Development of Novel Assays for Lignin Breakdown and Identification of a New Bacterial Lignin Degrading Enzyme

By

Mark Ahmad

A thesis submitted in partial fulfilment of the requirements of the degree of Doctor of Philosophy

University of Warwick, Department of Chemistry

September 2010

Table of Content

List of Figures

List of Tables

Abbreviations

ABTS	2,2'-azino-bis(3-ethylbenzthiazoline-6-sulphonic acid
AFU	arbitary fluorescence units
A. globiformis	*Arthrobacter globiformis*
APPL	acid perceptible polymeric lignin
AU	arbitary units
Bn	benzyl
br	broad
B. subtilis	*Bacillus subtilis*
B. licheniformis	*Bacillus licheniformis*
Bz	benzoyl
^{o}C	degrees Celsius
CCP	cytochrome c peroxidise
d	doublet
Da	Dalton
DCM	dichloromethane
dd	doublet of doublets
d. e.	diastereomeric excess
DEAE-Sepharose	diethylaminoethyl-cellulose
DMF	dimethylformamide
DNA	Deoxyribonucleic acid
DNP	2,4-Dinitrophenylhydrazine
d	doublet
ESI-MS	electrospray ionisation mass spectrometry
FITC	fluorescein isothiocyanate

FITC-lignin	lignin derivatised with fluorescein isothiocyanate
GC	gas chromatography
GC/MS	gas chromatography mass spectrometry
GSH	glutathione
GSSG	glutathione disulfide
GPC	gel permiation chromatography
Hz	hertz
HPLC	high pressure liquid chromatography
HV	high voltage
IAF	4(5)-iodoacetamido) fluorescein
iTRAQ	isobaric tag for relative and absolute quantificaiton
IR	Infra red
kDa	kilodalton
LB	Luria Broth
LC/MS	liquid chromatography mass spectrometry
LC/MS/MS	liquied chromatography tandem mass spectrometry
LDA	Lithium diisopropylamide
LiP	Lignin Peroxidase
L. mesenteroides	*Leuconostoc mesenteroides*
m	multiplet
Me	methyl
Mn	number average molar mass
Mp	gel permiation average molar mass
MnP	Manganese Peroxidase
Mv	viscosity average molar mass

Mw	weight average molar mass
Mz	Z average molar mass
Mz+n,	Z+n average molar mass
NAD^+	nicotinamide adenine dinucleotide, oxidized
NADH	nicotinamide adenine dinucleotide, reduced
N. asteroids	*Nocardia asteroids*
N. autotrophica	*Nocardia autotrophica*
N. corallina	*Nocardia corallina*
N.globerula	*Nocardia globerula*
nm	nanometers
NOE	nuclear overhauser effect
N. opaca	*Nocardia opaca*
PCB	poly chlorinated biphenyls
P.chrysosporium	*Phanerochaete chrysosporium*
PDC	2-pyrone 4,6-dicarboxylc acid
Pdi	poly dispersity index
Ppm	parts per million
P. ovalis	*Pseudomonas ovalis*
P. putida	*Pseudomonas putida*
q	quartet
R. erythropolis	*Rhodococcus erythropolis*
R. jostii RHA1	*Rhodococcus jostii* RHA1
s	singlet

S. albus	*Streptomyces albus*
S. badius	*Streptomyces badius*
S. coelicolor	*Streptomyces coelicolor*
S. cyaneus	*Streptomyces cyaneus*
SDS-PAGE	sodium dodecyl sulfate polyacrylamide gel electrophoresis
S. griseus	*Streptomyces griseus*
S. rosusu	*Streptomyces rosusu*
S. phaechromogens	*Streptomyces phaechromogens*
S. paucimobilis SYK-6	*Sphingomonas paucimobilis* SYK-6
S. viridosporus	*Streptomyces viridosporus*
t	triplet
TLC	thin layer chromatography
T. mesophila	*Thermomonospora mesophila*
UK	United Kingdom
VP	Versatile Peroxidase
WOW	wealth out of waste
λ	wave length

Acknowledgements

I would like to thank all the people who have helped me on my PhD. Particularly I would like to thank Tim for giving me the chance to do a PhD and for all his help and guidance along the way. I would also like to thank Liz Hardiman for reducing my workload, purifying loads of protein and providing many a good chat. A big thank you to the rest of the Bugg group past and present, it's been a great three years.

Thanks to Dr Lijiang Song and Philip Aston for help and patience with all the mass spectrometry I have done. Big thanks to Anne Smith for keeping Chemical Biology running, for the media and the autoclaving. I would like to thank everyone in Chemical Biology for all their help over the time I have worked there. Also I would like to thank Dr G. Clarkson for many a helpful discussion over the course of my work.

I'm very grateful to all the people I have collaborated with. For Andy Clark and his postdocs Drs Alana Collis and Stuart Coles who helped with the electrospinning and with much discussion of results. I'm also grateful to the group of Prof. Eltis at UBC for providing the original DypB and all the knock out mutants.

I would like to thank the people I worked alongside at Warwick HRI. Especially Dr. K. Burton and Dr. D. Eastwood, who helped grow the white and brown rot fungi and Dr. G. Bending who taught me all about mycorrhizal fungi.

I would like to thank my friends and family, especially my wife Alison, for all their help and support through the course of my studies at Warwick. Finally I would like to thank Jesus for making a way, when so often there seemed no way.

Declaration

The work presented here is my own work unless otherwise acknowledged and has not been submitted for a degree at any other university. Work presented in Chapter III has previously been published:

Development of novel assays for lignin degradation: comparative analysis of bacterial and fungal lignin degraders; M. Ahmad, C. Taylor, D. Pink, K. Burton, G. Bending and T. Bugg, *Molecular Biosystems*, 2010, **6**, 815-821.

Abstract

Two novel spectrophotometric assays have been developed for high throughput screening of microbial lignin degradation. The first assay involves fluorescently labelled lignin, which gives a time dependent increase in fluorescence with lignin degradation. The second involves nitrated lignin where an increase is seen at 430nm when lignin is broken down. These assays have allowed identification of a number of new strains of lignin degrading bacteria including *R. jostii* RHA1. They have also allowed the comparison of bacterial and fungal degraders and a study of lignin specificity.

Bioinformatics has been used to identify two putative lignin degrading enzymes in *R. jostii* RHA1. Their role in lignin degradation was investigated by assaying of gene knockouts. This led to the detailed study of a new recombinant peroxidase, DypB, using lignin, lignocellulose and lignin dimer model substrates. This represents the first recombinant bacterial lignin degrading enzyme to be characterised.

In addition methods for studying the products of lignin breakdown by HPLC, GC/MS and LC/MS have been developed. This has led to the identification of several low molecular weight aromatic products including ferulic acid. It has also been shown that the products released from lignin model compounds can be controlled by addition of the reductive enzyme diaphorase.

CHAPTER I: Introduction

1.1 Sustainable energy and raw materials

The world currently makes great use of crude oil to produce transportation fuel, materials, fine chemicals and energy. Diminishing reserves and increased concern about green house gas emissions have produced a strong desire to find alternative methods of meeting these needs.[1] Currently the world demand for oil is eighty-four million barrels a day and this is expected to grow to one hundred and ten million barrels by 2030 as developing economies such as China and India continue to grow.[2]

Several different methods have been suggested for providing electrical power: solar, wind, geothermal, nuclear and biomass. However, the options for fuel are less and for (raw) materials still fewer.[3] Currently one of the key technologies being applied to the problem is the fermentation of biomass to produce ethanol.[4] This technology has a long history in the UK for manufacture of beer, wine and spirits but now is being investigated for more practical reasons.[5] Ethanol can be employed as a fuel, and can be reduced to ethane, which can be used to make materials.[6] The process of fermentation currently uses readily available sugars that enzymes breakdown into ethanol.[1, 7] Ethanol produced in such a manner is described as a first generation biofuel.[6]

First generation biofuels are derived from sucrose, starch, vegetable oil or animal fats using current technology. Commonly used feedstocks are wheat/

corn grain and rapeseed. First generation biofuels include bioethanol, biodiesel and starch derived biogas.[2]

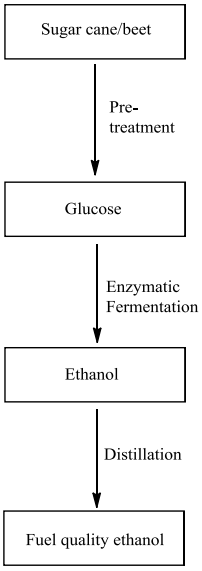

Figure 1.1 Schematic representation of a first generation bioethanol production process.

There are two significant limitations to 1st generation biofuels. Firstly, that the process can be restricted to a specific geography. Brazil is the second largest producer of first generation bio-ethanol, and it uses sugar cane as its main feedstock.[2] This is only possible because sugar cane grows in high yields in Brazil,[2] but in the UK it does not, thus the same system cannot be employed. Whilst other crops (e.g. sugar beet) can be used in the UK there are only a limited number of plants that produce high quantities of easily fermentable sugars.[1] The second limitation is that energy crops compete with food crops for land. These two limitations combine; lower yields obtained due to poor climate require the use of more land. The more land used for energy crops the less food one can grow and the less food grown the higher the cost of food. This makes first generation biofuels unpopular with the general public.[1]

1.2 Biorefineries and second generation biofuels

To overcome the limitations on first generation biofuels it has been proposed that agricultural waste be employed as the feedstock for ethanol production. The UK's main agricultural produce[8] is wheat: 435 thousand tons of domestic wheat were milled in the July 2010.[9] The majority of the straw from this wheat is not used, and is thus considered a waste product. This waste has the potential to become a useful feedstock for second-generation bioethanol production.[2]

Wheat straw is not the only waste material that can be used. For every kg of grain harvested, 1-1.5 kg of straw, cobs and other residue is generated. In the US 940×10^6 tons of organic solid waste is produced, much of which is cellulosic.[10] This represents a considerable raw material, which can be employed for biofuels and biomaterial production.

Second generation biofuels are produced from non-food sources with developing technology. They aim to breakdown the lignocellulose to form both fuel and chemicals.[2] This has given rise to the concept of a biorefinery: a place, where biomass is sustainably processed into a range of marketable products. [3]

A number of chemicals and materials have previously been produced from bioresources such as wood, cellulose and amino acids. However they have not been produced as part of an integrated process, and not on the scale now imagined. In a biorefinery, a diverse array of feedstocks including: agricultural material (both dedicated crops and residue); forestry; industrial/ domestic waste and marine culture (algae and seaweed) will be valorized at a local level to

provide energy, heating and chemicals. Bio-refineries will form the cornerstone of a sustainable bio-economy.[2]

A diverse array of processes are used to transform biomass into products in a biorefinery, Figure 1.2 provides a schematic overview.[11] There are two core types of process that are used, thermochemical and biochemical.[2, 11] The main thermochemical processes are pyrolysis and gasification. In gasification high temperatures and low oxygen concentrations are used to turn the biomass into a mix of H_2, CO, CO_2 and CH_4. This gas mixture is refered to as syngas. Syngas can be used directly as a fuel, for example to power the biorefinery or it can be converted into higher density fuels such ethanol or isobutanol. In addition, it can be used to make chemicals such as alcohols and organic acids. Pyrolysis uses temperatures of 300-600^{o}C and no oxygen to form bio-oil and charcoal.[2] Both of these have potential value as fuels. Biochemical processes consist of fermenting the cellulose and separating out the residue. From the residue, protein can be extracted for animal feed, and the remainder can be burnt. From the cellulose, sugars and alcohols can be produced.[11]

Fermentation of cellulose cannot only produce alcohols for fuels, but also feedstock chemicals. The fourteen leading feedstock chemicals proposed by the US energy department[12] are shown in Figure 1.3.[2]

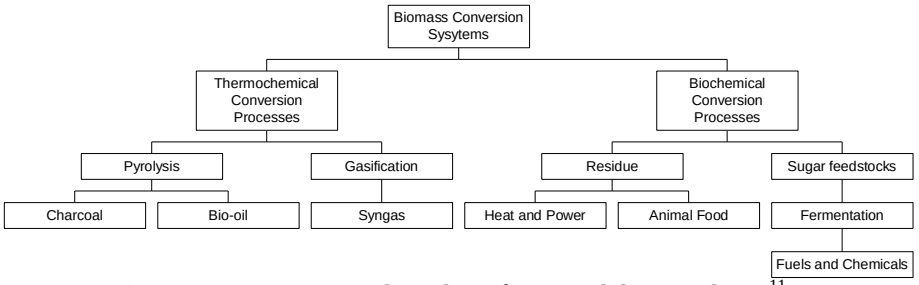

Figure 1.2 Processes used in a biorefinery and their products.[11]

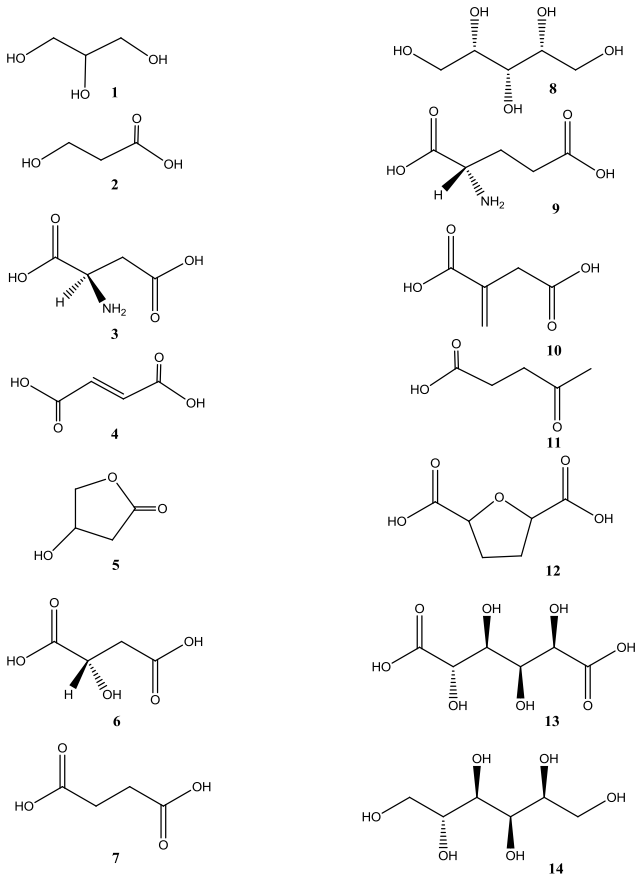

Figure 1.3 The 14 leading renewable feedstock chemicals; glycerol **1**; 3-hydroxy propionic acid **2**; L-aspartic acid **3**; fumaric acid **4**; 3-hydroxy butyrolactone **5**; L-malic acid **6**; succinic acid **7**; (S, R, R,)-xylitol **8;** L-glutamic acid **9**; Itaconic acid **10**; levulinic acid **11**; 2,5-furan-di-carboxylic acid **12**; glutaric acid **13** and sorbitol **14**.

The feedstock chemicals detailed above can be used to produce a wide range of different chemicals, providing a sustainable alternative to the petrochemical industry. Levulonic acid **11** is a potential feedstock chemical: it is produced by

the acid hydrolysis of C6 sugars. It has a mix of functionality, which means that it can be modified by a number of different chemistries. It can be used to produce methyltetrahydrofuran **15,** a biofuel that can be blended with petrol. It can be used to make δ–aminolevulinic acid **16**, which is a herbicide. It can be polymerised with phenols to give polydiphenolic acid, which can be used as a material. Finally it can be reacted with ethanol to form ethyl levulinate **17,** a transport biofuel, which can be added to conventional diesel and used without any need for engine modification.[2, 13]

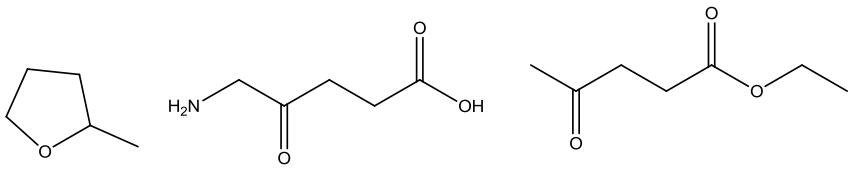

15 **16** **17**

Figure 1.4 Methyltetrahydrofuran **15**, δ-aminolevlininic acid **16**, and ethyl levulinate **17.**

Bio-refineries have great potential to provide sustainable energy and chemicals. They can provide solid, liquid and gaseous fuels and also provide a source of platform chemicals from which other materials can be manufactured.

The limitation of bio-refineries and second-generation biofuels is that cellulose, from which many useful things can be made, is closely bound to the plant polymer lignin.[2] The removal of lignin from the lignocellulose requires a high energy pre-treatment step.[3, 11] The current preferred method for this is steam explosion. In this process the wood is treated with pressurised steam at 200-250^{o}C.[14] This requires a significant amount of energy and makes the process cost ineffective.[7]

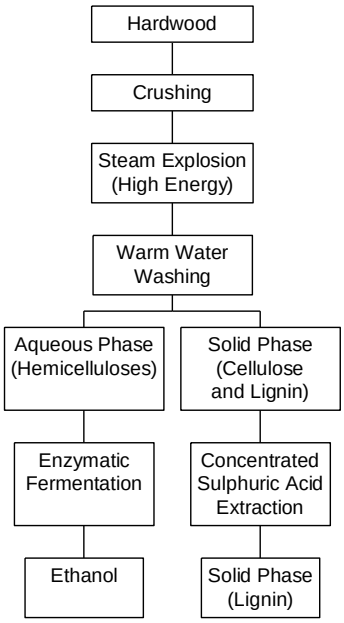

Figure 1.5- A schematic representation of a biorefinery with the high energy steam explosion step marked.[11]

1.3 Lignin and lignocellulose

Lignocellulose was first identified in 1838 by Anselne Payen who noticed that most of wood was lost after it was treated with concentrated nitric acid. He named the material that remained cellulose.[15] To comprehend why lignocellulose is so difficult to breakdown one must understand its structure, which is illustrated in Figure 1.6.

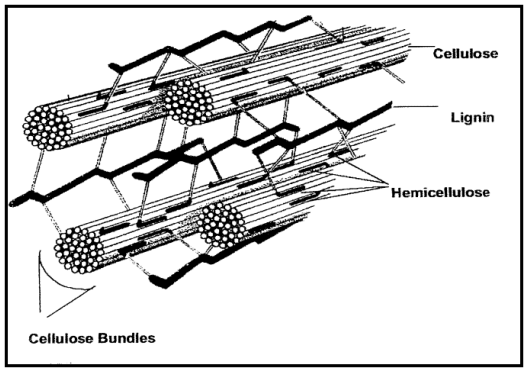

Figure 1.6 Cellulose as found in plant cells.[16]

Cellulose is a homopolymer of β-D-glucopyranose. These are linked together by (1→4) glycoside bonds. This is illustrated in Figure 1.7. The cellulose molecules are linear and have a strong tendency to aggregate into fibrils. This is driven by hydrogen bonding and van der Waals interactions. Cellulose differs from starch which is composed of α-1,4 linkages which are illustrated below (Figure 1.7).[15]

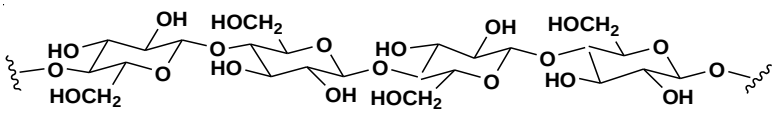

Figure 1.7 Cellulose, a linear 1,4 polymer of β-D-glucopyranose.[15]

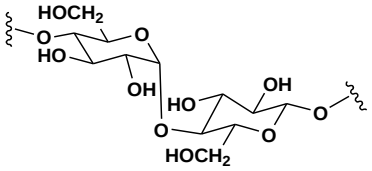

Figure 1.8 The α−1,4 linkage which is found in starch.[15]

Starch molecules are consequently not linear and tend to form helicies in the solid state and solution. They also tend to be branched, via 1,6 glycosidic linkages.[15] This combines to make it difficult for them to stack together, so they do not aggregate. These molecular differences lead to starch being soluble whilst cellulose is not.[17] Being soluble makes starch much easier to breakdown. Whilst plants rich in starch have been readily developed for first generation biofuels, those where the sugar is mainly in cellulose have not been.[1, 7]

The difference in macromolecular shape is not the only thing that leads to lignocellulose being difficult to break down. The other reason is that cellulose closely adheres to the plant polymer lignin and is even possibly bound to it

under some situations.[18] The lignin aids nutrient transport in plants, provides structural support and defence against micro-organisms.[19] This effect is increased by the anti-fungal properties of its breakdown products.[20] The structure of lignocellulose is illustrated in more detail in Figure 1.9. Hemicellulose is also part of lignocellulose it is found linking the cellulose and the lignin together.[15, 21] Hemicellulose has a diverse structure composed of five and six carbon sugars, which vary depending on the plant type.[15] The structure of a typical hemicellulose chain can be seen if Figure 1.9.[21]

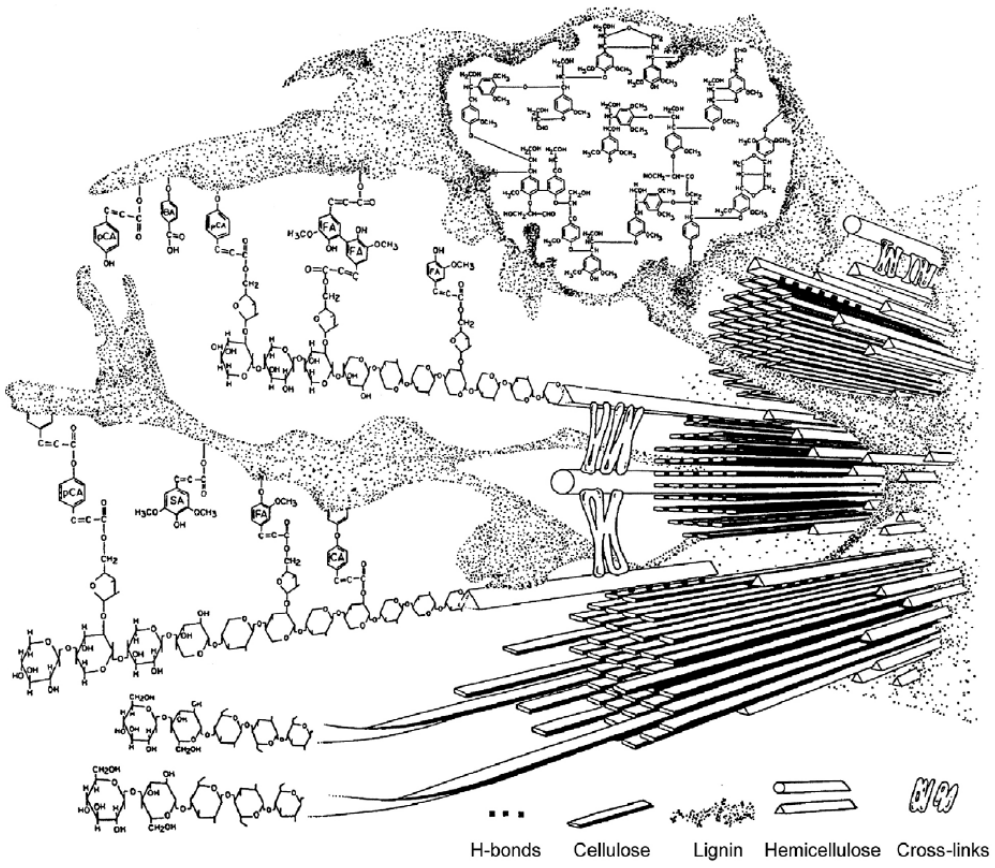

Figure 1.9 A detailed diagram of the structure of lignocellulose. Illustrating the molecular structure of lignin, cellulose and hemicellulose and how the three interact on a macromolecular level.[21]

Lignin is a three dimensional amorphous polymer consisting of methoxylated phenyl propane units. It has a diverse structure made of three types of subunit, which can be joined together in a number of ways. The three subunits are derived from the three biosynthetic building blocks of lignin: coniferyl alcohol **18**, sinapyl alcohol **19** and coumaryl alcohol **20**.[15]

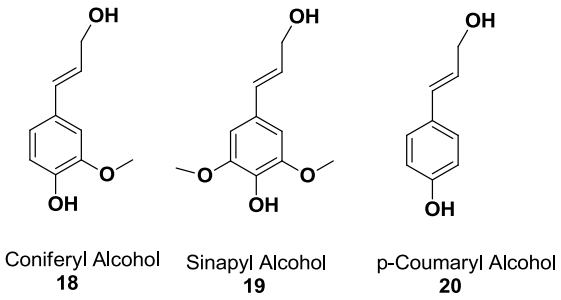

Figure 1.10 Lignin precursors.

These monomers are coupled together through a series of radical reactions that are initiated but not controlled by redox enzymes.[22] The monomers can be linked together into a number of different dimer structures. These dimer units occur in different amounts in different plants.[15] The factors affecting dimer formation are not well understood, but the concentration of monomers, the ratio of the three alcohols **18**-**20** at the polymerisation site, presence of antioxidants and the natural variation in electron density between the three resonance of the monomer units shown in Figure 1.11 are all proposed to be involved.[22]

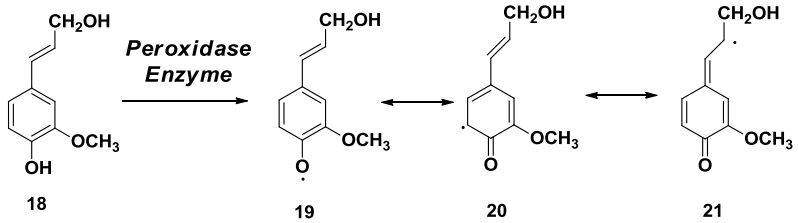

Figure 1.11 Resonance structures for the radical of coniferyl alcohol.[15]

The different types of lignin dimer that occur in nature are shown in Table 1 along with their relative abundance in different lignin types. The most common lignin dimer is the β-aryl ether dimer, which makes up around 50% of the dimer units.[23] The proposed mechanism of formation is given in Figure 1.12. The other linkages can be formed through analogous mechanisms with the exception of the

spirodienone linkage and dibenzodioxocin linkages, which are formed by slightly different mechanisms as illustrated in Figure 1.13 and 1.14 respectively.

Linkage			β-O-4	5-5	β-5	Spirodienone
Structure			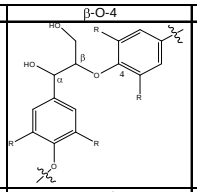	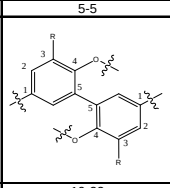	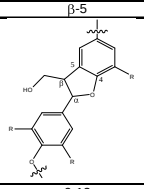	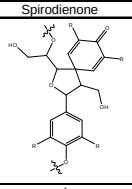
Abundance per 100 C9-units	Softwood	Spruce (23,24)	45-50	19-22	9-12	nd
		Spruce (25)	nd	22	12	nd
		Spruce (26)	45	24-27	9	nd
		Spruce (27)	45	24-27	9	2
	Hardwood	Birch (23, 24)	60	9	6	nd
		Eucalyptus grandis (28)	61	6	3	nd
		Eucalyptus grandis (29)	61	3	3	5
		Paulownia fortunei (30)	62	nd	11	3
Linkage			4-O-5	β-1	Dibenzodioxcin	β-β
Structure			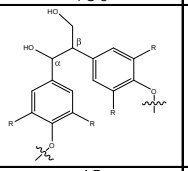	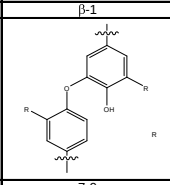	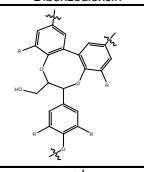	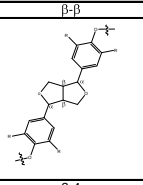
Abundance per 100 C9-units	Hardwood	Spruce (23,24)	4-7	7-9	nd	2-4
		Spruce (25)	nd	2	5	2.5
		Spruce (26)	nd	1	7	2
		Spruce (27)	nd	1	7	6
	Softwood	Birch (23, 24)	6.5	7	nd	3
		Eucalyptus grandis (28)	9	1	<1	3
		Eucalyptus grandis (29)	9	2	nd	3
		Paulownia fortunei (30)	nd	1	2	12

Table 1.1 The different lignin dimers and their relative abundances in different wood types. R= H or OMe.[23, 24, 25, 26, 27, 28, 29, 30, 31]

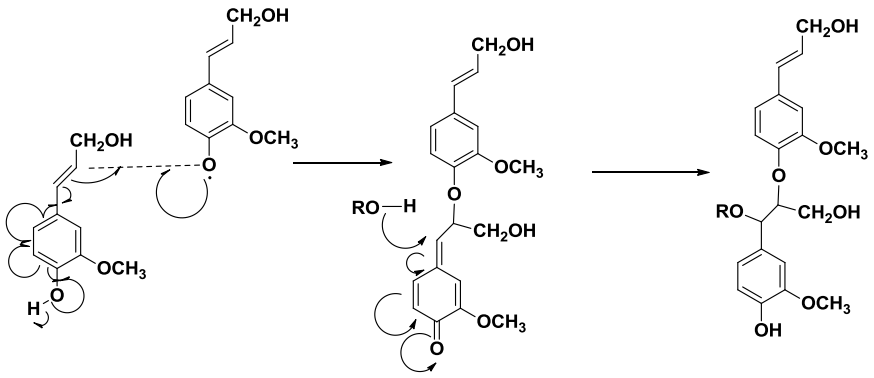

Figure 1.12 Mechanism for formation of β-aryl ether lignin dimer unit, this linkage is also refered to as a β-O-4 linkage.

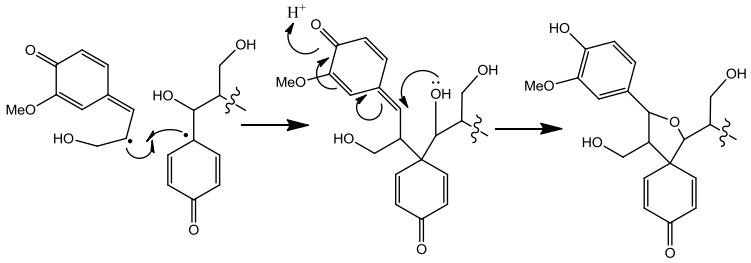

Figure 1.13 Mechanism for spirodienone dimer formation.[22]

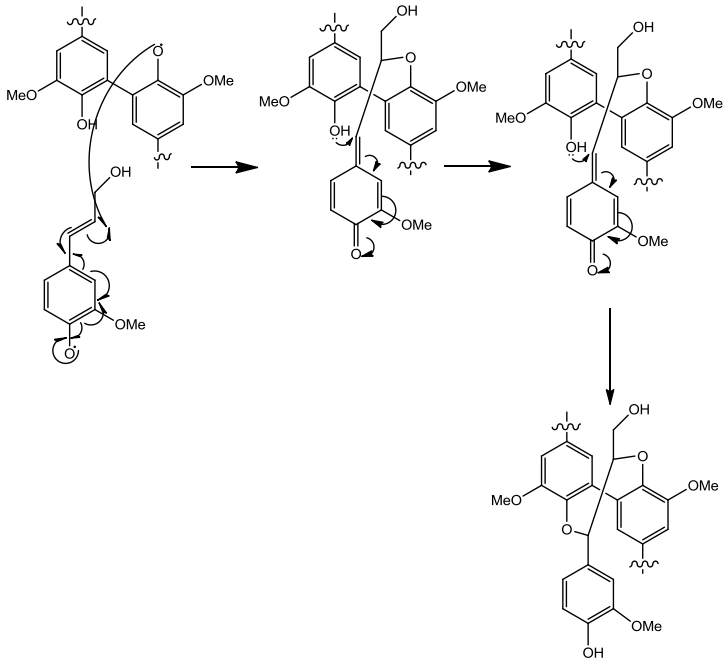

Figure 1.14 Mechanism for dibenzodioxocin dimer formation.[22]

Recently the 'uncontrolled' model of lignin polymerisation has been challenged by Davin and Lewis. [32] They have proposed that lignin formation is controlled by proteins that bind monolignols and control their polymerisation, producing lignin with a defined primary sequence. The main evidence for this is observations of distinct sites of nucleation,[22] differences in lignin properties within different cell types within plants[32] and some evidence of preferred lignin motifs.[33] This new perspective has so far failed to find widespread support, as no evidence of proteins being able to make any more than lignin oligomers has been shown, and the differences in lignin properties and the distinct sites of nucleation can be explained within the existing scheme.[22]

The structure of lignin varies significantly, not only due to variations in linkage type, but also due to variations in type of lignin monomer. There are three

monomers and they are present in varying amounts in different types of wood.[15] This is the main way that lignin is characterised and is summarised in Table 2.[34]

Predominant Lignin Type	Wood Type	Lignin Type	% H	% G	% S	Av. No. of MeO/ unit
G	Hardwood	G	0-15	85-100	0-5	0.85-1
GS	Softwood	GS1	0-10	70-95	5-20	0.95-1.2
		GS2	0-10	55-75	25-35	1.1-1.3
		GS3	0-5	50-65	35-45	1.25-1.4
		GS4	0-5	25-50	45-70	1.35-1.7
HGS	Grasses	HGS	20-40	35-55	5-45	0.8-1.1

Table 1.2 Lignin characterisation. G corresponds to guaiacylpropane subunits which are derived from confieryl alcohol. S corresponds to syringylpropane subunits which are derived from sinapyl alcohol. H corresponds to 4-hydroxyphenylpropane subunits which are derived from p-coumaryl alcohol.[34]

The lignin structures rich in methoxy groups are generally found in hardwoods as they are less likely to form branches, which are produced by the biphenyl type of linkage. This lack of branching gives rise to greater rigidity.[22] Where GSH lignins occur the wood is generally more flexible due to the increased branching.[15]

The heterogenous aromatic nature of lignin makes it inert. The high degree of structural variety has been proposed as a powerful defensive mechanism making it difficult for pathogens to develop effective methods of degradation.[22] The aromatic rings linked by alkyl ethers is a chemically resistant motif that grants lignin a high degree of stability to many chemical methods of breakdown. However, there have been a number of methods to degrade lignin chemically that have been discovered.[23]

1.4 Chemical lignin valorization

Lignin breakdown by chemical means has been an area of extensive study, starting in 1938 with the discovery that copper-chromium oxide could be used as a hydrogenation catalyst to produce propylcyclohexanols and methanol.[35] Since then, there have been three main types of reaction, which have been investigated crackin/hydrolysis reactions, reductive reactions and oxidative reactions.[23]

Cracking and hydrolysis generally produces lower molecular weight lignin fragments by C-C bond cleavage and ether cleavage.[36] Cracking is often accomplished with procedures modified from the petrochemical industry, thus zeolites are thus heavily employed to produce mixtures of aromatic and aliphatic hydrocarbons.[23] Hydrolysis, especially using basic conditions has been investigated and shown to produce lower weight lignin fractions, but has been limited by the poor solubility of some types of waste lignin.[23]

Reductive reactions have been generally found to produce breakdown products with lower degrees of functionality. Studies have focused on using a variety of heterogenous catalysts to carry out hydrogenation of lignin.[23] Although a little work has also shown how homogenous reactions can be carried out to depolymerised lignin through a reductive method for example using $NaBH_4$ and iodine.[37]

Oxidative reactions for modifying lignin tend to increase functionality and this has the potential to produce useful feed chemicals.[23] The main focus to date of

this research has been on cleaning the waste effluence of paper mills using photobleaching and TiO_2. [23, 38]

In the paper industry there has been a long history of removing lignin. One of the most common methods is through the kraft process. This involves cooking lignocellulose in alkaline solution with sodium sulfide at 170^{o}C.This produces a black waste stream of sulphonated lignin fragments.[39] The scale of this process is shown by the fact that twenty million tonnes of kraft lignin were produced in 1995 in the United States.[40] Kraft lignin provides a significant source of renewable aromatic compounds that is currently not fully utilised.[41]

Despite extensive efforts the various chemical methods thus far investigated have not given rise to an effective method of lignin valorisation.[23] The main reason for this is that the heterogenous nature of lignin when combined with harsh chemical treatment inevitably leads to a diverse array of products. Another disadvantage is that lignin streams in biorefineries are in practice heavily contaminated with a variety of chemical and biological moieties they are thus very prone to poisoning catalysts and side reactions.[23] It is hoped that a more controlled reaction by microorganism can overcome these two limitations. A number of micro-organisms are known to be able to degrade lignin, with fungi being the most well studied.[42]

1.5 Fungal degradation of lignin

The most well characterised lignin degraders are white rot basidiomycetes.[43] These fungi produce a number of extracellular enzymes that are effective in breaking down lignin. These are Lignin Peroxidase (LiP), Manganese

Peroxidase (MnP), laccases and Versatile Peroxidase (VP),[43, 44] but not all of these enzymes are expressed by any one fungal species. For example *Phanerochaete chrysosporium* (Figure 1.15) produces LiP and MnP but not VP or laccases.[43]

Figure 1.15 *P. chrysosporium* growing on wood chips.[45]

LiP, MnP and VP are all heme peroxidases that share a common folding structure similar to cytochrome c peroxidise (CCP) with ten helices which compose approximately 50% of the molecule.[46, 22] They all have two domains and sandwiched between these a single heme group tethered by a histidine residue.[22] They each work through a common mechanism given schematically in Figure 1.16, where hydrogen peroxide binds opposite the tethered histidine and iron-porphyrin, and undergoes a two electron oxidation to form Fe(IV) porphyrin radical cation. This is referred to as compound I. In some of proteins like LiP the radical can be centred on an amino acid. Compound I undergoes a one electron reduction with the substrate to give compound II and a further one electron reduction to give the resting enzyme.[47]

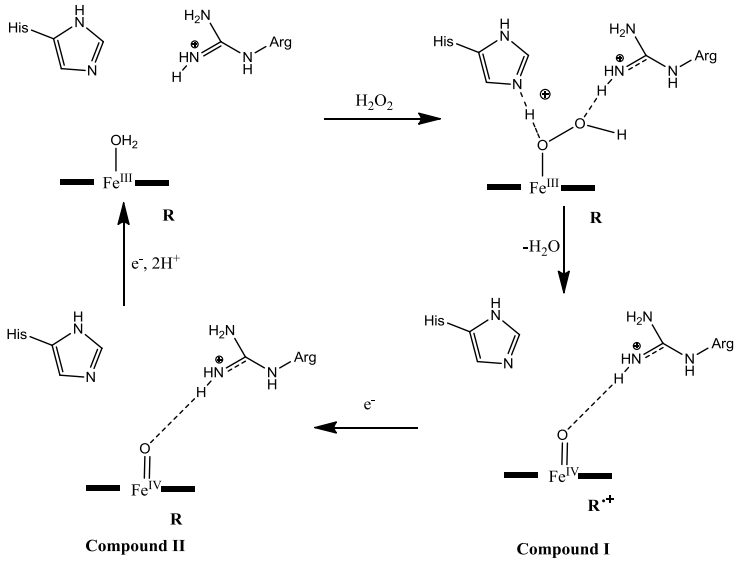

Figure 1.16 Catalytic cycle for a heme peroxidase. $R^{\bullet+}$ is a protein or porphyrin radical depending upon the enzyme.[47]

The mechanism above is based on that of CCP. Early studies in this enzyme using hydroperoxides showed quantitative release of alcohol this suggested that the O-O bond cleaved heterolytically to leve an oxeme.[48] The redox state of the iron was determined as IV by magnetic suspetability[49] studies and Mossbauer spectroscopy.[50] The additional electron needed was proposed to come from the porpherine ring consistent with what was observed with model heme systems.[51] However, EPR studies showed that no porphrin radical was observed but instead a protein radical was seen.[52] Further studies showed the radical to be located on Trp171 which was shown to be required for activity by mutagenesis.[53] The active site of CCP is dominated by a distal histidine and arginine residue. His52 assists in the formation of Compound I whilst Arg48 is involved in increasing the stability of compound I.[47]

LiP is an enzyme with a weight of between 38 and 43kDa depending on degree of glycosylation. It has an iron heme group in a 1:1 molar ratio with protein.[43] The crystal structure is known[54, 55] and shown in Figure 1.17.

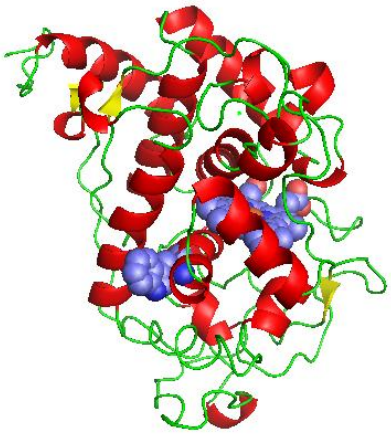

Figure 1.17 Crystal structure of LiP with Trp 171 and the heme highlighted. Deposited with the PDB, 1llp.[54]

Early work suggested that LiP mediated the oxidation of veratryl alcohol.[43] This was thought to happen at two active sites: one near the metal in the inside of the enzyme, and one on the surface near Trp171 (shown in Figure 1.17), which has a post-translational hydroxylation on the β-carbon in the crystal structure.[54] This is thought to be formed by the trapping of the tryptophan radical by water when no substrate is present.[54] Mutation of tryptophan 171 to phenylalanine leads to the loss of all activity further supporting the theory that this residue plays a vital role.[54]

There are two possible mechanisms by which this could occur. These are illustrated in Figure 1.18. The redox potential for tryptophan is 1.19 V[56] whilst for veratryl alcohol it is 1.4V,[57] meaning that the first step of the mechanism is thermodynamically easier than reaction of LiP compound I with substrate.[54] The

radical that is formed would be in equilibrium with the neutral radical at pH 4.5. This could then react in two ways. In route A it can react with the enzyme to form the cation which can lose a proton to form an α, β-unsaturated imine, which can under go a Michael –type addition of water. Route B for the neutral radical to react is via reaction with oxygen, which can then be eliminated as superoxide to give the modified amino acid. [54]

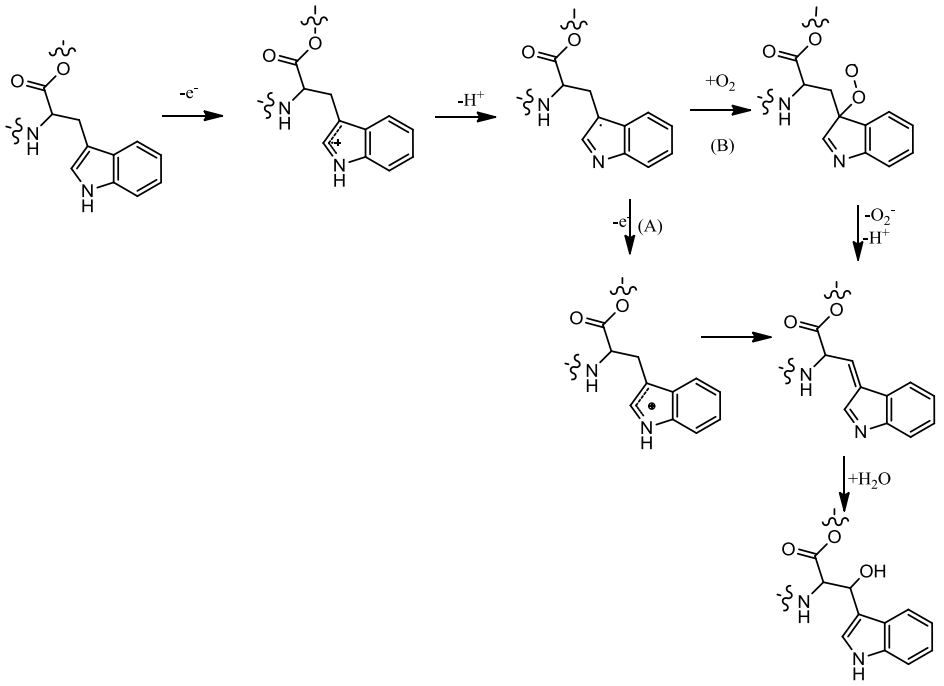

Figure 1.18 Two possible mechanisms for the formation of β-hydroxylated tyrosine in LiP from *P. chrysosporium*.[48]

However, resonant mirror biosensor techniques showed that LiP was capable of binding synthetic lignin.[58] This suggested that LiP might not always need a small molecule mediator. The mechanism of action for LiP has been studied using a number of model compounds.[59] With β-aryl ether linkage model compounds, a number of different methods of cleavage were apparent. The following mechanisms for cleavage where elucidated with deuterium labelled

model compounds.[59] Three different degradation routes were proposed, each starting with formation of a radical cation, from here there could be C-C bond cleavage between the α and β carbons, in one case proceeded by intermolecular cyclisation and in the other case proceeding directly. The third method of break down is by cleavage of the ether bond after addition of water to the radical cation.[59]

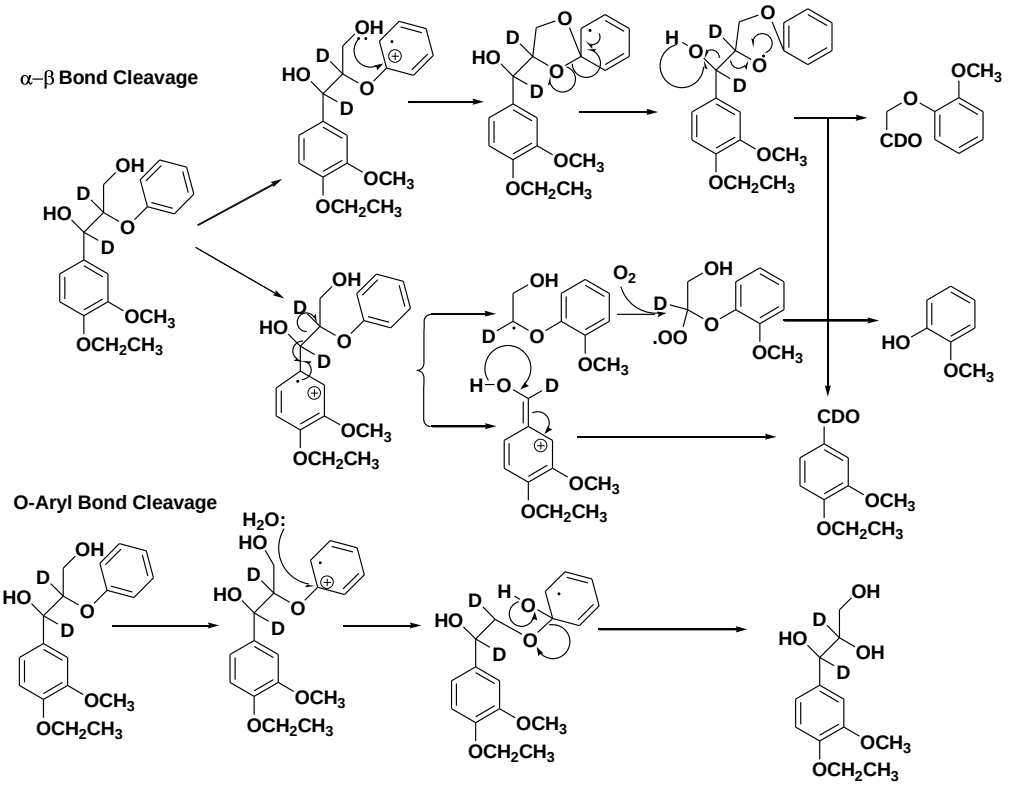

Figure 1.19 Degradation of deuterated β-aryl ether linkage lignin dimers by LiP of *P. chrysosporium.*[59]

Lignin from wood degraded by white rot fungi was compared with undegraded wood,[60] and it was found that aromatic ring fission could happen prior to cleavage. After further model studies, the mechanism illustrated in Figure 1.20 was proposed.[59] In this mechanism, the enzyme forms a radical cation, which can go onto to react with water or oxygen to give ring cleavage.

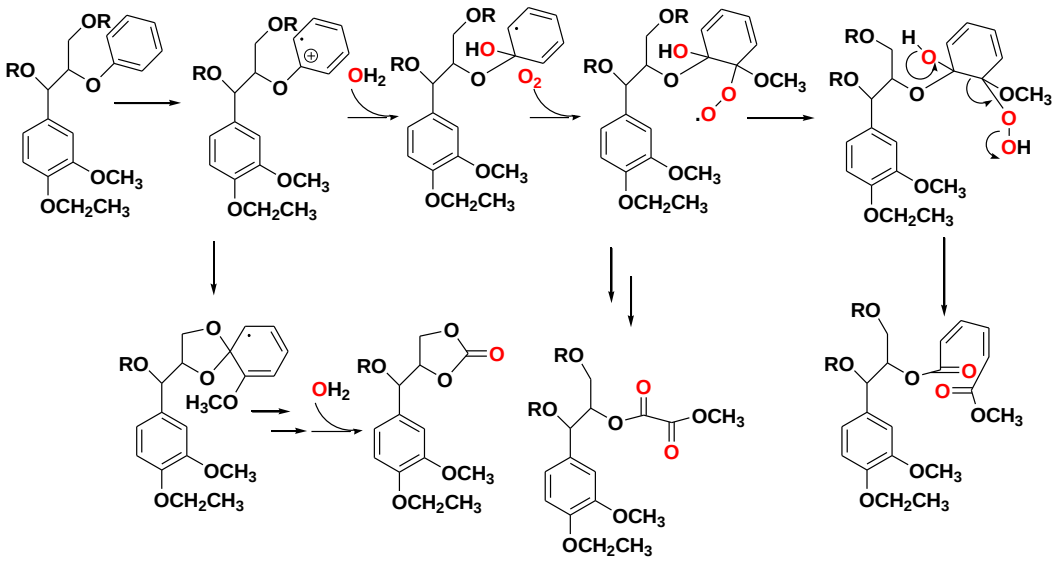

Figure 1.20 Proposed mechanism for ring cleavage. The red atoms correspond to ^{18}O.[59]

LiP from *P. chrysosporium* has been extensively studied by stopped flow kinetics. This method has shown that compound I formation is pH independent between pH 3 and pH 7, but that the reaction of compound I and compound II is faster at pH 3. This is consistent with the low pH optimum observed under steady state conditions. This low pH optimum suggests the role of ionisable groups with a pK_a under 5 in either the binding or oxidation of the substrate.[61] Subsequent mutation studies have shown that acidic residues near Trp171 may have an important role. The oxidation of mediators such as veratryl alcohol may be responsible for this pH sensitivity.[62]

MnP is found in almost all white rot fungi.[63] It is an iron heme, containing enzyme with a mass of 45-47 kDa, the structural fold is similar to that of LiP and cytochrome c peroxidase.[43,64] MnP oxidises Mn^{2+} to Mn^{3+} and this is then stabilized by chelators produced by the fungi such as oxalic acid or unsaturated fatty acids. These types of complexes have been found to degrade β–aryl ether model compounds.[65] They have shown to be been effective at degrading model

compounds both with phenolic groups and without. This suggests MnP has activity against both the end of lignin molecules and the main body of the polymer. The breakdown of non-phenolics is proposed to be carried out via abstraction of a backbone hydrogen, as shown in Figure 1.22.[63]

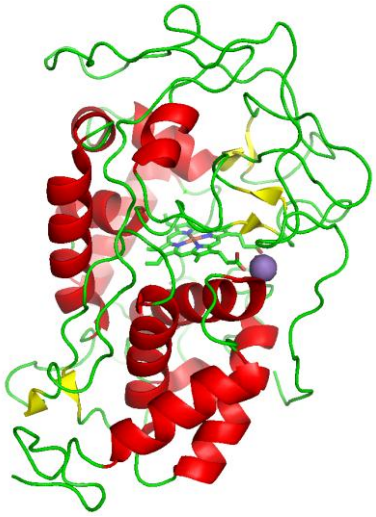

Figure 1.21 Crystal structure of MnP with Mn^{2+} and heme highlighted. Deposited with the PDB, 1MNP.[65]

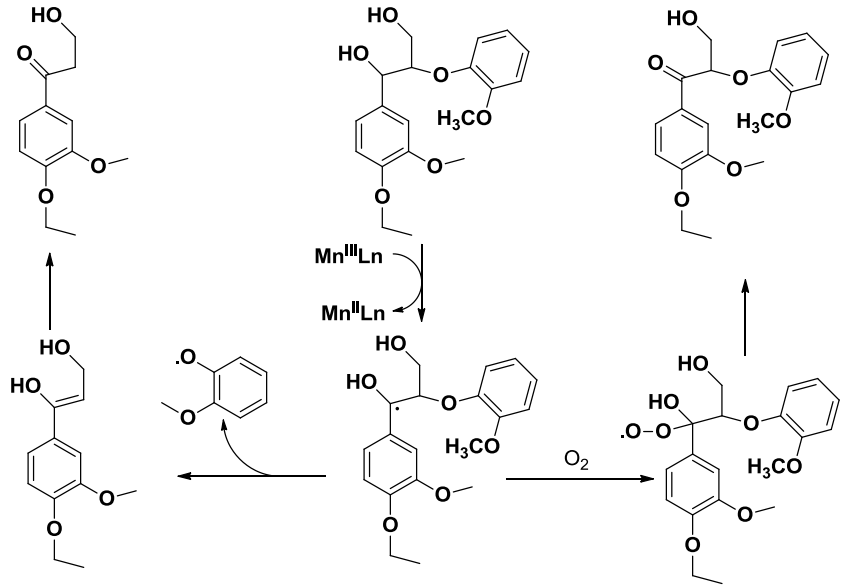

Figure 1.22 Proposed scheme for the oxidation of non-phenolic β-aryl ether lignin model dimers by Mn^{2+} with chelators. Ln= ligand, such as oxalic acid.[63]

MnP can react directly with both Mn^{2+} and lignin oligomers. The activity of recombinant MnP from *P. chrysosporium* expressed in *E. coli* was shown to be specific for Mn^{2+} by stopped flow studies. The rate of reaction of MnP compound I was shown to decrease rapidly with lignin oligomer size from 1.0 x 10^5 M^{-1} s^{-1} with guaiacol to 1.1 x 10^3 M^{-1} s^{-1} with lignin tetramer. With LiP from *P. chrysosporium*, such a decrease was not observed, a rate of 1.2 x 10^6 M^{-1} s^{-1} was observed with guaiacol and 3.6 x 10^5 M^{-1} s^{-1} with lignin tetramer. This shows that under natural conditions, the rate of reaction with Mn^{2+} would be much faster than with Mn^{2+} than with lignin.[66]

VP has been purified from *Pleurotus* and *Bjerkandera*, it has shown similar affinity for both aromatic compounds and Mn^{2+}.[67] The structure of VP is similar to that of LiP but it contains an additional Mn^{2+} binding site near to the bound heme, illustrated in Figure 1.23.[68] As in LiP there is a surface Trp, which has been identified to be involved in the oxidation of high redox potential aromatic substrates via long range electron transfer.[69]

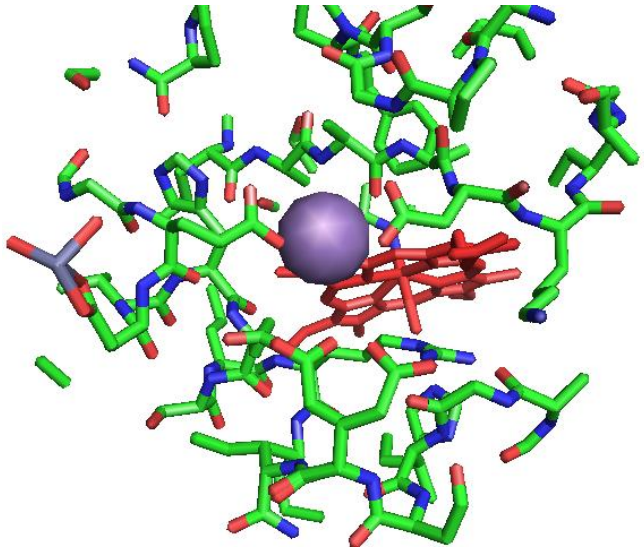

Figure 1.23 Mn^{2+} binding site in VP in close proximity to a nearby heme group. The crystal of VP is deposited with the pdb as 2BOQ.[70]

Laccases are a family of multicopper oxidases whose presence was found to be diagnostic of wood degrading fungi.[71] Laccases are blue copper proteins, which catalyse four sequential one electron oxidations of substrate molecules with reduction of oxygen. This enzymatic ability is centred around four copper atoms designated T1-T4. T1 forms the site of reaction with the substrate and is linked to T2, T3 and T4, which form a trinuclear copper centre by an electron transport chain. The enzyme carries out 4x one electron oxidations of the substrate after this the enzyme is regenerated by oxygen binding to the trinuclear copper centre and reacting to form two molecules of water. The general mechanism for the reaction of a substrate with a laccase is given in Figure 1.24.[68]

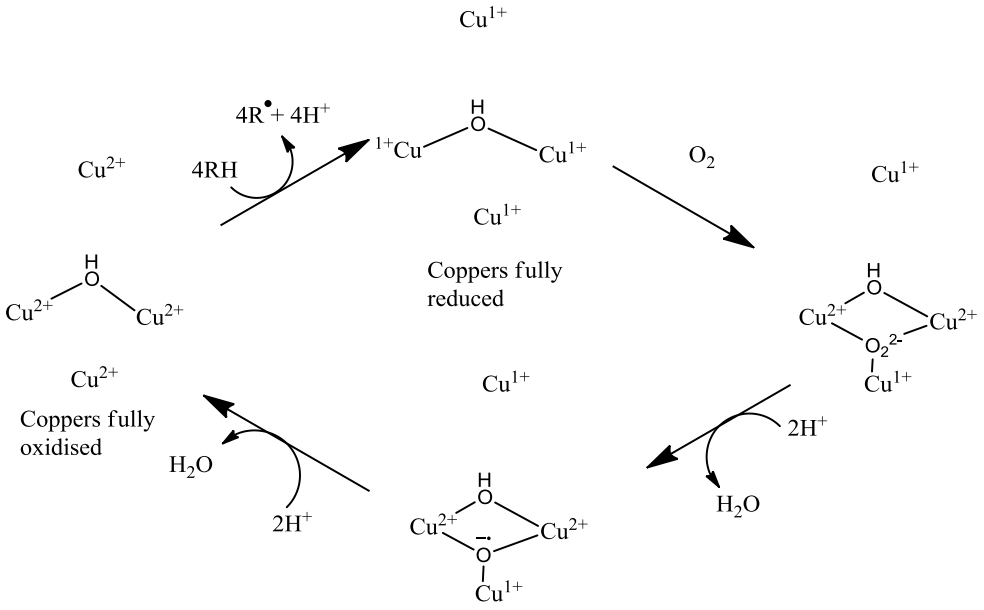

Figure 1.24 General laccase mechanism.[68]

Laccases have been observed to carry out a number of reactions on model compounds, which suggests they can degrade lignin. They can cause: C_α and C_β cleavage; causing alkyl-phenyl cleavage; α carbon oxidation and demethylation.[43] The mechanism used to carry out these transformations on model compounds is thought to be analogous to that used on lignin. Figure 1.24 gives the mechanism for cleavage of a lignin dimer.[44] There are two methods of breakdown for the dimer: one proceeds by oxidative cleavage between the ring and the benzylic carbon; in the other method there is oxidation of the benzylic alcohol followed by C_α-C_β cleavage.[44]

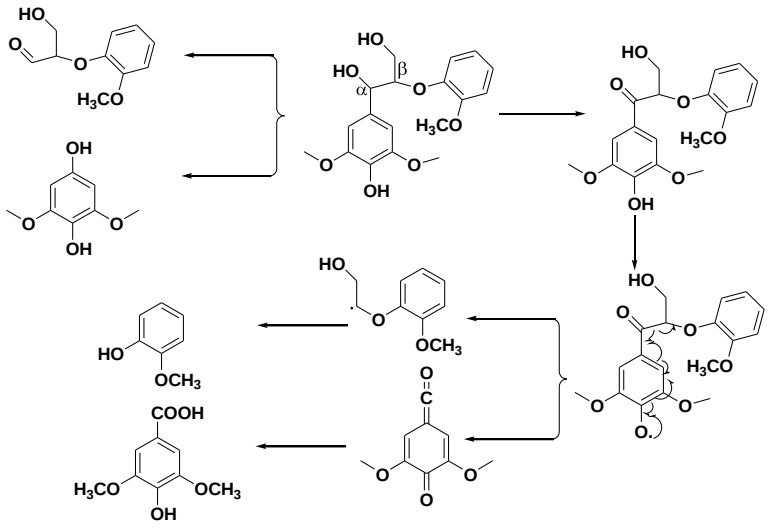

Figure 1.25 The proposed mechanism by which LA hydrolyses β aryl ether lignin dimers.[44]

Whilst laccasses have been shown to catalyse lignin degradation they can also polymerise lignin oligomers to form.[72, 73] The factors that control whether polymerisation or degradation occur are not well understood.

There has been on going resistance to accepting that laccases play a key role in lignin degradation, due to the inability of laccases to be effective on non-phenolic model compounds.[74] However, some fungi such as *Pycnoporus cinnabarinus* lack extracellular peroxidase activity, but can still effectively degrade lignin.[75] Mediators such as 2'2-azinobiz-(3-ethylbezthiazoline-6-sulfonate) (ABTS) and 1-hydrozybenzotriazole (HOBT) have been found to be effective mediators, increasing the oxidative range of many laccases.[60] In addition, lignin-derived compounds such as syringaldehyde and acetosyringone have been shown to be effective mediators as well.[76]

Laccases can show specificity depending upon the redox potential of both the enzyme and the substrate. High redox potential laccases are able to

accommodate a wider array of substrates compared with low redox potential substrates. High redox potential enzymes demonstrate faster reaction with lignin model systems.[77] Syringyl compounds react faster than guiacyl compounds as the extra methoxy group leads to more electron rich rings. The presence of aldehyde groups, such as in vanillin, decreases the rate of reaction substantially, as they make the ring more electron poor. This can give laccases specificity and further specificity may result from binding interactions.[77]

In addition to the enzymes above that react directly with lignin, there are a number of supporting enzymes that help to degrade lignin indirectly. These include glucose 1-oxidase, aryl alcohol oxidase, superoxide dismutase and glycoxal oxidase that produce hydrogen peroxide.[78] There are also believed to be secondary degradative enzymes such as low redox peroxidases and protocatechuate 3,4 dioxygenase: whilst ineffective at lignin degradation by themselves, they have been proposed to offer a synergistic advantage to lignin degradation when combined with other enzymes above. [78]

MnP, LiP, VP and laccases have all been shown to individually and concertedly to degrade lignin. However, fungal systems have as yet not given rise to any industrial processes for lignin remediation. This has partly been due to over efficiency[79] and partly due to limitations in the stability of the enzymes to the desired reaction conditions, particularly to pH.[21] There are also practical difficulties in genetic manipulation of fungi. This has drawn our attention towards bacterial lignin degraders, as they occur in a wide range of ecological niche environments, and are more amenable to genetic manipulation.

1.6 Bacterial degradation of lignin

A number of studies have shown bacteria can directly degrade lignin,[41, 80] but there has been little work on the enzymology of this process. Prior to the current study, only one enzyme from bacteria has been purified and conclusively shown to degrade lignin.[81] However, a broad range of bacteria have been shown to degrade lignin, as summarised in Table 3.[41, 80, 82, 83, 84, 85, 86, 87] These strains have predominantly been identified through use of laborious radiochemical assays. It can be seen that the majority of strains so far identified are Actinomyces, with two other clusters of strains focused around Bacillales and γ-Proteobacteria. It has been proposed that there is another cluster of degrading organisms among the α-Proteobacteria.[88] However, these degraders have yet to be confirmed.

Organism	Reference	Organism	Reference
γ-Proteobacteria		**Actinomycetes**	
Pseudomonas		*Nocardia*	
Pseudomonas spp.	41	*N. autotrophica*	72
P. ovalis	41	*N. corallina*	72
P. putida	75	*N. opaca*	72
Other γ-Proteobacteria		*N. asteroides*	72
Xanthomonas	43	*N.globerula*	72
Acinetobacter	43	*Streptomyces*	
Aeromonas	43	*Streptomyces sp.* EC22	74
γ-proteobacterium JB	78	*S. albus*	79
Bacillales		*S. badius*	41
B. megaterium	43	*S. cyaneus*	41
Aneurinibacillus aneurinilyticus	76	*S. rosusu*	41
Paenibacillus sp.	77	*S. viridosporus*	41
Bacillus sp.	77	*S. griseus*	74
Actinomycetes		*S. phaechromogens*	74
Actinomadura	41	*Saccharomonospora viridis*	74
Arthrobacter spp.	41	*Thermomonospora fusca*	74
Corynbacterium	41	*T. mesophila*	41
Mycobacterium	41	**Other Bacteria**	
Rhodococcus	41	*Flavobacterium*	41

Table 1.3 Literature reports of lignin degrading bacteria. To be included the bacteria had to have shown some aptitude for breaking down whole lignin not just model compounds. Note that some bacterial strains show varying activity in different papers.[80, 83, 89]

There have only been two bacteria studied in great detail for their ability to degrade lignin: *Streptomyces viridosporus*[81] and *Sphigomonas paucimobilis SYK-6*.[90]

S. viridosporus produces an extracellular lignin peroxidase, called LiP.[8]1 The amount of protein purified was very small and silver staining was needed to visualise it on gels. SDS-PAGE allowed the mass of the protein to be estimated as 17'800 Da. However, no sequence data or kinetic characterisation is available for this enzyme.[81] The lignin degrading ability of the protein was assessed by studying the breakdown products formed from model compounds and by observing the increase in turnover of hydrogen peroxide in the presence of lignin and lignocelluloes. Lignin degradation by *S. viridosporus* is much less susceptible to changes in nitrogen concentration than fungal degradation: an advantage of a bacterial system. [81]

LiP has been shown to degrade lignin to low molecule weight lignin fragments, which precipitate from solution with the addition of acid referred to as acid perceptible polymeric lignin (APPL). Yields of APPL are unfortunately low at 0.5% by weight.[91] UV light induced mutations have been shown to produce strains of Streptomyces that give higher yields 0.8%.[92] A study of the chemical composition of APPL from *S. viridosporus* showed that it had been substantially demethylated, dearomatised and oxidised at a number of benzylic carbons.[93]

A series of other bacteria have been investigated in the attempt to identify thermophilic lignin degrading strains including *Saccharomonospora viridis*

BD127, *Streptomyces sp.* EC22 and *Thermomonospora fusca* BD25. All of these strains showed some ability to produce APPL. *T. fusca* BD25 produced the most, approximately double that of *S. viridosporus*. Of particular note was the optimum temperature and pH, which were 60^{o}C and 7 respectively.[82] *T. fusca* has recently been subject to analysis by high throughput isobaric tag for relative and absolute quantificaiton (iTRAQ) with LC/MS/MS. This method allows the quantification and identification of extracellular proteins in the supernatant. When *T. fusca* was grown in the presence of lignocellulose, there was induction of cellulases, hemicellulases and transport proteins. High levels of novel Dyp-type peroxidases were reported as well as the presence of superoxide dismutase.[94]

One of the strangest examples of lignin degradation reported is with *Xanthomonas sp* strain 99. This bacteria was assayed with radioactive lignin of different sizes, those lignins of lower size gave a greater release of lignin. The assay was carried out over fourteen days and after this time some lignin remained in each case but no more ^{14}C labelled CO_2 was being released, a sign that the remaining lignin was resistant to degradation. Further analysis showed that the bacteria degraded only lignin fragments between the weights of 600-1000. The reason for this has not been fully investigated, but it was proposed that *Xanthomonas* could uptake small lignin fragments and then degrade them inside the cell. This is postulated to explain why so many bacteria show positive results in radiochemical studies when bacteria were commonly believed not to degrade lignin.[95]

In the same study it was reported that pre-treatment of the lignin samples with crude fungal supernatant from *P. chrysosporium* containing enzymes like LiP increased the molecular weight of lignin.[95] This is consistent with other observations by Haemerli *et al*[96] and shows that under some situation lignin degrading enzymes catalyse lignin polymerisation.

The down stream metabolism of lignin in *S. paucimobilis* SYK-6 has been extensively studied.[90] In this bacteria a very different mechanism is used to degrade lignin dimers than that reported in the fungal system. In this case the α carbon is oxidised by the enzyme LigD, and then cleaved by glutathione transfer by LigE,F and G. This is shown in Figure 1.26.[90] This same set of proteins has been shown to degrade synthetic lignin *in vitro*, however, *S. paucimobilis* SYK-6 has failed to show lignin degrading abilities.

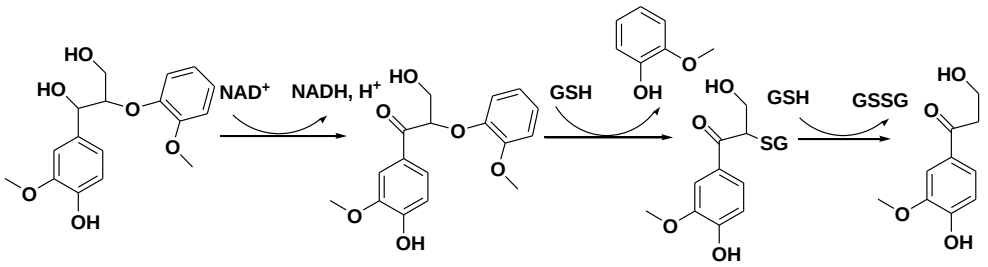

Figure 1.26 The oxidation of β-aryl lignin dimer and subsequent cleavage via glutathione transfer catalysed by LigEFG. Abbreviations: NAD, nicotinamide adenine dinucleotide; GSH, glutathione; GSSG, glutathione disulfide.

A full pathway for the degradation of lignin dimers has been proposed, illustrated in Figure 1.27, and many of the key proteins and the corresponding genes have been identified.[90, 97] Of particular interest is the identification of LigV that is responsible for the conversion of vanillin to vanillic acid.[97] The understanding of the molecular genetics of downstream lignin degradation has

allowed the cloning of *ligAB* and *ligC* genes of *S. paucimobilis* SYK-6 into *P. putida*, where they were shown to lead to the production of 2-pyrone 4,6-dicarboxylc acid (PDC) on a 10g/L from protocatechuate.[98] PDC has been shown to be polymerisable into a number of useful materials.[99, 100, 101, 102, 103] By including a lignin derived moiety, the polymer often gained better properties such as increased biodegradability.[103]

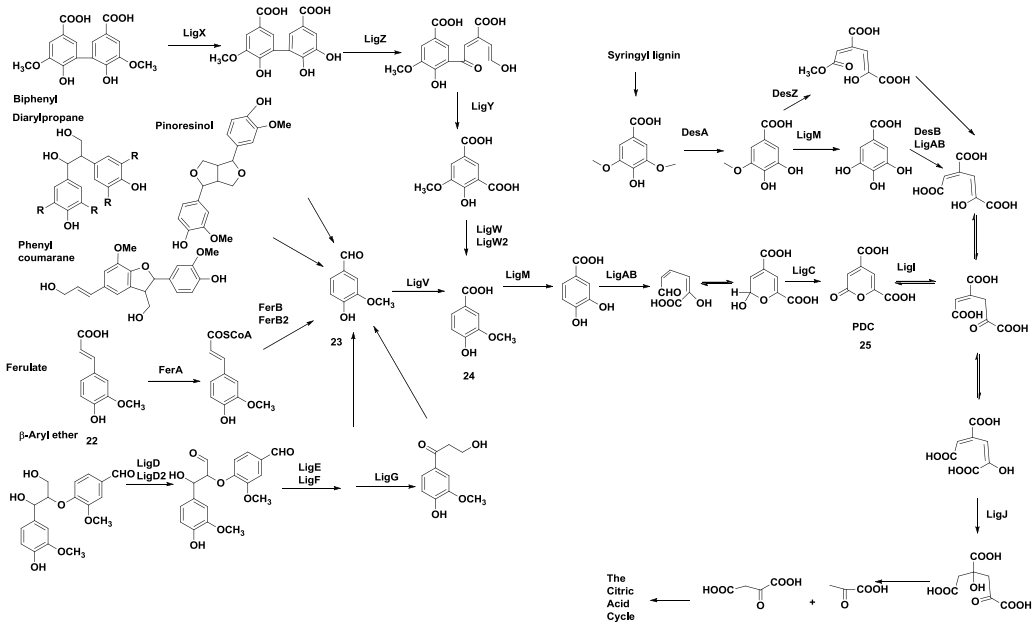

Figure 1.27 Catabolic pathway for degradation of lignin by *S. paucimobilis* SYK-6.[90, 97]

In *S. coelicolor* and *S. viridosporus* there is an alternative downstream pathway for breakdown of lignin derived compounds: this is the β-ketoadipate pathway, shown in Figure 1.28. This pathway has been shown to be induced by 4-hydroxybenzoate and protocatechuate.[104] The action of enzymes from the β-ketoadipate is consistent with the observed changes in lignin after it has been partially degraded to APPL by *S. viridosporus*.[93]

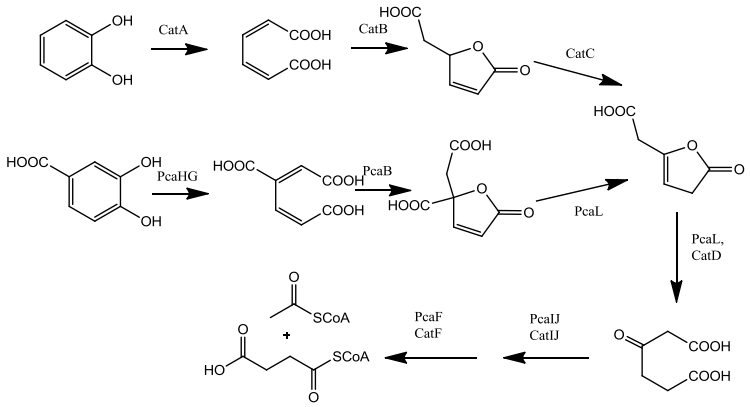

Figure 1.28 β-ketoadipate pathway.[104]

A laccase from the alkali tolerant *γ-proteobacterium* JB has been purified and shown to be active on a number of small aromatic monomers. The enzyme was shown to work at an optimal temperature of 55^{o}C and be stable after 60 days over a pH range of 4-10.[86] The enzyme has been shown to be able to decolourise dyes such as indigo carmine as well as soda pulp.[86, 105] The bleaching of soda pulp requires the removal of residual lignin from the cellulose fibre and is an important part of paper production.[106] Treatment with the laccase was found to reduce the need for hypochlorite by 10% without any reduction of paper quality. The greatest limitation on the process is that it needs 2,2'-azino-bis(3-ethylbenzthiazoline-6-sulphonic acid (ABTS) as a mediator, which is not cost effective on an industrial scale. The effectiveness of the laccase in industrial bleaching is indirect evidence of lignin degrading abilities, however, further studies are needed to confirm this. [105]

Bacterial laccases are on the whole less well studied than those in fungi but they are still widespread. In a recent study, over 100 different bacterial laccase sequences were identified from DNA that had been isolated from forest soil.[107]

However, not all of these will be active on lignin as bacterial laccases generally have a lower redox potential. However, it may be possible to rectify this by directed evolution.[21]

Bacteria seem to have potential to be powerful tools in lignin breakdown. However, this capacity has not been fully realised due to lack of good assay methods.[108, 109] Assays for lignin degradation will be fully discussed in Chapter II. Bacteria seem to have the potential to offer a degree of control over the products formed from lignin. A good example of this potential is the work done on PDC with *S. paucimobilis* SYK-6.[98] This highlights the capacity of lignin to provide a renewable source for unsaturated compounds. There are a number of compounds that are currently of commercial interest that could be sourced from lignin through a bio-refinery.

1.7 Industrially relevant compounds from lignin

The molecules shown below are of considerable interest for being sourced from lignin. In the case of vanillin **22**, guaiacol **24** and ferulic acid **26** there are already substantial markets developed. Vanillic acid is of interest as a potential feedstock from which other chemicals can be produced and 4-hydroxy benzaldehyde has the potential for use as polymer feedstock and can be used as a flavour compound.[110, 111]

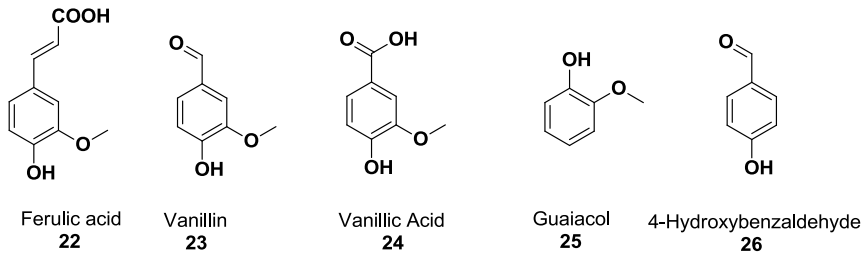

Figure 1.29 Small aromatic molecules of interest for acquisition from sustainable sources. Ferulic acid **22**, vanillin **23**, vanillic acid **24**, guaiacol **25** and 4-hydroxybenzaldehyde **26**.

Vanillin is the number one aroma chemical, as measured by tons used per year.[112] It is heavily used in the food and flavour industry, for example in products such as ice cream. Natural vanillin is produced from the vanilla bean and can cost $1800 /lb, whereas synthetic vanillin costs $7/lb. Hence, synthetic vanilla is used in most cases.[112] Production of vanillin from lignin by biotechnology would allow it to be marketed as 'natural' and this would offer a considerable commercial advantage. Such a process seems distinctly possible, as vanillin has been shown to be on the metabolic pathway for lignin.[90] However, current attempts by chemical and genetic intervention have not given high yields of lignin.[113] This may be because vanillin itself is toxic to many micro-organisms and thus they have multiple methods for assuring it does not accrue. This is one of the reasons why there has been interest in vanillic acid. This compound can be a potential precursor for production of vanillin by chemical and biological means and is less toxic to the cell. It has been already shown that *Aspergillus fumigatus* can produce vanillin from vanillic acid in 72% yields over 112h.[113]

Currently, vanillin is produced from guaiacol or lignin. The production from lignin is by chemical degradation and has been used since 1937 but in recent

years changes in pulping practice has meant that the sulphate waste stream needed for this process has become less available and so its use has decreased.[112]

Ferulic acid **22** has been shown to be produced from bacterial degradation of lignin.[114, 115] It is an antioxidant chemical, which can have a variety of uses.[116] It can be used as a feedstock in bioconversion by *Amycolatopsis* sp. and *S. setonii*, which can produce vanillin in commercially attractive yields.[113] Ferulic acid is of interest for its self by having potential anti-cancer properties,[117] potential as a cardiovascular drug[118] and potential use in skin care products as it reduces oxidative stress when topically applied.[119] Finally, it can be used as a food additive to cover bitter tastes.[120]

The main interest in guaiacol has been its use as a precursor for vanillin production and for production of eugenol another important flavour compound.[113] It can also be derivatised, as shown in Figure 1.30, to make commercially relevant drugs such as the expectorant Guaigensin part of a number of commercial cough remedies.[121]

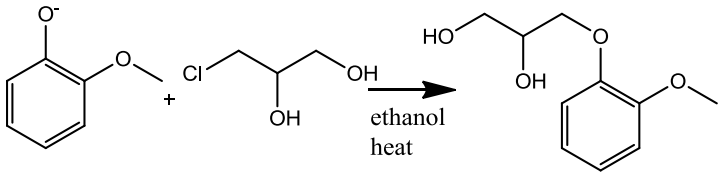

Figure 1.30 Synthesis of guaifensin.

Guaiacol and benzaldehyde can potentially be made from the corresponding benzoic acid via decarboxylation as illustrated in Figure 1.31. The

bioconversion of vanillic acid by *Nocardia sp.* NRRL 5646 to give guaiacol proceeds at a yield of 69%.[122] Since vanillic acid is a key compound on the breakdown pathway of lignin it seems reasonable to hypothesis that guaiacol could be produced from lignin.

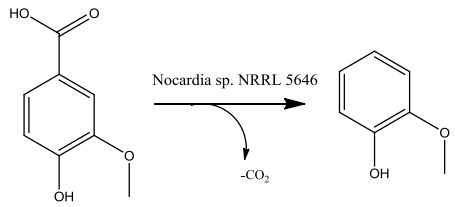

Figure 1.31 Vanillic acid and other aromatic acids could be decarboxylated to give guaiacol and related products.

In addition to monoaromatics lignin can provide a source of partially degraded polyaromatics. Such waste lignin streams from chemical processes have already been used to make high quality plastics for applications such as childrens toys.[123]

Lignin represents a potential source of useful aromatic compounds if its degradation can be controlled. It is hypothesised that bacteria and their enzymes have the ability to do this. This PhD will focus on investigating this process.

1.8 Aims of the project

This project was part of a larger collaboration with Warwick Manufacturing Group and Horticultral Research Institute called Wealth Out of Waste (WOW). The aim of the project is to develop methods for a microbial treatment of lignin, which produces renewable chemicals.

My PhD aims to develop the fundamental tools needed to investigate the bacterial degradation of lignin, through providing methods to assay lignin breakdown by both bacteria and proteins. It aims to provide methods for analysing and identifying products formed by micro-organisms when they degrade lignin with a particular focus on chemicals which are of industrial interest.

The aim of this project is to develop methods for high throughput assaying of lignin degradation by using fluorescent and nitrated lignin. These assays will allow identification of new bacterial lignin degrading strains and the breakdown products from these organisms will be identified. Lignin degrading enzymes will be purified and characterised from strains of interest and they will be applied to lignocellulose.

CHAPTER II: Synthesis of lignin model compounds

2.1 Introduction

Dimeric lignin model compounds have been used to study the molecular mechanism of fungal peroxidases and laccases.[44] Three variations of the β-aryl ether linked dimer, compounds **27**-**29**, a biphenyl dimer **31** and the coumaryl dimer **32**, were chosen to be synthesised. These dimers, illustrated in Figure 2.1, were chosen as they represent some of the most common lignin structures. β-aryl ether linkages make up around 50%, biphenyl units contribute another 10-11% and the phenylcoumaran 9-12%.[15] The aim of synthesising these molecules was to use them as standards when studying lignin degradation and as enzyme substrates in later studies (Chapter VI).

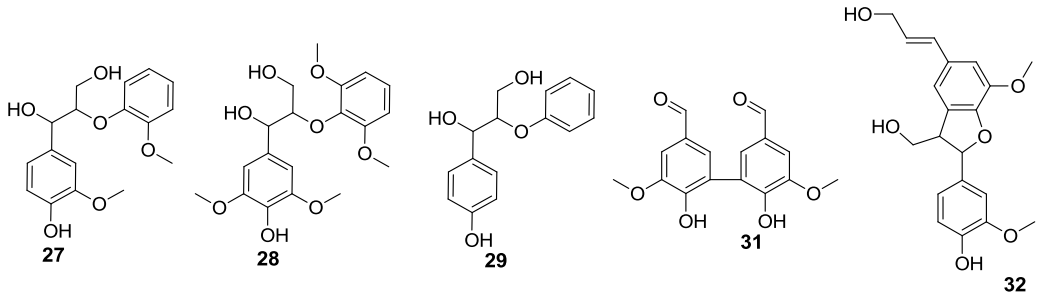

Figure 2.1 Lignin dimers, from left to right, 2-(2-methoxyphenoxy)-1-(4-hydroxy-3-methoxyphenyl) 1,3-propanediol **27**, 2-(2,6-dimethoxyphenoxy)-1-(4-hydroxy-3,5-dimethoxyphenyl)-1,3-propanediol **28**, 1-(4-hydroxyphenyl)-2-phenoxy-1,3-propanediol **29**, 3,3'-dicarboxaldehyde, 6,6'-dihydroxy-5,5'-dimethoxy-1,1'-biphenyl **31** and 2,3-dihydro-2-(4-hydroxy-3-methoxyphenyl)-5-(3-hydroxy-1-propen-1-yl)-7-methoxy-3-Benzofuranmethanol **32**.

In addition to lignin dimers, two lignin breakdown products were also synthesised. These are shown in Figure 2.2. Compound **33** is of interest because

it has been hypothesised to be a breakdown product from compound **27**, Figure 2.3.[82] Compound **34** was synthesised to help characterise the nitrated lignin formed in chapter III and to be used as a standard in analytical studies of the breakdown of nitrated lignin. The three different β-aryl ether lignin dimers that are synthesised are the product of the homocoupling of the three different lignin monomer feedstock types.

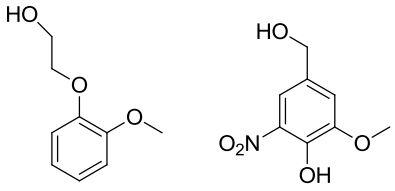

Figure 2.2 Possible lignin breakdown products compound **33** and **34**.

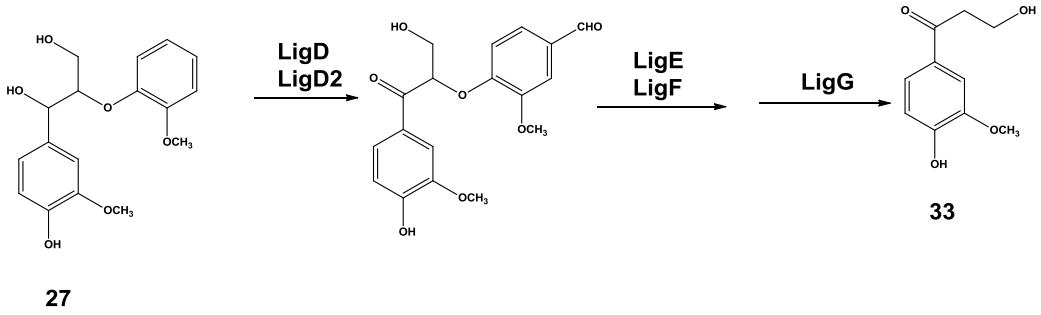

Figure 2.3 Possible breakdown route for β-aryl ether dimer **27** via compound **33.**[82]

2.2 Synthesis of β-aryl ether lignin dimers

There are two literature methods by which the β-aryl ether lignin dimer can be synthesised. The earliest of these methods was developed by Adler, and is a linear synthesis that proceeds through the bromination of acetovanillone, followed by displacement of the bromide by guaiacol, then a one carbon extension by reaction with formaldehyde, followed by a ketone reduction and deprotection.[124] The newer method is a convergent synthesis developed by

Nakatsubo where the key reaction is a crossed aldol. The Nakasubo route has less steps and a high overall yield, 72%.[125] The two methods are summarised in Figure 2.4.

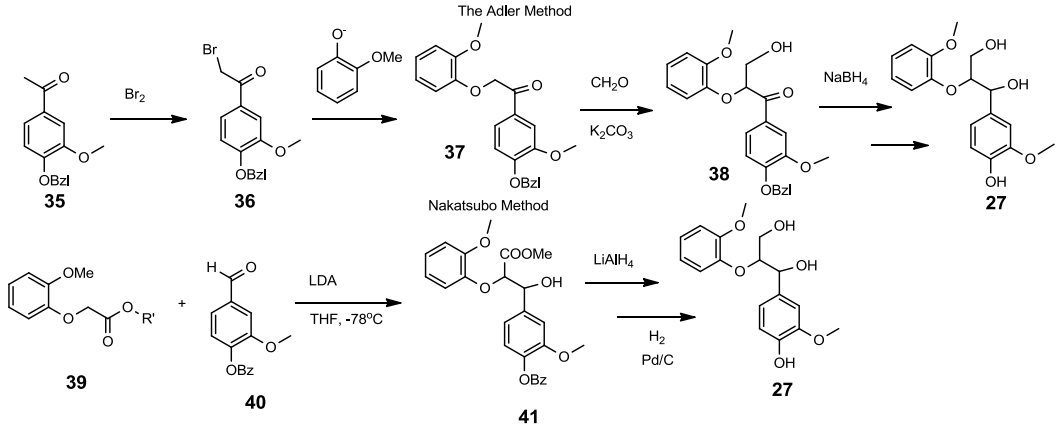

Figure 2.4 The Adler and Nakatsubo methods of synthesising β-aryl ethers.[126]

In both methods diastereomeric purity is important. Two diastereomer isomers can form, at the adjacent chiral centers on the propyl backbone. These are the *erythro* and *threo* diastereomers. The terms *erythro* and *threo* are derived from sugar chemistry and there is a degree of conflict in how they are used in the literature. Here the definitions of B. Davis and A. Fairbanks will be used.[127] For an *erythro* isomer one can draw the Fisher projection of the molecule so that the highest priority group on both chiral centres are on the same side. In the case of the *threo* isomer the two highest priority groups are on different sides. In the case of the β-aryl ethers the *erythro* isomer corresponds to the S,R diastereomer and the *threo* isomer to the R,R. Figure 2.5 summarises the *erythro* and *threo* diastereomers. In lignin both diastereomers are present as a mixture.[22]

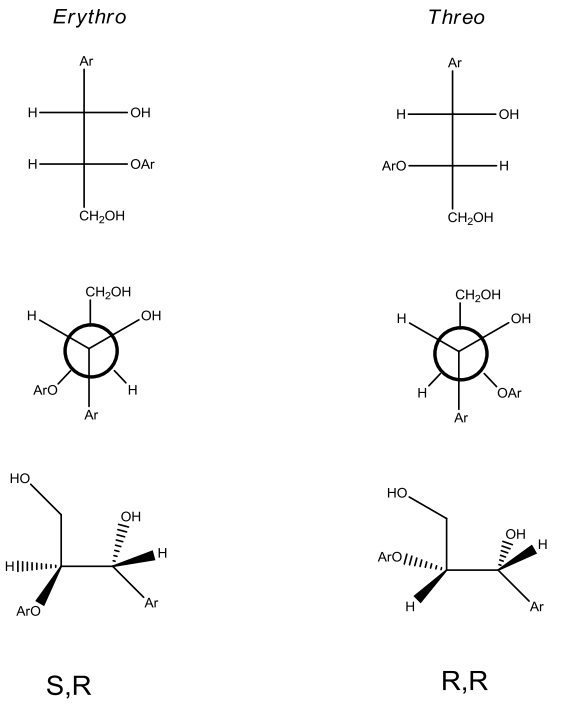

Figure 2.5 The Fisher, Newman and CIP assignments for a general structure. Ar = aromatic ring similar to those seen in Figure 2.1

First the route of Adler was explored. Benzoylation of acetovanillone with pyridine and benzoyl chloride using the method of Crestini and D'Auria giving a yield of 63%.[128] However, the method of Erdtman,[129] using a smaller ratio of pyridine to acetovanillone the yield increased to 86%.

The second step of the Adler method is a mono bromination of methyl ketone. The literature method used 1:1 $CHCl_3$: CCl_4 as solvent, at 5^oC for twenty minutes and then gradual heating to 40^oC. Due to the extreme environmental toxicity of carbon tetrachloride, the reaction was run in chloroform, but a mixture of products was obtained, shown by mass spectrometry to contain di- and tri-brominated products. The method was then carried out in acidic conditions, using either HCl or acetic acid, but with no heating in either case. However, in these cases no product was formed. Consideration of the

mechanism lead to the development of a new method where aluminium chloride (0.1 eq) was used to activate the bromine (1 eq) and the product was formed in a 72% yield. At this point it was decided to abandon the Adler route, as the methods reported in the literature could not be easily repeated and more success had been obtained using the Nakatusbo route.

The Nakatsubo route is shown in Figure 2.6 along with the yields achieved.

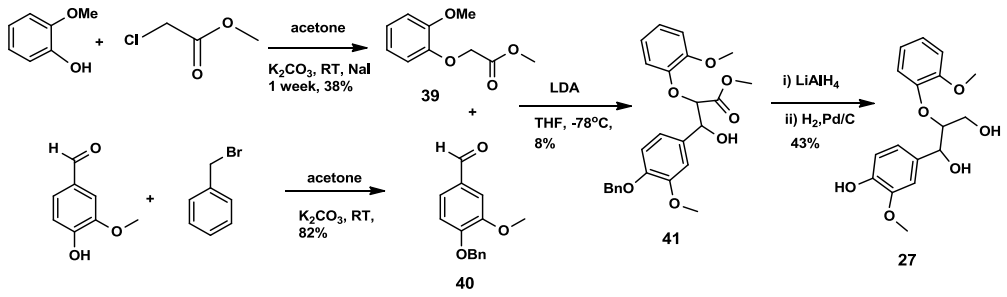

Figure 2.6 The Nakatsubo synthesis for compound **27** and the yields achieved

Firstly, vanillin was protected with a benzyl group, in acetone with potassium carbonate in 82% yield. The derivatisation of guaiacol with methyl chloroacetate went in only 38% yield, due to the production of a large amount of inorganic salt, which required vigorous washing to separate from the product.

The crossed aldol reaction that lies at the heart of the Nakatsubo is synthesis,[125] in this reaction compound **39** and **40** are mixed at -78^{o}C with LDA. The product was purified by silica column chromatography and two diasteomers proved difficult to separate. The yield of 8% was low, but this was because a significant amount of material was lost in the purification.

The crossed aldol reaction preferentially forms the *erythro* product. The reaction begins by formation of the lithium enolate. Two enolates are possible the E and the Z. Presuming a chair style transition state as postulated for other metal catalysed aldol reaction,[130] the Z enolate would go on to form the *erythro* product whilst the E would give the *threo*. In the formation of compound **41** it seems likely that both enolates would form but that the Z enolate would react faster as it would proceed by a lower energy transition state giving the a preference towards the *erythro* product. The threo product would be disfavoured as it places the bulky aryl ether group axial where there is more steric hinderance. This is illustrated in Figure 2.7.

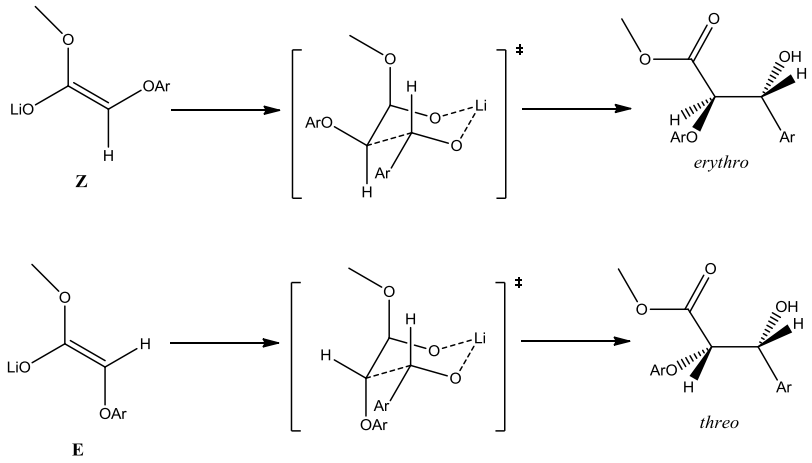

Figure 2.7 Formation of *threo* product from the E-enolate leads bulky aromatic group being place axial making the transition state higher in entergy. Ar = aromatic ring.

The final product **27** was formed by reduction of the ester with lithium aluminium hydride and debenzylation with H_2 and Pd/C. A low yield of 43% was initially obtained, because the product was prone to sticking to the palladium on carbon. When synthesising subsequent analogues yields were considerably improved by including several additional washings of the catalyst

after the debenzylation was finished. The original method of Nakatsubo was further adapted for the reduction, by heating the reaction to 60^{o}C. The heating allowed the reaction to be carried out in one hour rather than three. In the workup dry ice is added to produce an inorganic salt. Dilution prior to this was found to improve the yield as less product was lost when filtering. The final product was achieved with the *erythro* isomer in a diastereomeric excess (d. e). of 72%.

2.2.1 Synthesis of b-aryl ethers: 2-(2,6-dimethoxyphenoxy)-1-(4-hydroxy-3,5-dimethoxyphenyl)-1,3-propanediol, 28 and 1-(4-hydroxyphenyl)-2-pehnoxy-1,3-proapanediol, 29

Two other analogues of the β-aryl ether where there were either two or no methoxy groups joining the aromatic ring, compounds **28** and **29**. These syntheses are summarised in Figure 2.8.

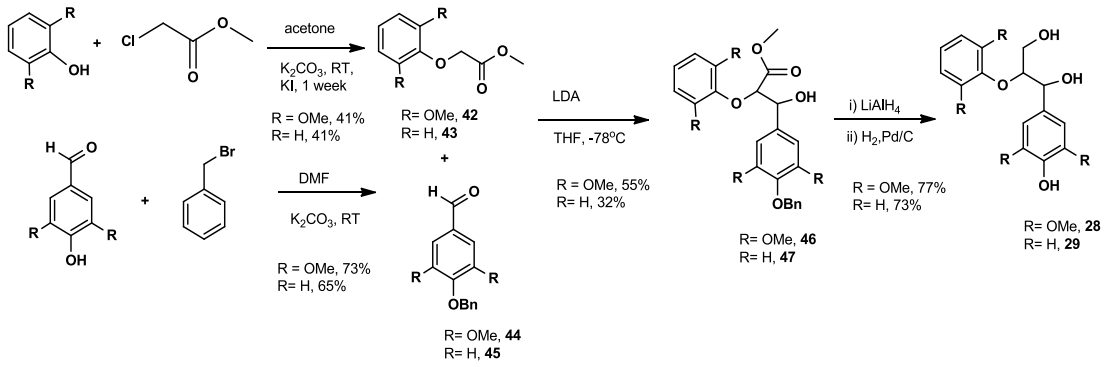

Figure 2.8 Synthesis of compounds **28** and **29**.

For both of the analogues the synthesis was similar to that detailed above, however, the benzylation step was carried out in DMF, in order to more fully solublise the reaction mixture. The DMF was subsequently removed by forming

an azeotrope with dichloromethane. In both cases the yields were lower than those seen in the synthesis of compound **27**.

The crossed aldol reaction was carried out as before but with four hours less stirring after the starting materials were mixed. This was suggested by the method of Sipilä and Syrjänen.[126] The yield was much higher than my previous attempt 55% for compound **46** and 32% for compound **47**. In the case of **46** the *erythro* isomer could be enriched by flash silica column to a d.e of 82%. In the case of compound **47** the *erythro* compound could be crystallised allowing it to be produced pure.

Compound *erythro*-**46** was found to have a strange proton spectrum with an unexpected sharp doublet at 4.54 ppm with a coupling constant of 7.3 Hz. The coupling for the peak at 4.87 ppm was also 7.3 Hz. Suggesting, that these two peaks are coupling partners. It is proposed that this extra peak is from H_{17} illustrated in Figure 2.9. The large coupling constants are generated by this proton forming an intramolecular hydrogen bond with the carbonyl group of the ester. The proton spectrum for the propyl backbone for both diastereomers of compound **46** is summarised in Table 2.1.

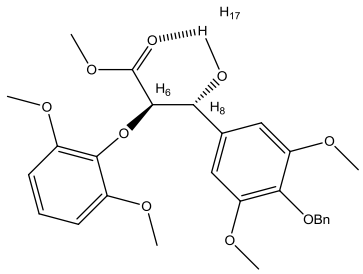

Figure 2.9 The intramolecular hydrogen bond found in compound **46.**

Erythro				*Threo*			
Assignment	Shift	Multiplicity	Coupling Constant (Hz)	Assignment	Shift	Multiplicity	Coupling Constant (Hz)
H_{17}	4.54	d	7.3	H_6	5.13	d	18.5
H_6	4.65	d	3.9	H_8	5.31	d	18.3
H_8	4.87	dd	3.9 + 7.3	H_{17}	Not Seen		

Table 2.1 Table of key ^{1}H NMR peaks and coupling constants for *erythro* and *threo* isomersof compound **46.**

When the NMR sample was shaken with d_4-methanol, as describe in the Experimental section 8.2.10, this greatly reduced the intensity of the doublets at 4.54 and resolved the doublet of doublets at 4.87 to a doublet. This is illustrated in Figure 2.10. The reason for the change in the spectrum is that H_{17} can now exchange with the deuterium from the methanol and thus become NMR silent. The deuterium shake allowed peak 4.54 to be assigned as H_{17} , this then lead to the assignment of its coupling partner at 4.87 as H_8 and finally the peak at 4.65 as H_6. In the *threo* compound a similar set of peaks with even larger coupling constants was observed.

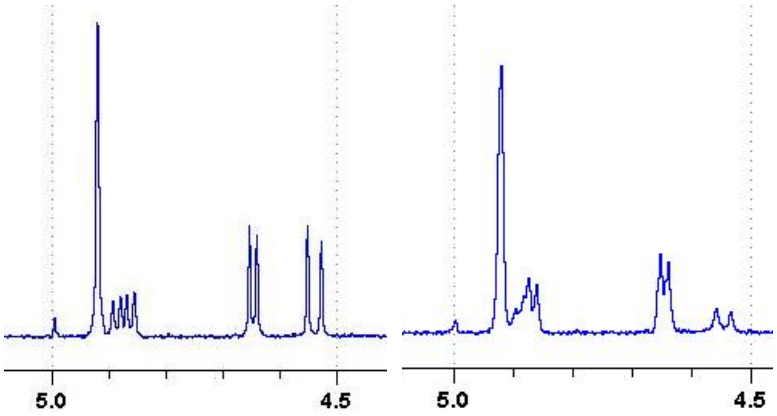

Figure 2.10 Left hand side^{1}H NMR spectrum for compound **46** between 5 and 4.5 ppm before being shaken with d_4-methanol. Right hand side 1H NMR spectrum for compound **46** between 5 and 4.5 ppm after being shaken with d_4-methanol. The intensity of the doublet at 4.54 ppm is reduced and the splitting of the doublet of doublets at 4.87 ppm has resolved towards a doublet.

This suggests that rotation is restricted along the propyl chain, this could once again be caused by an intramolecular hydrogen bond or it may be an example of rotational isomerism. In cases of restricted rotation the dihedral angel has a significant effect on the coupling constant observed. The relationship between the dihedral angle and splitting is given by the Karplus equation, Equation 1.

$$^{3}J = J^{0} \cos^{2} \phi - 0.28 \ (0^{o} \leq \phi \leq 90^{o})$$

$$^{3}J = J^{180} \cos^{2} \phi - 0.28 \ (0^{o} \leq \phi \leq 90^{o})$$

Equation 1 The Karplus equation. Where J^{0} and J^{180} are constants that depend on the substitution of the carbon atom.

If one builds a model of the *erythro* and *threo* isomers it can be seen that the *threo* isomers has a much smaller dihedral angle between H_6 and H_8, as illustrated in Figure 2.10 This eclipsed position gives rise to extreme coupling as predicted by equation 1 as here theta would be close to zero. In the *erythro* isomer the smaller but still considerable coupling constant of 7.3Hz comes from H_{17} demonstrated by the fact that it is removed by shaking with deuterated methanol. Once again the restricted rotational motion leads to a large coupling constant but in this case theta is closer to 60^{o} giving a smaller coupling constant than seen in the *threo* isomer. The structures of the two diastereomers is shown in Figure 2.10. H_{17} cannot be observed in the *threo* isomer presumably because it exchanges with the solvent, this argues against the existence of an intramolecular hydrogen bond as these hydrogens are generally harder to exchange. However, its difficult to see how the large coupling constants reported for the *threo* isomer could be formed without the adoption of a

staggered conformation which would only happen in the case of a hydrogen bond. Even with this explanation the coupling constant is larger than the theory would predict.[131]

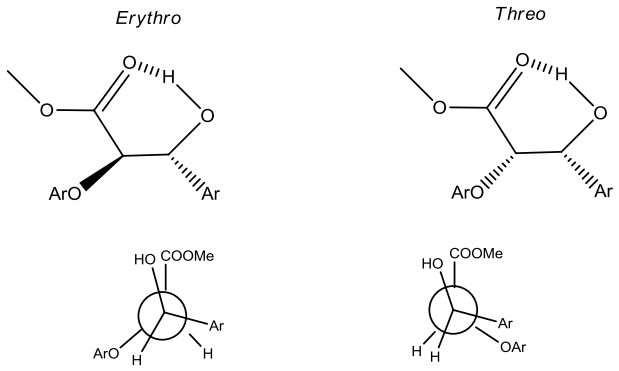

Figure 2.11 Illustrating that for the *erythro* and *threo* isomers in an eclipsed confirmation assuming the existence of an intramolecular hydrogen bond. Ar = aromatic ring.

The final step went in good yields following a method analogous to that given above to give compound **28** in 77% yield and compound **29** in 73%.

2.3 Synthesis of biphenyl lignin dimer, 3,3'-dicarboxaldehyde, 6,6'-dihydroxy-5,5'-dimethoxy-1,1'-biphenyl, 31

The biphenyl compound was synthesised by a literature procedure[132] by boiling vanillin in water with $K_2S_2O_8$ and $FeSO_4$. This gave the product as an insoluble brown solid. Two key pieces of evidence for the product being formed was the lack of doublets in the aromatic region of the spectra and the observation of a mass spectrum ion of 205 m/z corresponding to the MNa^+ for the dimer. The mechanism for this reaction probably proceeds via a phenol radical coupling.

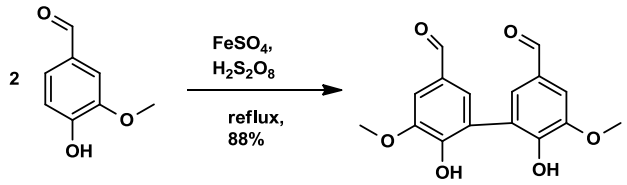

Figure 2.12 Synthesis of biphenyl dimer, compound **31**.

2.4 Synthesis of coumaryl lignin dimer, 2,3-dihydro-2-(4-hydroxy-3-methoxyphenyl)-5-(3-hydroxy-1-propen-1-yl)-7-methoxy-3-Benzofuranmethanol, 32

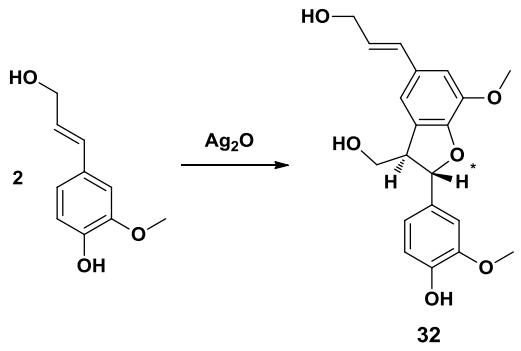

Figure 2.13 Synthesis of coumaryl lignin dimer, **32.**

A small amount (yield = 0.6%) of the coumaryl lignin dimer was synthesised by the silver (I) mediated coupling of two coumaryl alcohol units as reported in the literature.[18] A single disastereomer was isolated by HPLC. To investigate the stereochemistry of two chiral centers on the benzofuran ring an NOE difference experiment was carried out on the doublet of 5.43 ppm that corresponds to H^*. No effect was then seen in the rest of the spectra suggesting that the two protons

of the benzofuran ring are not near each other in space. This means the trans isomer was formed.

2.5 Synthesis of 2-(2-methoxy-pehnoxy)ethanol, 33

Compound **33** was synthesised as an authentic standard for use in analytical studies of lignin degradation. Using the protected intermediate **41** for compound **27**, shown below, as a starting point, compound **33** was formed by lithium aluminium hydride reduction, in 98 % yield.

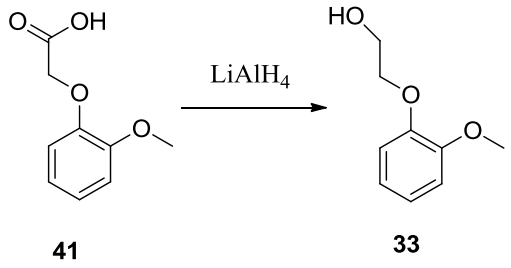

Figure 2.14 Synthesis of compound **33**.

2.6 Synthesis of nitrovanillic alcohol compound 34

Nitrovanillic alcohol was synthesised to help characterise the nitrated lignin formed in Chapter III and was used as an authentic standard when studying the breakdown of nitrated lignin. Nitrovanillin was reduced with sodium borohydride in basic aqueous solution at room temperature.[133] A number of different alcohols were tried as the solvent for this reaction but the starting material was poorly soluble in them. The final yield of the reaction was 65%.

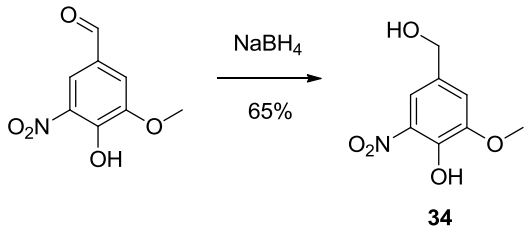

Figure 2.15 Synthesis of nitrovanillic alcohol, **34.**

2.7 Conclusion

Organic synthesis has been used to form a number of useful molecules that can now be used to help study lignin degradation. With these tools further analysis by spectroscopy, HPLC, LC/MS and GC/MS were made possible. Five lignin dimers have been successfully formed as well as two other small molecules that were of interest.

Of the two synthetic methods for synthesising the β-aryl ether lignin dimers the Nakatsubo route was found to be the best. This route offered better yields and the reactions were readily accomplished. However, the route does not allow easy access to purified versions of the *threo* diastereomer, which can be formed by the Adler synthesis.

CHAPTER III: Assays for lignin degradation

3.1 Introduction

Detailed studies of bacterial lignin degradation have been hindered by a lack of a convenient assay for lignin breakdown.[108, 109] Previously there have been a number of methods in the literature: these have used a mixture of techniques but none have allowed easy and accurate assessments of a bacteria's lignin degrading abilities. They have also been either inappropriate or unreliable when used on protein samples, hampering efforts to purify lignin-degrading enzymes.

One method of screening is to grow micro-organisms on agar plates which contain either an aromatic dye or lignin. For the aromatic dyes the micro-organism should give a clear ring around it if it degrades lignin.[134] Dyes can also be used in liquid culture and the decolourisation observed relative to a standard.[135] If lignin is used in the agar then the plate needs to be stained with a 1:1 ratio of 1% $FeCl_3$: $K_3[Fe(CN)_6]$, but once again a clear area is produced around the growth of lignin degrading micro-organisms.[136] These methods are cheap but it takes ten days to grow the plate to see if there is an effect and it is only qualitative. The major limitation is there is often poor correlation between dye degrading abilities and lignin degrading ability.[133] Even in the lignin assay care needs to be taken as often industrial lignins are used, but these are already partly degraded and thus much easier for micro-organisms to degrade.

^{14}C-labelled lignin has been used to identify several degraders,[42, 137] however this method requires preparation of radioactively-labelled lignin and is then very

slow as radioactive CO_2 must be counted as it expired by the bacteria over one to two weeks.[42] The length of time required by the assay means that it is not amenable to use in large-scale screening, protein purification or kinetic studies. The strength of the assay is it is quantitative and as long as the radioactive label was on the core structure of the lignin, is unlikely to produce false positives. Although there is some debate about this in the literature as discussed in the introduction.[95]

There are a number of general peroxidase and laccase assays used in studying lignin degradation. These assays use a mixture of substrates including ABTS **48,**[86] guaiacol **49**,[138] and 2,4-dichlorophenol **50**.[81] Whilst these have the advantage of being fast and easy to use they are not specific to lignin and give many false positives as they only pick up general peroxidase or laccase activity. A large number of extracellular peroxidases or laccases does not necessarily correlate with high lignin degrading ability.[139] Consequently these assays are of little use for screening and protein purification, however, they can be of use for studying the kinetics of purified enzymes.

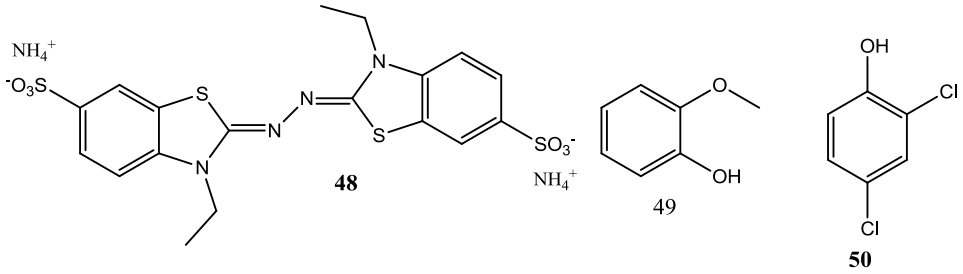

Figure 3.1 Structures for ABTS **48**, guaiacol **49** and 2,4-dichlorophenol **50**.

There is a stopped assay that reacts diazotised sulfanilic acid **51** with lignin to give a red colour. This can then be compared to a standard curve to give the amount of lignin in the solution.[109] This is a good method of quantifying the amount of lignin in a solution but as it is a stopped assay it is a laborious method of carrying out kinetics. It requires several days and a large growth of material to get a reading this makes it quite cumbersome for screening purposes.

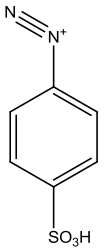

51

Figure 3.2 Diazotised sulfanilic acid **51**.

Fluorescent synthetic lignin has been prepared by the method illustrated in Figure 3.3 and used to analyse the ability of *Sphingomonas paucimobilis* to degrade lignin. This assay is very sensitive.[140] However, it does not use native lignin because synthetic lignin is often very different structurally, having less β-aryl ether linkages and more coumaryl linkages.[141]

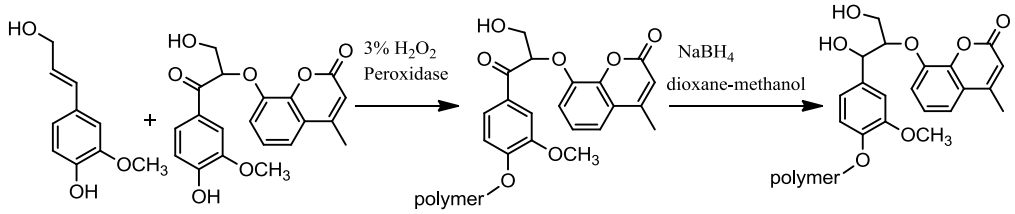

Figure 3.3 Enzymatic synthesis of fluorescent liginin incorporating a fluorophore.

The development of two new spectrophotometric assays for lignin breakdown will be described in this chapter. Both can be carried out on 96 well microtitre

plates, which allows for rapid screening of the lignin degrading ability of micro-organisms. The first assay involves the attachment of a fluorophore to the lignin polymer. Breakdown of the lignin by a degrading strain leads to a change in environment of the fluorophore, and hence an increase in fluorescence. The use of native lignin represents an improvement on the previous fluorescent lignin assay. The second assay involves chemically nitrated lignin – breakdown of the lignin structure then releases nitrated phenols, leading to an increase in UV/vis absorbance (see Figure 3.4).

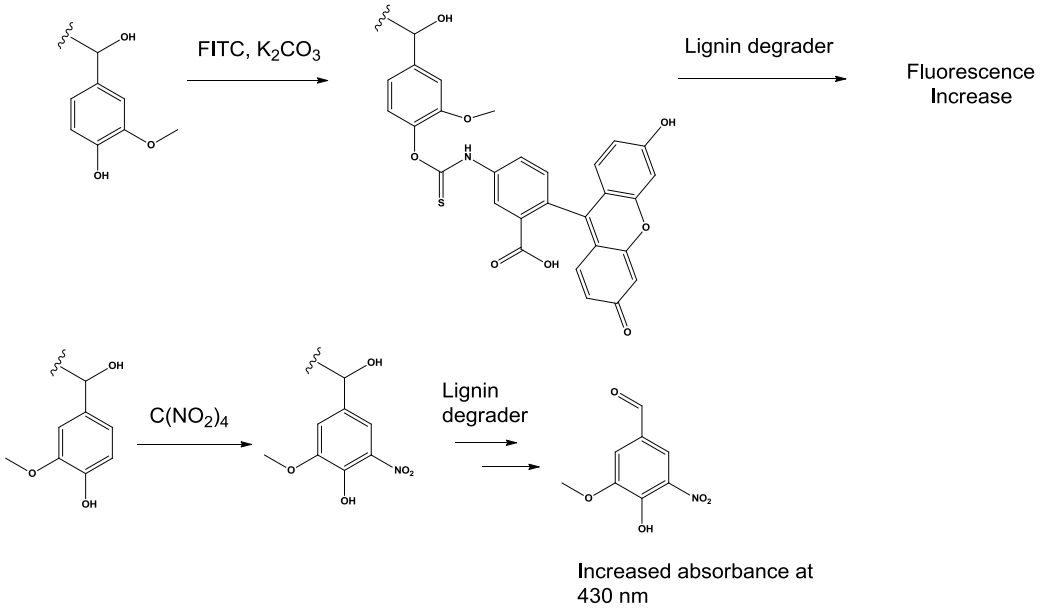

Figure 3.4 Top- Synthesis for fluorescent lignin. FITC is attached to lignin by reaction with phenolic hydroxyl group. Exposure to a lignin degrading microorganism gives an increase in fluorescence. Bottom- Tetranitro methane is used to nitrate lignin. When this nitrated lignin is exposed to lignin degrading micro-organisms an increase at 430 nm is observed due to release of nitrated lignin monomers. Only a representative lignin end unit is shown.

These assays have then been used to investigate both bacterial and fungal degradation of lignin, looking to identify new degraders and compare the

activity of the respective kingdoms. In addition the molecular specificity of different micro-organisms is also examined.

3. 2 Isolation of different lignins

Lignin from different plants have different structures it was hypothesised that such structural differences may lead to changes in how each lignin is degraded. To study the specificity of bacteria for lignin, three different types were isolated from natural sources. Lignin was purified from miscanthus, pine and straw. These three plants were chosen as they each represent a potential biofuel feedstock.[1]

Miscanthus, wheat and pine milled wood lignins were prepared as described in the literature by a series of milling steps followed by extraction into dioxane.[142] Milled wood lignin is defined as lignin that is first heavily milled to increase solubility before being extracted into dioxane. The process is thought to preserve the main elements of lignin structure whilst decreasing the length on the molecule sufficiently to allow material to be solublised.[143] First, the biomass was milled with a Willey mill to pass through a 4mm mesh to increase its density. This material was then washed with a 9:1 acetone: water mix to remove waxes and lipids. The resulting material was then rotary ball milled through an approximately 0.1mm mesh and then vibratory ball milled for 1 hour. The ball milling was done in 20-minute steps to avoid the material becoming too hot. The material was dispersed in 9:1 dioxane: water and stirred for one day. The extractant was then separated from the solid material with a sintered frit. The extraction was then with 1:1 dioxane: water. After this both extractions were

repeated. The combined extractants were then evaporated under reduced pressure to gave a solid brown crystalline product. Yields of 6, 3 and 1% were achieved for miscanthus, wheat and pine respectively. The yield was determined by dividing the amount of lignin recovered by the total starting mass and then multiplying by one hundred. The yield for the pine may have been less due to the fact it was harder and thus not milled as finely.

The lignins were studied by IR, ESI-MS and UV-visible spectrometry. Due to its complex heterogenous nature, lignin cannot be easily studied by NMR. The IR spectra were consistent with that of previously studied lignins, a characteristically sharper ether peak was seen for the pine lignin, illustrated in Figure 3.5.[144] This is because there are less ether environments in pine lignin, this is typical of the GS lignin found in soft woods. The wheat and miscanthus spectra were typical of HGS lignins with an additional peak in around 1130 nm. Fuller assignments of the IR spectra are given in the experimental.

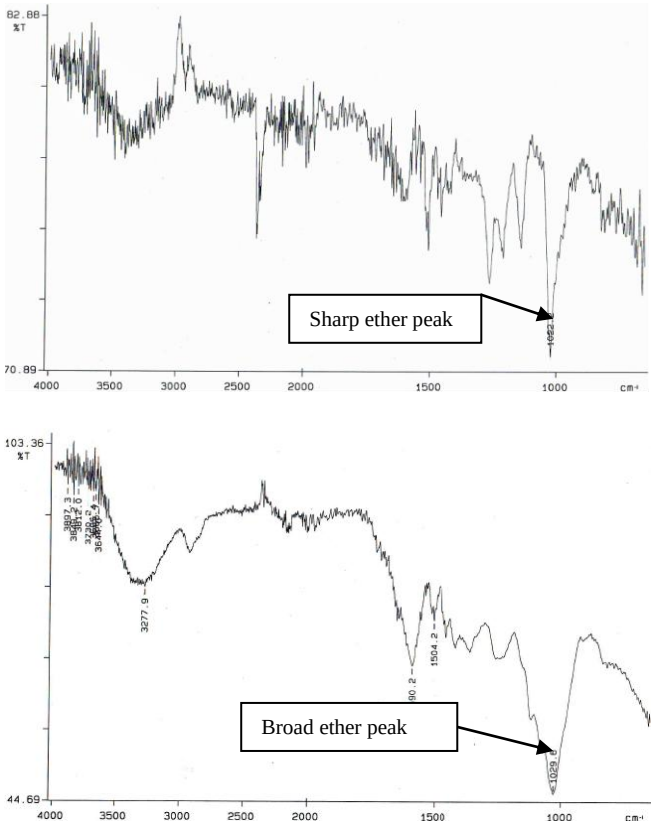

Figure 3.5 Top- The IR spectrum for miscanthus milled wood lignin with a sharp ether peak 1022 cm^{-1}. Bottom- The IR spectrum for Hereward wheat milled wood lignin with a broad ether peak at 1029 cm^{-1}.

UV-visible spectrometry showed a single peak at around 280nm for the three lignins, this is suggestive of aromatic rings. Mass spectrometry showed that there was a range of molecules of different sizes present with the average weight for the wheat lignin being 1539 *m/z*, for the miscanthus lignin 1451 *m/z* and for the pine lignin 1418 *m/z*. This confirmed that the lignin was still polymeric in nature.

3.3 Synthesis of fluorescent lignin

Prof. H. Dalton supplied some industrial lignin, unfortunately little was known about the source of this material or the method by which it was prepared, therefore it was analysed by IR and GPC was used. The IR spectrum had peaks at 1593, 1512 and 1250cm^{-1}; these were compared to the data gathered by O Faix[144] and seen to be characteristic of GS type lignin. Acquiring the GPC data was hindered by the poor solubility of the lignin, but a spectrum was obtained using PL-GPC 220 fitted with two PL PolarGel (300mm x7.5mm) columns in dimethyl acetamide. GPC showed that the lignin sample was polydisperse (Pdi =9.8) meaning that there were both long and short chains. The GPC data is summarised in Figure 3.6 where Mp is the mode weight, M_n, M_w, M_z, M_{z+1} are different ways of calculating the average molecular weight. The large difference between M_n and M_w is a consequence of there being a wide range of chain lengths in the sample. M_v corresponds to the molecular weight as determined by the viscosity of the sample.

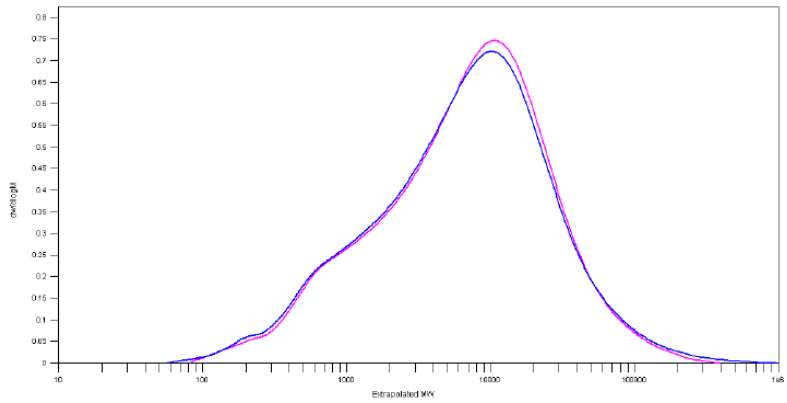

Sample Name	Molecular Weight Averages / g mol^{-1}						
	M_p	M_n	M_w	M_z	M_{z+1}	M_v	Pdi
Lignin	6528	1242	12145	51060	131586	9393	9.7786

Figure 3.6 The GPC data for the lignin provided by Prof. H. Dalton. The two lines represent two repeats. Mp is the mode weight, M_n, M_w, M_z, M_{z+1} are all types of average molecular weight and M_v corresponds to the molecular weight as determined by the viscosity of the sample. Pdi is the polydispersity index and is a measure of how different the chains are in length. GPC was acquired by polymer labs using a PL-GPC 220 fitted with two PL PolarGel (300mm x7.5mm) columns in dimethyl acetamide.

Fluorescent lignin was formed by mixing 5mg of lignin or kraft lignin in water with K_2CO_3. This allowed the majority of the lignin to be dissolved by deprotonating the phenolic hydroxyl groups. The rest of the suspended material was removed by filtration through cotton wool. After this 100 μl of 0.2 mM fluorescein isothiocyanate (FITC), 4(5)-iodoacetamido) fluorescein (IAF) or dansyl chloride was added. The resulting solution was left overnight after which the lignin was precipitated by addition of HCl. With the kraft lignin, as it is soluble even in acidified water, it was separated from excess fluorescent material by dialysis. Once the fluorescent lignin samples where formed and purified, the fluorescence was examined. The dansylated material did not show any increase in fluorescence therefore it was not continued to further studies. Both the FITC derivative (FITC-lignin) and the IAF derivative formed fluorescent lignin with excitation at 494nm and emission at 520nm. In both of

these cases there was an increase in fluoresecnce comparative to the underivatised material but only in the case of the FITC-lignin was this concentration dependent, as shown in Table 3.1. Thus, the FITC-lignin was carried on for latter trials.

	Volume (μl)		
	10	20	30
FITC-lignin	17306	25374	45314
IAF-lignin	10964	6564	5903
FITC-kraft	8170	7951	7894
IAF-kraft	8444	8534	8565

Table 3.1 The fluorescence of lignin and kraft lignin after reaction with FITC and IAF. All the measurements had a total volume of 200 μl. The fluorescence was determined with excitation at 494 nm and emission at 520 nm. Note only in the case of the FITC-lignin was the degree of fluorescence dependent on the amount of material added.

3.4 Application of fluorescent assay

The fluorescent lignin was then used to screen a series of micro-organisms for lignin degrading ability using a plate reader.

3.4.1 Whole bacterial cells

The FITC lignin (0.2 mg fluorescent lignin/ ml) was mixed with liquid culture of *Rhodococcus sp., Nocardia autotrophica, Pseudomonas putida, Bacillus subtillis, Escherichia coli DH10B, Rhodococcus erythropolis, Leuconostoc mesenteroides* grown overnight and the change in fluorescence was observed over two hours with excitation at 494 nm and emission at 520 nm using a 96 well plate reader.

With the liginin-FITC there was no change with *L. mesenteroides*. There was a time dependant increase in fluorescence with the other bacteria, in the magnitude of 500-1000 AFU. These are summarised in Figure 3.7. The data presented in Figure 3.3 has been treated by having the control, where no bacteria was present subtracted from each fluorescent reading. All of the subsequent fluorescent data is treated in the same way. The data are treated because there is a natural quenching of the fluorophore verses time in the assay.

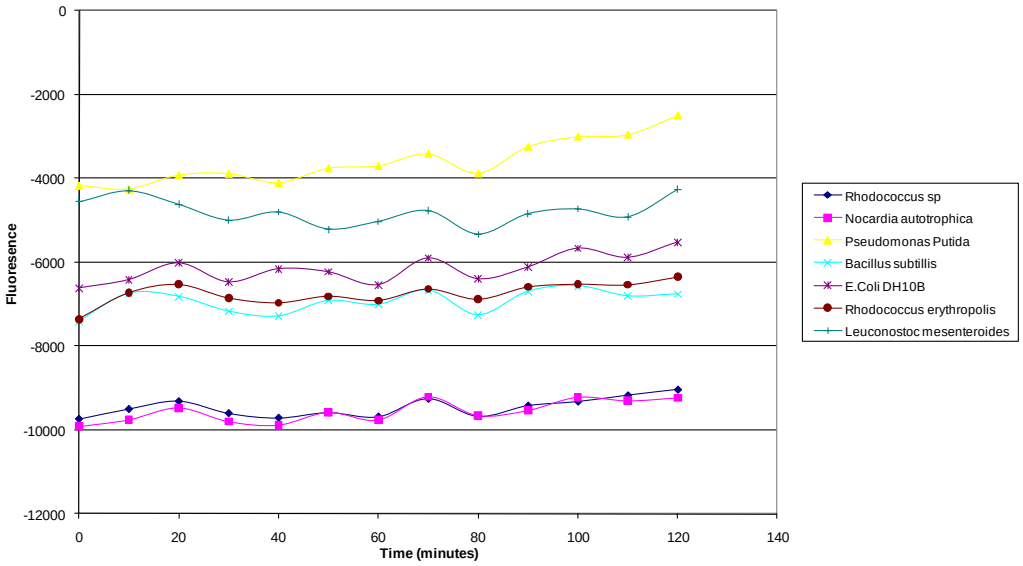

Figure 3.7 Changes in fluorescence with whole cell culture over two hours with FITC-lignin. FITC-lignin (0.2 mg fluorescent lignin/ ml) was mixed with bacterial cell culture (30 µl) and hydrogen peroxide (2 mM) the fluorescence was observed with excitation at 494 nm and emission at 520 nm.

For the approximatly first thirty minutes, there is no increase in fluorescence, as shown above, a possible explanation for this is lignin might first be adsorbed onto the surface of the bacteria. After thirty minutes a time dependent increase in fluorescence is observed which is interpreted as the result of lignin being broken down.

3.4.2 Whole bacterial cells with different concentrations of hydrogen peroxide

Many fungal systems that degrade lignin have been shown to use peroxidases,[68] thus the assays above was repeated with 5mM, 1mM, 0.1 and 0 mM of H_2O_2 solution. The data showed that activity was preserved even when no hydrogen peroxide was added. This observation can be rationalised by the hypothesis that cells can produce the hydrogen peroxide they need themselves. Alternatively the activity could be caused by lignin degrading enzymes that do not use hydrogen peroxide. Some loss of activity was seen at 5mM for all of the bacteria other than *P. putida*, which had previously shown activity. This loss of activity at high concentrations of hydrogen peroxide is probably due to enzymes involved being inhibited. The activity for *P. putida* is shown in Figure 3.8.

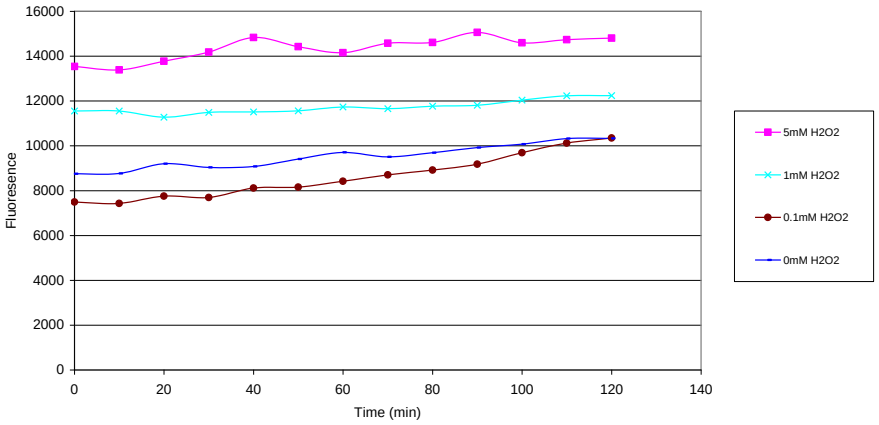

Figure 3.8 Changes in fluorescence with whole cell culture over two hours with FITC-lignin and *P. putida*. FITC-lignin (0.2 mg fluorescent lignin/ ml) was mixed with *P. putida* cell culture (30 µl) and various hydrogen peroxide (5 mM, 1mM, 0.1 mM and 0mM) the fluorescence was observed with excitation at 494 nm and emission at 520 nm. For *P.putida* an increase in fluorescence was seen at all hydrogen peroxide concentrations.

3.4.3 Concentration and time dependence of *P. putida* supernatant

P. putida gave the highest fluorescence change in studies with whole cells (Figure 3.7) therefore it was selected for further study. Previous work by Crawford et al.[81] has shown that *S. viridosporus* uses an extracellular peroxidase for lignin breakdown. To investigate whether the reaction we were observing was extracellular and to remove any complications caused by having cells in the assay mixture the liquid culture was spun for four minutes at 10000 rpm. After this the supernatant (30 μl) was taken and used in the assay with FITC-lignin (0.2 mg fluorescent lignin/ml) and hydrogen peroxide (2 mM). An increase of around 1000 AFU was observed over two hours. This increase was also proportional to protein concentration. This is shown in Figure 3.9 and 3.10. This strongly suggests that the fluorescence increase is due to an extracellular enzyme.

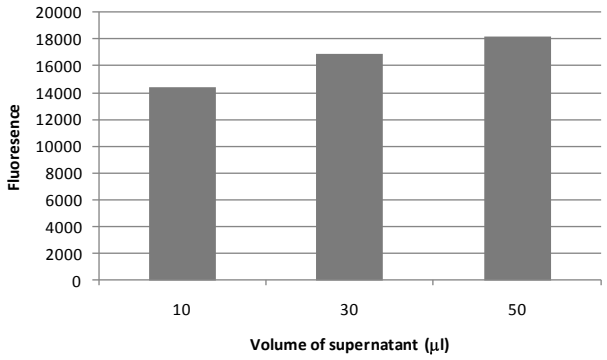

Figure 3.9 Fluorescence vs volume of *P. putida* supernatant added, in two hour assay. FITC-lignin (0.2 mg fluorescent lignin/ ml) was mixed with *P. putida* supernant (10, 30 and 50 μl) and hydrogen peroxide (2mM) the fluorescence was observed with excitation at 494 nm and emission at 520 nm.

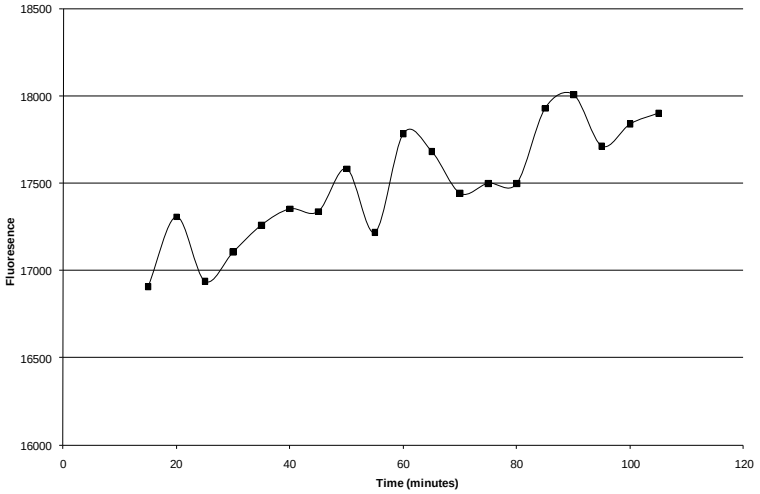

Figure 3.10 Time dependent increase with FITC lignin and *P. putida*. FITC-lignin (0.2 mg fluorescent lignin/ ml) was mixed with *P. putida* supernatant (30 μl) and hydrogen peroxide (2mM) the fluorescence was observed with excitation at 494 nm and emission at 520 nm measurements were taken over two hours.

3.4.4 Bacterial supernatants screened for lignin degrading ability

With the assay method developed in **3.4.3**, *S. viridosporus, B. subtilis, P. putida, Rhodococcus jostii* RHA 1, *Rhodococcus sp., N. autotrophica* and *L. mesenteroides* supernatants were assayed for their lignin-degrading ability. There was an increase in fluorescence of up to 600 units for the known degraders of *S. viridosporus,*[81] *P. putida,*[83] *Rhodococcus sp.,*[41] *N. autotrophica*.[80] An increase of around 250 units was also seen for *R. jostii* RHA1, consistent with it being a lignin degrading micro-organism. This micro-organism had not been previously studied for lignin degrading activity but is a known poly chlorinated biphenyl (PCB) degrader and its genome has been sequenced.[145] *L. mesenteroides* and *B. subtilis* showed a decrease in fluorescence. There are two possible explanations: firstly that as the fluorescent lignin is diluted by the other reagents you get a decrease in fluorescence; or if

there was any left over cellular residue that could stick to the lignin and decrease fluorescence. The data for this assay is summarised in Figure 3.11.

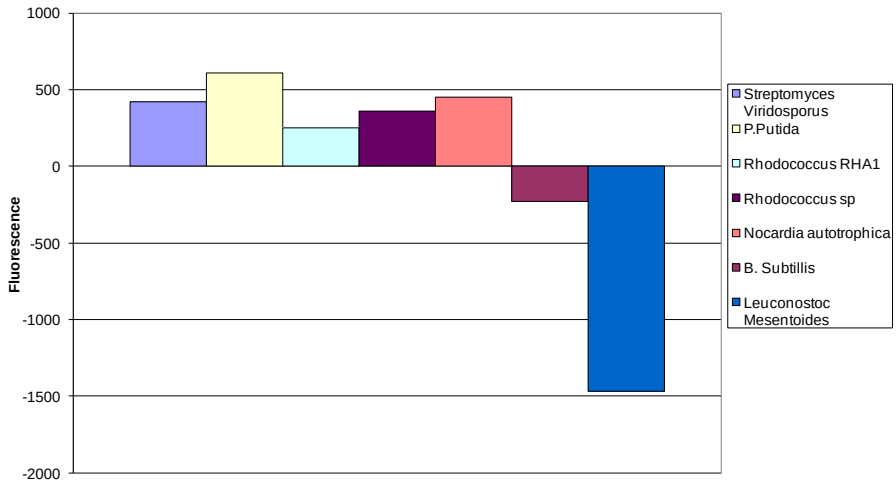

Figure 3.11 Bar chart showing the change in fluorescence over the first 10 minutes. FITC-lignin (0.2 mg fluorescent lignin/ ml) was mixed with bacterial supernatant (30 µl) and hydrogen peroxide (2mM) the fluorescence was observed with excitation at 494 nm and emission at 520 nm over ten minutes.

The above assay was repeated without any hydrogen peroxide present. For *S. viridosporus* the increase in fluorescence was reduced and for *N. autotrophica* no increase was not observed at all. *P. putida, Rhodococcus jostii RHA1* and *Rhodococcus sp*. were unaffected by the presence of H_2O_2. This can be seen in the following figure.

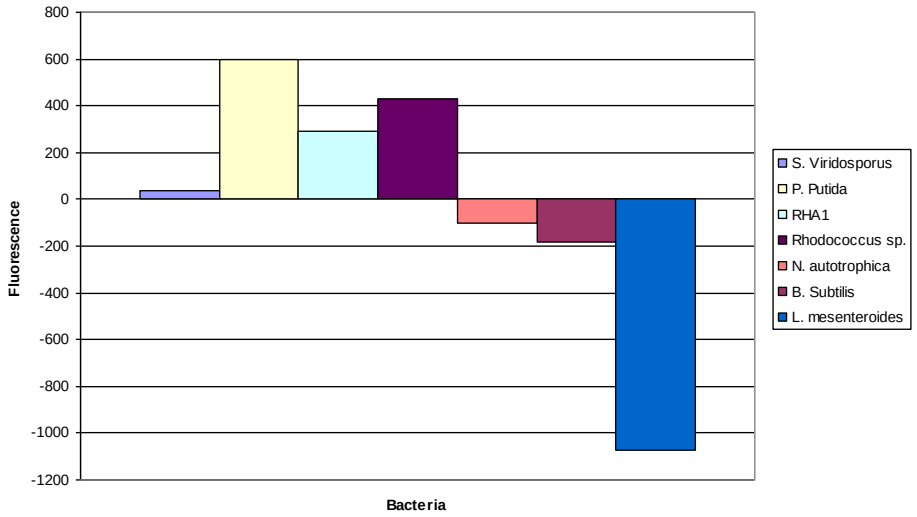

Figure 3.12 Bar chart showing change in fluorescence over the first ten minutes when no hydrogen peroxide is available. FITC-lignin (0.2 mg fluorescent lignin/ ml) was mixed with bacterial supernatant (30 μl) the fluorescence was observed with excitation at 494 nm and emission at 520 nm over ten minutes.

Where lignin degradation is dependant on hydrogen peroxide it suggests peroxidases are involved in the breakdown process. In the other cases degradation must either involve other enzymes that do not require hydrogen peroxide e.g. laccases or there are extracellular enzymes that produce hydrogen peroxide. An alternative explanation is that there may be enough hydrogen peroxide intrinsically in the assay to provide some activity. Considering that the assay is carried out with cell supernant this does not seem likely.

It should be noted in none of our assays with the supernatant did we observe the initial lag in fluorescence increase. This was only seen with the whole cells. This supports the hypothesis of the lignin being adsorbed onto the cell surface.

3. 5 Synthesis of nitrated lignin

An attempt was made to functionalise the milled wood lignins with FITC, however, this was unsuccessful. Whereas treatment of the industrial lignin with FITC gave a precipitate, treatment of the milled wood lignin gave no precipitate. Attempts to assay any lignin retrieved from the process gave no increase in fluorescence, when the material was mixed with bacterial supernatant and hydrogen peroxide.

Therefore the milled lignins were nitrated with tetranitromethane following an analogous procedure for that used to nitrate tyrosine residues in proteins.[146] The material was characterised by IR, UV-visible and mass spectrometry. The nitration could be seen to clearly take place by the emergence of a new peak at 350 nm in the UV-visible spectrum. The degree of nitration for each lignin was estimated from the extinction coefficient of 5-nitrovanillyl alcohol (λ_{340} = 1134 mol dm^{-3} cm^{-1}) calculated from the Beer-Lambert law. The degree of nitration and the average M_r determined by ESI for each lignin is given in Table 3.2. The degree of nitration was estimated by calculating the concentration of lignin from absorbance at 280nm, which is proportional to the number of aromatic rings and calculating the concentration at 340nm, which is proportional to the amount of nitrated aromatic rings. Hence the ratio of these two number gives the ratio of nitrated to un-nitrated rings.

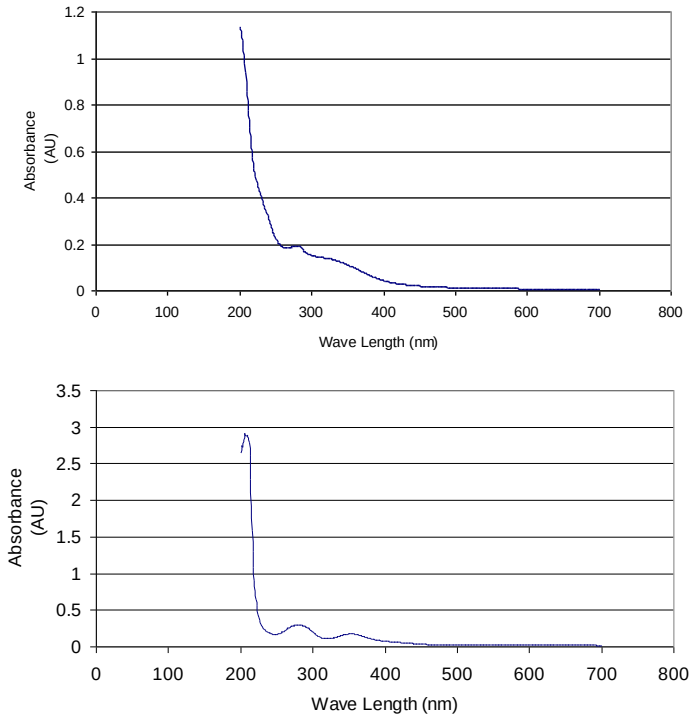

Figure 3.13 Top- UV-visible of lignin from miscanthus (0.02mg/ml); Bottom- miscanthus nitrated lignin from miscanthus (0.01mg/ml) a new peak been seen around 340 nm.

Lignin	Mass by ESI	Absorbacne @340 nm	Concentration estimated from absorbance at 340 nm	Absorbance @280 nm	Concentration estimated from absorbance at 280 nm	Nitration ratio ($concentration_{340}$/ $concentration_{280}$)
Wheat	1449	0.111	9.79E-05	0.0358	1.41E-05	7.0
Miscanthus	1472	0.220	0.000194	0.0530	2.08E-05	9.3
Pine	1529	0.250	0.000220	0.0595	2.34E-05	9.4

Table 3.2 Approximate mass and degree of nitration of milled wood lignins. A molality 0.0125 mg/ml was used for the concentration estimates by UV-visible spectroscopy.

Further evidence for nitration was gathered by IR spectroscopy where peaks at around 1636, 1540 and 1383 cm^{-1} appeared in each of the lignin samples. The peak at 1636 is broad and composed of two bands caused by O=N-O. The peaks at 1540 and 1383 are caused by the symmetric and anti symmetric stretching of $C\text{-}NO_2$.

3.6 Ascertaining the concentration and time dependence of nitrated lignin assay

Treatment of the nitrated lignin with bacterial supernatant in pH 7.4, 750mM Tris buffer with 2 mM H_2O_2 solution gave a time dependent and concentration dependent change in absorbance at 430nm. Initially a high buffer concentration was used by mistake, but later attempts to vary the concentration lead to inconsistent data. The increase is in the magnitude of 0.002 AU over twenty minutes. These results are shown below.

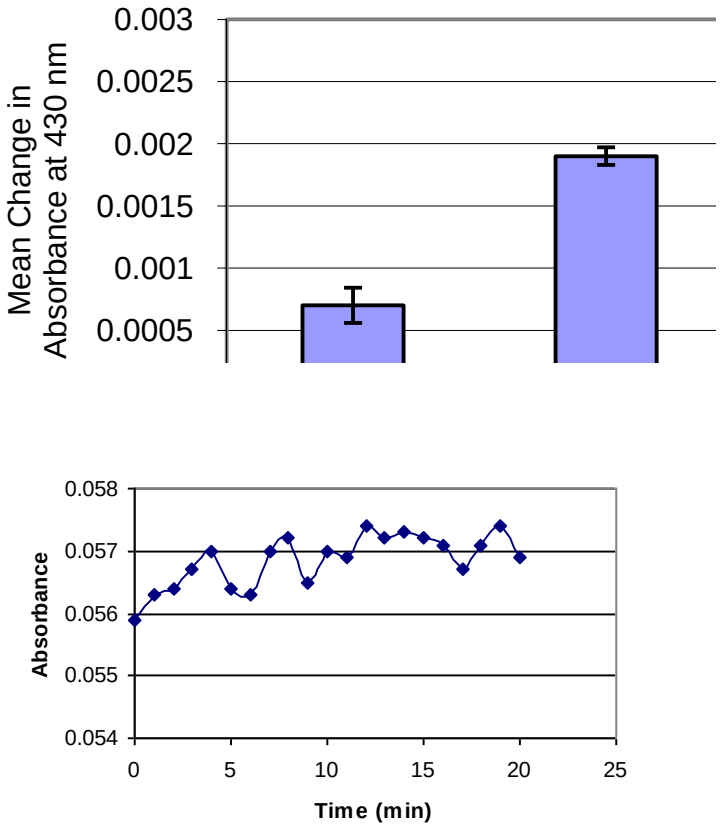

Figure 3.14 Top- Concentration dependence of UV-visible assay based on amount of supernatant added. Bottom- Time dependence of UV-visible assay. Results are for nitrated wheat straw with *P. putida*. For both graphs nitrated lignin (0.01 mg/ml) was mixed with *P. putida* supernatant (30 μl) in the presence of hydrogen peroxide (2 mM).

This suggested that the nitrated lignin was being degraded to small nitrated molecules that then absorb more strongly at 430nm.

In order to examine the molecular basis for the observed changes in absorbance, 5 ml cultures of *Rhodococcus jostii* RHA1, *P. putida*, *S. viridosporus*, and *B. subtilis* were grown in the presence of 0.04mg/ml nitrated MWL overnight, and the resulting solution was analysed by reverse phase HPLC. A number of new peaks with absorbance at 430nm were observed. In the case of *S. viridosporus*, a large peak was observed at retention time 4.8 min, which showed the same retention time and UV-vis spectrum as an authentic sample of 5-nitrovanillin. A smaller peak at the same retention time was observed in the case of *Rhodococcus jostii* RHA1. Treatment with *B. subtilis* showed no new peaks, compared to control samples while RHA1 and *P. putida* produced a number of other peaks absorbing at 430nm. For *P. putida* these had a retention time of 3.6, 10 and 26.5 minutes. For *R. jostii* RHA1 new peaks were at 8.6, 11.5, 30.2 and 35.0 minutes.

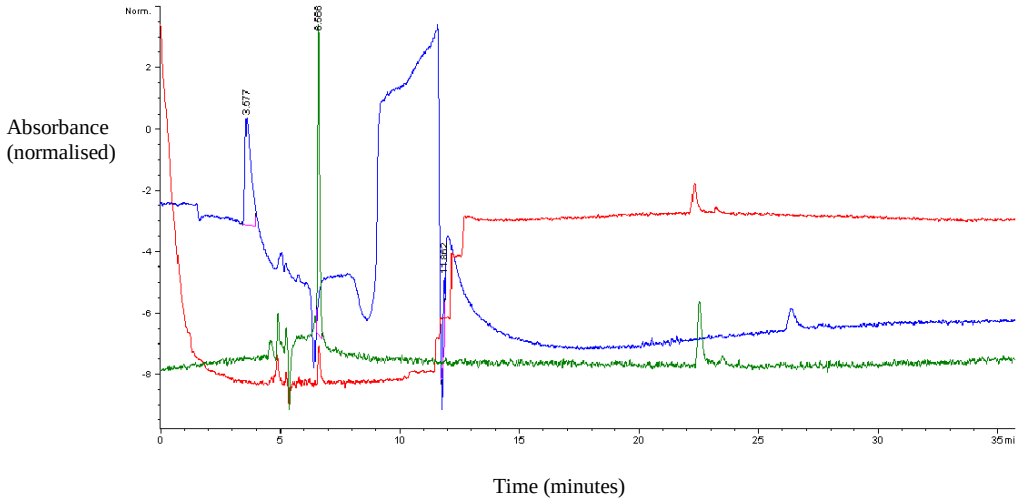

Figure 3.15 HPLC trace for breakdown of nitrated lignin (0.04mg/ml) by *P. putida* grown in LB for 24 hours, shown in blue. In red is the HPLC trace for *P. putida* grown in LB with no lignin and in green is the HPLC trace lignin in LB with no *P. putida* present. In all cases looking at 430 nm.

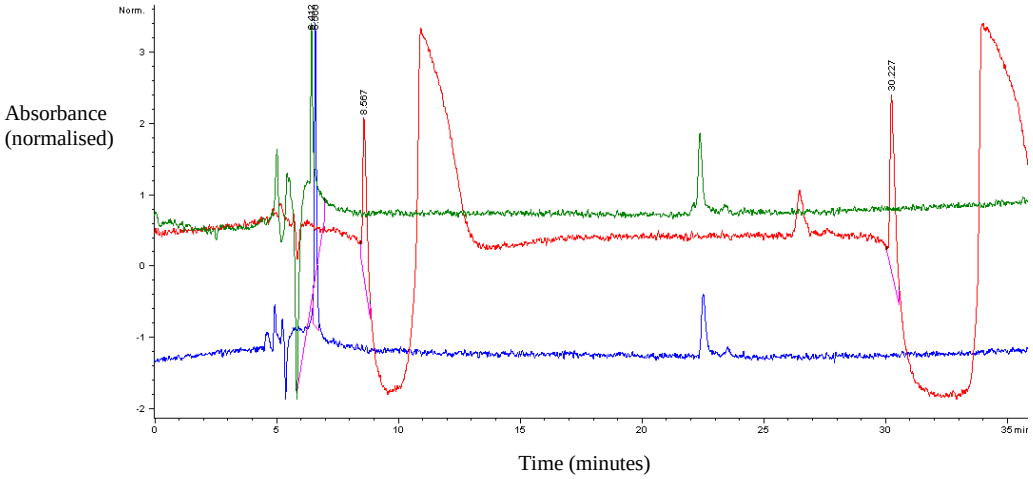

Figure 3.16 HPLC trace for breakdown of nitrated lignin (0.04 mg/ ml) by *R. jostii* RHA1 grown in LB shown for 24 hours shown in blue. Shown in red is the HPLC trace for R. jostii RHA1grown in LB and in green is the HPLC trace for lignin in LB with no bacteria present. In all cases looking at 430 nm

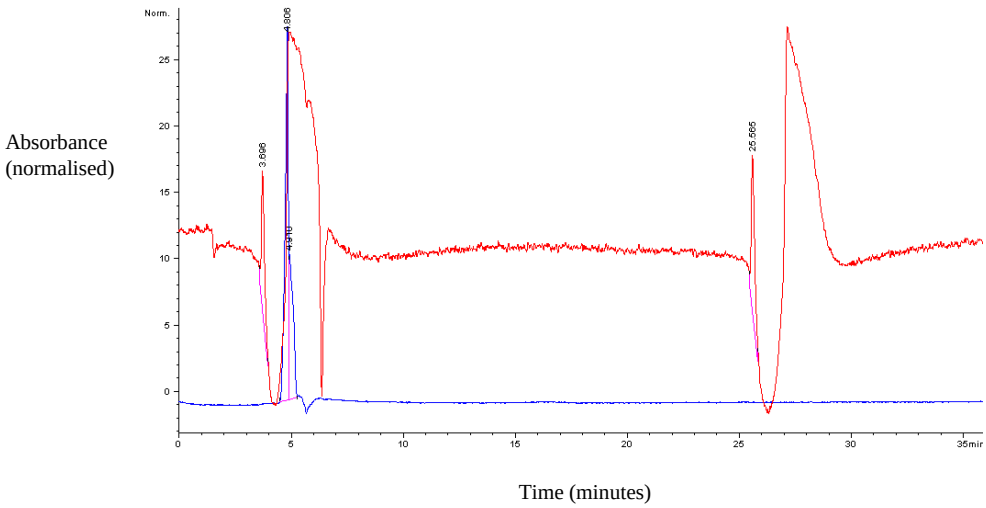

Figure 3.17 HPLC trace for *S. viridosporus* with nitrated lignin (0.04mg/ml) grown in LB for 24 hours shown in red. HPLC trace for nitrovanillin shown in blue. In both cases observing at 430nm.

In order to verify that the observed absorbance changes were not due to degradation of cell wall carbohydrates, cellulose and glucose were both subjected to the same nitration conditions, and the treated samples were incubated with cultures of *Rhodococcus jostii* RHA1 and *P. putida*. In neither case was any change in absorbance at 430 nm observed over 20 min in the presence of a lignin degrader.

Different pHs where studied to see if they had an effect on the nitated lignin assay. At both pH 9.0 and 4.7 no consistent increase could be observed for known degrading strains. This could be due to the fact that the enzymes involved in lignin breakdown generally prefer acid pHs and thus become inactive under alkali conditions. The lignin assay itself does not work under acid conditions, as it needs to create a nitrophenolate anion to have a strong absorbance at pH 7 due to the delocalisation of the charge.

3.7.1 Application of the nitrated lignin assay to screen bacterial supernatants for lignin degrading activity

The nitrated lignin assay was first tested on the same set of bacteria as the fluorescence assay and the results are shown in Figure 3.18. Absorbance increases were observed for four lignin degraders (*S. viridosporus*, *P. putida*, *Rhodococcus* sp., *Rhodococcus jostii* RHA1). No increase was seen with the non-degraders *L. mesenteroides* (shown on the the far righ hand side of Figure 3.17) and *B. subtillis*. *N. autotrophica* also gave no absorbance increase with miscanthus MWL, but, with that exception, the assay was able to distinguish lignin degraders from non-degraders.

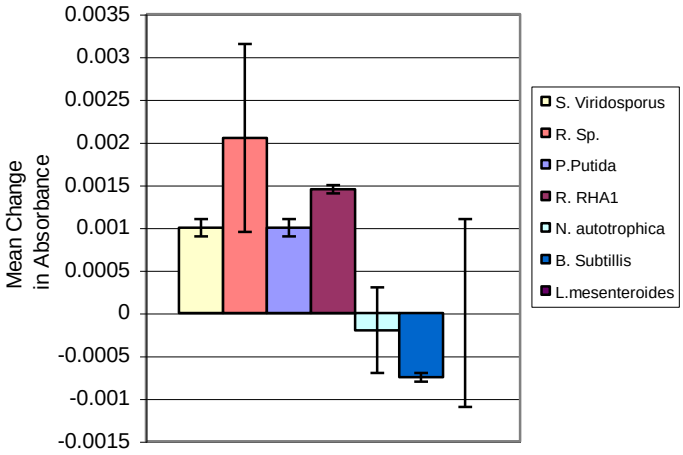

Figure 3.18 Change in absorbance at 430 nm over 0-20 min for bacterial lignin degraders and non-degraders with 2 mM H_2O_2 and nitrated miscanthus lignin (0.01mg/ml). The assay method is described in the Experimental Section. Left to right: *Streptomyces viridosporus* (cream), *Rhodococcus sp*. (peach), *Pseudomonas putida* (blue), *Rhodococcus jostii* RHA1 (purple), *Nocardia autotrophica* (turquoise), *Bacillus subtilis* (royal blue), *Leuconostoc mesenteroides* (purple).

Since the nitrated milled wood lignin seemed to be giving data consistent with the literature and the fluorescence assay, it was further employed to screen a range of bacteria against the three milled wood lignins previously prepared. The results of these assays are summarised in Table 3.3. It can be seen that *N. autotrophica*, which was active in the fluorescent assay (Figure 3.11), showed no activity with wheat, but lignin was active with the other lignin types. This is one of a number of examples microbial preferences for a specific lignin type: other examples in the data are *Arthrobacter globiformis*, *Rhodococcus erythropolis*, *Acinetobacter* PC/4 and *S. coelicolor* 1010. *R. erythropolis* showed the highest activity of any of the species screened, but was very specific for wheat lignin. The highest consistent activity was shown by *S. coelicolor* M110. This screen shows that there are a range of bacteria which show activity for lignin. Most of the bacteria found to be active are actinomycetes and the exceptions are *Acinetobacter* PC/4 and *P. putida* which are both γ-proteobacteria.

Micro-organism	Change in Absorbance (mAU)		
Bacteria	Wheat	Miscanthus	Pine
Streptomyces			
S. coelicolor M110	21.9	16.5	30.4
S. coelicolor ISP 5233	1.2	1.3	1.85
S. coelicolor JCM 3279	4.3	3.1	3.3
S. coelicolor 1010	0.8	0.8	3.8
S. coelicolor M1190	<0	1.1	2.1
S. coelicolor M145	1.15	0.6	2.65
S. avermitilis 41443 DSM	<0	<0	5.1
S. viridosporus	1	0.7	1
P. putida 33015	0.6	1	0.25
Rhodococcus erythropolis	68.3	0.55	0.9
Rhodococcus jostii RHA1	1.5	2.7	2.5
R. sp	2.05	4.1	<0
Acetobacter PC/4	2.35	0	<0
Arthrobacter globiformis	10.1	0.35	12.3
N. autotrophica	<0	0.25	1.95
B. licheniformis	1.1	<0	1.55
B. subtillis	<0	0	0.3
L. mesenteroides	0	<0	<0

Table 3.3 Activities observed in UV-visible assay for extracellular supernatants from a collection of bacteria, against nitrated lignin from wheat, miscanthus, and pine. No change in absorbance relative to controls was seen with *B. licheniformis, B. subtilis and L. mesenteroides*.

3.7.2 Application of the nitrated lignin assay to screen fungi for lignin degrading activity

The UV-visible assay was used to compare the activity of the bacterial strains identified above with a selection of known lignin[43, 70, 147, 148, 149] degraders and some mycorrhizal fungi, and to assess the relative activity of each strain towards the three lignin types. In each case, a 30 µl sample of extracellular solution was used in the assay. The data is shown in Table 3.4.

The mycorrhizal fungi listed in Table 3.4 were grown on MMN media by researchers from the group of Dr G. Bending from Warwick HRI. The

mycorrhizal media was used for the assay after filtration through a 0.2μm Whatman filter. The white and brown rot fungi were grown on straw by Drs K. Burton and D. Eastwood. To assay these fungi, they were washed and the resulting solution was centrifuged. This final solution was then used in the nitrated lignin assay.

The highest activity was observed using the well studied white-rot fungus *Phanerochaete chrysosporium*, which gave an increase of 400-700 mAU at 430 nm over 20 min. Other white- and brown-rot fungi showed lower activities of 0.2-32 mAU. A set of 7 mycorrhizal fungi composed of *Pauxillus involutus*, *Suillus luteus*, *Laccaria bicolour*, *Lactarius controversus*, *Lactarius rufus*, *Cenococcum geophilum* and *Suillus bovinus* were also tested in the assay, several of which showed activity in the assay. Highest activity was observed with *Paxillus involutus* and *Suillus luteus* with values in the range 0.8-2.3 mAU. There have been previous investigations into whether *Suillus luteus* could degrade lignin, but the results have been inconclusive.[150, 151] These results suggest it does degrade lignin but not as strongly as the basidiomyces. The specificity of *Suillus luteus* is consistent with its role in nature where it is a symbiotic fungus for coniferous trees.[150]

Micro-organism	Change in Absorbance (mAU)		
Fungi	Wheat	Miscanthus	Pine
White and Brown rot			
Phanerochaete chrysosporium	459	832	297
Lepista nuda	42.7	7.45	26.5
Serpula lacrymans	5.9	14.0	28.5
Schizophyllum commune	6.45	10.1	11.9
Trametes versicolor	1.1	4.25	1.5
Mycorrhizal			
Pauxillus inv.	6.65	6.83	8.95
Suillus luteus	1.73	1.08	2.4
Laccaria bicolour	1.63	0.8	1.48
Lactarius controversus	4.58	4.88	3.6
Lactarius rufus	2.95	3.33	1.95
Cenococcum geophilum	4.65	4.68	3.73
Suillus bovinus	1.48	2.53	2.40

Table 3.4. Changes in absorbance observed in UV-visible assay for extracellular samples from a collection of fungi, against nitrated lignin from wheat, miscanthus, and pine. No change in absorbance relative to controls was seen with *Cenococcum geophilum*, *Lactarius rufus* and *Suillus bovines*.

Comparison of the changes in absorbance in Table 3.3 and 3.4 show that the most active micro-organism was *Phanerochaete chrysosporium*. The activity of white and brown rot fungi can generally be seen to be greater than that of mycorrhizal fungi. The activity of bacteria is generally lower still but with some exceptions. *R. erythropolis*, *A. globiformis* and *S. coelicolor* M110 all give activity comparative with the basidiomycetes fungi.

3.7.3 Application of the nitrated assay to protein purification

The nitrated milled wood lignin assay can also be used in protein purification. An attempt was made to purify lignin degrading enzymes from wild type *R. jostii* RHA1. It was determined that proteins in the extracellular supernatant which had activity in the nitrated lignin assay might adhere to an anion

exchange column (DEAE-Sepharose) and could be eluted with KCl 1M gradient wash and activity could be recovered, as shown in Figure 3.19. Activity was assessed using the UV-visible assay detailed above. At least two peaks of enzyme activity were observed. Unfortunately, only very small amounts of protein, in the order 7-8 μg were recovered from a 500ml culture. At this point in the project, two putative recombinant heme peroxidases became available as explained in Chapters 5 and 6 this meant that purification of material from the wild type strain was not necessary.

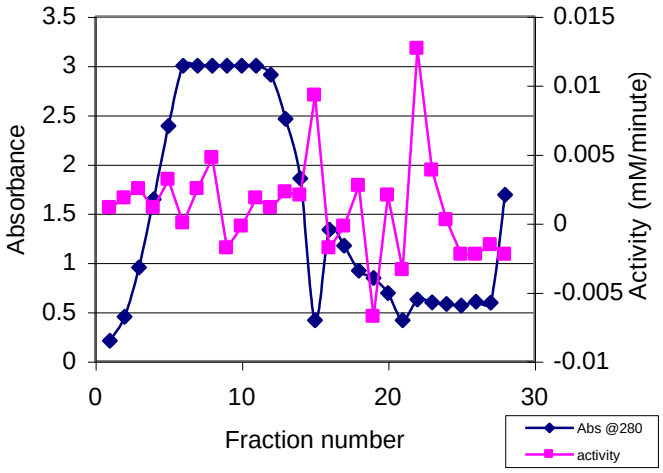

Figure 3.19 Plot of activity and absorbance after DEAE-Sepharose column. Nitrated lignin assay can be used to observe increase in activity of protein samples after they are washed off of ion exchange columns.

3.8 Plate assay

In order to test whether the nitrated lignin assay could be used on agar plates to detect lignin degrading activity, nitrated lignin (1mg/100ml) was sprayed onto bacteria that had been grown on agar plates and incubated for two days. This gave a strong yellow colour for *P.putida* 33015 and *R. sp* RHA1 and no change

for *Leuconostoc mesenteroides* and *B. subtilis*. (see Figure 3.20). This is consistent with a yellow colour being observed for lignin degrading bacteria.

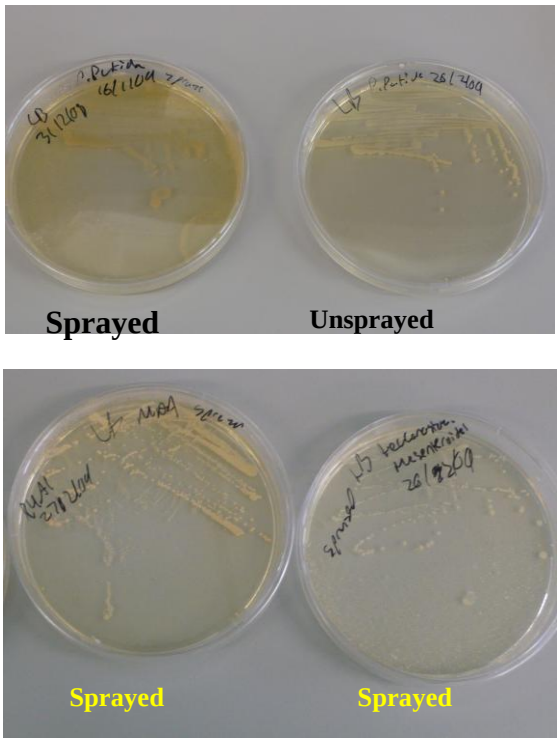

Figure 3.20 Top- *P.putida* grown on LB agar sprayed with nitrated myscanthus lignin solution (0.01 mg/ml) compared with *P. putida* grown under the same conditions but without having been sprayed. Bottom- *R. sp* RHA1 (left) and *L. mesenteroides* (right) both after having been sprayed with nitrated myscanthus lignin solution (0.01 mg/ml). All plates were incubated for two days before photos were taken.

This sort of plate based assay could therefore be used for bioprospecting work such as looking for thermophilic lignin degraders.

3.9 Conclusion

Two new spectrophotometric assays have been developed that are well suited for the rapid screening of bacteria and use in protein purification. Both assays are quick, sensitive and amenable to use in a 96 well plate reader. The nitrated

milled wood lignin can also be used in a spray to allow screening on solid media.

The nitrated lignin degradation assay showed substantial scatter in the data collected. This was found to be greatly reduced by doing experiments in triplicate. If the assay is to be used for protein purification it is advisable to originally screen for activity with a general peroxidise assay to save time and nitrated lignin. Active fractions can then beinvestigated specifically for lignases with the nitrated lignin assay.

The fluorescent assay which was originally used showed evidence that lignin might become attached onto bacterial cells. This is consistent with work from the literature that shows lignin can be recognised by bacterial cell walls in *Xanthonas*.[95]

In the course of our studies *R. jostii* RHA1, *Acinetobacter* PC/4 and a number of *S. coelicolor* strains showed positive results for ability to degrade lignin. These strains represent new bacterial lignin degraders. *R. jostii* RHA1[145] and *Acinetobacter* PC/4[152] have previously been shown to be involved in aromatic breakdown. This is perhaps unsurprising as lignin is the one of largest sources of aromatic compound in nature.

The fluorescent assay in particular highlighted that a number of the bacteria studied may also use laccases to degrade lignin. This is of interest as laccases are more amenable to being used in industrial procedures, as they do not require

stoichiometrics amounts of hydrogen peroxide to accomplish degradation. The role of laccases in *R. jostii* RHA1 is further discussed in chapters V and VI.

The microbial screening with different lignin types drew out two points of interest. The first that microorganisms can be quite specific for different types of lignin, an observation not previously made in the literature. The reason for this specificity is not known but it could be due to enzymes directly binding the lignin. Previously there has been little suggestion of this although it has been recently shown in the case of LiP.[58] Another reason could be due to differences in the redox potential of different lignin dimer structures. Work by Spila has shown this to be the case in laccase from *Melanocarpus albomyces* and *Trametes hirsuta*.[72] Whatever its cause, the specificity of lignin degraders needs to be considered carefully in the development of a biotechnological process because mixed feedstocks have been suggested for second generation processes and thus micro-organisms with a broad specificity are important.

The second point that emerged from the screening of micro-organisms was that some bacteria had comparable activity to some fungi which are commonly associated as good lignin degraders. Whilst none were as effective as *P. chrysosporium*, this organism has proven disappointing when practically employed as its degrading power is so great as to leave little material remaining after its own metabolic needs have been met. Bacteria, however, may be prove more useful as they can offer considerable activity but not too much. This combined with the comparative ease with which bacteria can be genetically

manipulated offers a wealth of opportunities for application of bacteria to lignin degradation.

CHAPTER IV: Lignin breakdown products

4.1 Introduction

Due to its heterogeneous nature lignin breaks down into many components, which has been a limitation of both fungal and chemical lignin degradation. The bacterial degradation of lignin has so far been only given the most cursory of studies.[137] Having established that *R. jostii* RHA1 and *P. putida* were active in the lignin degrading assays we wished to study whether small molecule aromatic products were formed upon degradation of lignin. Further investigation aimed to identify products of lignin degradation by HPLC, GC/MS and LC/MS.

Degradation of kraft lignin by *Bacillus sp.* and *Aneurinibacillus aneurinilyticus* has been studied by GC/MS and a number of products have been confidently identified: *trans*-4-hydroxycinnamic acid **52**, 3,4,5-trimethoxy benzaldehyde **53**, gallic acid **54** and ferulic acid **22**.[114] In a similar study the effect of *Aeromonas formicans* on waste paper effluent was studied by GC. 4-Hydroxy benzoic acid **55**, vanillic acid **56**, protocatechuic acid **57**, syringic acid **58**, *trans*-4-hydroxycinnamic acid and ferulic acid were identified.[115] In both cases there were many more products that could not be comprehensively assigned a structure.

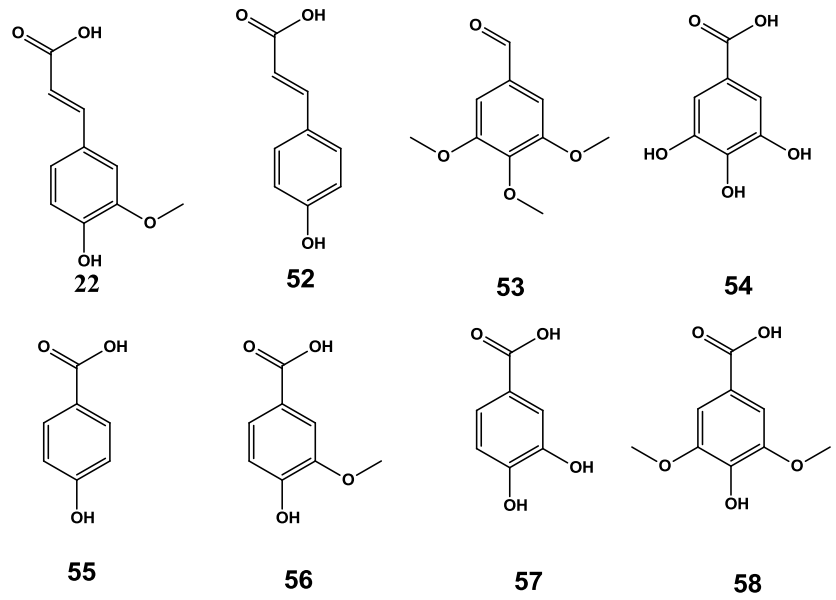

Figure 4.1 Previously identified products from bacterial lignin degradation. Ferulic acid **22,** *trans*-4-hydroxycinnamic acid **52**, 3,4,5-trimethoxy benzaldehyde **53**, gallic acid **54,** 4-Hydroxy benzoic acid **55**, vanillic acid **56**, protocatechuic acid **57** and syringic acid **58**.

The presence of ferulic acid is of particular interest, as the compound has been of significant industrial interest. It can be used as a food additive, due to its anti-oxidant effects, or alternatively as a feedstock for other products.[113, 116] These studies illustrate the potential of bacteria in bioconversion of lignin to fine chemicals, however, they also outline the ongoing challenge of controlling the breakdown to produce desired compounds in high yields.

4.2 Analysis of lignin degradation by HPLC

To ascertain the validity of the nitrated lignin assay, two positives *R. jostii* RHA1 and *P. putida* and one negative result, *B. subtilis*, were taken and grown at 30^{o}C on lignocellulose from miscanthus in 22 ml of LB for one week. At time intervals of 4 hours, 1 day, 2 day and 7 days, samples were taken and studied by HPLC, LC/MS and GC/MS. Products formed by lignin degradation have

previously been studied by HPLC.[153] In the case of *R. jostii* RHA1 and *P. putida*, significant changes in the HPLC chromatograms were observed, compared with the control where lignin was present under sterile conditions as shown in Figure 4.2 and 4.3. The peaks at 6.9, 13.0 and 25.1 minutes shown in green are not observed when bacteria are present. Also some new peaks form at 20.7 minutes in the case of *R. jostii* and 11.5 minutes for *P. putida*. For B. subtilis no changes were observed verses time. The changes seen by HPLC seemed to confirm the results of the nitrated lignin assay that *R. jostii* and *P. putida* are able to degrade lignin, whilst *B. subtilis* is not, though at this stage we did not know the identity of the peaks observed.

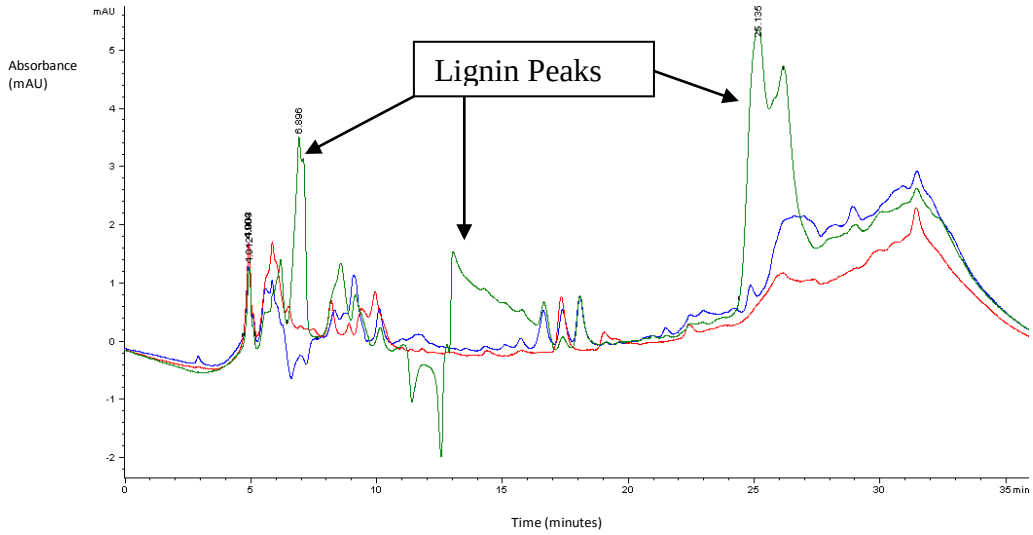

Figure 4.2 HPLC trace of *P. putida* with lignin in Luria Broth (LB) after 1 day (blue), compared with lignin in LB after 1 day (green) and bacteria growing in LB after 1 day (red). Note disappearance of lignin peaks between green and blue line.

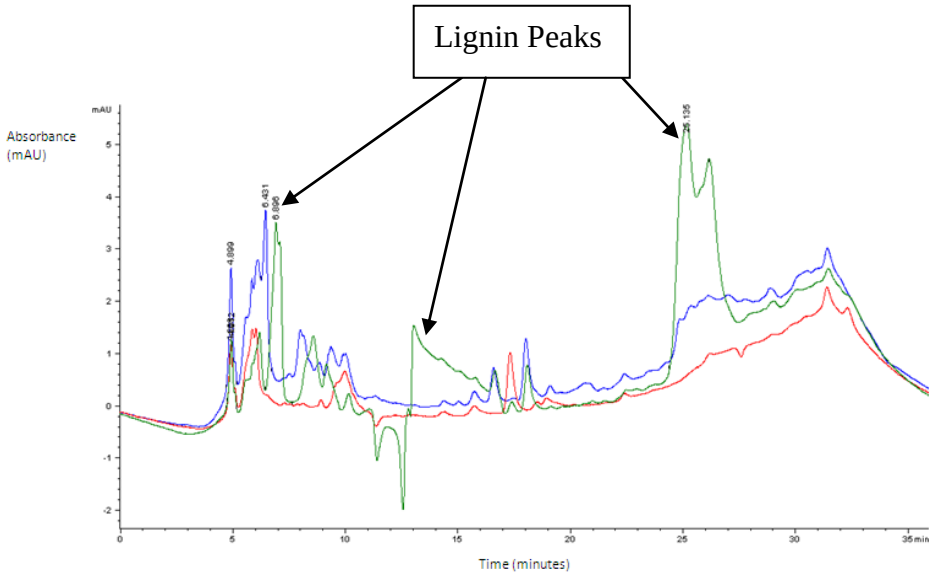

Figure 4.3 HPLC trace of *R. jostii* RHA1 with lignin in LB after 1 day (blue), compared with lignin in LB after 1 day (green) and bacteria growing in LB after 1 day (red). Note the disappearance of the lignin lignin peaks from the green to the blue line.

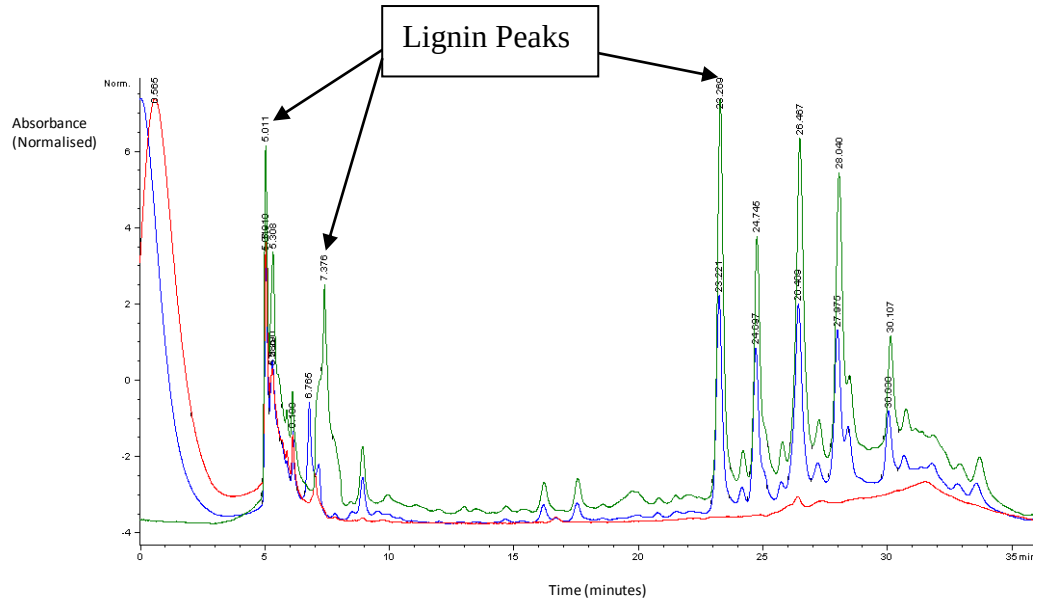

Figure 4.4 HPLC trace of *B. subtilis* with lignin in LB after 1 day (blue), compared with lignin in LB after 1 day (green) and bacteria growing in LB after 1 day (red). Note lignin peaks remain.

4.3 Product identification

Samples from each bacteria at each time point were extracted into DCM and derivatised in preparation for analysis by GC/MS. Each sample was reacted with 200µl N, O-bis(trimethylsilyl)acetamide and 10µl chloro-trimethylsilane samples and was then diluted by a factor of one hundred. This process causes silylation of active hydrogens, giving increased volatility to compounds in the mixture. GC/MS analysis of the samples from *R. jostii* RHA1 and *P. putida* gave complex total ion chromatograms, as shown in Figure 4.4. This demonstrates that multiple products are being formed.

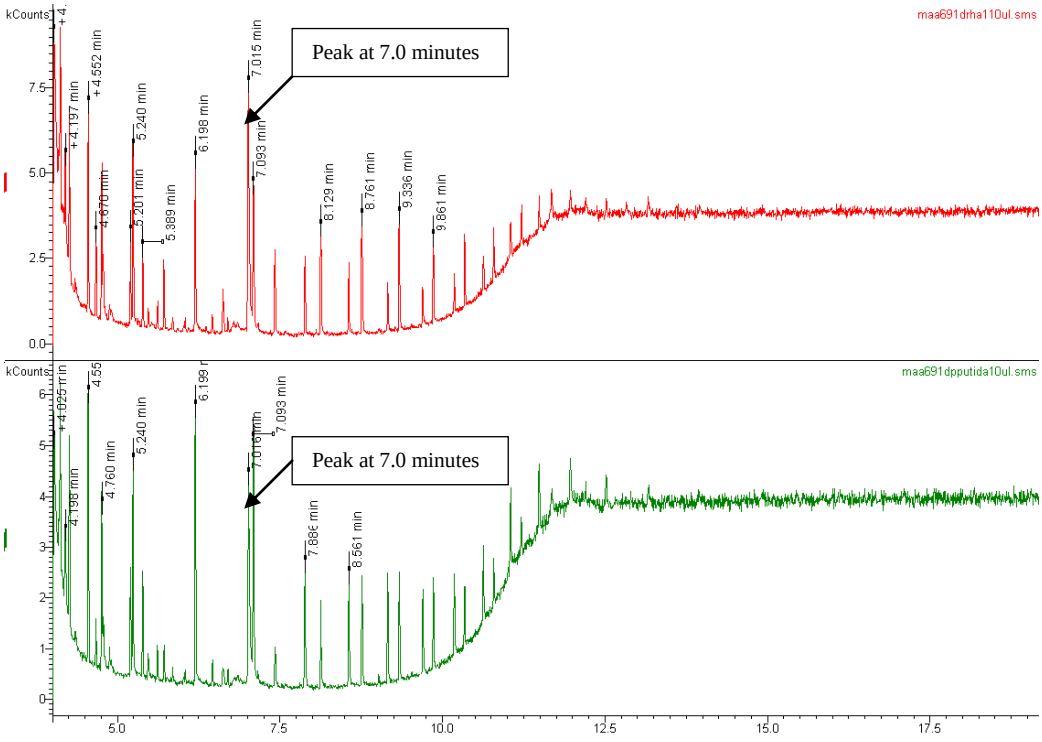

Figure 4.5 GC-MS total ion chromatograms. Top- *R. jostii* RHA1 and lignocelluloses (25 mg/ml) grown in LB after 1 day. Bottom- *P. putida* and lignocelluloses (25 mg/ml) grown in LB after 1 day.

The peak at 7.0 minutes was observed in all samples for both bacteria, this peak gave the mass fragmentation pattern illustrated in Figure 4.5. An assignment of

fragments is given in Table 4.1 and the proposed structure is given in Figure 4.6. In addition a peak with a retention time of 4.3 minutes and a mass of 235 which corresponds to the MK^+ of the underivatised compound **59**. Treatment of the LC/MS sample with dinitrophenol hydrazine (DNP) and a drop of HCl lead to the formation of a small amount of red precipitate. Subsequent analysis of the sample by LC/MS revealed that the peak at 4.3 minutes was no longer present. This is consistent with the proposed structure, as DNP forms a red precipitate with ketones. The structure proposed in Figure 4.6 is both consistent with the data gathered and is a known product from lignin degradation.[90] The peak at retention time 7.0 minutes in the GC/MS represents the largest peak not in controls in the samples and thus, as the method of ionisation is electron impact, represents the most abundant product. Electron impact is semi-quantitative as the method of ionisation is so harsh it ionises all of the compound present.

m/z	Fragment
268	M^+
267	M^+-H
266	M^+-2H
253	M^+-CH_3
195	M^+-$SiMe_3$
180	M^+-CH_3-$COCH_2CH_2OH$
122	M^+-$SiMe_3$-$COCH_2CH_2OH$

Table 4.1 Assignment of fragments from the electron impact ionisation of compound **59**.

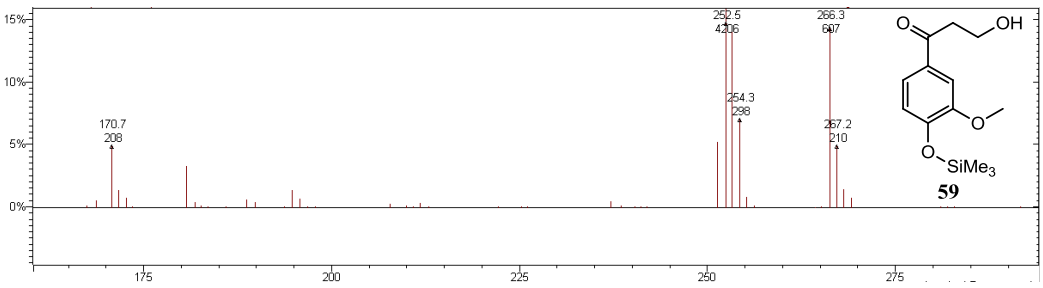

Figure 4.6 Mass spectrum for retention time 7.0 shown for *R. jostii* RHA1 1 day. Right hand side- Compound **59** derivatised.

The GC/MS total ion chromatogram has a small peak at retention time 5.85 minutes. This gave the fragmentation shown in Figure 4.7 and Table 4.2. The fragmentations and the retention time were the similar to those produced by the commercial standard of ferulic acid. When the commercial standard was run it was found to give a broad peak due to the acid moiety. The LC/MS gave a peak at *m/z* of 195 and retention time of 5.25 this is consistent with the MH^+ adduct of ferulic acid.

m/z	Fragment
265	M^+-H
251	M^+-CH_3
222	M^+-CO_2
221	M^+-CO_2-H
207	M^+-CO_2-CH_3
193	M^+-$SiMe_3$
149	M^+-$SiMe_3$-CO_2

Table 4.2 Assignment of fragments from the electron impact ionisation of ferulic acid, compound **22**.

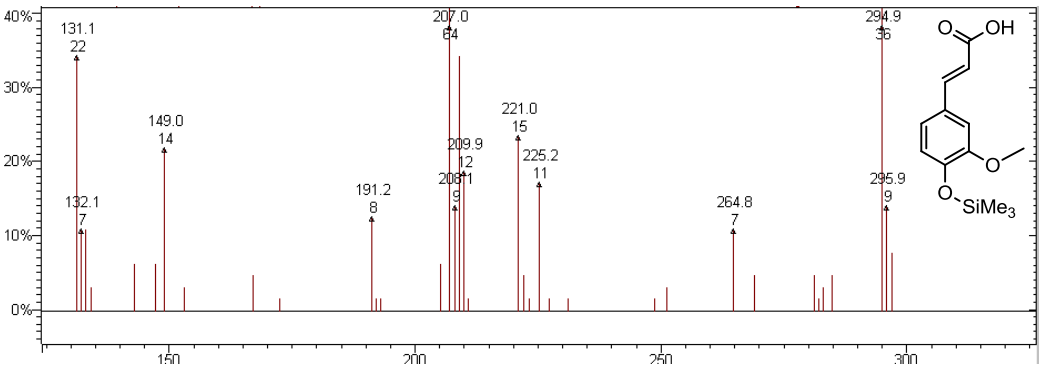

Figure 4.7 Mass spectrum for retention time 5.85 minutes shown for *P. putida* 1 day. Right hand side- derivatised fereulic acid **22**.

A small peak was observed in the GC/MS at retention time 6.0 minutes (see Figure 4.5) with all the samples tested for *P. putida* and all bar the 4 hour

sample for *R. jostii* RHA1. This peak corresponds, with respect to retention time and fragmentation, with the disilylated commercial standard compound **60**. The GC/MS fragmentation is shown in Figure 4.8 and assignments are given in Table 4.3. The LC/MS had a peak at retention time 5.8 minutes and an *m/z* of 251, consistent with the MK^+ of an underivatised compound **60**.

m/z	Fragment
341	M^+-CH_3
325	M^+-$2CH_3$-H
239	M^+-$SiMe_3$-CO_2
209	M^+-$2(SiMe_3)$-H

Table 4.3 Assignment of fragments from the electron impact ionisation of the diacid compound **60**.

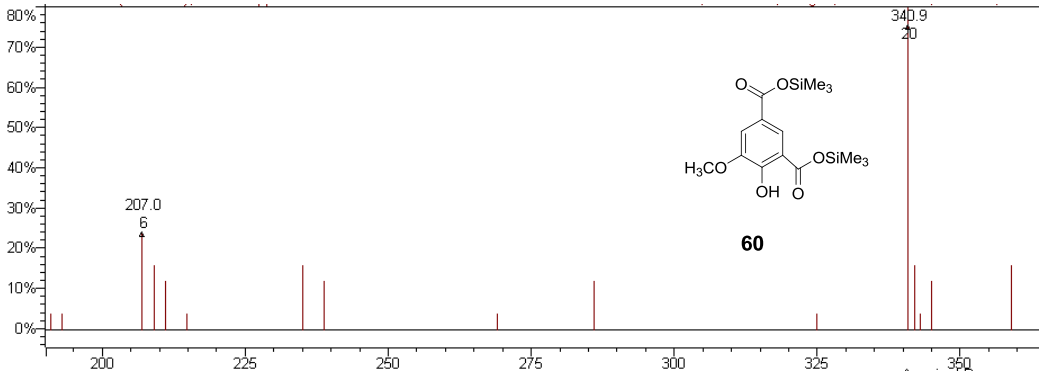

Figure 4.8 Mass spectrum for retention time 6.0 shown for *P. putida* 1day. Right hand side compound **60** derivatised with trimethylsilyl groups, position of silyl groups is representative.

In all samples a peak was observed at 4.4 minutes, which had the fragmentation pattern seen in Figure 4.9 and which is assigned in Table 4.4. The retention times and fragments were the same as that of the commercial standard for oxalic acid. In addition there was evidence of the same compound but monosilated at a retention time of 5.3 minutes once again the fragmentation was similar to that of the standard. At both retention times there was a large fragment with a mass of

149, which was also in the authentic standard but this could not be assigned a structure.

m/z	Fragment
189	M^+-3Me
147	M^+-$SiMe_3$-2Me
132	M^+-$SiMe_3$-2Me-O
116	M+-2($SiMe_3$)

Table 4.4 Assignment of fragments from the electron impact ionisation of oxalic acid compound **61**.

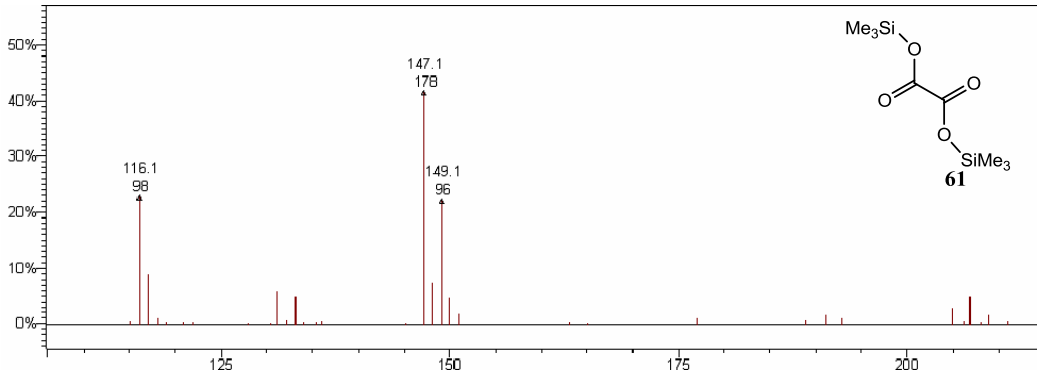

Figure 4.9 Mass spectrum for retention time 4.4 minutes shown for *P. putida* 2 days. Right hand side oxalic acid derivatised with trimethyl silyl groups **61**.

The peak heights observed in the total ion chromatogram vary with time for each product. Due to the fact that method of ionisation used was electron impact the intensities of the total ion current recorded are proportional to the amount of material present. Therefore variations in the peak heights are proportional to variations in the amount of product. These changes are summarised in Table 4.5. The ketone compound **59** can be seen to be the most abundant product, which forms quickly and is later degraded. The amount of compound **60** and **22** is consistently low. In the case of ferulic acid there is some evidence of abundance increasing with time. Oxalic acid was strongly present in all the samples. There

are two different sets of time points for the two bacteria as some samples were lost in the process of being derivatised.

	P.putida			*R. jostii* RHA1			
Compound	4hrs	1day	2 days	4hrs	1day	5 days	1 week
Ketone, **59**	12.25	4.25	1	2.1	8	3.5	<1
Diacid, **60**	0.8	0.45	0.6	Not present	0.5	<1	<1
Ferulic acid, **22**	Not present	0.65	1.5	Not present	0.75	4.5	Not present
Oxalic acid, **61**	7.25	5	10.2	4.5	6.8	3.75	3

Table 4.5 Variation of product from lignocellulose breakdown in accordance with time. Values in kcount.

The HPLC, LC/MS and GC/MS data all show more compounds present than have been characterised. There are ongoing studies by both the Bugg and Clark group to investigate the products produced by bacterial and fungal degradation of lignin. To support this work, Appendix 1 contains a tabulation of the major peaks observed by the LC/MS and speculative assignments. The volume of data generated by the GC/MS meant that no similar table was compiled for this data. The only structural assignments with a high degree of confidence are those outlined above. Despite this, some trends are apparent upon examination of Appendix 1, that within the first day predominantly high mass structures are observed (m/z greater than 500). As time progresses, these high mass structures become less prominent and few are left by day 3. In later samples there are compounds in the mass range of lignin dimers and monomers.

4.4 Production of APPL from lignin

Previously Crawford *et al.* had produced a low molecular weight variation of lignin by treating lignocellulose with *S. viridosporus*.[91] This material was named acid percipitable polymeric lignin (APPL). We attempted to isolate some APPL

to use as a possible bioproduct. Miscanthus lignocellulose, which had been partially ground, was incubated for eight weeks with *S. viridosporus* in minimal media 1(For 1L $K_2HPO_4.3H_2O$ 4.25g, NaH_2PO_4 1.0g, NH_4Cl 2.0g, $MgSO.7H_2O$ 0.2g, $FeSO_4.7H_2O$ 12mg, $MnSO_4.H_2O$ 3mg, $ZnSO_4.7H_2O$ 3mg, $CoSO_4.7H_2O$ 1mg, nitrilotriaceticacid 0.1g and Yeast extract 3g) at 30^oC. After this the residue was filtered out and the filtrate acidified to give a precipitate. This precipitate proved very difficult to isolate but eventually some of the material was separated by centrifugation. Attempts to filter the material failed as it adhered very strongly to the filter paper. It could be found to be resolublised by washing with aqueous sodium bicarbonate.

Studies by IR and mass spectrometry were consistent with this material being a form of APPL. In the IR spectrum (Figure 4.10) there was a peak at 1644 cm^{-1} this is consistent with the presence of aryl or $\alpha\beta$ unsaturated ketones. There were also peaks at 1555 and 1430 that would not normally be found in lignin; these are consistent with a carboxylate ion. In addition to these three peaks not seen in miscanthus lignin there were peaks at 3362, 2913, 1143 and 1030 cm^{-1} that were consistent with the spectrum for miscanthus lignin[144] but all the peaks were much broader as would be expected for a partly degraded species.

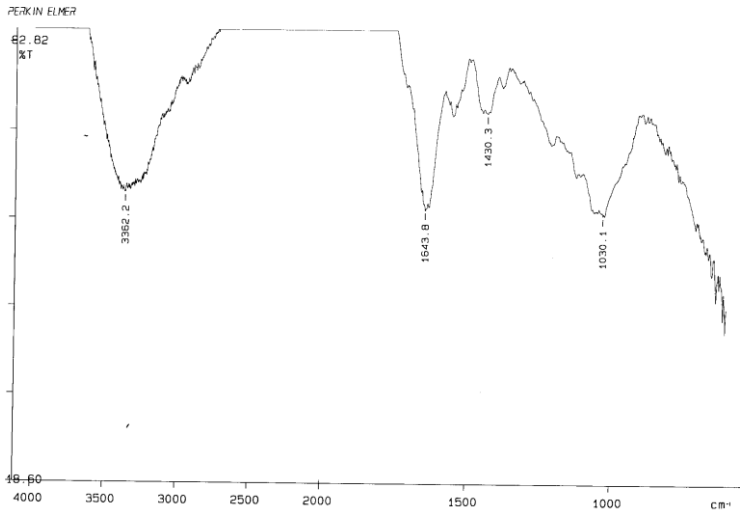

Figure 4.10 The IR of APPL formed from miscanthus lignin after eight weeks of treatment with *S. viridosporus*. Note the peak at 1644 cm^{-1} which is consistent with the presence of aryl or αβ unsaturated ketones.

Prior studies on the structure of APPL have suggested that there is oxidation of benzylic hydroxyl groups and a loss of aromaticity.[93] The most likely method for this loss of aromaticity is by the activities of enzymes like protocatechuate 3,4 dioxygenase and CatA on the β-ketoadipate pathway. Equivalent systems have been shown to work on polymeric lignin in fungi and to be present in *S. viridosporus*.[104, 78] These pathways give carboxylates as products and this is consistent with what is observed by IR. ESI mass spectrometry of the sample gives a series of peaks mainly between 122-696 *m/z* with major mass peaks being approximately 140 mass units apart. This is consistent with a group of oligomers composed of a number of different aromatic monomers.

The APPL was subsequently tested by Dr S. Coles for its properties when electrospun. This is a process where polymer nano fibres are made by applying a

high voltage electrical potential to charge the surface of the polymer and thus induce the ejection of the material through a spinarette. This process is summarised in Figure 4.11. The nano fibres produced typically have a diameter between 50 nm – 500nm and this morphology grants them several unique characteristics including a very high surface area per unit of mass, high porosity and excellent mechanical properties.[154]

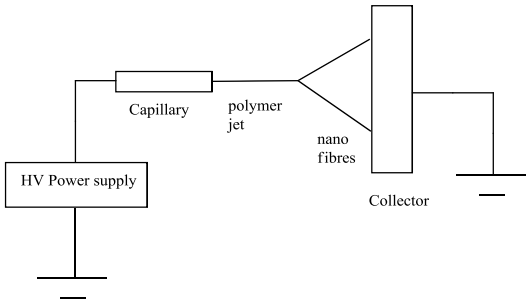

Figure 4.11 Simplified schematic of electrospinning system. Polymer solution is forced out of small capillary by high voltage (HV) and shot against a collector plate were nano fibres form.[143]

APPL at a concentration of 300 mg mL^{-1} was not viscous enough in solution by itself to be electrospun but could be co-spun with poly vinyl alcohol at concentrations of 25 mg^{-1} ml and 100 mg^{-1} ml to give fibres as illustrated in Figure 4.12. The low viscosity of APPL was almost certainly due to its low weight and if larger lignin fragements could be isolated it is possible they would be better for spinning.

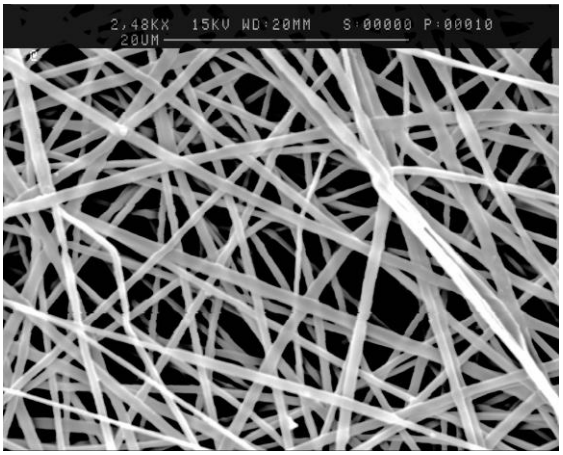

Figure 4.12 SEM picture of APPL cospun with polyvinyl alcohol.

4.5 Conclusion

This chapter has shown two different ways in which bacteria can be implemented to the breakdown of lignocellulose. The first of these, illustrated by the *R. jostii* RHA1 and *P. putida*, is the breakdown of lignocellulose to form small molecules. The second way bacteria can breakdown lignin is to solublise it as lower weight oligomers. Both of these methods are potentially useful.

A number of products were formed from the actions of *R. jostii* RHA1 and *P. putida*. However, the quantities of some products were very small and the fact that they are part of a larger mixture represents a considerable challenge for future industrial applications.

Ferulic acid was of interest as it has been heavily studied as renewable feedstock. It also has a place in the current market as a food preservative and dietary supplement due to its antioxidant properties.[105, 108] Ferulic acid is often observed in lignin degradation studies.[106, 107] This is because it is often incorporated into lignin and forms sites of attachment to hemi-cellulose.[18, 21]

Compound **59** was one of the most abundant compounds in the media. This compound has substantial functionality, which could make it an interesting potential feedstock chemical. The fact that it is one of the most abundant products in the mixture makes it easier to purify.

Compound **59** has previously been reported in studies of aromatic breakdown by *Sphigomonas paucimobilis SYK-6*. In this case it is believed to occur by the following route.[90]

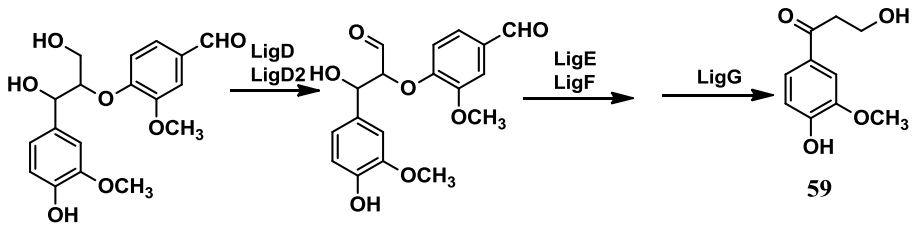

Figure 4.13 The route and enzymes involved in the degradation of β-arylether lignin dimers by S. *paucimobilis SYK-6*.[90]

In *S. paucimobilis SYK-6* it is postulated that compound **59** is metabolised to vanillin, however, no enzymes that carry out this transformation could be found nor any evidence to support this hypothesis although future studies may shed more light on this.[90] It is possible that the structure is a bottleneck in lignin breakdown and as such has a tendency to accrue in the media of bacteria grown with lignocellulose.

In our studies it was found that the other compounds, ferulic acid **22** and aromatic diacid **60**, which are also on the aromatic degradation pathway, were not present in large amounts. We would postulate this is because the bacteria

quickly metabolise them. This means that if one wishes to produce vanillin or any other substance directly on the lignin breakdown pathway it will be necessary to interrupt or redirect the natural degradation process.

Oxalic acid was observed by GC/MS and this may have been present due to the cells' natural metabolism or it may be more directly linked to lignin breakdown. In fungi, oxalic acid has been shown to be the final product of a series of oxidation of glycoxal by glyoxal oxidase, producing two equivalents of hydrogen peroxide.[155] This hydrogen peroxide can then be used by peroxidases to breakdown lignin. In addition, oxalic acid has been shown to be a mediator for manganese peroxidase so can thus further aid lignin degradation.[156] Oxalic acid precursors can be made from enzymatic degradation of lignin dimer compounds.[157] This means that lignin degradation can lead to hydrogen peroxide formation as illustrated in Figure 4.14. Oxalic acid could thus be both from lignin breakdown and play a role in aiding it. The co-production of hydrogen peroxide and oxalic acid is consistent with the observation of lignin degrading activity without hydrogen peroxide in the spectrophotometric assays, as micro-organisms may be able to produce the majority of the hydrogen peroxide they need.

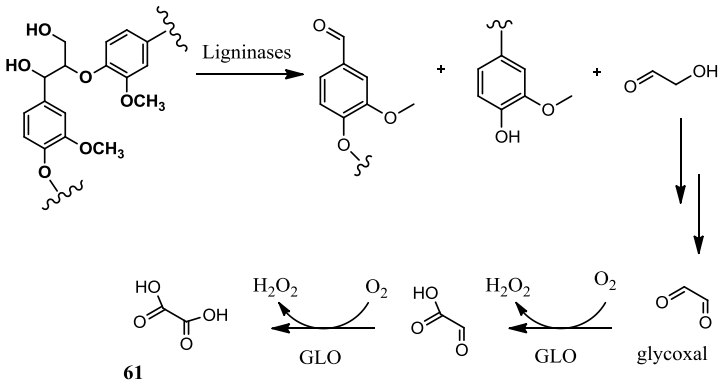

Figure 4.14 Possible route by which oxalic acid **61** and hydrogen peroxide could be formed from lignin like compounds based upon known biochemical reactions in fungi.

Oxalic acid was one of the most abundant compounds found in medium after the bacteria had been grown on lignocellulose. Oxalic acid is employed as a bleach and mordant for use in dyes. Ironically, one of its main uses is wood pulping.[158] It is possible that further investigation could allow the development of a method of producing oxalic acid from lignocellulose on a larger scale.

The LC/MS data for the breakdown of the lignocellulose showed a distinctive pattern where oligomers formed early on and monomers and dimers were predominantly produced latter, although compound **59** represents an exception to this. It is hypothesised that this pattern of breakdown products is the consequence of a suite of enzymes acting on lignocellulose. Some of these enzymes break large lignin molecules into smaller oligomers. Others are involved in cutting down these smaller molecules into monomers and dimers and perhaps yet other enzymes work by endocleavage producing monomer like compound **59**.

Two compounds that were not positively identified were vanillin and vanillic acid both of these compounds are of industrial interest and lie on the proposed pathway for lignin breakdown.[90] There was some evidence for vanillic acid by LC/MS but the commercial standard had a different retention time. These two compounds were possibly not seen as the bacteria may further metabolise them very quickly and thus they do not accrue in the media.

APPL was successfully produced from miscanthus lignocellulos by *S. viridosporus*. This material was later shown to capable of being formed into nanofibres which can be further developed for use in materials. It is hoped that further testing will show that the fibres possess anti-oxidant properties because of the presence of phenolic species from the lignin. Such fibres would be of interest for making materials that could enhance wound healing.

CHAPTER V: Bioinformatics

5.1 Introduction

Having previously identified some lignin degrading bacteria (Chapter 3) and having made an attempt to purify the proteins responsible, (Chapter 2), bioinformatics was then used to identify genes that would encode for proteins that would be of further interest. Identification of genes that encoded for lignin degrading proteins is important to produce strains of bacteria that over express the desired protein. Bioinformatics also allowed reflections on what bacteria would be good for further study and how different enzymes can be improved via genetic manipulation.

5.2 Bioinformatic analysis- Peroxidases

Nocardia farcinica was used as a starting point as its genome had been sequenced and it was closely related to *Nocardia autotrophica*, which was known to have lignin degrading activity. *N. farcinica* contains seven peroxidases: four of known function (2 catalases, 1 glutathione peroxidase and 1 alkylhydroperoxidase) and three unannotated peroxidase genes (accession numbers Q5YV75, Q5YZF4, Q5YPL4).[159] Searches using the BLAST algorithm revealed that Q5YPL4 shared homologues in *Streptomyces coelicolor* (accession number Q9FBY9, 66% identity), *Mycobacterium tuberculosis* (accession number A0R4G9, 63% identity), *Pseudomonas fluorescens* (accession number Q4KA97, 56% identity), *Rhodococcus jostii* RHA1 (accession number Q0SE24, 52% identity), and *Zymomonas mobilis* (accession

number Q5NM63, 55% identity). A protein alignment between Q9FBY9, Q4KA97, Q0SE24 and Q5YPL4 the above is shown in Figure 5.1.

There are several sections that are conserved between the different proteins; this suggested they have similar function. The work in chapter 2 highlighted *R. jostii* RHA1 and *S. coelicolor* as lignin degrading bacteria. In addition *P. putida*, a related strain to *P. fluorescens*, was also identified. *R. jostii* was of particular interest to us as it could be easily grown, and it's molecular biology had been well studied by our collaborators in the Eltis Group.[145]

```
S. coelicolor Q9FBY9     --------MGGEVEEPEPQMVLSPLTSAAIFLVVTIDSGGED--TVRDLL 40

N. farcinica Q5YPL4      --------MG------EPQPILEPLTPAAIFLVATIDEGGEA--IVRDLL 34
P. fluorescens Q4KA97    MEPIMTQPSSLAERKPEPQAICNPITRSAIFIVATLAPGAAAAQTVRDWC 50
R. jostii, RHA1 Q0SE24   --------MPGPVARLAPQAVLTPPSAASLFLVLVAGDSDDDRATVCDVI 42
                                    ** :  * : :::*:* .   .      * *

S. coelicolor Q9FBY9     SDVASLERAVGFRAQPDGRLSCVTGIGSEAWDRLFSGARPAGLHPFRELD 90
N. farcinica Q5YPL4      EDLPGLRRSVGFR-IPGANLSCVTSIGSQAWDRLFTGPRPAELHVLREFV 83
P. fluorescens Q4KA97    TDIAALTRSVGKR-VPGGNLSCVCGFGSSAWDRLFGGPHPASLHPFIEVG 99
R. jostii, RHA1 Q0SE24   SGIDGPLKAVGFR-ELAGSLSCVVGVGAQFWDRVSASSKPAHLHPFVPLS 91
                          .: .  ::** *    . **** ..*:. ***:  ..:** ** :  .

S. coelicolor Q9FBY9     GPVHRAVATPGDLLFHIRASRLDLCFALATEIMGRLRGAVTPQDEVHGFK 140
N. farcinica Q5YPL4      GAKHRAPSTPGDLLFHIRAEVHDACFELAMAIGDRLAGAATIVDETVGFR 133
P. fluorescens Q4KA97    VEGRRAPSTPGDLLLHIRAEQMDLCFELATQLLKPLGDSIKVVDEVQGFR 149
R. jostii, RHA1 Q0SE24   GPVHSAPSTPGDLLFHIKAARKDLCFELGRQIVSALGSAATVVDEVHGFR 141
                            : * :******:**:*   * ** *.  :   * .: .  **. **:

S. coelicolor Q9FBY9     YFDERDMLGFVDGTENPTGAAARRAVLVGAEDPAFAGGSYAVVQKYLHDI 190
N. farcinica Q5YPL4      YFEQRDLLGFVDGTENPEGAAAAAATLVGQEDPDFAGGSYVVVQKYLHPL 183
P. fluorescens Q4KA97    YFDMRSMVGFVDGTENPEGREAVDFTLVGDEDPQFCNGSYVLVQKYLHNM 199
R. jostii, RHA1 Q0SE24   YFDSRDLLGFVDGTENPTDDDAADSALIGDEDPDFRGGSYVIVQKYLHDM 191
                         **: *.::********* .  *   .*:* *** * .***.:****** :

S. coelicolor Q9FBY9     DAWEGLSVEAQERVIGRRKMTDVELSDDVKPADSHVALTSVTGPDGSDLE 240
N. farcinica Q5YPL4      DEWRALSVEEQERIIGRTKLDDFELPDDVKPADSHVAVNTVVDPDGTERQ 233
P. fluorescens Q4KA97    TAWNELTVEAQERIIGRTKLSDIELDDAVKPSCSHSSLTTLEE-NGEEVK 248
R. jostii, RHA1 Q0SE24   SAWNTLSTEEQERVIGRTKLENVELDDDAQPSNSHVTLNTIVDDDGVEHD 241
                           *. *:.* ***:*** *: :.** * .:*: ** ::.::   :* : .

S. coelicolor Q9FBY9     ILRDNMPFGSVGREEFGTYFIGYARTPEVTETMLERMFLGTASAPHDRIL 290
N. farcinica Q5YPL4      ITRANMPFGSVREGRFGTYYIAYAATPTVTETMLSRMFEGTEEAAYDRIL 283
P. fluorescens Q4KA97    ILRDNMPFGRPGAGEFGTYFIGYARSPRPVEQMLENMFVGRPAGNYDRLL 298
R. jostii, RHA1 Q0SE24   ILRDNMAFGSLGEAEYGTYFIGYAKDPAVTELMLRRMFLGEPPGNYDRVL 291
                         * * **.**     .:***:*.**  *  .* ** .** *   . :**:*

S. coelicolor Q9FBY9     DFSTAVTGSLFFTPAADFLEDLPARP------------------------ 316
N. farcinica Q5YPL4      DFSVAVTGTLFFAPPLDFFDDLPDPPTAAAAVDDDAEAAAAVASELRVLG 333
P. fluorescens Q4KA97    DFSTAVTGGLFFVPSADLLEDLAERAPTGL--------------------- 328
R. jostii, RHA1 Q0SE24   DFSTAATGTLFFVPSRDVLESLGDEPAGAESAPEDPVEPAAAG-----PY 336
                         ***.*.** ***.*. *.::.*   .

S. coelicolor Q9FBY9     --------------
N. farcinica Q5YPL4      DGSLGIGTLKRSTL 347
P. fluorescens Q4KA97    --------------
R. jostii, RHA1 Q0SE24   DLSLKIGGLKGVSQ 350
```

Figure 5.1 Protein alignment for unknown peroxidase (Q5YPL4) from *Nocardia farcinica* peroxidase with homologues from *Rhodoccus jostii* (Q0SE24), *Streptomyces coelicolor* (Q9FBY9) and *P. fluorescnenes* (Q4KA97). Alignment carried out using CLUSTAL 2.0.12

The gene identified in *R. jostii* RHA1 (ro2407) encodes a 350 amino acid dyp-type peroxidase (Mr 37,222). *R. jostii* RHA1 also contains a second dyp-type peroxidase (ro5773). We have designated ro5773 and ro2407 as *dypA* and *dypB* respectively. An alignment of *R. jostii* RHA1 DypB, with the related previously studied bacterial dye decolourising peroxidase TyrA, was carried out (Figure 5.3). The biological substrate of TyrA is unknown but it is thought to be involved in melatin biosynthesis.[160] The sequence alignment gave 29 % of residues as identical and 45% as similar. Highlighted in red are a number of important conserved residues of known function in TyrA. Asp151 in TyrA is conserved as Asp152 and is the distal active site aspartic acid that is involved in compound I formation along with Arg242 conserved as Arg 243 in DypB. This conserved apartate residue is the equivalent of the conserved histidine found in other heme peroxidises as discussed in more detail in section 6.1. The heme moiety is bound by His224 in TyrA and this is conserved as His 225 in DypB. Asp284 is conserved as Asp 287.[160] The aspartate in TyrA is thought to be involved in a hydrogen bonding interaction with His224. This Asp-His-Fe motif is seen in the plant peroxidase superfamily[161] where it plays a role in tuning the redox potential of the iron and in orientating the tyrosine residue which bears the coupled radical in compound I.[160]

Study of the genome of *R. jostii* RHA1 shows that there is another gene just down stream from DypB that encodes for encapsulin. This is a protein that forms a nanoparticle. The genomic context of DypB is given in Figure 5.2. The position of the two genes suggests that they are expressed together.[145]

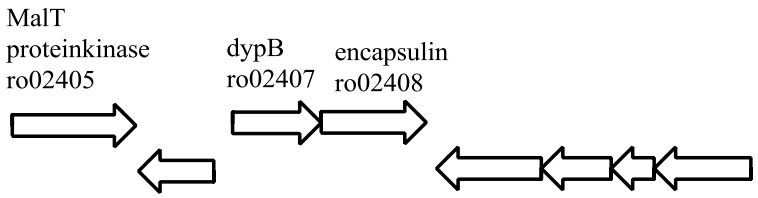

Figure 5.2 The genomic context for, *dypB* ro02407.

There are very few gaps in the alignment until residue 315 of DypB. After this there is a substantial overhang on the DypB sequence. This is believed to contain a targeting sequence for directing DypB to the encapsulin compartment. The targeting motif is believed to be GSLXIGSLKG although in some occasion it is not all preserved.[162] In DypB two of the residues are missing thus the sequence is present as XSLXIGXLKG; these residues are highlighted in lilac.

```
TyrA            GMDIQNMPREQLGVCAEGNLHSVYLMFNAN--DNVESQLRPCIANVAQYI 48
DypB            -MPGPVARLAPQAVLTPPSAASLFLVLVAGDSDDDRATVCDVISGID
                 *          .* :  .  *::*:: *.  *: .: :   *:.:   :

TyrA            YELTDQYSDSAFNGFVAIGANYWDSLYPESRPEMLKPFPAMQEGNREAPA 98
DypB            KAVGFRELAGSLSCVVGVGAQFWDRVSASSKPAHLHPFVPLSGPVHSAPS 99
                  :  :   .::. .*.:**::** : ..*:*  *:** .:.   :.**:

TyrA            IEYDLFVHLRCDRYDILHLVANEISQMFEDLVELVEEERGFRFMDSRDLT 148
DypB            TPGDLLFHIKAARKDLCFELGRQIVSALGSAATVVDEVHGFRYFDSRDLL 149
                   **:.*::. * *: . :..:* . : . . :*:* :***::*****

TyrA            GFVDGTENPKGRHRQEVALVGSEDPEFKGGSYIHVQKYAHNLSKWHRLPL 198
DypB            GFVDGTENPTDDDAADSALIGDEDPDFRGGSYVIVQKYLHDMSAWNTLST 199
                *********.. . :**:*.***:*:****: **** *:.* *: *.

TyrA            KKQEDIIGRTKQDNIEYESEDKPLTSHIKRVNLKDENGKSIEILRQSMPY 248
DypB            EEQERVIGRTKLENVELDDDAQPSNSHVTLNTIVDDDGVEHDILRDNMAF 249
                ::** :***** :*:* :.: :* .**:.  .: *::* . :***:.*.:

TyrA            GSL--KEQGLMFISTCRTPDHFEKMLHSMVFGDGAGNHDHLMHFTSALTG 296
DypB            GSLGEAEYGTYFIGYAKDPAVTELMLRRMFLGEPPGNYDRVLDFSTAATG 299
                ***   * *  **. .: *   * **: *.:*: .**:*:::.*::* **

TyrA            SSFFAPSLDFLMQFDN---------------------------------- 312
DypB            TLFFVPSRDVLESLGDEPAGAESAPEDPVEPAAAGPYDLSLKIGGLKGVS 349
                : **.** *.* .:.:

TyrA            -
DypB            Q 350
```

Figure 5.3. Protein alignment between DypB (Q0SE2) from *R. jostii* RHA1 and TyrA (Q8EIU4) from *S. oneidensis*. Highlighted in red are key conserved residues and in lilac is the possible encapsulin targeting sequence. Alignment carried out using CLUSTAL 2.0.12

DypB was compared to similar proteins in fungi using a blast algorithm. There were seven hits of which three where from *Aspergillus* strains: Q0CIQ8 from *Aspergillus terreus* NIH2624 65% identity; B8NQM9 from *Aspergillus flavus* NRRL3357 50% identity and Q2UBB0 from *Aspergillus oryzae* RIB40 50% identity. *Aspergillus* species are known to be good lignin degrading strains.[163] A protein from *Nectria haematococca mp*VI (C7ZEG5), another lignin degrading strain, was also found and it had 53% idenity.[164] The remaining three hits were B6H985 from *Penicillium chrysogenum* 51% identity, B8M7R5 from *Talaromyces stipitatus* 50% identity and B6QFT7 from *Penicillium marneffei* 50% identity. *P. chrysogenum* is a known lignin degrader[165] and *T. stipitatus* produces a fereulyl esterase that is involved in plant cell wall degradation.[166] The fact that so many fungi involved in cell wall breakdown show proteins with such high degrees of identity, is striking, and supports the hypothesis that DypB might be involved in lignin degradation.

5.3 Bioinformatic analysis- Laccase

We identified a gene (accession number Q0SE54, RHA1 designation ro2377) in *Rhodococcus jostii* RHA1 which shares 28% sequence identity with a fungal laccase, Tvl (accession number Q12718), from *Trametes versicolor*, that shows activity in lignin breakdown.[167] This was done by using a blast search to look for bacterial protein sequences that had a similarity to Tvl. We have designated the putative *Rhodococcus jostii* RHA1 multi-copper oxidase as *mco*. The encoded Mco protein contains 494 amino acids (Mr 53,262) and contains a TAT protein export signal sequence. The alignment of these two sequences are shown in Figure 5.4.

In the crystal structure of Tvl there are four coppers, three of these form a cluster and one of them is separate. The binding for the cluster is made up of eight histidine residues (H64, 66, 109, 111, 398, 400, 452 and 454) these are all conserved in mco (H139, 141, 163, 165, 431, 433, 475 and 477). The three ligands that bind the lone copper atom are conserved (H396, H458 and C453) but F463 which is near the active site is mutated to M486. This change generally lowers the redox potential lacases because the methionine binds, increasing the electron density around the copper centre.[167] In Tvl there is a hydrogen bond between E460 and S113 that extends the Cu-N bond length for H395. This has the effect of deshielding the copper and raising the redox potential.[167] In mco E460 and S113 are not conserved there positions in the alignment are instead held by A482 and D167 resptectivly. One would expect this to also lower the redox potential for mco.

```
mco           MPGNRPLDPQLSRRRVLQWGAGAALLGLTGACARSDDTEAAIGPDSPEVR 50
Tvl           ----------------------------------------AIGP------ 4
                                                        ****

mco           AYAESEERRFPGGRPIAYELSATQSDVDIAGTRTAAWLYNTQLPGPILRA 100
Tvl           ----------------AASLVVANAPVSPDGFLRDAIVVNGVFPSPLITG 38
                             * .* .::: *.  *    * : *  :*.*:: .

mco           DVGDRVQVRFRNQLP-----DPTTVHWHGLAIR--NDMDGVPDVTQAPIP 143
Tvl           KKGDRFQLNVVDTLTNHTMLKSTSIHWHGFFQAGTNWADGPAFVNQCPIA 88
              . ***.*:.. : *.     ..*::****:     *  ** . *.*.**.

mco           AGTEFVYDFIPPD-SGTYWYHTHGDLQRGRGLYGALIVDDPAAPAN---- 188
Tvl           SGHSFLYDFHVPDQAGTFWYHSHLSTQYCDGLRGPFVVYDPKDPHASRYD 138
              :* .*:***  ** :**:***:* . *   ** *.::* **  *

mco           -YDAEFVVVLSDWLTDRTPSQVFDELRGGRMTSMAEMTSPVLSGDSGDVR 237
Tvl           VDNESTVITLTDWYHTAAR-------LGPRFPLGADATLINGLGRS---- 177
                : . *:.*:**    :         * *:.  *: *     * *
mco           YPVYLLNGKPPGDPAVFTARPGQRARIRLINAGDDTAFRVALGGHRLTVT 287
Tvl           ------ASTPTAALAVINVQHGKRYRFRLVSISCDPNYTFSIDGHNLTVI 221
                     ..*..  **:..: *:* *:**:. . *. : .::.**.***

mco           DTDGFPVEPVDTDSVLIGMGERYDAVVTLQD-------GAFPLVAVAEGK 330
Tvl           EVDGINSQPLLVDSIQIFAAQRYSFVLNANQTVGNYWIRANPNFGTVGFA 271
              :.**:  :*: .**: *  .:**. *:. ::        * * ....

mco           GAQGFAVVRTGGGAAPDPAVVPRELGPPPLTVADLRATDAVRLP--VVDP 378
Tvl           GGINSAILRYQGAPVAEPTTT-QTTSVIPLIETNLHPLARMPVPGSPTPG 320
              *. . *::*  *....:*:.. :  .  **  ::*:.   : :*   .

mco           GVTLEASLGGDMKQYVWTVNGRAYP-----------------------D 404
Tvl           GVDKALNLAFNFNGTNFFINNASFTPPTVPVLLQILSGAQTAQDLLPAGS 370
              **    .*. :::   : :*. ::.                      .

mco           HTPLTVHRDQRVRLVYTNPT-MMFHPMHLHGHTFAVARPDGSGPR----- 448
Tvl           VYPLPAHSTIEITLPATALAPGAPHPFHLHGHAFAVVRSAGSTTYNYNDP 420
                 **..*   .: *  *  :    **:*****:***.*. ** .

mco           -----KDTVIVLPGQTVAADIDTTNPGRWITHCHNDYHLAAGMATIFSYV 493
Tvl           IFRDVVSTGTPAAGDNVTIRFQTDNPGPWFLHCHIDFHLEAGFAIVFAED 470
                    .*    .*:.*:  ::* *** *: *** *:** **:* :*:

mco           S---------------------------- 494
Tvl           VADVKAANPVPKAWSDLCPIYDGLSEANQ 499
```

Figure 5.4 Protein sequence alignment between Tvl from *T. versicolor* (Q12718) and mco (Q0SE54) from *R. jostii* RHA1. Alignment carried out using CLUSTAL 2.0.12

In addition to mco there was a laccase from *Rhodoccus sp*., B5ABG9, which showed sequence similarity with Tvl. It has 28% sequence identity. However, since prior work had also identified an interesting peroxidase from *R. jostii* RHA1 we focused are efforts on this micro-organism.

5.4 Bioinformatic analysis- Versatile Peroxidase

Another protein that is used by fungi to degrade lignin is Versatile Peroxidase (VP).[69] A blast search was carried out to find similar proteins in bacteria. A number of similar hits were found: a catalase, Q21DT6, from *Saccharophagus degradans*, which had 31% identity and 51% positives; B6B0P8 from *Rhodobacterales bacterium* 30% identity and 40% positives; A1TZH9 from *Marinobacter aquaeolei*, which had 27% identity and 41% positives; EEB59661.1 (sequence from GenBank) from *Pseuonmonas syringe pv. tomato T1* which had 27% identity and 44% positives. *S. degradans* is known to have some ability to grow on lignin.[168] If so it could be that up regulation of Q21DT6 could give an increased lignin degrading ability. *P. syringe* is also of interest as it is a known plant pathogen thus it seems like a likely lead bacterium for future searches for lignin degrading enzymes.[169]

5.5 Bioinformatic analysis- Encapsulin

As mentioned above, DypB seems to include a targeting sequence for encapsulin. This lead us to use a blast algorithm to search for fungi and bacteria with encapsulin hololog ues to see if this corresponded with lignin degrading micro-organisms. Dyp proteins are often closely associated with encapsulin.[162] The blast search was performed with the encapsulin sequence from *Thermotoga miaritima* (B1L7S2), the first encapsulin protein identified and characterised. This produced over 200 highly conserved (67-100% identity).

Among these hits a number of bacteria stood out as being of interest. From the original Dyp homologues identified in section 5.2 *N. farcinica* and

mycobacterium tuberculosis had encapsulin homologues (Q5YPL3 99% and Q7U190 99% identity). In addition *Rhodococcus opacus* (C1B1V8) and *Rhodoccus erythropolis* (C3JL93), which separate work in our group has also shown to have DypB homologues, also had encapsulin homologues. These are positioned directly downstream from the DypB homologues analogous to the situation in *R. jostii* RHA1.

5.6 Conclusion

Bioinformatics showed two proteins of interest from *R. jostii RHA1*. These are DypB and mco. DypB was identified by its homology with other peroxidases of unknown function in other known degrading species. The laccase mco was identified due to its similarities to a homologous laccase in the known fungal degrader *T. versicolor*.[167] As both these proteins came from the *R. jostii* RHA1 and because this strain has shown activity in the nitrated lignin and fluorescence assay they were chosen for further study. The laccase was of particular interest as it can work without hydrogen peroxide and this makes it far more applicable to industrial applications than a peroxidase.

The similarities between fungal proteins and bacterial proteins seemed very high and this caused us to consider whether horizontal gene transfer might be involved. This is a phenomenon where genes are exchanged between different species.[170] However, on careful scrutiny of the lacase structure it was clear that this was not the case as the fundamental way in which the enzyme worked had changed substantially, illustrated by key changes around the mono nuclear copper site. In the case of DypB, a phylogram illustrates that the bacterial and

fungal proteins are each most closely related to themselves. This is consistent with a normal evolutionary process. It is noted that the TyrA sequence has less similarity to DypB than do the other bacterial proteins. This is probable because whilst all are dye decolourising peroxidases, the biological role of TyrA is probably very different to that of DypB.

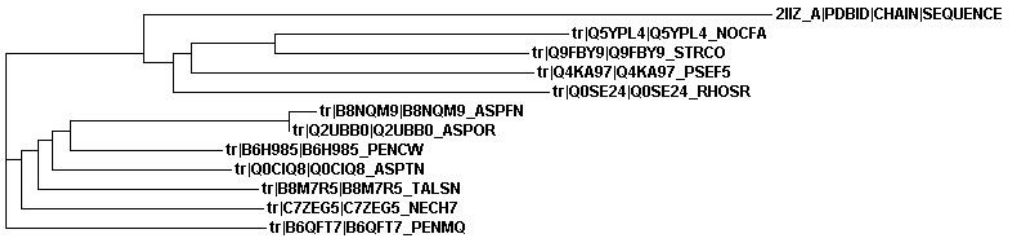

Figure 5.5 Phylogram of TyrA(2IIZ_A) from *S. oneidensis*, Q5YPL4 from *N. farcinica*, Q9FBY9 from S. coelicolor, Q4KA97 from P. fluorescens and DypB (Q0SE24) from *R. jostii* RHA1.

Whilst mco and DypB will be the focus of this study, the bioinformatics above has highlighted a number of other bacterial species that are of further interest from the perspective of finding lignin degrading enzymes. The versatile peroxidase homologues in *P. syringe* seems a particularly promising lead as it seems likely that a plant pathogen which disrupts the plant outer cell wall will have a method for dealing with lignin.

The fact that DypB and encapsulin often occur together may explain why the high salt concentrations are needed for the nitrated and fluorescence assay. High salt concentrations could break up the encapsulin, allowing the DypB to come into contact with the lignin.

Mycobacterium tuberculosis is something of a curiosity in the above study having both Dyp and encapuslin homologues. It seems dubious as to whether this has anything to do with lignin degradation. There has been an example of Dyp proteins being involved in iron scavenging by removing iron from heme rings.[171] This activity would definitely be an advantage to *M. tuberculosis*. If this is the case it could prove an interesting site for therapeutic intervention, however this lies well beyond the scope of this work, but any further understanding gained on how Dyp proteins work can only be of help.

CHAPTER VI Identification and Molecular Characterisation of DypB from *Rhodoccus jostii* RHA1 as a Lignin Peroxidase

6.1 Introduction

Rhodoccus jostii RHA 1, a previously known polychlorinated aromatics degrader,[145] has been shown to degrade lignin (Ch II). Bioinformatics research has identified two genes of interest: ro5773 and ro2407 (Ch V). These encode for dye decolourising peroxidases (Dyps).

The first example of this type of enzyme was isolated from the fungus *Thanatephorus cucumeris*.[172] This enzyme had a number of peculiarities when compared to previous peroxidases. The most striking of these is that the distal histidine, which is involved in the formation of an Fe^{4+} oxoferryl center and a porphyrin based cation radical is replaced with an aspartic acid group.[172] The two mechanisms for compound I formation are illustrated in Figure 6.1.[173] In the mechanism hydrogen peroxide binds to the heme iron and interacts with the distal aspartate/histidine and arginine. The oxygen oxygen bond then cleaves homolytically to give water and an iron (IV) oxeme known as Compound I. This is a cation radical species where the radical is predominantly found on protein residues in heme peroxidises.[47] The elucidation of this mechanism is discussed in detail in section 1.5.

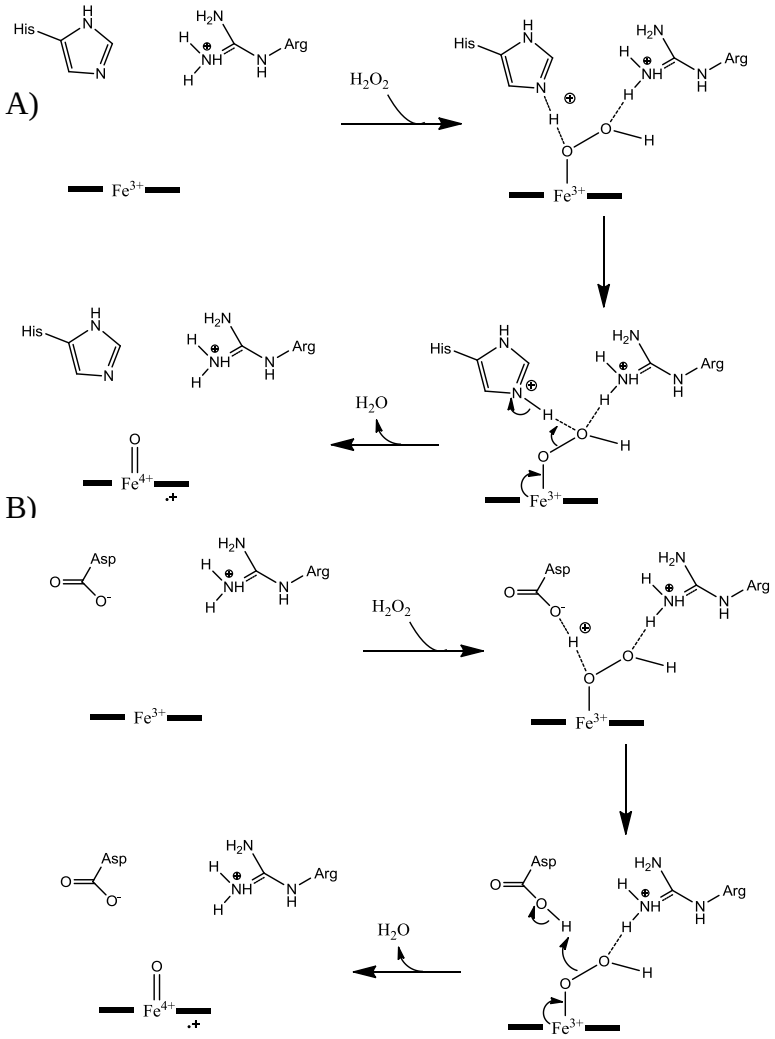

Figure 6.1 A) Classical mechanism for compound I formation; B) Possible mechanism for compound I formation in Dyp proteins where the distal histidine is replaced with an aspartic acid.[173]

Consequently the enzyme has a lower optimal pH (3-3.2) than a traditional plant peroxidase,[174] but the optimum is similar to that of LiP (~3.0).[175] It also has a wider activity for aromatic dyes. Finally, no compound II has been detected by spectroscopy for a Dyp protein.[176] These three features, combined with its lack of homology with previous peroxidases, has lead to the proposal of dye decolourising peroxidases being seen as a new family of heme peroxidases.[176]

The precise function of the Dyp from *T. cucumeris* is unknown.[176] Its activity towards dyes is consistent with an activity towards lignin, but the fungus' overall lignin degrading ability is modest.[177] In *E. coli* there are two Dyp homologues EfeB and YfeX. Phylogenetic analysis shows EfeB clusters with DypA and YfeX clusters with DypB.[178] EfeB and YfeX have been shown to have activity as deferrochelatases.[171] This activity is consistent with the presence of Dyp proteins in a number of different bacteria including some pathogenic strains, which one would expect to have no use for a lignin degrading enzyme e.g. *Mycobacterium tuberculosis*. DypA and DypB may under some circumstances play a similar role in iron scavenging. DypA and YfeX have TAT secretion sequences whilst EfeB and DypB do not. DypB has been shown to have a targeting sequence that in other cases has been shown to target export to a nanocompartment formed of the protein encapsulin.[163] The deferrochelatase activity above has been shown to be intracellular. This adds an extra degree of confusion to what the function of DypA and DypB may be, as encapsulin complexes are extracellular.[163] Here the nitrated lignin assay is combined with kinetic studies and LC/MS studies on the break down of model compounds in order to study the role of DypB in lignin degradation. The nitrated lignin assay is also used to study a gene knock out of a potential laccase.

6.2 UV-visible assays of gene deletion mutants and recombinant DypB and DypA

To investigate the function of DypA and DypB the extracellular supernatent of gene deletion mutants (provided by Prof. L. Eltis) were assayed with the nitrated lignin assay for activity in lignin degradation. In addition, a knock out of the

multi copper oxidase (mco) was also assayed. In Figure 6.2 the *dypB*$^-$ strain shows a marked decrease in activity in both the presence and absence of hydrogen peroxide, whereas the *dypA*$^-$ strain retains activity, consistent with a role for DypB in lignin breakdown. The *mco*$^-$ strain shows activity in the presence of hydrogen peroxide, but no activity in the absence of hydrogen peroxide, consistent with a possible role as a laccase enzyme in lignin breakdown.

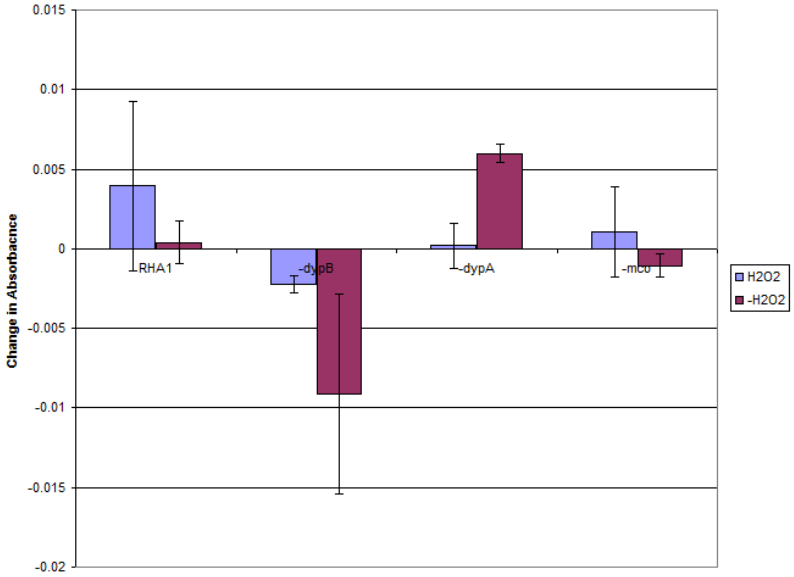

Figure 6.2 Activity of culture supernatant (30 µl) obtained from wild-type RHA1 and gene deletion mutants in ro2407 (dypB), ro5773 (dypA), and ro2377 (mco) for nitrated lignin (0.01mg/ml), in the presence (blue) and absence (purple) of hydrogen peroxide (2mM). Measuring change in absorbance at 430 nm over ten minutes.

Recombinant DypB and DypA were overexpressed (by Prof. L. Eltis) and assayed with nitrated lignin. Each protein was assayed with 0.015mg/ml of protein and 9.75µM of nitrated lignin and without 2mM hydrogen peroxide. As shown in Figure 6.3, DypA had no activity whilst DypB was active in the presence of hydrogen peroxide but not without. This is consistent with DypB

being a lignin degrading peroxidase but suggests that DypA serves another purpose.

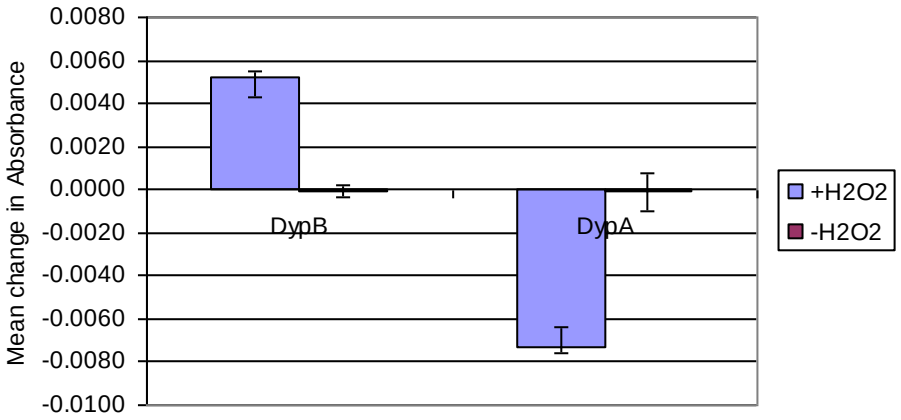

Figure 6.3 Activity of recombinant DypA and DypB protein (15 μg/ml) with nitrated lignin (10 μM), in the presence (blue) or absence (purple) of hydrogen peroxide (2mM). Measuring change in absorbance at 430 nm over ten minutes.

The nitrated lignin assay was subsequently implemented in the presence of 1 mM Mn^{2+} and a four fold increase in absorbance was observed, see Figure 6.4. This suggests that the Mn^{2+} might play a role as a cofactor, similar to in MnP. Small organic molecules have also been postulated to be able to aid enzymatic lignin breakdown.[43, 179] To investigate this the assay was repeated in the presence of 1 mM syringaldehyde. However, the background increase in absorbance was very high even when no protein was present, presumably through a background chemical reaction of the syringaldehyde such as oxidation.

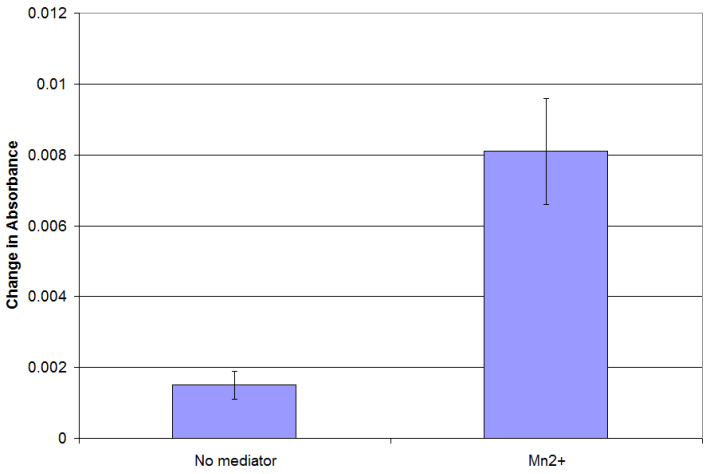

Figure 6.4 Activity of recombinant DypB for nitrated lignin in the presence and absence of Mn^{2+}. Dyp B (15 μg/ml), was mixed with nitrated lignin (10 μM) with and without Mn^{2+} (7.5 mM) in the presence of hydrogen peroxide (2 mM) at pH 7.4 in 750 mM tris buffer the change in absorbance at 430 nm was then observed over ten minutes.

6.3 Scale up-reactions of DypB on lignin and lignocellulose

DypB's lignin-degrading activity was then tested against samples of lignin and lignocellulose. When incubated with wheat straw lignocellulose 1 mg/ml in the presence of 1 mM $MnCl_2$, with 0.3 mM glucose and 0.5 μg/ml glucose oxidase to provide a source of H_2O_2, large changes in the resulting reverse phase HPLC chromatogram were observed after 48 hours, as shown in Figure 6.5. In the case of the control where no DypB was present, no change was observed.

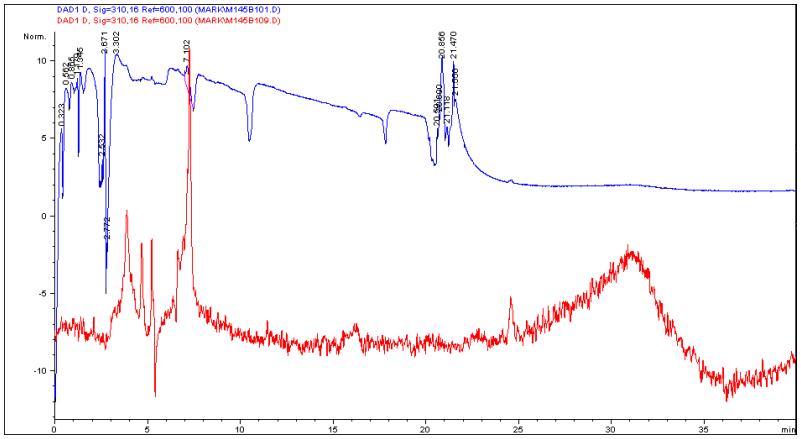

Figure 6.5 Effects of recombinant DypB upon lignocellulose. Analysis by reverse phase HPLC of extracts from an incubation of 2 μg/ml DypB and 1mg/ ml lignocellulose, in the presence of 1 mM $MnCl_2$, 0.3 mM glucose and 0.5 μg/ml glucose oxidase after 48h (blue) and without DypB (red).

No changes were observed in the absence of Mn^{2+}, implying that Mn^{2+} plays an important role in the breakdown of lignocellulose by DypB. In addition, no change was seen when hydrogen peroxide was used directly. With lignin the changes in the HPLC were smaller but still visible. After 24 hours peaks at 17 and 21.5 minutes could be seen to decrease, as shown in Figure 6.6. For the control where no DypB was present no change in the HPLC spectrum was observed.

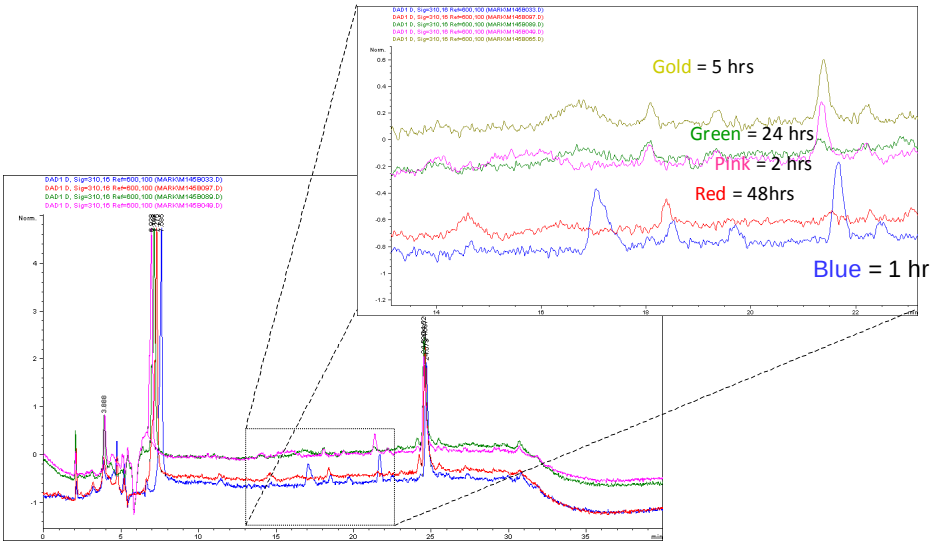

Figure 6.6 Effects of recombinant DypB on lignin. Analysis by reverse phase HPLC of extracts from an incubation of 2 μg/ml DypB and 1mg/ ml wheat lignin, in the presence of 1 mM $MnCl_2$, 0.3 mM glucose and 0.5 μg/ml glucose oxidase.

6.4 Kinetic evaluation of recombinant DypB and DypA

Incubation of DypB with samples of Kraft lignin (see section 8.7.5) was found to result in a time-dependent change in the UV-visible spectrum at 465 nm. This wavelength had previously been used to study enzymatic modification of kraft lignin.[85] Kinetic measurements at this wavelength at a range of $MnCl_2$ concentrations followed Michaelis-Menten kinetics, allowing the measurement of an approximate K_m value of 8.4 (error = +16 – 6.4) mM for Mn^{2+}, and a k_{cat} value of 7.7 (error = + 8.8 -3.4) s^{-1}. The Eadi-Hofstee, Lineweaver Burk and rate Vs [S] plots for Mn^{2+} are given in Figure 6.7. This is consistent with the Mn^{2+} being both bound and turned over.

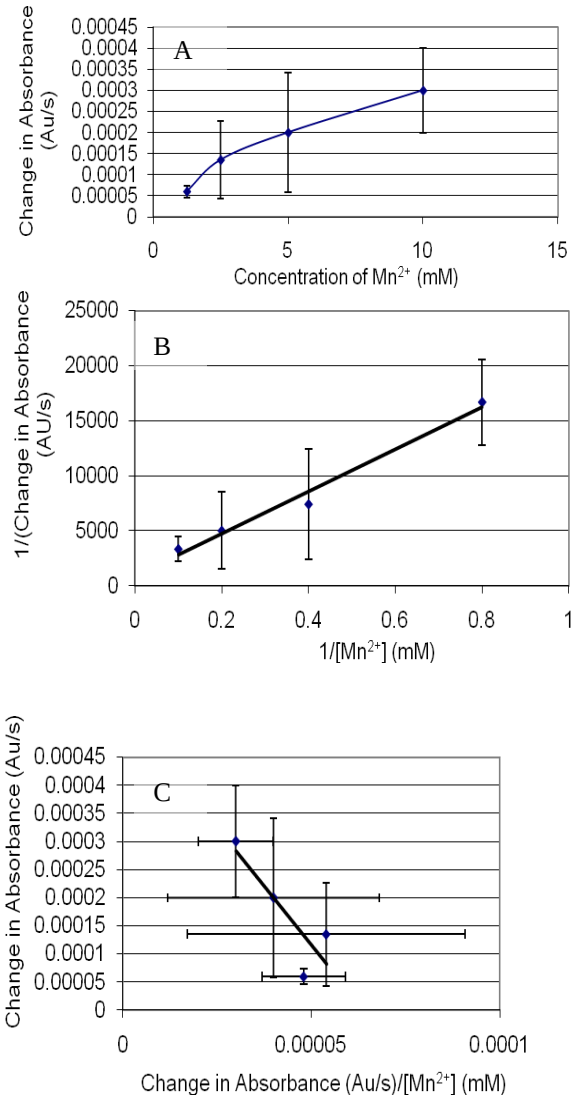

Figure 6.7 Kraft lignin (0.25 mg/ml), DypB 25 (μg/ ml), hydrogen peroxide (2 mM), Mn^{2+} (various) and pH 5.5 succinate buffer (50 mM) were mixed in a 1ml cuvette and the change in absorbacne was measured at 465nm. This allowed the determination of approximate k_{cat} and K_m values. A) Mn^{2+} concentration Vs Change in Absorbance; B) $1/Mn^{2+}$ concentration Vs 1/Change in Absorbance. This gave a K_m = 19.8 (error = +12.5 -16.5) mM and a k_{cat}= 16 s^{-1} (error = +16 -11); C) Change in Absorbance/ Mn^{2+} concentration Vs Change in Absorbance. This gave a K_m = 8.4 (error = +16 – 6.4) mM and a k_{cat} = 7.7 (error = + 8.8 -3.4) s^{-1}.

Michaelis-Menten kinetics were also observed for the kraft lignin. Allowing the measurement of a K_m value of 8.2 (error = +190 -4.7) μM and a k_{cat} of 6 (error = +63 -2) s^{-1} The Eadi-Hofstee, Lineweaver Burk and rate Vs [S] plots for kraft lignin are given in Figure 6.8. The K_m, and k_{cat} observed are consistent with the kraft lignin being both bound and turned over. This suggests that DypB has a binding site for lignin. Similar values for K_m and k_{cat} have been measured for TyrA with dye substrates.[160] However, there is substantial uncertainties in the K_m and k_{cat} values reported. Uncertainty is introduced by the small number of

data points used and by the fact that the kraft lignin concentration is calculated with an average molecular mass 10000.

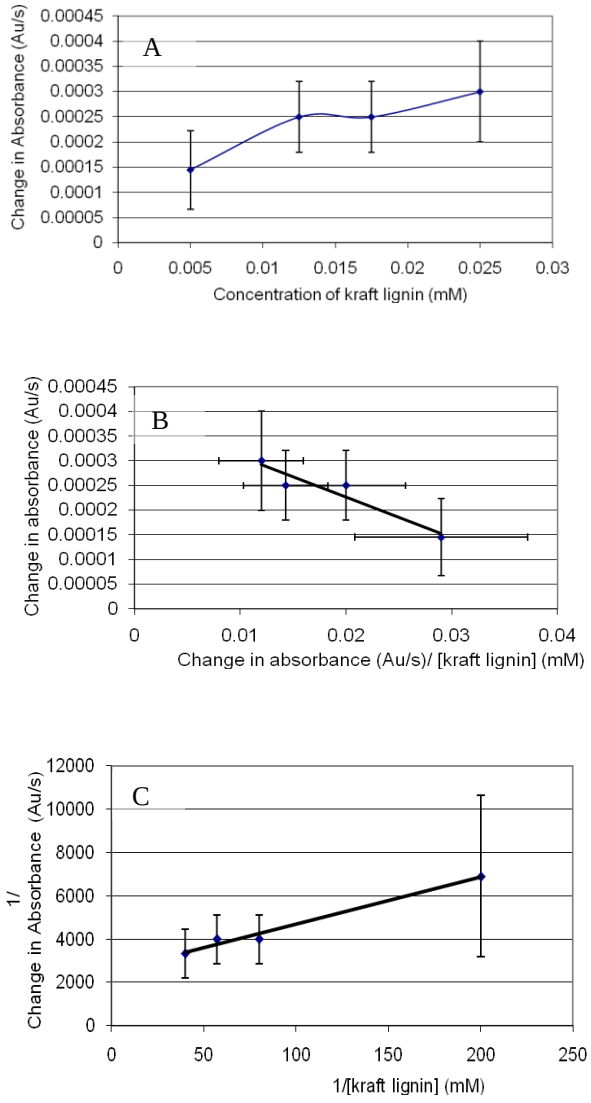

Figure 6.8 Kraft lignin (0.25 various), DypB 25 (μg/ ml), hydrogen peroxide (2 mM), Mn^{2+} (10 mM) and pH 5.5 succinate buffer (50 mM) were mixed in a 1ml cuvette and the change in absorbacne was measured at 465nm. This allowed the determination of approximate k_{cat} and K_m values. A) Kraft lignin concentration Vs Change in Absorbance; B) 1/kraft lignin concentration Vs 1/Change in Absorbance. This gives a K_m = 8.7 (+18 – 1.4) μM and a k_{cat} = 6.0 (±6) s^{-1}; C) Change in Absorbanc/kraft lignin concentration Vs Change in Absorbance. This gives a K_m = 8.2 (+190 -4.7) μM and a k_{cat} = 6.0 (+63 -2) s^{-1}

Further information on the rate of lignin degradation was gathered by testing DypB activity against the compound **27** at a starting concentration of 2 mM. Compound **27** was synthesised in chapter II. Quntitative HPLC was then used to monitor the rate of β-aryl ether disappearance, by measuring the decrease in the peaks at 28.2 and 28.8 minutes over time. These two peaks corresponded to the *erythro* and *threo* distereomers of compound **27**. The activity was estimated by

taking the integral of each peak at a given time point and converting this to a concentration through comparison to a known standard. The experiment was done with 1 mM Mn^{2+} and without. This then allowed change in concentration to be plotted against time, Figure 6.9. The rate with Mn^{2+} was for the *erythro* 0.0528 $\pm$ 0.00317 mM h^{-1} and 0.0141 $\pm$ 0.000141 mM h^{-1} for the *threo*. Without Mn^{2+} the rate was effectively zero. The rate can be converted into a specific activity by converting into μM $min^{-1}$and then accounting for the amount of protein which was 2 μg. The results for this calculation are summarised in Table 6.1. The specific activity with Mn^{2+} for the *erythro* isomer was 440 $\pm$ 264μM min^{-1} mg^{-1}. The specific activity for the *threo* isomer with Mn^{2+} is 117.5 $\pm$ 1.2 μM min^{-1} mg^{-1}. The activity plots for loss of compound **27** with Mn^{2+} are shown in Figure 6.10. This is a low activity but subsequent investigation has shown that the enzyme is not at its ideal pH (Section 6.7) where rates could it is a promising sign for the overal activity of the enzyme for lignin like material.

Rate (mM h^{-1})	Rate (mM min^{-1})	Rate (μM min^{-1})	Specific Activity (μM $minutes^{-1}$ mg^{-1})	Error (±)
0.0528	0.00088	0.88	440	26.4
0.0141	0.000235	0.235	118	1.2

Table 6.1 The specific activity of DypB for *erythro* and *threo* isomers of **27** with Mn^{2+} based upon a total amount of protein of 2 μg and the rate of disappearance observed in Figure 6.10.

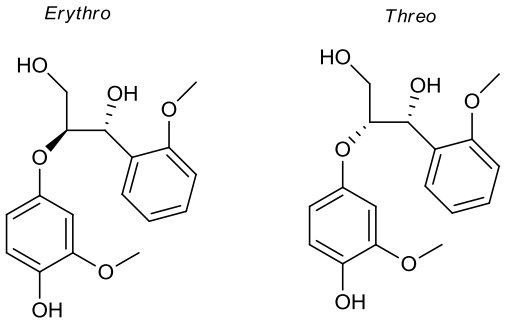

Figure 6.9 The two diasteomers of compound **27**. The *erythro* isomer corresponds to the S, R diastereomer and the *threo* to the R, R. 2-(2-methoxyphenoxy)-1-(4-hydroxy-3-methoxyphenyl) 1,3-propanediol.

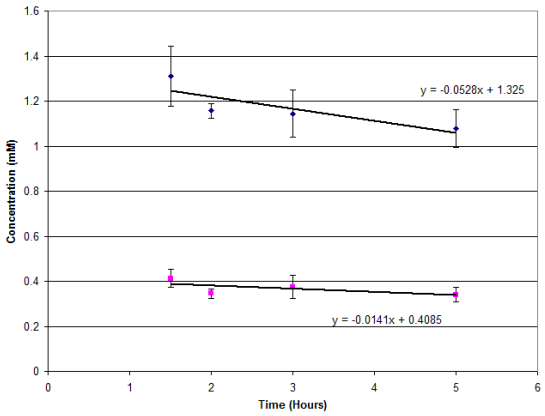

Figure 6.10 Rate of conversion for erythro (blue) and threo (pink) diastereomers of compound **27** (2 mM) with DypB (2 μg/ml), Mn^{2+} (1mM) and hydrogen peroxide (0.8mM).

6.5 Study of products formed from lignin model compounds

DypB (0.5 μg/ml) was mixed with guaiacol (2mM), which can be considered a lignin monomer unit,[180] in succinate buffer pH 5.5. The guaiacol was turned over and a wide variety of products were made as shown by the multiple peaks in Figure 6.11.

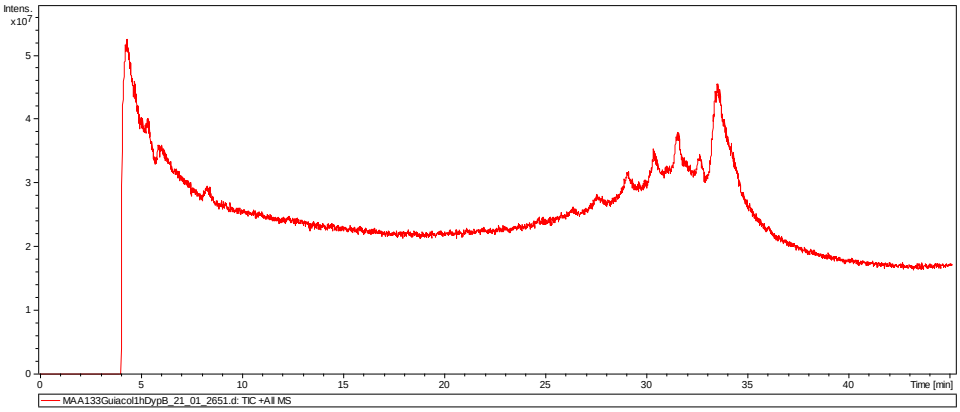

Figure 6.11 Total ion chromatogram for sample of for DypB (0.5μg/ml) with guaiacol (2mM) in 50mM succinate buffer at pH 5.5 with hydrogen peroxide (0.8 mM) after 1 hour.

An extracted mass chromatogram was used to highlight the presence of a peak at a retention time of 27.5 minutes where the major product has an m/z of 407. This corresponds to MK^+ for a guaiacol trimer, compound **62**. In the same experiment there is a strong peak at 391 m/z this would correspond to the Na^+ adduct. The structure for the guaiacol trimer is that suggested from chemical oxidation of guaiacol.[181]

A)

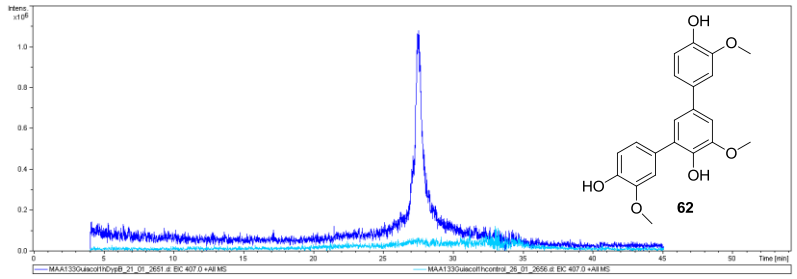

B)

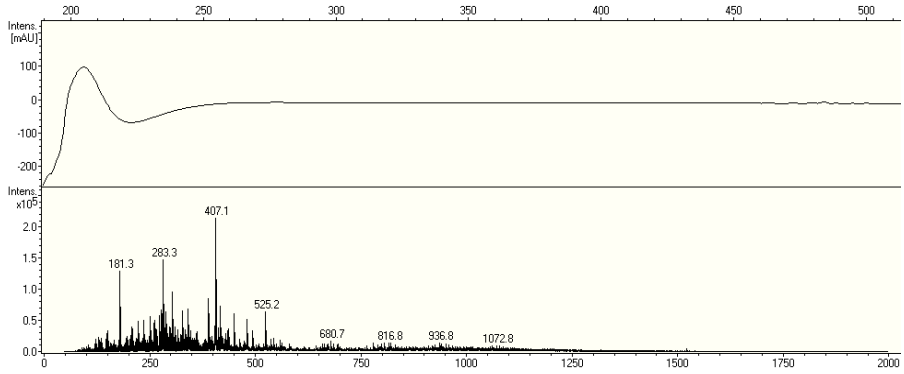

Figure 6.12 Extracted ion chromatogram 407 m/z after 1hour for DypB (0.5µg/ml) with guaiacol (2mM) in 50mM succinate buffer at pH5.5 (dark blue) with hydrogen peroxide (0.8 mM). In light blue is the control where no DypB is present. Trimer structure shown in right hand corner. B) Mass spectum for between 26.5 and 29 minutes.

The trimer is present in the 1-hour sample but not in samples from latter time points. However, the structure for an analogous pentamer at the 5 h time point is seen, as shown in Figure 6.13. None of the above oligomers are seen when no DypB is added to the solution which suggests that guaiacol is being polymerised by the DypB.

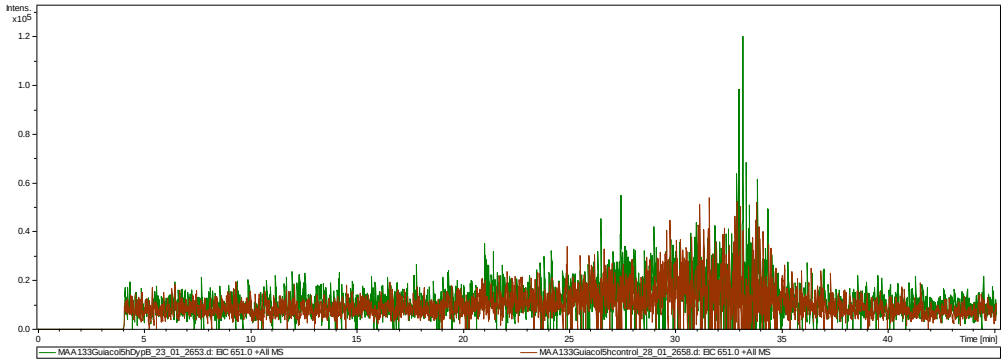

Figure 6.13 Extracted mass chromatogram 651m/z, possible guaiacol pentamer (MK^+), from 5 hours sample of DypB (0.5μg/ml) with guaiacol (2mM) in 50mM succinate buffer at pH 5.5 (green) with hydrogen peroxide (0.8 mM). In brown is the control with no DypB present.

Further studies were carried out to see if DypB would degrade the lignin dimer, compound **27**, and to investigate what products would form from such a reaction. DypB (2μg/ ml) were combined with β-aryl ether **27**, (2 mM) in pH 5.5 succinate buffer (50 mM) and the products formed were studied by LC/MS. A number of new peaks were present on the chromatogram but the mass spectra contained many peaks with masses mainly between 400-800m/z. Figure 6.14 illustrates that a number of new compounds are formed and that the original dimer is still present. The dimer peak is in both the yellow (control) and red chromatograms at 36 minutes. The main mass peak seen here is 343 m/z (shown in C Figure 6.14), which corresponds to the sodium adduct of compound **27**. The mass spectrum shown in Figure 6.14 comes from between 28 and 34 minutes and shows the wide variety of mass peaks that are present including a number of peaks from contaminating polyethylene glycol, the most clear of which are 446, 490, 534, 578 and 622. These peaks can be recognised by their regular envelope with peaks 44 mass units apart.

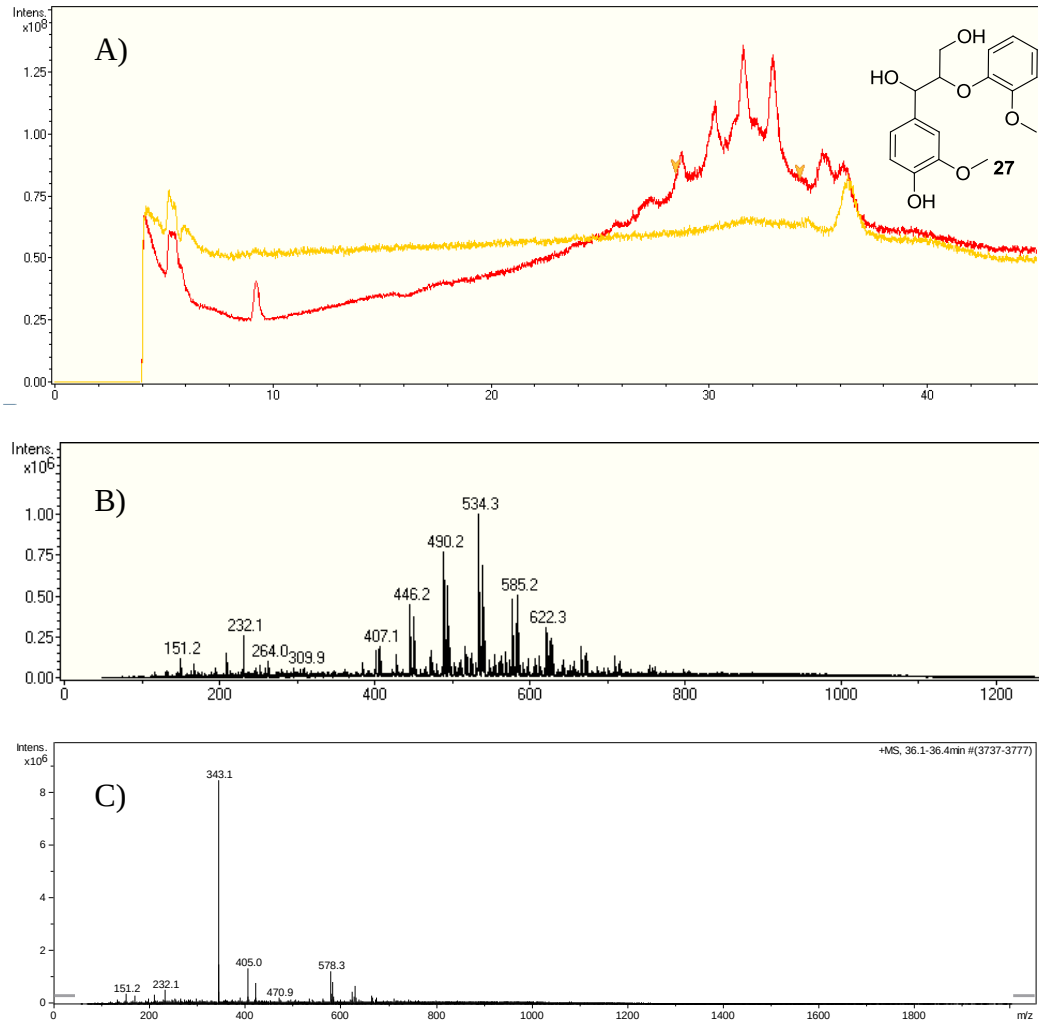

Figure 6.14 A) In red total ion chromatogram, for DypB (0.5µg/ml) with β-aryl ether, **27**, (2mM) in 50mM succinate buffer at pH5.5 with hydrogen peroxide (0.8 mM) after 1 hour. In yellow is the control where no DypB was present after 1 hour. The structure for β-aryl ether, **27** is given in the right hand corner. B) The mass spectrum for between 28-34 minutes for the red chromatogram. C) The mass spectrum for between 36.1-36.4 minutes for the red chromatogram.

Using an extracted mass chromatogram to simplify the total ion spectrum above, it could be seen that a single peak with a mass of 341 m/z at a retention time of 27 minutes was observed that was not seen in the controls. The extracted ion mass chromatogram is used to allow a simple visual manner of observing changes in the abundance of a specific mass ion. This is shown in Figure 6.15. It is suggested that this corresponds to a single oxidation of the β-aryl ether **27**, a

possible structure is given in Figure 6.15. The main evidence for this is it would have the correct mass and that it has been previously observed with other bacterial enzymes, although by a different mechanism.[90] In addition the guaiacol trimer was also observed in the 1h, 3h and 5h samples.

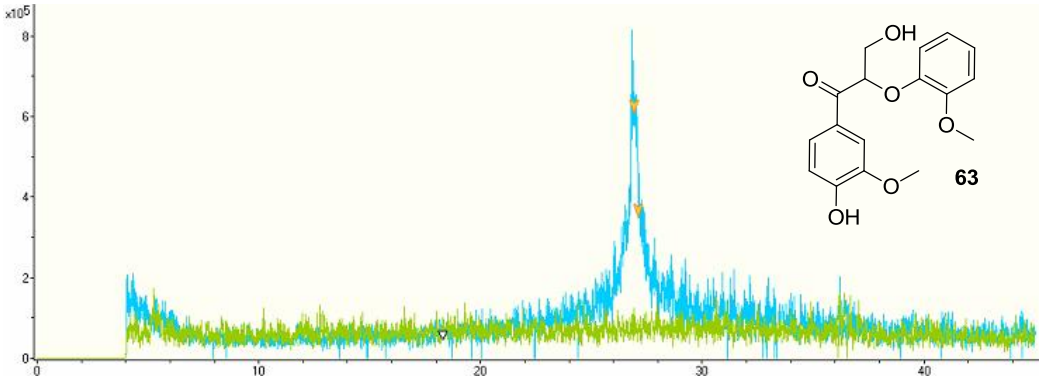

Figure 6.15 In blue is the extracted ion chromatogram 341 m/z for DypB (0.5μg/ml) with β-aryl ether, **27**, (2mM) in 50mM succinate buffer at pH 5.5 after 1hour and the proposed structure compound **63** is given in the right hand corner.

When the above reaction was repeated in the presence of Mn^{2+}, three peaks with a mass of 341 were visible in the extracted ion chromatogram, Figure 6.16. One of these peaks was also in the control. The other two could correspond to the two different structural isomers of the single oxidation product of compound **27**. The guaiacol trimer is clearly in the 1h sample and at a trace level in the 3h sample.

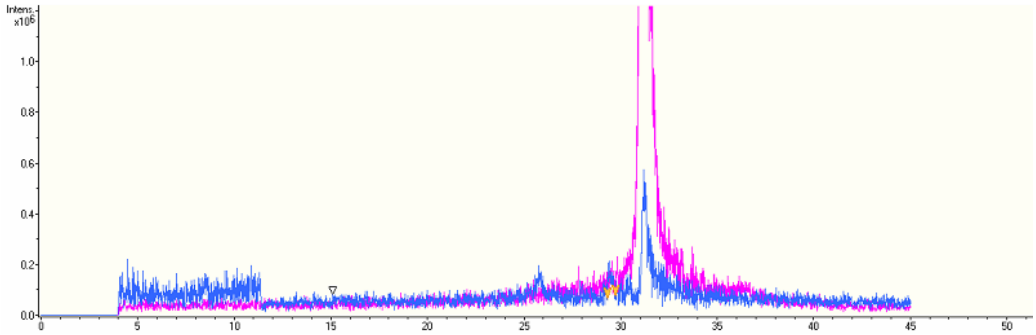

Figure 6.16 In blue is the extracted ion chromoatogram 341 m/z for DypB (0.5μg/ml) with β-aryl ether, **27**, (2mM), $MnCl_2$ (1 mM) in 50mM succinate buffer at pH5.5 with hydrogen peroxide (0.8 mM) after 1hour. In pink is the control where no DypB was present.

It was postulated one of the reasons why the total ion chromatogram given in Figure 6.14 is so complex was because of recombination of radicals formed by DypB. The sort of radical species that could be formed is illustrated in Figure 6.17.

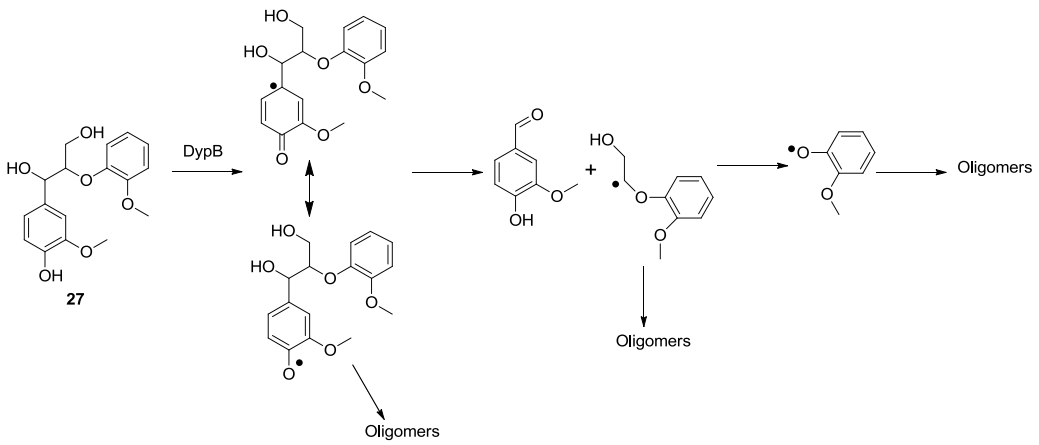

Figure 6.17 Possible route by which radicals and subsequently oligomers could be formed by DypB reacting with compound **27**.

It has been noted that the FAD binding protein dihydrolipoamide dehydrogenase, is very abundant in the proteome of the micro-organism proposed lignin degrading micro-organism *T. fusca*. This enzyme plays an

important role in redox homeostasis quenching radicals.[94] We hypothesised that this enzyme may quench the radicals formed in lignin breakdown in nature.

To investigate the above hypothesis DypB and β-aryl ether **27**, were mixed in succinate buffer pH 5.5 with 1mM Mn^{2+} and 8 enzyme units of diaphorase from *Clostridium kluyveri*. Diaphorase, also known as Lipoyl dehydrogenase, is a related protein to dihdrolipoamide dehydrogenase. With the addition of diaphorase more products could be identified. An extrated ion chromatogram for the ion 191 m/z, showed a peak at a retention time of 28.6 minutes the same as for the authentic standard for compound **33** as seen in Figure 6.18. This is strong evidence for the presence of the compound.

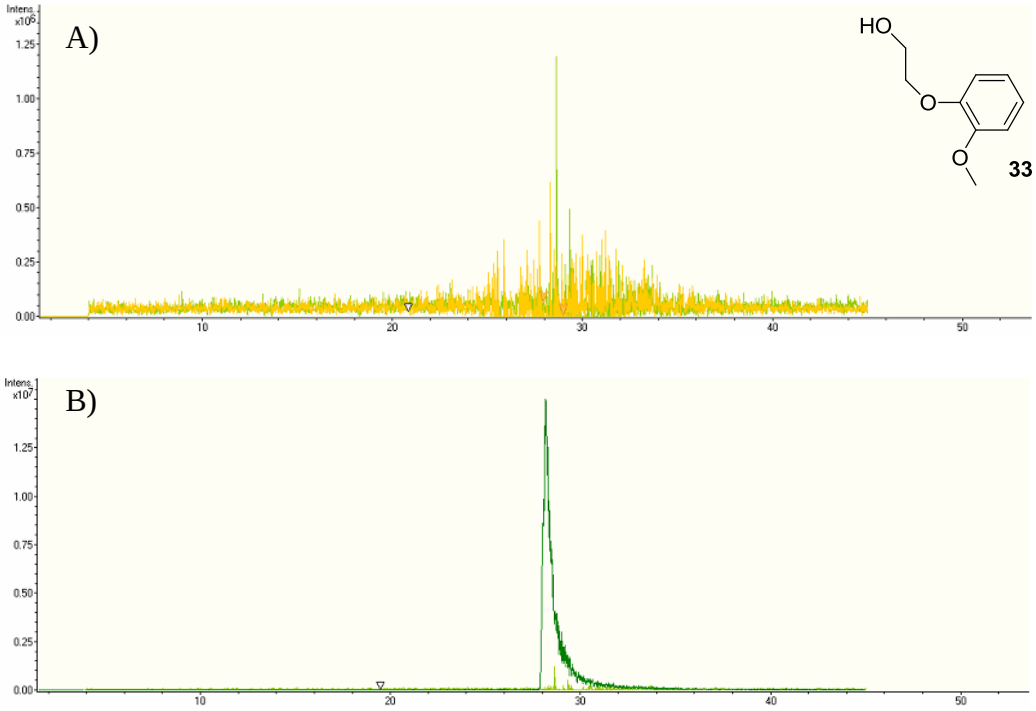

Figure 6.18 A) In green extracted ion chromatogram 191 m/z for DypB (0.5μg/ml) and diaphorase (0.4mg/ml) with β-aryl ether, **27** (2mM), $MnCl_2$ (1 mM) in 50mM succinate buffer at pH5.5 with hydrogen peroxide (0.8 mM) after 1 hour. In yellow is the control with no DypB present. Right hand corner, compound **33**. B) In light green is the same extracted ion chromatogram for 191m/z given in A. In dark green is the extracted chromatogram ion 191 m/z for the authentic standard of compound **33**, with a retention time of 28.6 minutes.

Under the same conditions a peak is seen in the extracted mass chromatogram for ion 153 m/z and retention time of 28.4 minutes, this is shown in Figure 6.18. This is the same as the major ion as for the vanillin **23** standard and at the same retention time. The observation of compound **33** and vanillin is suggestive of C-C cleavage as outlined in Figure 6.20. The observation of the above two products is believed to be because the diaphorase is quenching radicals formed in the reaction and thus allowing intermediates to accumalate. The guaiacol trimer was also observed and this too can be rationalised by the proposed

scheme as even with the diaphorase present some radicals go on to react to form guaiacol and then these go on to oligomerise.

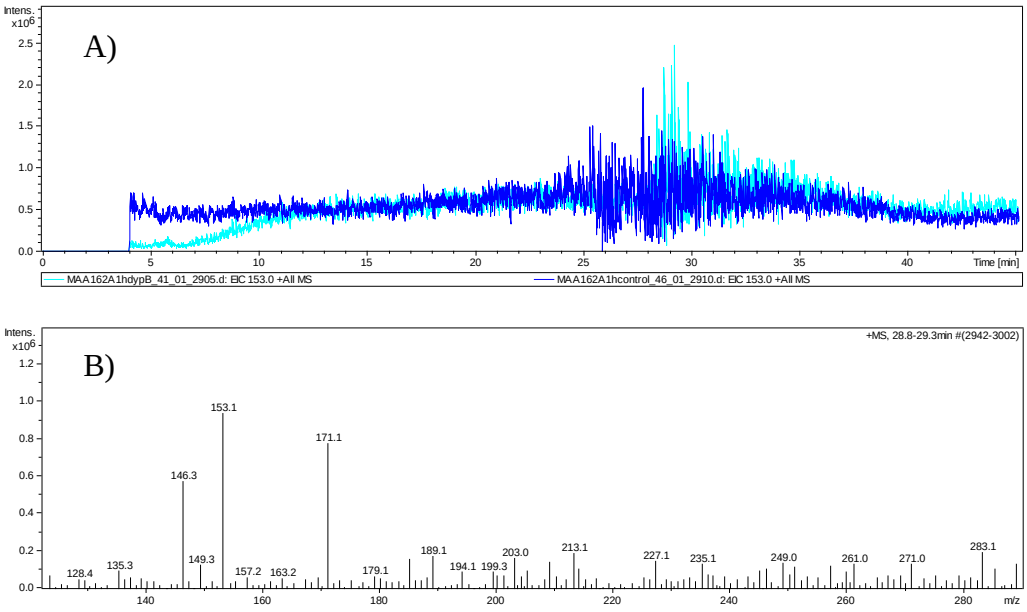

Figure 6.19 A) In light blue the extracted ion chromatogram 153 m/z for DypB (0.5µg/ml) and diaphorase (0.4mg/ml) with β-aryl ether, **27** (2mM), $MnCl_2$ (1 mM) in 50mM succinate buffer at pH5.5 with hydrogen peroxide (0.8 mM) after 1 hour. In dark blue is the control were no DypB was present. B) Mass spectum for between 28.5 and 30 minutes.

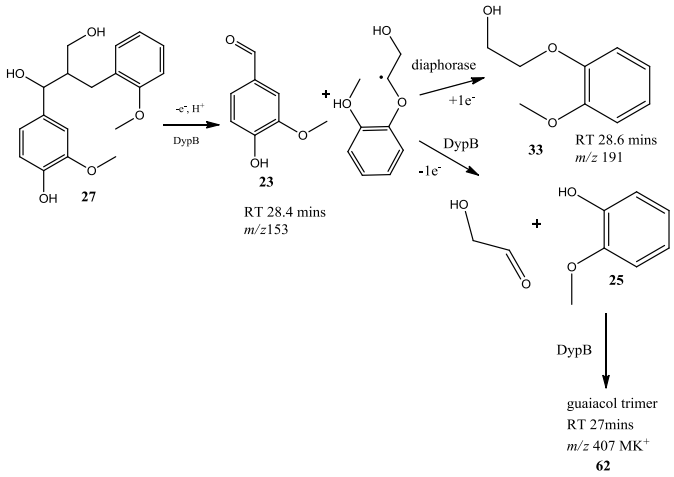

Figure 6.20 Proposed route for formation of vanillin **23**, compound **33** and **62** from β-aryl ether **27** by C-C bond cleavage with subsequent radical quenching by diaphorase.

When the reaction was carried out with diaphorase and with NADH (0.8mM), which the enzyme turns over to regenerate FADH no new products are observed at any mass. This is probably because the diaphorase is now quenching radicals so efficiently that no reaction can occur. This suggests that the cleavage of the β-aryl ether occurs when the β-aryl ether is not bound to DypB.

The reaction was repeated with the four compounds shown in Figure 6.21. In each case no reaction was observed. Representative HPLC traces for compounds **28** and **64** are given in Figure 6.22 to show that nothing happens on mixing with DypB.

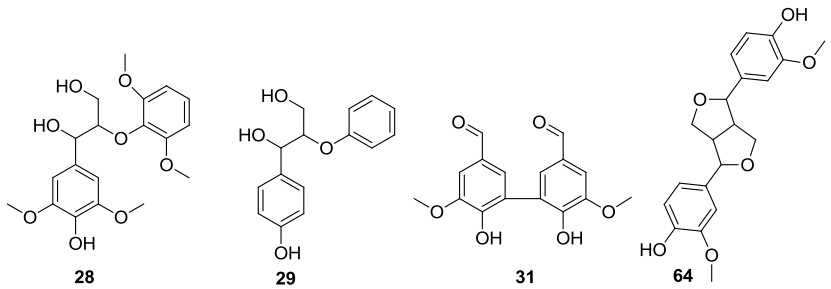

Figure 6.21 From left to right, 2-(2,6-dimethoxyphenoxy)-1-(4-hydroxy-3,5-dimethoxyphenyl)-1,3-propanediol **28**, 1-(4-hydroxyphenyl)-2-phenoxy-1,3-propanediol **29**, 3,3'-dicarboxaldehyde, 6,6'-dihydroxy-5,5'-dimethoxy-1,1'-biphenyl **31,** and pinoresinol **64**.

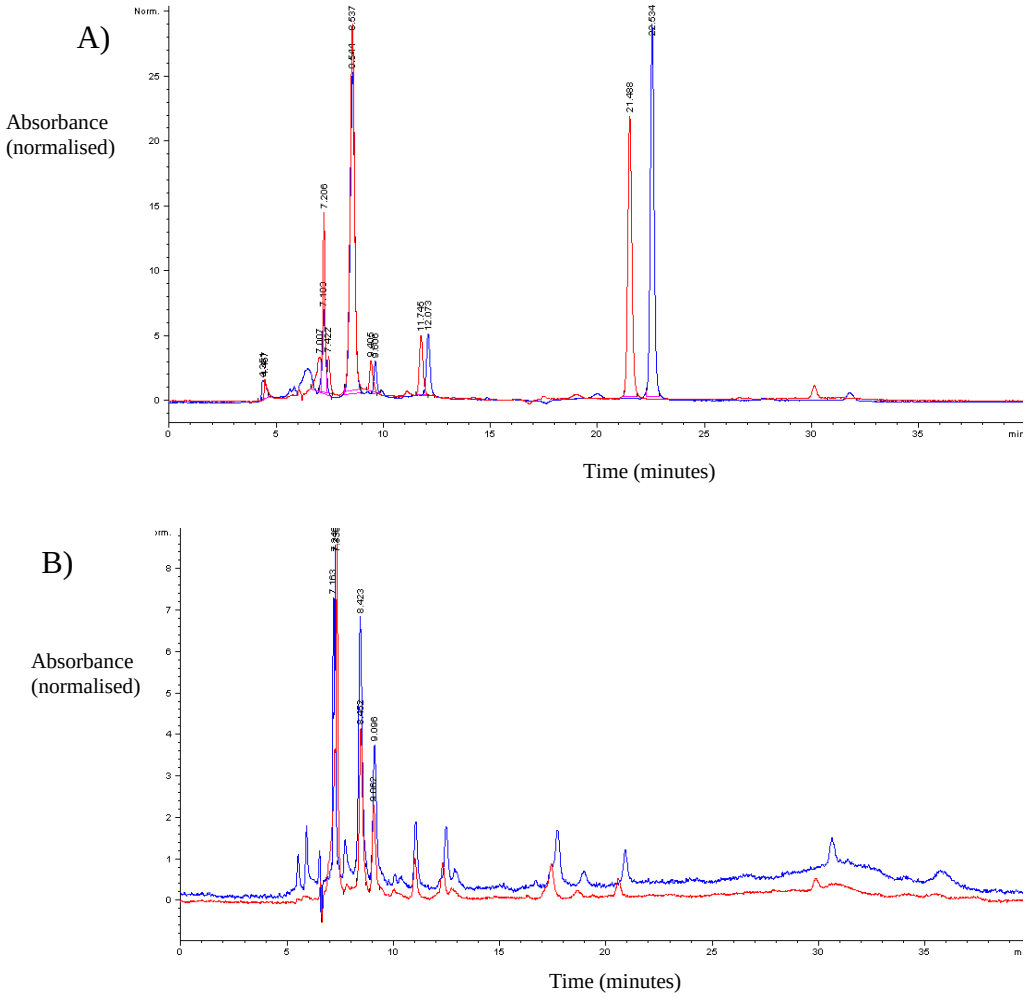

Figure 6.22 A) HPLC trace of β-aryl ether trimer **28** (2 mM) with DypB (0.5 μg/ml), Mn^{2+} (1 mM) and hydrogen peroxide (0.8 mM) in pH 5.5 succeinate buffer (50mM). B) HPLC trace of pinoresinol (2 mM) **64** with DypB (0.5 μg/ml), Mn^{2+} (1 mM) and hydrogen peroxide (0.8 mM) in pH 5.5 succeinate buffer (50mM).

6.6 Pre-steady state kinetics study of DypB

Stopped flow kinetics was used to study the breakdown of lignin dimer **27**, with the aim of understanding whether DypB has a preference for lignin-like material such as dimer **27** or Mn^{2+}. In the literature three types of enzyme have been identified from fungi: lignin peroxidases which oxidise lignin model compounds faster than Mn^{2+}, manganese peroxidases which oxidise Mn^{2+} faster then lignin

model compounds and versatile peroxidise which oxidises them both at similar rates. The stopped flow investigation aimed to identify which of these enzymes DypB was most like. The study was carried out in tandem with the group of Professor L. Eltis, they showed that a compound I-like intermediate: with a λ_{max} at 397 nm, was formed[182] and that DypB turned over a variety of commercial lignin monomers such as guaiacol and vanillin.

A series of stopped flow experiments were carried out with recombinant DypB, pre-mixing 8 μM enzyme in citrate-phosphate buffer pH 6.0 with 1 equivalent hydrogen peroxide and then reacting it with 1 or 10 equivalents of $MnCl_2$ and/or β-aryl ether **27** and monitoring the reaction either at 397 nm (for compound I) or 417 nm (isosbestic point for compound II).[183] The study originally used a pH of 3.6, which is the optimal pH of the enzyme (see section 6.7), however, the reaction was then very fast and no intermediates could be observed following the dead time of the instrument (4 ms). Experiments were then carried out at pH 5.5 but at the high concentrations of enzyme needed for stopped flow the protein precipitated. Finally, the study was carried out at pH 6.0.

The first experiment looked at observing the formation and decay of Compound I at 397nm with the mixing of DypB and H_2O_2. A typical trace fitted with a single exponential for this style of reaction is given in Figure 6.23. The decay of compound I could be clearly observed but the formation fell within the dead time (4 ms). If the k_{obs} of 0.841 s^{-1} is divided by the initial enzyme concentration (8 μM), a theoretical bimolecular rate constant for reaction with hydrogen

peroxide of 1.1 x 10^5 $M^{-1}s^{-1}$ is generated, which is consistent for with the observations of the Eltis group.[182]

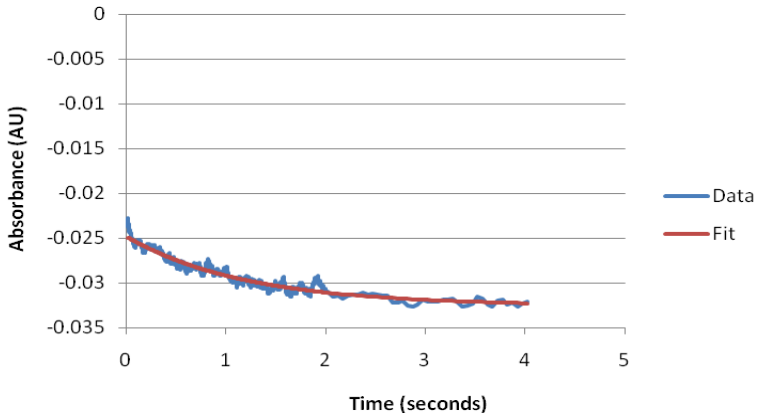

Figure 6.23 DypB (8 μM) mixed with hydrogen peroxide (8 μM) in citrate phosphate buffer at pH 6.0. The decay of compound I was observed at 397 nm. The data was fitted to a single exponential with a good fit shown by a χ^2= 5.03 x10^{-4}. A k_{obs} 0.841 s^{-1} and amplitude of 0.00740 were observed.

Once the rate of decay of compound I without substrate was known we looked at the decay of Compound I in the presence of Mn^{2+}, dimer 27 and a mixture of Mn^{2+} and dimer **27**. These experiments where done in a 1:1:1 ratio of enzyme: H_2O_2: substrate. Typical traces are given in Figure 6.24.

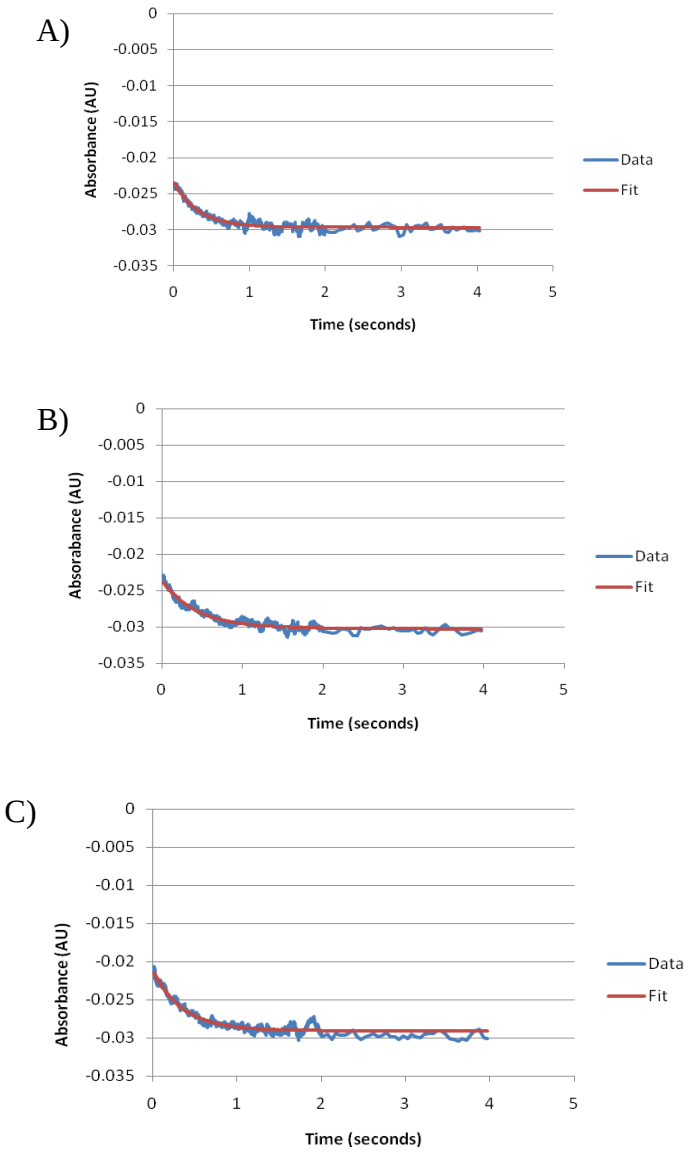

Figure 6.24 A) DypB (8 μM) pre-mixed with hydrogen peroxide (8 μM) and then mixed with dimer **27** (8 μM). Compound I breakdown observed at 397 nm. Data was fitted to a single exponential which gave a good fit shown by a $\chi^2 = 5.03 \times 10^{-4}$. A $k_{obs} = 3.10\ s^{-1}$ and amplitude = 0.00614 were observed. B) DypB (8 μM) pre-mixed with hydrogen peroxide (8 μM) and then mixed with Mn^{2+} (8 μM). Compound I breakdown observed at 397 nm. Data was fitted to a single exponential which gave a good fit shown by a $\chi^2 = 4.17 \times 10^{-4}$. A $k_{obs} = 2.35\ s^{-1}$ and amplitude = 0.00630 were observed. C) DypB (8 μM) pre-mixed with hydrogen peroxide (8 μM) and then mixed with dimer **27** (8 μM) and Mn^{2+} (8 μM). Compound I breakdown observed at 397 nm. Data was fitted to a single exponential which gave a good fit shown by a $\chi^2 = 5.15 \times 10^{-4}$. A $k_{obs} = 2.81\ s^{-1}$ and amplitude = 0.00762 were observed.

The k_{obs} for the decay of Compound I without substrate was determined as 0.841 s^{-1} This was found to increase in the presence of Mn^{2+} to 2.35 s^{-1} and in the presence of dimer **27** to 3.14 s^{-1}. Whilst these are not large increases they still are significant and show that compound I interacts with both substrates. The rate of decay is similar with both Mn^{2+} and dimer **27** suggesting the enzyme has a similar affinity for the two substrates similar to the fungal enzyme versatile peroxidise.[70]

The experiment was repeated with a 1:1:10 ration of DypB: H_2O_2: dimer **27**. In this case a more complex decay was observed which did not fit a single exponential. This is illustrated in Figure 6.25. The data was refitted as a double exponential which gave an improved fit. The k_{obs} were 0.00631 and -0.00177 s^{-1} and the amplitudes were 2.11 and 0.384. This corresponds to two processes: the decay of compound I with substrate and another slower process. This slower process seems to occur on a longer time scale than a single turnover i.e. the time for the ezyme to react with a single equivalent of substrate.

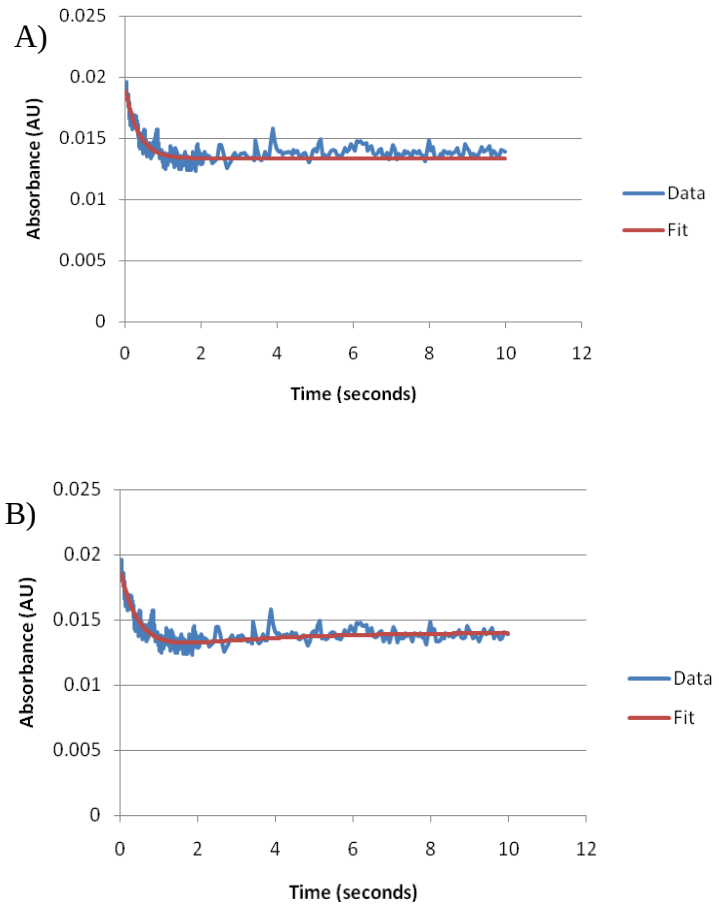

Figure 6.25 DypB (8 μM) pre-mixed with hydrogen peroxide (8 μM) and then mixed with dimer **27** (80 μM). Compound I breakdown observed at 397 nm. A) Data was fitted to a single exponential which gave poor fit with a $\chi^2 = 6.7 \times 10^{-4}$, a $k_{obs} = 2.88\ s^{-1}$ and an amplitude = 0.00547. B) The data was refitted with a double exponential which gave a better fit with a $\chi^2 = 5.90 \times 10^{-4}$, $k_{obs} = 2.11$ and $0.384\ s^{-1}$ and an amplitudes = 0.00631and -0.00177.

The reaction of DypB with Mn^{2+} was also investigated with a higher concentration of Mn^{2+} the data in this case fitted a single exponential as shown in Figure 6.26. Fitting the data to a second exponential was investigated but it gave a negligible increase in χ^2. In this case a $k_{obs} = 1.99\ s^{-1}$ and amplitude = 0.00830 was observed.

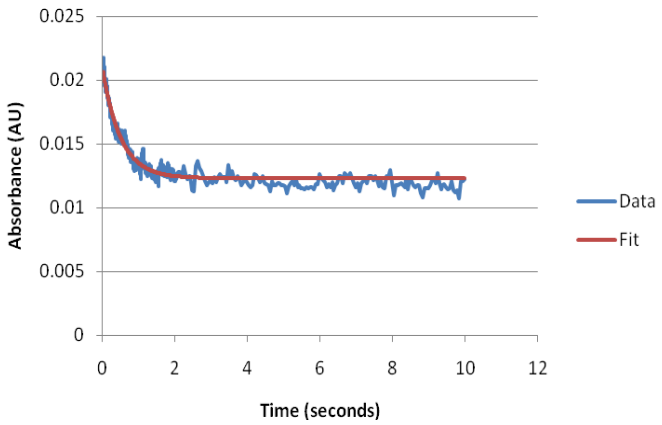

Figure 6.26 DypB (8 μM) pre-mixed with hydrogen peroxide (8 μM) and then mixed with Mn^{2+} (80 μM). Compound I breakdown observed at 397 nm. A) Data was fitted to a single exponential which gave a good fit shown by a $\chi^2 = 4.86 \times 10^{-4}$, a $k_{obs} = 1.99\ s^{-1}$ and an amplitude = 0.00830 were observed.

Previously, no compound II has been observed for a Dyp peroxidise[187] and so we decided to investigate at 417 nm, an isosbestic point between compound II and resting enzyme used in the literature, to observe compound II in other peroxidases.[183] Whilst in the presence of Mn^{2+} no compound II could be seen. But in the case when there was no substrate and when dimer **27** was used, a species could be observed. Despite a substantial amount of noise and low amplitudes the traces still fitted to single exponentials as shown in Figure 6.27 These observations led to collaborators in the Eltis group investigating possible compound II formation and they too observed such a species under certain reaction conditions.

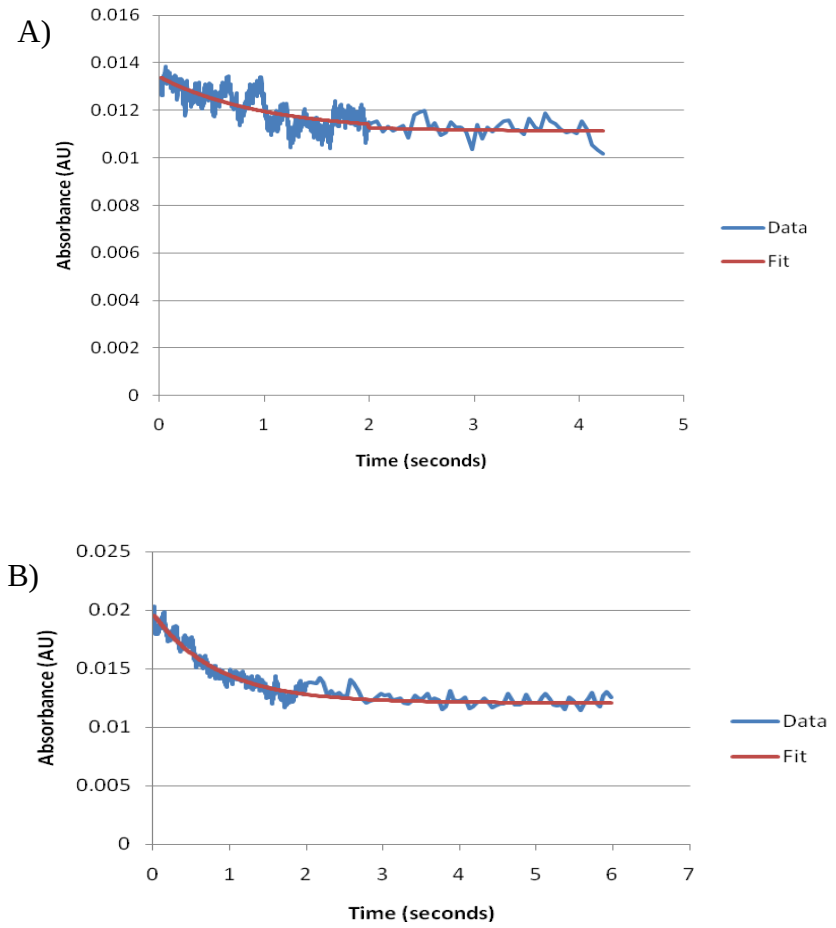

Figure 6.27 A) DypB (8 μM) mixed with hydrogen peroxide (8 μM) in pH 6.0 buffer and observed at 417 nm. A possible compound II species was observed the decay of which fitted a single exponential with a $\chi^2 = 4.32x10^{-4}$, a $k_{obs} = 1.01$ and an amplitude 0.00229. B) DypB (8 μM) mixed with hydrogen peroxide (8 μM) in pH 6.0 buffer with dimer **27** (8 μM) and observed, at 417 nm. A possible compound II species was observed the decay of which fitted a single exponential with χ2 = 5.69x10-4, a k_{obs} 1.18 and an amplitude = 0.00749.

Despite the noise of some of the spectra k_{obs} observed in the studies above are considerably faster than the calculated k_{cat}, 0.1 s^{-1}, at pH 6.0 based on the rate with ABTS assay as reported in section 6.7, suggesting that a pre-steady-state phenomena are being observed. On the whole the data fitted well to single exponential decays, further reinforcing the conclusion that the data is reliable.

The stopped flow studies above confirm that DypB can interact with both DypB and Mn^{2+} and it does this with similar rate constants. The compound II like species seen represents the first data of such a species for a Dyp type peroxidise.

6.7 Additional characterisation of DypB

The optimal pH of DypB was investigated using the ABTS assay and over a pH range of 2.8 to 6.6 The largest change in rate was seen at pH 3.6-4. as showing in Figure 6.28. This is consistent with what is reported for other Dyp peroxidases.[174]

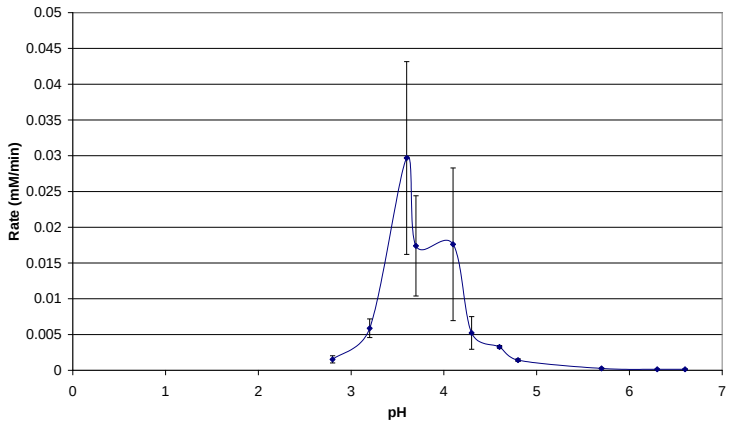

Figure 6.28 pH rate profile for DypB (0.5 mg/ ml), rate was determined with ABTS (10 mM), Mn2+ (10 mM) and hydrogen peroxide (10 mM). An increase in absorbance at 430 nm was observed and the buffer used for all pHs was citrate 0.1 M- phosphate 0.2M.

6.8 Conclusion

This study shows that *R. jostii* RHA1 produces an enzyme DypB that is active against lignin. This enzyme can both directly and indirectly interact with lignin causing its degradation. DypB's activity is greatly enhanced by the presence of Mn^{2+}.

DypB is active against the lignin dimer **27**. This is proposed to occur through the following radical mechanism. This mechanism is consistent with the two transient intermediates observed by stopped flow and the products observed in the LC/MS studies.

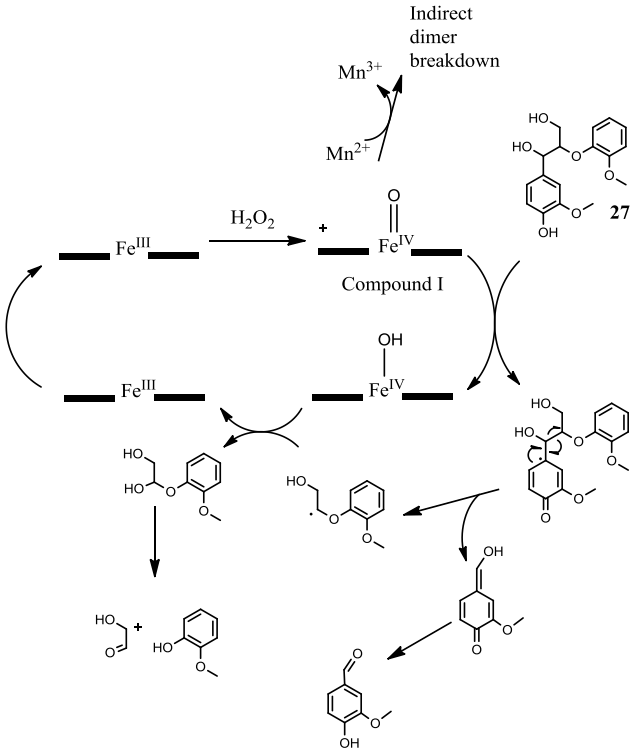

Figure 6.29 Mechanism for the reaction of DypB with β-aryl ether **27**.

The specificity of DypB for dimer **27** over the other lignin dimers is surprising especially considering that activity against lignin is still maintained. However, this is consistent with the way that some bacteria show specificity for some lignin types. Perhaps this specificity is dominated by the abundance of different lignin dimer units.

There is evidence that DypB can interact directly with lignin in the kraft lignin kinetics assay, where a K_m of 8.2 μM was observed, suggesting strong binding

of lignin. The stopped flow data also suggests that the dimer is bound by DypB as the reaction between DypB and the dimer is not proportional to dimer concentration. Previous work has suggested other Dyp peroxidaes can bind dyes.[160] Note, such direct action on lignin has not been reported for versatile peroxidase but has been seen for LiP.[58]

DypB was shown to be more effective in the presence of Mn^{2+}. This was seen in the nitrated lignin assay, in the experiments on lignin dimer **27** monitored by HPLC and directly on lignin and lignocellulose. However, despite this some activity was still observed without Mn^{2+} in the nitrated lignin assay, the stopped flow work and the LC/MS studies. In particular the turnover of guaiacol was clearly observed when there was no Mn^{2+} present. This is consistent with a mode of activity similar to versatile peroxidase, which can use both Mn^{2+} and small organic molecules as substrates.[70]

The presence of the diaphorase was found to quench the reaction of the dimer entirely. This suggests that the β-aryl ether is released prior to cleavage but after a radical has been formed on it. The effectiveness of the diaphorase at quenching the reaction was consistent with our hypothesis that dihydrolipoamide dehydrogenase may be involved in controlling the production of radicals produced *in vivo* when lignin is degraded. It also provides a lead for further work in controlling product formation from lignin. The presence of diaphorase was shown to allow intermediates in lignin breakdown to be identified. This provides a potential solution to the problem of controlling lignin

breakdown. We have shown DypB is capable of degrading lignin like material to the industrially valuable compound vanillin.

The stopped flow work showed a species at 417nm that decreased with time this is consistent with the presence of a compound II intermediate that has not been previously observed for Dyp type peroxidases.[176] It was only clearly visible in the presence of the lignin dimer, this once again suggests specificity, as a natural substrate is required for the enzyme to progress through a classical peroxidase mechanism.

In conclusion, a novel manganese-dependent lignin peroxidase, DypB, has been identified. This provides a potential reagent for the future conversion of lignocellulose to renewable chemicals.

CHAPTER VII: Conclusion

7.1 Conclusions and future work

During the course of this PhD new methods have been developed for the high throughput screening to determine the lignin degrading ability of micro-organisms. Application of these assays has led to the identification of *R. jostii* RHA1, *Acetinobacter* PC/4 and a number of *S. coelicolor* strains as being lignin degraders. In addition, the assays allowed the identification of the peroxidase DypB, the first recombinant bacterial enzyme shown to degrade lignin. The nitrated lignin and fluorescence assay represent a step forwards in lignin degradation assays, as they are fast and more specific than conventional general peroxidase assays.

In the future there are further opportunities for the assays developed here. Currently in other projects within the Bugg group the nitrated lignin assay is being employed to help purify more lignin degrading proteins, with ongoing studies focusing on *R. erythropolis* and *R. jostii* RHA1, as well as new lignin-degrading bacteria. The solid agar plate assay is currently being employed to screen for new degrading strains from geothermal soils and composted straw (with aim of finding thermophilic strains).

The studies of the genetic knockouts of *R. jostii* RHA1 showed a potentially interesting laccase encoded for by the gene ro2377. This enzyme is currently undergoing further studies in our group. As postulated in Chapter V its activity

towards lignin seems low, but it is possible that this could be enhanced by the selective mutations to increase its redox potential. Alternatively, it could be that the use of mediators or other supporting enzymes may increase its activity.

It was shown that growing *R. jostii* RHA1 and *P.putida* on lignocellulose gave rise to a number of small organic compounds. These included oxalic acid and ferulic acid for which there are already established commercial markets. This highlights that there is potential in the use of bacteria to valorise lignin. However, these studies were hampered by the formation of a wide mixture of products similar to the results of chemical degradation.[23] In the studies on DypB it was found that product formation could be controlled by addition of the enzyme diaphorase. It is particularly interesting that vanillin could be formed. This is a potential tool to access higher yields of products of interest. In addition, current studies in our group are also looking at using enzyme inhibitors to interfere with the degradation of aromatic compounds by bacteria and then examining changes in the products formed using the methods developed in Chapter IV.

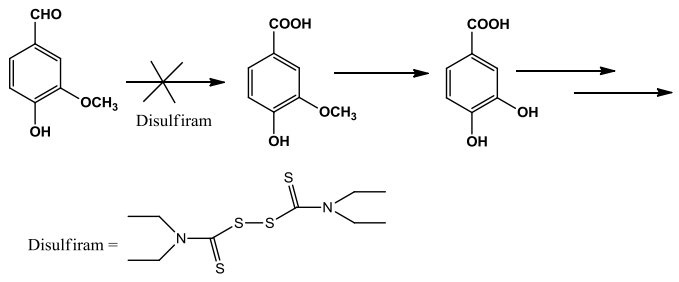

Figure 7.1 Metabolism of vanillin could possibly be stopped by the general aldehyde dehydrogenase inhibitor disulfiram leading to an increase in the amount of vanillin in the culture supernatants.

Evidence has been gathered to suggest that bacteria have a specificity for particular types of lignin. This is a new observation with little prior discussion in the literature.[81] At a molecular level it was shown that DypB was specific for β-aryl ether **27**, such enzymes specificities may be responsible for the specificity of the parent organism. The preference of different micro-organisms for different feedstocks should be considered carefully when designing potential processes for a biorefinery. There is need for ongoing work to look at variation in product formation with different lignin types as this too will have a significant effect on what material and micro-organism will be best for industrial application. The nitrated lignin assay is well suited to screening a set of lignin degraders against a range of plant feedstocks (e.g. varieties of wheat).

The cellular location of DypB must logically be extracellular, since activity is seen with the R. *jostii* RHA1 supernatant but not with the supernatant from the DypB knockouts. The protein sequence for *Rhodococcus jostii* RHA1 DypB contains neither a Sec signal sequence nor a Tat signal sequence, though DypB homologues in some other bacteria do contain possible Tat signal sequences.[151] As discussed in chapter V the gene encoding for DypB is immediately adjacent to the gene encoding encapsulin in *R. jostii* RHA1. It is probable that the transportation of DypB to the outside of the cell is related to encapsulin but the mechanism for this is unknown at this time.

In nature DypB is probably one of a suite of enzymes, as proposed in chapter IV, hence its modest activity towards lignin *in vivo* (Figure 6.6). This is analogous to the fungal system and without all of the pieces lignin degrading

activity can be expected to be low.[78] Despite this DypB represents the first recombinant bacterial lignin peroxidase to be kinetically characterised.

The observation of oxalic acid in the culture media of bacteria grown on lignocellulose offers the first explanation of how the hydrogen peroxide for lignin degradation is generated in bacteria. Previous work on the fungal system has shown that oxalic acid is the final product of a series of oxidations each of which reduces oxygen to hydrogen peroxide.[78]

This PhD has produced a number of tools for investigating lignin degradation, it has also identified a number of new lignin degrading bacterial strains. It has identified a number of products formed by *R. jostii* RHA1 and *P. putida* from lignin. It has also provided the first detailed characterisation of a recombinant bacterial protein. It is hoped that the tools developed here will be of further help to develop methods of using bacteria to form renewable chemicals.

CHAPTER VIII: Experimental

8.1 Materials and equipment

The NMR spectra were recorded using a Bruker DPX300 (300 MHz for ^{1}H-NMR, 75.5 MHz for ^{13}C-NMR), Bruker DRX500 (500MHz for ^{1}H-NMR, 125 MHz ^{13}C-NMR) and a Bruker AVIII (600MHz for ^{1}H-NMR, 150 MHz ^{13}C-NMR). The solvents were $CDCl_3$, DMSO d_6, acetone d_6 and MeOH d_4. The residue solvent or tetramethylsilane was used as internal standards. The multiplicity of the spectra is expressed as s (singlet), d (doublet), t(triplet), q (quartet), br (broad signal) and m (multiplet).

The mass spectra were recorded by ESI (Electro Spray Ionization) technique using a Bruker Esquire 2000. The high resolution spectra were obtained using a Bruker Micro TOF. The IR spectra were recorded using a Perkin Elmer Spectrum One instrument. The fluorescence was measured using TECAN GENios plate reader. The plates used were 96 well Nunclon Δ Surface from Nunc or 96 well tissue culture plates from Falcon. Stopped flow kinetics measurements were taken with a MOS 450-Biologic spectrophotometer and an SFM 300 observation chamber, equipped with a 1-cm observation cell at 25^{o}C. GC-MS was carried out on a Varian 3800 machine, using a Varian Factor Four column, 30m x 0.25mm x 0.25μm, with electron impact ionisation at 750eV. HPLC analysis was carried out using a Phenomenex Luna 5μ C18 100Å 50x4.6 mm on a Hewlett Packard Series 1100 analyser. UV-visible Spectrometry was carried out with a Perkin Elmer Lambda 35 UV-visible spectrometer.

Chromatography was performed with silica gel 40-63 u 60A from Fluochem.TLC (Thin Layer Chromatography) was performed using silica gel 60 F_{254} on aluminium sheets from Merck.

The reagents and solvents were purchased from Aldrich and used without further purification, with exception of pinoresinol, which was purchased from Arbre Nova. The industrial lignin was obtained from Prof. H. Dalton at the University of Warwick. The *Rhodococcus jostii RHA1* strain came from Lindsay Eltis from the University of British Columbia, as did the recombinant DypA and DypB as well as the genetic knockouts of *R. jostii* RHA1. The *Streptomyces viridosporus* 39115, *Pseudomonas putida* 33015 and *Rhodococcus erythropolis* 11048 were from the American Type Culture Collection (ATCC).The *Nocardia autotrophica* 43083 and *Rhodococcus sp.* 43230 was supplied from the Deutsche Sammlung von Mikroorganismen und Zelkulturen GmbH (DSMZ). The *Leuconostoc mesenteroides* NCIMB 8023 came from the National Collection of Industrial Bacteria (NCIMB)**.** *Bacillus subtilis*, *Acetobacter* PC/4 and *Bacillus Licheniformis* from our own laboratory supply were also used. *Arthrobacter globiformis* D45 was provided by A. Morgan from warwick Horticultral Research Institute (HRI). *S. coelicoler* M110, *S. coelicoler JCM* 3279, *S. coelicoler* M145, *S. coelicoler* ISP 5233, *S. coelicoler* M1190, *S. coelicoler* 1010 and *S. avermittilis* 41443 DSM where provided by Prof. E. Wellington. Solid fungal cultures of *Lentinula edodes*, *Lepista nuda*, *Phanerochaete chrysosporium*, *Pleurotus ostreatus*, *Schizophyllum commune*, *Serpula lacrymans* and *Trametes versicolor* were provided by Dr K. Burton and

D. Eastwood from Warwick HRI. Liquid fungal cultures of *Suillus luteus, Paxillus involutus, Suillus bovines, Laccaria bicolour, Cenococcum geophilum, Lactarius rufus* and *Lactarius controversus* were provided by Dr G. Bending from Warwick HRI.

Hereward wheat straw was provided by Warwick HRI by Prof. Pink. Miscanthus lignocellulose was proved from Rothamstead and Scots pine was provided by the British Forestry Association.

8.2 Synthesis

8.2.1 Synthesis of β-aryl ether lignin dimers

Adler Synthesis

8.2.1.1 Synthesis of 3-Methoxy-4-(benzyloxy)benzaldehyde (35)[129]

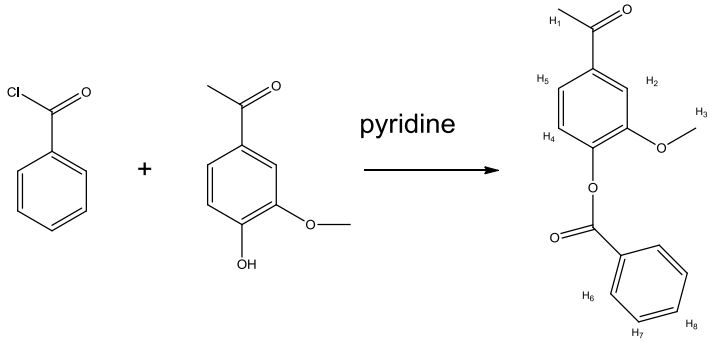

35

Modified from the procedure of H. Erdtman and B. Leopold.[129] Acetovanillone (10.00g, 60.0mmole) was dissolved in pyridine (20ml) and cooled on ice. After this benzoyl chloride (7.0ml, 60.2mmole) was added. After thirty minutes 60ml of water was added and a white precipitate was formed. This was collected by filtration and dried under vacuum. The product was recrystallized from ethyl acetate: hexane (1:1) giving white crystals (14.0g, 86%). Mp 106-110^{o}C (lit 108-109^{o}C)[184]; IR (neat) 1721 (saturated ketone), 1598 (aryl), 1505 (aryl) 1264 (aryl-O-CH_3) cm^{-1}; ^{1}H NMR (300MHz, $CDCl_3$) 8.23 (2H,d, ^{3}J=5.6, H_6) 7.67 (3H, m, H_5, H_2, H_8), 7.55 (2H, t, ^{3}J=6.6, H_7) 7.27 (1H, d, ^{3}J= 5.6, H_4) 3.90 (3H, s, H_3) 2.65 (3H, s, H_1) ppm; ^{13}C NMR (75MHz, $CDCl_3$) 196.42, 163.68, 151.02, 143.49, 135.37, 133.15, 139.77, 128.34, 128.01, 122.34, 121.41, 110.89, 55.48, 25.99 ppm; ESI-MS (low res.) 271 MH^{+}.

8.2.1.2 Synthesis of 1-(4-Benzoyloxy-3-methoxyphenyl)-2-bromoethanone (36)

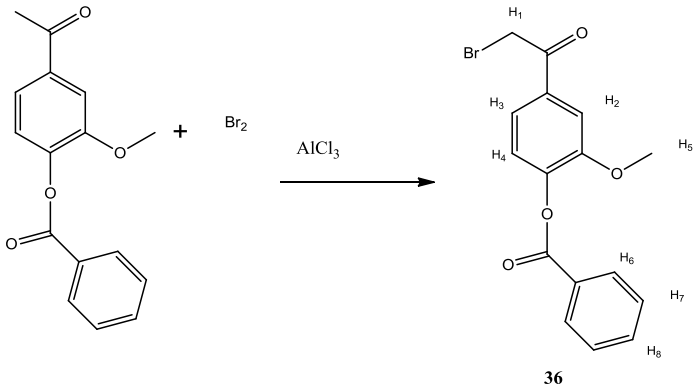

36

Benzoylated acetovanillone **35**, (5g, 0.0185 moles) was dissolved in dichloromethane (10cm^3) in a 250ml round bottom flask. $AlCl_3$ (0.00185 moles, 0.2467g, 0.1eq) in diethyl ether (1 ml) was then added, followed by Br_2 (47ml of 0.39 Molar stock). The mixture is then left stirring two hours. Once no colour change was occurring, TLC was used to confirm the reaction had gone to completion. The reaction was then washed with sat. bicarbonate solution (~150ml) an effervescence was observed. The reaction was left to stir until fizzing stopped. After this the organic layer was dried, filtered and evaporated under vacuum. This gave brown crystals which where recrystallised twice in ethanol. Mp 108-109^{o}C (lit 105-106^{o}C)[121]; IR (neat) 1734 (Ester carbonyl), 1685 (aldehyde carbonyl), 1595 (aryl), 1508 (aryl), 1236 (aryl-O-CH_3), 1206 (aryl-OCH_3) cm^{-1}; ^{1}H NMR (300MHz, $CDCl_3$) 8.10 (2H,d, ^{3}J=7.1, H_6) 7.62-7.52 (3H, m, H_2, H_3, H_8), 7.42 (2H, t, ^{3}J=7.9, H_7) 7.18 (1H, d, ^{3}J= 8.2, H_4), 4.35(2H, s, H_1) 3.78 (3H, s, H_5) ppm; ^{13}C NMR (75MHz, $CDCl_3$) 189.71, 163.55, 151.35, 144.19, 133.25, 132.10, 129.79, 128.20, 128.04, 122.61, 121.80, 111.75, 55.55,

29.96 ppm; ESI-MS (low res.) 349/351 MH^+ and 371/373 MNa^+ (The two peaks were caused by the two main isotopes of bromine).

Nakatsubo Synthesis

8.2.1.3 Synthesis of 4-(phenyloxy)-3-methoxybenzaldehyde (40)[185]

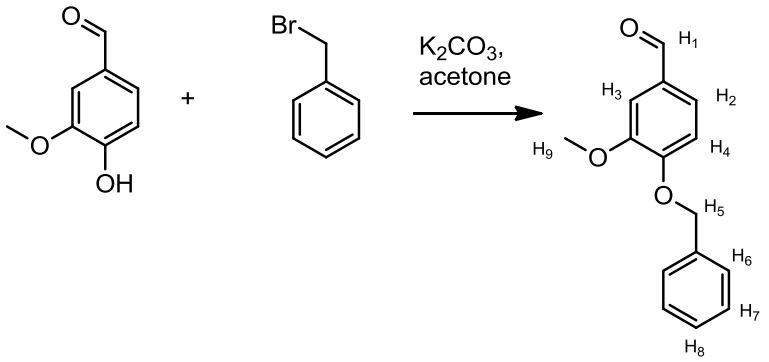

40

Vanillin (15.2g, 0.1 mole) was vigorously stirred in acetone (300ml) at room temperature. Powdered K_2CO_3 (75g, 0.54 mole) was added slowly to the solution followed by benzyl bromide (11.9ml, 0.1 mole). The suspension was refluxed for 2 hours and then cooled to room temperature. Inorganic salts were then removed by filtration. The filter cake was washed with acetone (150ml). Then the solvent was removed *in vacuo*. The resulting dirty white crystals where recrystallised (diethyl ether/ pet. ether 1:2) to give white crystals (19.84g, 82%). Mp 60-62^{o}C (lit. 61-62^{o}C)[186]; TLC (4 hexane: 1 Ethyl acetate) Rf = 0.8; IR(neat) 2841(-O-CH_3), 1671(aryl aldehyde), 1583(Aryl) and 1505 cm^{-1}(Aryl); ^{1}H NMR (300MHz, $CDCl_3$,) 9.84 (1H, s, H_1), 7.48-7.30 (7H, m, H_2, H_3, H_6, H_7, H_8), 7.00 (1H, d, ^{3}J=7.1 Hz, H_4), 5.26 (2H, s, H_5), 3.96 (3H, s, H_9)ppm; ^{13}C NMR (75.5MHz, $CDCl_3$) 199.0, 153.6, 150.0, 136.0, 130.2, 128.8, 128.2, 127.2, 126.7, 112.3, 109.2, 65.9, 56.1 ppm; ESI-MS (low res.) 243 (MH^+) 265 (MNa^+).

8.2.1.4 Synthesis of 4-(benzyloxy)-3,5-dimethoxybenzaldehyde (44)[187]

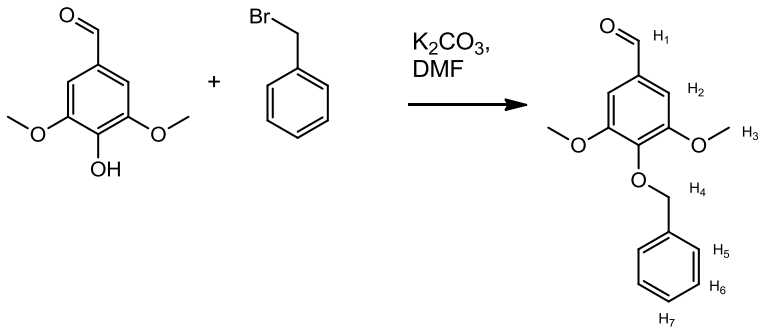

44

Adapted from the method of C. Bennette *et al.*[187] Syringylaldehyde (15.0g, 0.0823 mole) and K_2CO_3 (22.78g, 0.16 mole) were added to stirring DMF (300ml). Benzyl bromide was then added (9.81, 0.0823 mole) and the solution was then stirred for 64 hours. The solution was then poured into dichloromethane (500ml). The solution was then washed five times and dried with $MgSO_4$. It is then concentrated to a brown oil *in vacuo* and crystallized from hexane, giving white crystals (16.47g, 73%). Mp 61-62^oC (Lit. 61-62^oC)[188]; IR (neat) 3000 (C-H), 2986 (C-H), 2841 (Aryl-O-Me), 1682 (aldehyde),1588 (Aryl), 1498 (Aryl)cm^{-1}; ^1H NMR (300MHz, $CDCl_3$) 9.80 (1H, s, H_1), 7.40 (2H, d, ^3J= 8.0Hz, H_5), 7.31-7.23 (3H, m, H_6, H_7), 7.04 (2H, s, H_2), 5.06 (2H, s, H_4), 3.83 (6H, s, H_3) ppm; ^{13}C NMR (75.5 MHz, $CDCl_3$) 190.41, 153.37, 141.73, 136.56, 131.27, 127.82, 127.62, 127.50, 106.04, 74.44, 55.63 ppm; ESI-MS (low res.) 273 (MH^+), 295 (MNa^+).

8.2.1.5 Synthesis of 4-benzyloxy-benzaldehyde (45)[189]

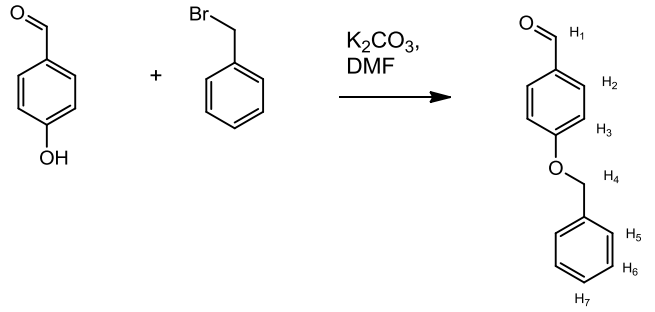

45

4-Hydroxybenzaldehde (10.0g, 0.0819 mole) and K_2CO_3 (24.88g, 0.18 mole) were added to stirring DMF (100ml). This was heated to 90^oC overnight and the solvent was removed *in vacuo*. The residue was extracted with ethyl acetate (200ml). The combined ethyl acetate layers where then washed with 1M NaOH. Then the solution is washed with brine and dried over $MgSO_4$. Then the solvent is removed *in vacuo*. This is then recrystallised from ethylacetate: hexane giving white needle like crystals. (11.35g, 65% yield). Mp = 68-70^oC (Lit. 70-71^oC)[190]; IR (neat) 1684 (Aryl-O-Me) 1597 (Aryl), 1507 (Aryl) 1162 (C-O) cm^{-1}; ^1H NMR (300MHz, $CDCl_3$) 9.89 (1H, s, H_1), 7.84 (2H, d, ^3J=8.8, H_2) 7.47-7.33 (5H, m, H_5, H_6, H_7), 7.09 (2H, d, ^3J=8.8, H_3), 5.16 (2H, s, H_4) ppm; ^{13}C NMR (75 MHz, $CDCl_3$) 190.21, 163.12, 135.32, 131.41, 129.50, 128.14, 127.74, 126.90, 114.53, 69.66 ppm; ESI-MS (low res.) 213 (MH^+).

8.2.1.6 Synthesis of methyl 2-methoxypheoxyacetate (39)[125]

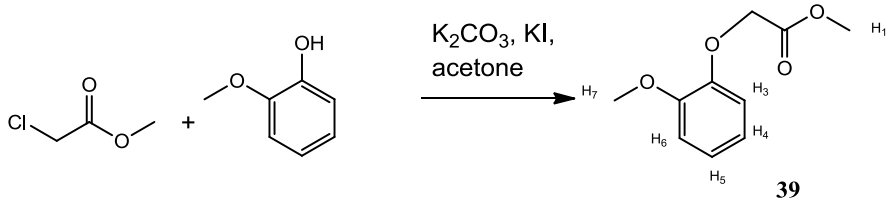

39

Methylchloroacetate (4.43ml, 0.046 mole), guaiacole (5.0ml, 0.05 mole), K_2CO_3 (13.8g, 0.1 mole) and NaI (3.5g, 0.231 mole) were mixed in acetone (65ml) with

stirring for one week. The inorganic salts were then removed by filtration and washed with acetone (4x50ml). The filtrate was concentrated to a yellow oil *in vacuo*. This was then suspended between brine solution (50ml) and diethyl ether (50ml). The organic later was washed with 10% KOH solution and then dilute acid HCl in NaCl solution. The organic layer is then dried with $MgSO_4$. This is then evaporated *in vacuo* to give a white solid (3.41g, 38%). Mp 50-51^oC (lit. 33^oC)[191]; 1757 (aryl ester), 1594 (Aryl), 1502 (Aryl), 1428 (C-H); ^1H NMR (300MHz, $CDCl_3$) 6.97 (1H, t, ^3J=7.5Hz, H_4 or H_5), 6.96-6.74 (3H, m, H_3, H_4 or H_5, H_6), 4.68 (2H, s, H_2), 3.86 (3H, s, H_1) 3.77 (3H, s, H_7) ppm; ^{13}C NMR (75MHz, $CDCl_3$) 149.42, 146.97, 120.56, 120.41, 114.10, 111.88, 60.59, 55.66, 52.03 ppm; ESI-MS (low res.) 197 (MH^+), 219 (MNa^+).

8.2.1.7 Synthesis of methyl 2,6-methoxy-phenoxyacetate (42)[125]

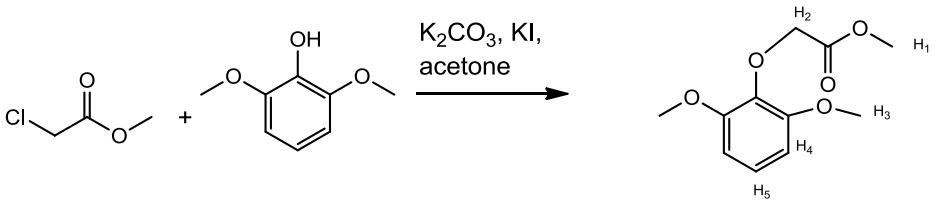

42

Adapted from the work of Nakatsubo.[117] Syringyl alcohol (10g, 0.0649 mole), methylchloroacetate (5.87ml, 0.066mole), K_2CO_3 (19.7g, 0.1435 mole) and KI (5.39g, 0.032 mole) were mixed in acetone (100ml) with stirring for one week. The inorganic salts were then removed by filtration and washed with acetone. The filtrate was concentrated to a black oil in vacuo. This was then suspended between brine solution (25ml) and diethyl ether (25ml). The solution was then extracted repeatedly with 10% KOH (20ml) until the aqueous layer was clear. This took eight extractions. The organic layer was then extracted with 10% HCl

in sat. NaCl solution (20ml) and dried with $MgSO_4$. The solution was evaporated *in vacuo* to give white crystals (6.0516g, 41%). Mp =60°C (Lit. 58°C)[192]; IR (neat) 2909 (C-H), 2841 (O-Me), 1754 (Aryl Ester), 1597 (Aryl), 1495 (Aryl) cm^{-1}; ^1H NMR (300 MHz, $CDCl_3$) 6.94 (1H, t, ^3J= 8.4 Hz, H_5) 6.50 (2H, d, ^3J=8.4 Hz, H_4), 4.56 (2H, s, H_2), 3.77 (6H, s, H_3), 3.74 (3H, s, H_1) ppm; ^{13}C NMR (75MHz, $CDCl_3$) 169.99, 153.00, 136.16, 124.10, 105.20, 105.20, 69.59, 56.11, 52.02 ppm; ESI-MS (low res.) 227 (MH^+), 249 (MNa^+); ESI-MS (high res.) 249.0733 (MNa^+) observed, 249.0733 (MNa^+) calculated.

8.2.1.8 Synthesis of methyl phenoxyacetate (43)[125]

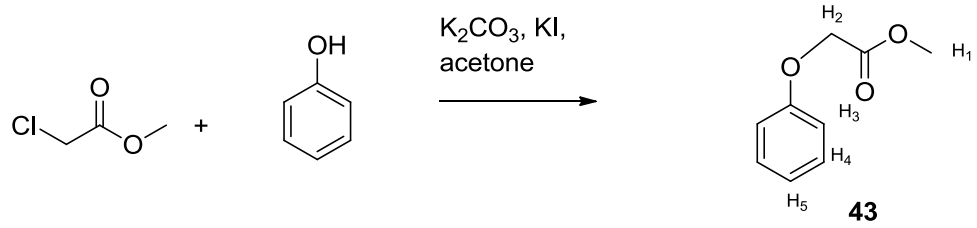

43

Adapted from the work of Nakatsubo.[117] Phenol (23.5g, 0.22 mole), methylchloroacetate (22ml, 0.23mole), K_2CO_3 (69g, 0.5mol) and KI (19.5g, 0.117 mole) were mixed in acetone (325ml) with stirring for one week. The inorganic salts were then removed by filtration and washed with acetone. The filtrate was concentrated to a yellow/white residue *in vacuo*. This was then suspended between brine solution (25ml) and diethyl ether (25ml). The solution was then extracted four times with 10% KOH (25ml). This took eight extractions. The organic layer was then extracted with 10% HCl in sat. NaCl solution (20ml) and dried with $MgSO_4$. The solution was evaporated *in vacuo* to give to a yellow liquid this was further purified by reduced pressure distillation. Finally giving a clear liquid (15.84g, 41%). B.p. = 92°C @ 16mm Hg (lit. 90-

90.5 @ 8mmHg)[193], IR (neat) 1758 (aryl ester), 1600 (Aryl), 1493 (Aryl), 1436 (C-H), 1199 (Aryl-O-) cm^{-1}; 7.20 (2H, t, ^3J=,7.9 Hz, H_4), 6.90 (1H, t, ^3J= 7.5 Hz, H_5), 6.83 (2H, d, ^3J= 8.4, H_3), 4.52 (2H, s, H_2), 3.67 (3H, s, H_1) ppm; ^{13}C NMR (75MHz, $CDCl_3$) 169.39, 151.39, 129.59, 121.71, 114.58, 64.69, 51.68 ppm; ESI-MS (low res.) 189 (MNa^+); ESI-MS (high res.) 189.0556 (MNa^+) observed 189.0522 (MNa^+) calculated.

8.2.1.9 Synthesis of 3-(4-benzyloxy-3-methoxy-phenyl)-3-hydroxy-2-(2-methoxy-phenyl)-propionic methyl ester (41)[125]

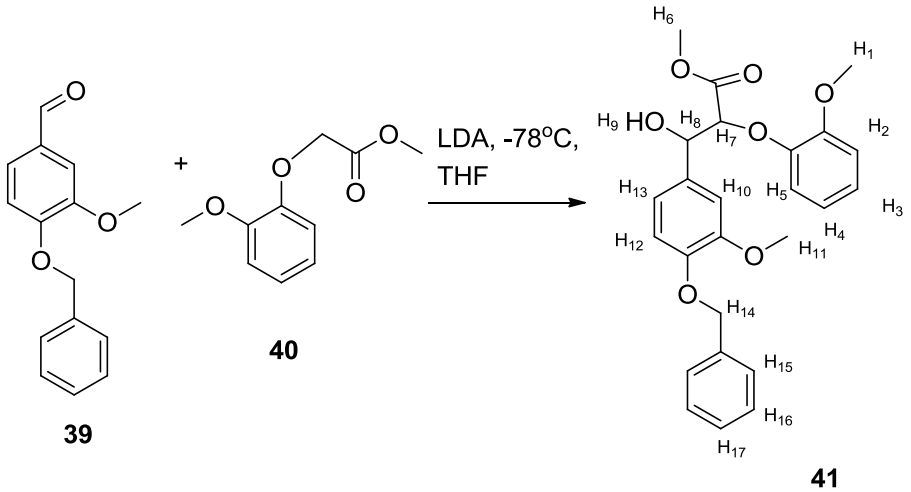

Benzyl vanillin and methyl 2-methoxypheoxyacetate were dried in a dessicator over P_2O_5 for 2 days. All glassware was dried for two days in an oven at 100°C before use.

A solution of diisopropyl amine (3.9ml, 0.0276mole) in anhydrous THF (24ml) was cooled on ice. Over five minutes 2.5M n-butyllithium in hexane solution (11.0ml, 0.0276 mole) was added. The solution was then stirred for forty minutes and then cooled with dry ice and acetone to –78°C. Methyl 2-methoxphenoxyacetae **40** (5.00g, 0.0255 mole) in anhydrous THF (23ml) was

then added over fifteen minutes. This was followed by benzyl vanillin **39** (6.09g, 0.0255 mole) in anhydrous THF (23ml) over forty minutes. The pale yellow solution was then stirred for a further five and a half hours with care to keep the temperature at –78^{o}C. After this the solution was transferred to a separating funnel and brine (25ml) was added. This solution was then neutralised with 10% HCl. The reaction mixture was extracted with diethyl ether (120ml) and then twice more (30ml). The combined ether layers where then washed with brine (12ml). The ether was then dried with $MgSO_4$ and evaporated *in vacuo*, giving a yellow oil (3.81g, crude yield 34%). This material contained a mix of *erythro* and *threo* isomers in a ratio (5:1). Half of this material was further purified with flash chromatography on silca gel (eluent Pet. ether: ethyl acetate 2:1) giving a yellow oil (0.8567g, 8%) with a ratio of *erythro* to *threo* of 3:1. TLC (Pet. Ether: ethylacetate 2:1) R_f (*threo*) = 0.35 R_f (*erythro*) = 0.2; IR (neat) 3484 (O-H), 2951 (CH_3/ CH_2), 1744 (sat. ester), 1593 (Aryl), 1500 (Aryl), 1253 (aryl-O-Me) cm^{-1}; ^{1}H NMR (300MHz, $CDCl_3$) *erythro* 7.45 (2H, d, ^{3}J=7.1Hz, H_{15}) 7.37 (2H, t, ^{3}J=6.7Hz, H_{16}), 7.33 (1H, t, ^{3}J=6.9Hz, H_{17}), 5.19 (2H, s, H_{14}), 5.16 (1H, d, ^{3}J=6.9Hz, H_8), 4.75 (1H, d, ^{3}J=5.1, H_7) 3.91(3H, s, H_1 or H_{11}), 3.87 (3H, s, H_1 or H_{11}), 3.69 (3H, s, H_6);

threo 3.91 (3H, s, H_1 or H_{11}), 3.87 (3H, s, H_1 or H_{11}), 3.69 (3H, s, H_6) ppm;

^{13}C NMR (125 MHz, $CDCl_3$) *erythro*169.88, 150.59, 149.47, 147.97, 147.26, 137.15, 131.16, 128.53, 127.81, 127.28, 123.97, 121.09. 119.12, 118.91, 113.60, 112.30, 110.57, 83.97, 73.86, 60.41, 55.96, 55.85, 52.00;

threo 85.38, 74.83 ppm;

ESI-MS (low res.) 461 (MNa^+); ESI-MS (high res.) 461.1595 (MNa^+) observed, 461.1595 (MNa^+) calculated.

8.2.1.10 Synthesis of 3-(4-benzyloxy-3,5-dimethoxy-phenyl)-2-(2,6 dimethoxy-phenoxyl)-3-hydroxypropionic methyl ester (46)[125, 126]

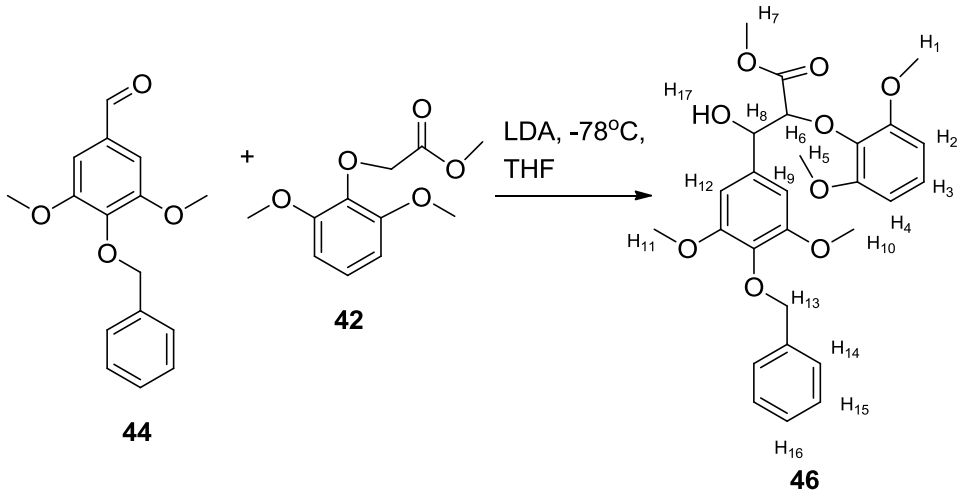

Adapated from the method of Nakatsubo and the method of Spilä and Syrjänen.[117, 118] Benzyl syringyl aldehyde **44** and methyl 2-methoxypheoxyacetate **42** was dried in a dessicator over P_2O_5 for 2 days and all glassware used was dried for two days in an oven at 100°C.

A solution of diisopropyl amine (2.23ml, 0.01591mole) in anhydrous THF (8.5ml) was cooled on ice. Over five minutes 2.5M n-butyllithium in hexane solution (6.1ml, 0.01591 mole) was added. The solution was then stirred for forty minutes and then cooled with dry ice and acetone to –78°C. Methyl 2-methoxphenoxyacetae **42** (3.00g, 0.01326 mole) in anhydrous THF (14ml) was then added over eight minutes. This was followed by benzyl syringlaldehyde **44**

(3.6110g, 0.01326 mole) in anhydrous THF (14ml) over thirty minutes. The rich yellow solution was then stirred for a further one and a half hours with care to keep the temperature at –78^{o}C. After this the solution was transferred to a separating funnel and brine (14ml) was added. This solution was then neutralised with 10% HCl. The reaction mixture was extracted three times with diethyl ether. The combined ether layers where then washed with brine (7ml). The ether was then dried with $MgSO_4$ and evaporated *in vacuo* giving a orange oil (6g, 91%). This material contained a mix of *erythro* and threo isomers in a ratio (4:1). This material was further purified with flash chromatography on silca gel (eluent ethyl acetate: toluene 1:1) giving an orange oil that was still impure, so was further purified with flash chromatography (eluent ethyl acetate: toluene 1:2). This gave two sets of material one with a ratio of *erythro* to threo of 3:1 (0.96g) and the second of 10:1 (2.69g). The total amount of pure material was 3.59g, 55%. The NMR sample was also shaken with d_4-methanol in the NMR tube. This lead to a reduction in the intensity of the doublet at 4.54 ppm and a change in the splitting of the doublet of doublets at 4.87 ppm to a doublet. TLC (Pet. Ether: ethylacetate 2:1) R_f (*threo*) = 0.18 R_f (*erythro*) = 0.08; IR (neat) 1672 (ester), 1597 (aryl), 1255 (aryl-O-CH_3), 1108 (C-O), 1018 (aryl-O-CH_3) cm^{-1};

^{1}H NMR (300 MHz, $CDCl_3$) *erythro* 7.42 (2H, d, ^{3}J=6.6 Hz, H_{14}), 7.24 (1H, t, ^{3}J=7.3 , H_{16}), 7.12 (2H, t, ^{3}J=7.5 Hz, H_{15}), 6.99 (1H, t, ^{3}J=8.4, H_3), 6.55 (2H, d, ^{3}J= 9.2, H_2 or H_4), 4.92 (2H, s, H_{13}), 4.87 (1H, dd, H_8, ^{3}J=3.9 + 7.3 Hz), 4.65 (1H, d, ^{3}J=3.9 Hz, H_6), 4.54 (1H, d, ^{3}J=7.3, H_{17}), 3.79 (6H, s, $H_{1/5}$ or $H_{10/11}$), 3.74 (6H, s, $H_{1/5}$ or $H_{10/11}$), 3.50 (3H, s, H_7)

threo 7.45-7.33 (2H, m, H_{14}), 7.24 (1H, t, ^{3}J=7.3, H_{16}), 7.30-7.20 (2H, m, H_{15}), 6.95-6.87 (1H, m, H_3) 6.55-6.38 (4H, m, $H_{2/4}$ + $H_{12/9}$), 5.31 (1H, d, ^{3}J=18.3Hz, H_8) 5.13 (1H, d, J=18.5Hz, H_6), 5.00 (2H, s, H_{13}), 3.77 (6H, s, $H_{11/10}$ or $H_{1/5}$), 3.70 (6H, s, $H_{11/10}$ or $H_{1/5}$) 3.47 (3H, s, H_7) ppm;

^{13}C NMR(175 MHz, $CDCl_3$) *erythro* 169. 88, 150.59, 149.47, 147.97, 147.26, 137.15, 131.16, 128.53, 127.81, 127.28, 123.97, 121.09, 119.12, 118.91, 113.60, 112.30, 110.57, 83.97, 73. 86, 60.41, 55.96, 55.85, 52.00,

threo 74.83, 85.38 ppm;

ESI-MS (low res.) 521 (MNa^+); ESI-MS (high res.) 521.1791 (MNa^+) observed, 521.1782 (MNa^+) calculated.

8.2.1.11 Synthesis of 3-(4-benzyloxy-phenyl)-2-phenoxyl-3-hydroxypropionic methyl ester (47) [125, 126]

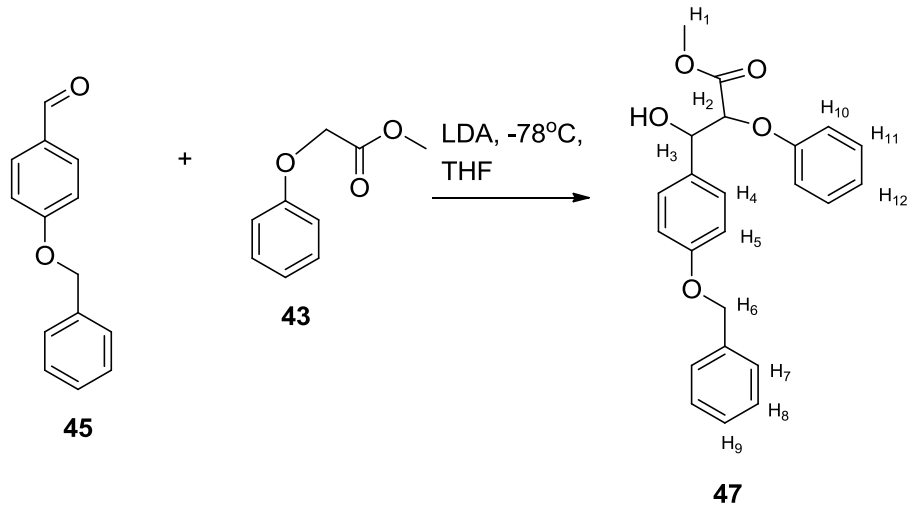

Benzyl vanillin **45** and methyl 2-methoxypheoxyacetate **43** were dried in a dessicator over P_2O_5 for 2 days. All glassware was dried for two days in an oven at 100^oC before use.

A solution of diisopropyl amine (2.6 ml, 18.1 mmole) in anhydrous THF (8.5ml) was cooled on ice. Over five minutes 2.5M n-butyllithium in hexane solution (7.25ml, 18.1 mmole) was added. The solution was then stirred for forty minutes and then cooled with dry ice and acetone to –78^oC. Methyl phenoxyacetae **43** (2.00g, 12.1 mmole) in anhydrous THF (12ml) was then added over fifteen minutes. This was followed by 4-benzyloxy-benzaldehyde **45** (2.5724g, 12.1 mmole) in anhydrous THF (23ml) over thirty minutes. The pale yellow solution was then stirred for a further two hours at –78^oC. After this the solution was transferred to a separating funnel and brine (10ml) was added. This solution was then neutralised with 10% HCl. The reaction mixture was extracted with diethyl ether (120ml) and then twice more (50ml). The combined ether layers where then washed with brine (40ml). The ether was then dried with $MgSO_4$ and evaporated *in vacuo* giving a orange/yellow solid this was recrystallised in ethylacetate and hexane to give a yellow solid. (1.4885g, crude yield 32%). This material was pure *erythro* enantiomer. TLC (Pet. Ether: ethylacetate 2:1) R_f (*threo*) = 0.6 R_f (*erythro*) = 0.5; m.p. =116-117^oC (no literature available) IR (neat) 1734 (ester carbonyl) 1228 (O-H stretching) 1585 (aryl) 1508 (aryl) cm^{-1}; ^1H NMR (300 MHz, $CDCl_3$) 7.35-7.21 (7H, m, H_7, H_8, H_9, H_{11}), 7.12 (2H, d, ^3J = 8.8 Hz, H_4), 6.86 (1H, t, ^3J= 7.13 Hz, H_{12}), 6.85 (2H, d, ^3J= 8.8 Hz, H_5), 6.74 (2H, d, ^3J= 7.7 Hz, H_{10}), 5.05 (1H, d, ^3J= 5.8 Hz, H_3), 4.95 (2H, s, H_6), 4.65 (1H, d, ^3J=6.1 Hz, H_2), 3.59 (3H, s, H_1); ^{13}C NMR (75 MHz, $CDCl_3$) 136.23, 130.85, 128.99, 127.99, 127.39, 127.30, 126.88, 121.54, 114.78, 114.14, 80.15, 73.31,

69.38, 51.76 ppm; ESI-MS (low res.) 401 (MNa^+); ESI-MS (high res.) 401.1359 (MNa^+) observed, 401.1355 (MNa^+) calculated.

8.2.1.12 Synthesis of 2-(2-methoxyphenoxy)-1-(4-hydroxy-3-methoxyphenyl) 1,3-propanediol (27) [196]

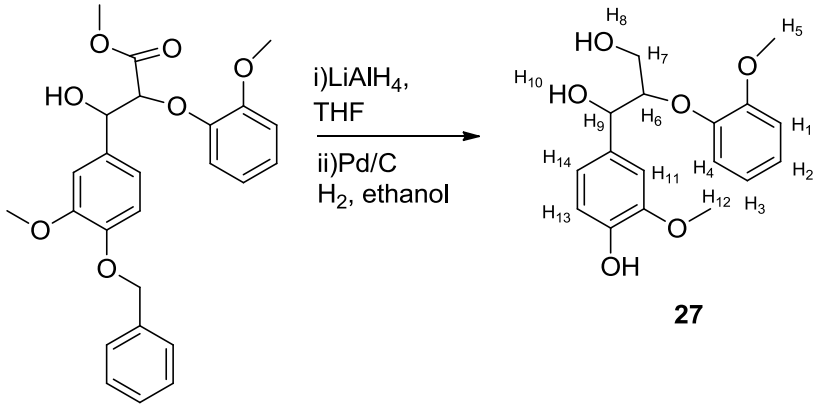

Adapted from two methods by Nakatsubo.[125, 194] Lithium aluminium hydride (0.27g, 7.2 mmole) was dissolved in anhydrous THF (10ml). This solution was stirred vigorously at 60°C under nitrogen and over twelve minutes compound **41**(1g, 2.4mmole) dissolved in THF (8ml) was added. This solution was left for two hours and then cooled to 0°C. This was followed by the dropwise addition of H_2O (0.5ml) in THF (10ml). Ethylacetate (15ml) was then added. After this dry ice is added until no further precipitate is formed. The inorganic salts formed are then removed by filtration and washed with ethanol. The filtrate was then dried with $MgSO_4$. The solution was then evaporated *in vacuo* giving a yellow oil. This material was then dissolved in ethanol (10ml) and 10% Pd/C (0.1g) was added. The solution was thoroughly degassed and then stirred with H_2 for 5 hours. The Pd/C was then removed and washed three times with ethanol (30ml). The combined filtrate were then evaporated *in vacuo* to give a light

brown oil. The final ratio of *erythro*: *threo* was 6:1. (0.322g, 43%). IR (neat) 3288 (O-H), 2943 (CH_3/CH_2), 1594 (Aryl), 1500 (Aryl), 1454 (C-H deformation), 1251(aryl-O-CH_3), 1021 (aryl-O-CH_3); ^{1}H NMR (300MHz, $CDCl_3$) *erythro* 6.95 (1H, d, ^{3}J= 8.41Hz, H_{14}) 6.90-6.78 (5H, m, $H_1 + H_2 + H_3 + H_4$), 6.75 (1H, s, H_{11}), 5.53 (1H, br. s, H_8 or H_{10}), 4.87 (1H, d, ^{3}J= 4.89 Hz, H_9), 4.06-4.00 (1H, m, H_6), 3.78 (6H, s, $H_5 + H_{12}$), 3.56-3.20 (2H, m, H_7) *threo* 3.80 (6H, s, $H_5 + H_{12}$). ^{13}C NMR (125MHz, $CDCl_3$) *erythro* 151.63, 146.85, 146.63, 145.12, 121.76, 124.29, 121.73, 119.02, 114.33, 112.19. 108.63, 87.46, 72.77, 60.72, 56.00, 55.91, *threo* 89.61, 74.04, 61.07; ESI-MS (low res.) 343 (MNa^+); ESI-MS (high res.) 343.1150 (MNa^+) observed, 343.1152 calculated.

8.2.1.13 Synthesis of 2-(2,6-dimethoxyphenoxy)-1-(4-hydroxy-3,5-dimethoxyphenyl)-1,3-propanediol (28) [196]

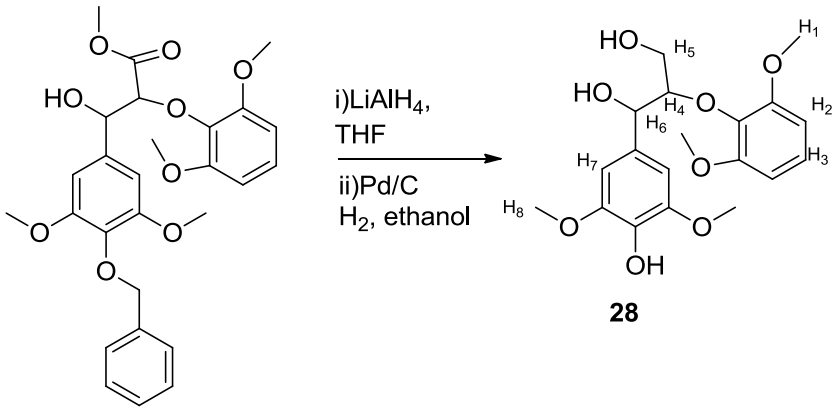

46 **28**

Adapted from two methods by Nakatsubo.[196] Lithium aluminium hydride (0.219g, 5.79 mmole) was dissolved in anhydrous THF (10ml). This solution was stirred vigorously at 60^{o}C under nitrogen and over thirty minutes compound **46** (1.85g, 4.87mmole) dissolved in THF (7ml) was added. This solution was left for two hours and then cooled to 0^{o}C. THF (15ml) was then added. Reaction checked by TLC. This was followed by the dropwise addition of H_2O (0.1ml) in

THF (1ml). After this dry ice is added until no further precipitate is formed. The inorganic salts formed are then removed by filtration and washed with ethanol repeatedly. The filtrate was then dried with $MgSO_4$. The solution was then evaporated *in vacuo* giving a peach liquid. This material was then dissolved in 40ml ethanol and 10% Pd/C (0.5g) was added. The solution was thoroughly degassed and then stirred with H_2 for 6 hours. The Pd/C was then removed and washed thoroughly with ethanol. The combined filtrate where then *evaporated in vacuo* to give a black oil (1.42g, 77%). In the case of the enriched *erthro* (ratio) The solution crystallised and was then recrystalised from ethylacetate (71.3mg, 5%). TLC (chloroform with 10% methanol) R_f (*threo*) = 0.66 , R_f (*erythro*) = 0.51; IR (neat) 3500 (O-H), 2955 (CH_2/CH_3), 1597 (aryl), 1608 (aryl) 1467 (CH_2/CH_3 deformation) 1085 (C-O stretch) ^{1}H NMR (300MHz, $CDCl_3$) *erythro* 6.98 (1H, t, ^{3}J=8.42, H_3), 6.54 (2H, d, H_2), 6.48 (2H, s, H_7), 4.89 (1H, d, ^{3}J= 3.31Hz, H_6), 4.25-4.18 (1H, m, H_4) 4.15-4.06 (1H, m, H_5), 3.78 (3H, s, H_1 or H_8), 3.76 (3H, s, H_1 or H_8), 3.36 (1H, br. s, H_8 or H_{10}), 3.09 (1H, br s, H_8 or H_{10}), *threo* 6.94-6.84 (1H, m, H_3), 6.53-6.48 (4H, m, H_2+H_7), 4.92 (1H, d, ^{3}J= 8.79, H_6), 4.46 (1H, dd, ^{3}J= 2.81 + 10.66, H_4), 4.31 (1H, m, H_5), 3.80 (6H, s, H_1 or H_8), 3.73 (6H, s, H_1 or H_8); ^{13}C NMR (125MHz, $CDCl_3$) 153.37, 147.16, 134.81, 133.90, 130.35, 124.52, 105.28, 102.72, 86.67, 72.46, 60.46, 56.21, 56.05; ESI-MS (low res.) 403 (MNa^+); ESI-MS (high res.) 403.1353 (MNa^+) observed, 403.1363 (MNa^+) calculated.

8.2.1.14 Synthesis of 1-(4-hydroxyphenyl)-2-phenoxy-1,3-propanediol (29)[195]

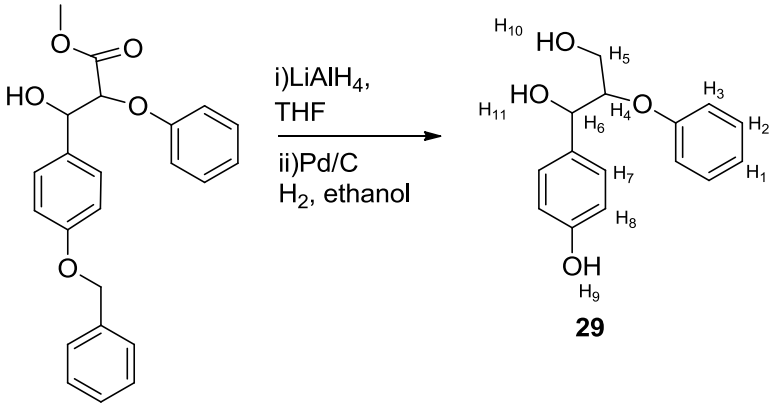

47 **29**

Lithium aluminium hydride (7.93 mmole, 0.309g) was dissolved in anhydrous THF (20ml). This solution was stirred vigorously at 50^{o}C under nitrogen and over thirteen minutes compound **47** (1g, 2.64 mmole) dissolved in THF (20 ml) was added. This solution was left for two hours and then cooled to 0^{o}C. This was followed by the dropwise addition of H_2O (4 ml) in THF (5 ml). After this dry ice is added until no further precipitate is formed. The inorganic salts formed are then removed by filtration and washed with ethanol. The filtrate was then dried with $MgSO_4$. The solution was then evaporated *in vacuo*. This material was then dissolved in ethanol (12 ml) and 10% Pd/C (0.15g) was added. The solution was thoroughly degassed and then stirred with H_2 for 30 hours. The Pd/C was then removed and washed three times with ethanol. The combined filtrate where then evaporated *in vacuo* to give a yellow oil. (0.5g, 73%). IR (neat) 3287 (OH), 1596 (aryl), 1490 (aryl), 1228 (aryl ether), 1034 (aryl ether); ^{1}H NMR (300MHz, $CDCl_3$) 7.24-7.38 (2H, m, H_2), 7.35-7.11 (2H, m, H_7), 6.86 (1H, t, ^{3}J=8.2 , H_1), 6.80 (2H, d, ^{3}J=8.4, H_3), 6.71 (2H, d, ^{3}J=8.5 Hz, H_8), 4.94 (1H,d, ^{3}J= 5.1, H_6), 4.28 (1H, q, ^{3}J=4.5 H_4), 3.80 (2H, dd, ^{3}J = 7.9,

^{3}J =11.8, H_5), 2.71 (1H, br s, $H_{9/10}$), 2.22 (1H, br s, H_9/H_{10}) ppm; ^{13}C NMR (75MHz, $CDCl_3$) 158.94, 156.62, 133.05, 129.65, 127. 70, 121.88, 116.59, 115.40, 81.90, 73.84, 61.38 ppm; ESI-MS (low res.) 283(MNa^+); ESI-MS (high res.) 283.0950 (MNa^+) observed, 283.0941 (MNa^+) calculated.

8.2.2 Synthesis of lignin dimers

8.2.2.1 Synthesis of biphenyl dimer, 3,3'-dicarboxaldehyde, 6,6'-dihydroxy-5,5'-dimethoxy-1,1'-biphenyl (31)[132]

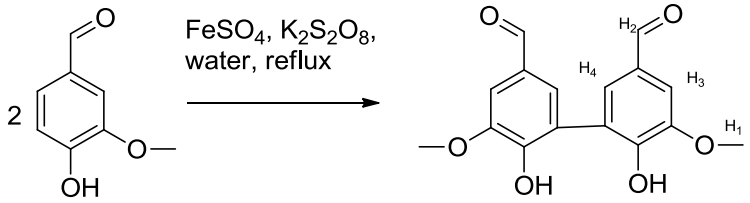

31

Vanillin (5.00g, 33mmole) was dissolved in hot water (200ml). $FeSO_4$ (200mg, 0.72 mmole) and $K_2S_2O_8$ (5g, 19 mmole) were then added creating a purple solution, which was then refluxed for two hours. After this the product had crystallised and was removed by filtration and allowed to dry in air. The final material was light brown in colour and similar to dry mud (8.74g, 88%). Mp 285-290^{o}C (lit. 300-305)[196] IR (neat) 3182 (O-H), 2955 (CH_3/CH_2), 1667 (C=O), 1577 (aryl), 1111 (C-O), 1040 (aryl-O-CH_3); ^{1}H NMR (300 MHz, DMSO) 9.81 (2H, s, H_2), 7.43 (4H, s, H_3, H_4), 3.93 (6H, s, H_1); ^{13}C NMR (75 MHz, DMSO) 191.24, 150.35, 148.09, 128.16, 127.68, 124.50, 109.04, 55.98; ESI-MS (High res.) 303.0861 (MH^+), 325.0677 (MNa^+).

8.2.2.2 Synthesis of 2,3-dihydro-2-(4-hydroxy-3-methoxyphenyl)-5-(3-hydroxy-1-propen-1-yl)-7-methoxy-3-Benzofuranmethanol (32)[18]

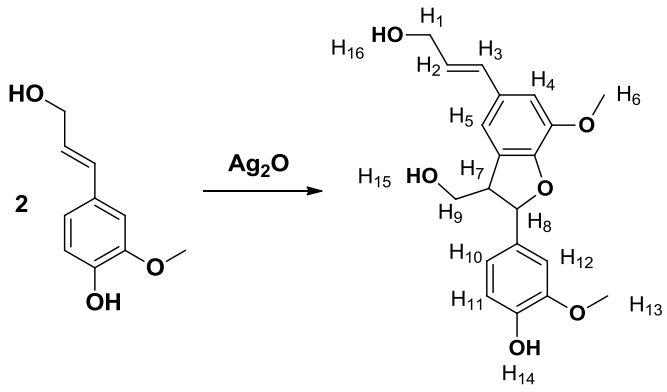

32

Coniferyl alcohol (80mg, 0.44 mmole, 1 eq) was dissolved in dry acetone (2ml) and Ag_2O (I) was added to the solution and stirred in the dark for three days. The solution was then diluted with acetone and filtered through celite and the solvent was removed in vacuo. The product was then purified by reverse phase HPLC in the same manner as the pinrenisol. Approximately 1mg. ^{1}H NMR (300MHz, acetone) 7.03 (1H, br s, H_{14} or H_{15} or H_{16}) 6.98 (1H, s, H_5), 6.95 (1H, s, H_4), 6.89 (1H, s, H_{12}), 6.76 (1H, d, ^{3}J= 8.0, H_{10}), 6.68 (1H, d, ^{3}J=8.2, H_{11}), 6.53 (1H, d, ^{3}J=15.9, H_3), 6.24 (1H, dt, ^{3}J= 15.9, 5.4, H_2), 5.43 (1H, d, ^{3}J=6.6, H_8), 4.19 (2H, d, ^{3}J= 5.1, H_9), 3.79 (2H, m, H_1), 3.73 (3H, s, $H_{6/13}$), 3.69 (3H, s, $H_{6/13}$), 3.40 (1H, q, H_7,^{3}J= 6.2, 6.3) ppm; ^{13}C NMR (150MHz, acetone) 148.93, 148.43, 147.34, 145.17, 134.36, 131.94, 130.53, 130.42, 128.37, 119.55, 116.10, 115.72, 111.67, 110.52, 88.53, 64.61, 63.38, 56.51, 56.48, 54.78 ppm; ESI-MS (low res.) 381 (MNa^+).

8.2.3 Synthesis of lignin degradation products

8.2.3.1 Synthesis of 2-(2-methoxy-phenoxy)-ethanol (33)[195]

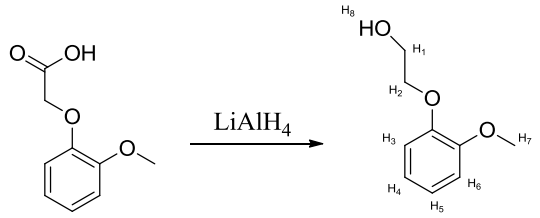

33

$LiAlH_4$ (0.156g, 4.11 mmoles, 3 equivalents) was dissolved in 5ml of dry THF. This was stirred vigorously and heated to 50^{o}C. Over thirty minutes the ester, (0.25g, 1.37 mmoles, 1 equivalent) dissolved in 5ml of THF, was added. The solution was stirred for three hours. After this the reaction was still incomplete, so a further three equivalents of $LiAlH_4$ dissolved in 5ml of dry THF was added and the reaction was left over night. After this the reaction was cooled to 0^{o}C and 5ml of wet THF was added. After this dry ice was added and the resulting solid removed by filtration. The remaining THF was dried with $MgSO_4$ and evaporated *in vacuo* to give a yellow oil (0.225, 98%) IR(neat), 2928 (CH_3/ CH_2 stretching), 1593(Aryl), 1503 cm^{-1}(Aryl), 1251 (Aryl-O-CH_3) and 1027(Aryl-O-CH_3); ^{1}H NMR (300MHz, $CDCl_3$) 6.93 (4H, m, H_3, H_4, H_5, H_6) 4.12 (2H, t, ^{3}J= 5, H_1), 3.91 (2H, t, ^{3}J= 5, H_2) 3.85(3H, s, H_7), 1.83 (br s, H_x) ppm; ^{13}CNMR (75.5MHz, $CDCl_3$) 149.5, 148.0, 121.8, 121.1, 114.2, 111.8, 71.4, 61.2, 55.8 ppm; ESI-MS (low res.) 191(M Na^{+}).

8.2.3.2 Synthesis of nitrovanillic alcohol compound 34[133]

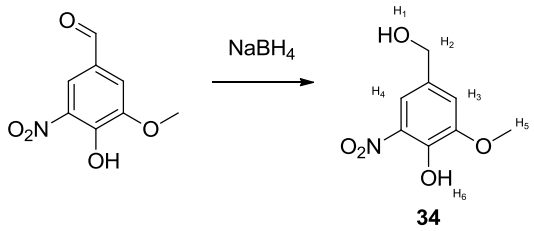

34

Nitrovanillin (0.5g, 2.6 mmoles, 1 equivalent) was dissolved in water (25 ml) and sodium borohydride solution (0.036g, 0.95mmoles, 0.37 equivalents in a solution of 10% 2M NaOH solution and 90% distilled water) was added dropwise. When no more temperature increase was seen on addition of sodium borohydride, the reaction mixture was then extracted with ether (30ml x 3) and dried with $MgSO_4$. The ether was then removed *in vacuo* to give solid. (0.3399g, 65%). Mp =112-113 (lit. 107-108^oC)[197] IR(neat), 3245 (OH), 1544 (NO_2 conjugated), 1500 (Aryl), 1329 (OH bending) 1263(Aryl-O-CH_3) cm^{-1}; ^1H NMR (300MHz, $CDCl_3$,) 10.77 (1H, br. s, H_1 or H_6), 9.90 (1H, br. s, H_1 or H_6), 7.69 (1H, s, H_4), 7.20 (1H, s, H_3), 4.69 (1H, d, J= 5.6, H_2), 3.97 (3H, s, H_5); ^{13}CNMR (75.5MHz, $CDCl_3$) 150.18, 145.75, 133.46, 32.11, 121.39, 116.38, 113.60, 64.15, 56.75 ppm; ESI-MS (low res.) 196 (M^-).

8.3 Preparations of lignin

8.3.1 Lignin Preparation[142]

Lignin from miscanthus, Hereward wheat and Scots pine was prepared using the following general method. The biomaterial (wheat straw 11.20g, pine 21.41g, miscanthus 21.36) was passed through a C&N laboratory mill size 8 rotary mill with a 5mm mesh. The resulting material is referred to as lignocellulose. This material was then washed with a soxhlet for three days with acetone and then

three days with acetone: water (9:1, v:v) (120ml). The material was then dried over phosphorous pentoxide and remilled on a Apex 529A rotary mill with a 1mm mesh. After this it was ball milled on a vibrating jar ball mill from Glen Creston ltd, Type: 14-5805, Serial number: 88.08.35 (1 hour total, in 20 minute steps). The remaining material was extracted with dioxane: water (9: 1, v:v) (100ml). This was followed by dioxane: water (1:1, v:v) (100ml). After this these two extractions where repeated. Each extraction was carried out for one day with stirring. Dioxane extracts were then combined and evaporated under reduced pressure giving a brown solid (Final masses: Wheat 0.2946g, 3%, pine 0.1099g, 0.6%, miscanthus 0.8065%, 5%).

Wheat lignin: UV-visible maximum 278 nm; IR (neat) 3278 (OH stretch), 2821 (C-H stretching in methyl groups), 1590 (aromatic stretching particularly in di methoxylated units), 1504 (aromatic skeletal vibrations particularly strong for monomethoxylated units), 1455 (C-H deformations, asymmetric in CH_3 and CH_2), 1228 (C-O and C-C in g rings), 1122 (typical for grass lignins), 1021 (aromatic ethers) cm^{-1}; ESI-MS A series of peaks were observed for the polymer between 900-2000 *m/z* the centre was at 1539 *m/z*.

Miscanthus lignin: UV-visible maximum 279nm; IR (neat) 3321 (OH stretching), 1500 (aromatic structural vibrations), 1464 (CH deformations asymmetric in CH_3 and CH_2 groups), 1268 (mono methoxylated ring), 1127 (typical for grass lignins), 1023 (aromatic ethers) cm^{-1}; ESI-MS A series of peaks were observed for the polymer between 900-1900 *m/z* the centre was at 1451.

Pine lignin: 3321 (OH stretching), 1434 (aromatic vibrations, combined with C-H in plane deformations), 1022 (aromatic ether) cm^{-1}. For pine lignin four distinct envelopes of peaks were observed. The first spread between 1100-1200 with the centre at 1149, the second between 1250-1350 with the centre at 1329, the third envelope was between 1450-1600 with the centre at 1507 and the fourth envelope was between 1600 and 1700 with the centre at 1661.

8.3.2 Synthesis of nitrated lignin[146]

Lignin (5mg) and K_2CO_3 (3mg) were mixed in H_2O (0.5ml), shaken thoroughly, and filtered to remove insoluble material. Tetranitromethane (100μl) was added, and the reaction was stirred under foil at room temperature for one hour, and then centrifuged (2 min, 10000 rpm). The aqueous layer was separated and evaporated under vacuum. This method yielded 1.3mg miscanthus lignin, 0.6 mg Scots pine lignin and 1mg of Hereward wheat lignin.

Nitrated wheat lignin: UV-visible maximum 348 nm; IR (neat) 3408 (OH), 1636 (O-N=O two bands), 1539 (C-NO_2), 1492(aryl), 1372 (C-NO_2), 1159 (C-O stretch), 1043 (aryl ether) cm^{-1}; ESI-MS A series of mass peaks where observed for the polymer, the envelope was between 950 and 1900 with the centre at 1449 *m/z*.

Nitrated miscanthus lignin: UV-visible maxima 353, 279 nm; IR (neat) 3411 (OH), 1646 (O-N=O two bands), 1543 (C-NO_2), 1496 (aryl), 1394 (C-NO_2), 1162 (C-O stretch), 1032 (aryl ether) cm^{-1};ESI-MS A series of mass peaks

where observed for the polymer the envelope was between 1000 and 2000 centred around 1472 *m/z*.

Nitrated pine lignin: UV-visible maximum 350 nm; IR (neat) 3409 (OH), 1636 (O-N=O two bands), 1540 (C-NO_2), 1482 (aryl), 1383 (C-NO_2), 1158 (C-O stretch), 1037 (aryl ether) cm^{-1}; ESI-MS A series of mass peaks where observed for the polymer and the envelope was between 950 and 1800 with main peak at 1529 *m/z*.

8.3.3 Producing Acid Precipitable Polymeric Lignin (APPL)[91]

This experiment was done in duplicate to get sufficient mass of APPL for further study. 5g of miscanthus lignocellulose was placed in a sterile conical flask with 50ml of minimal media 1 (For 1L $K_2HPO_4.3H_2O$ 4.25g, NaH_2PO_4 1.0g, NH_4Cl 2.0g, $MgSO.7H_2O$ 0.2g, $FeSO_4.7H_2O$ 12mg, $MnSO_4.H_2O$ 3mg, $ZnSO_4.7H_2O$ 3mg, $CoSO_4.7H_2O$ 1mg, nitrilotriaceticacid 0.1g and yeast extract 3g).[198] These were inoculated with 1ml log phase growth of *S. viridosporus*. After 4 weeks 40ml of LB was added to each. After an additional four weeks the solution was filtered through filter paper. The filtrate was then treated with 12M HCl. This gave a precipitate that was separated by centrifugation (one minute, 4000 rpm). The final amount of black brown solid material was 0.3067g. IR (neat) all peaks much broader than seen with unmodified lignin. 3362 (OH strerching) 2913 (C-H stretching in methyl groups) 1644 (Aryl/unsaturated ketone), 1553 (antisymetric carboxylate ion stretching), 1430 (symmetric carboxylate ion stretching), 1143 (typical for grass lignins) 1030 (aryl ethers) ESI-Ms a range of peaks observed with main ions 696, 556, 413 *m/z*. The envelope ran from 100 to 800 with the centre at 400 *m/z*.

8.3.4 Industrial lignin

The industrial lignin was provided by Prof. H. Dalton and characterised by IR and GPC. The GPC was done by Polymer labs ltd with PL-GPC 220 fitted with two PL PolarGel (300mm 7.5mm) columns in dimethyl acetamide. The molecular weights of Mp =6528, Mn = 1242, Mw =12145, Mz = 51060 Mz+1 = 131586, Mv = 9393 was observed and a polydispersity index of 9.8. IR (neat) 3339 (OH), 2920 (CH_2/CH_3), 2850 (CH_2/CH_3), 1592 (aromatic skeletal vibations), 1512 (aromatic skeletal vibations), 1454 (C-H in CH_3 and CH_2 groups), 1076 (aryl ethers), 810 cm^{-1} (C-H out of of plane deformations for G type monomer).

8.3.5 Synthesis of fluorescent lignin

Industrial lignin or kraft lignin (5mg) was mixed with H_2O (0.5ml) and K_2CO_3 (3mg, 0.02mM), shaken thoroughly and then filtered through cotton wool. A 100μl aliquot of a stock fluorophore solution (0.2mM stock in water) was added and left stirring overnight under foil. Fluorophores investigated were fluorescein isothiocyanate (FITC), 4(5)-iodoacetamido)fluorescein (IAF) or dansyl chloride. The solution was acidified, and the precipitate collected by centrifugation (2min at 10000rpm). Fluorescence observed from 30 ul of 0.1 mg/ml fluorescent lignin was as follows lignin: FITC 45314, Lignin IAF 5903, kraft lignin FITC 7894 and kraft lignin IAF 8565 AFU. No fluorescence was observed with the dansyl chloride derivatised material.

8.4 Fluorescent assay

8.4.1 Whole bacterial cells

Liquid cultures of *Rhodococcus sp., Nocardia autotrophica, Pseudomonas putida, Bacillus subtillis, Escherichia coli DH10B, Rhodococcus erythropolis* and *Leuconostoc mesenteroides* were grown for 16 hrs in LB.

Assays had a total volume 200µl and were carried out in 96 well plates, using a TECAN GENios plate reader. A stock solution of lignin-FITC solution (1 mg) was prepared in 750 mM Tris buffer pH 7.4 containing 50 mM NaCl, and then diluted into 4.5ml of the same Tris buffer. 160µl of this solution was then added to each well, followed by 30µl culture supernatant, and then 10µl of 40mM H_2O_2 (2 mM final concentration) solution. Measurements (λ_{ex} 490 nm, λ_{em} 520 nm) were taken every minute for the first ten minutes and after this every ten minutes for two hours. Duplicates of each assay were carried out, and controls were included where the lignin and/or bacteria solutions where both replaced with buffer. The entire assay was repeated as above but with the H_2O_2 being replaced by buffer. The control without bacteria was subtracted from each data point. Effect of H_2O_2 concentration was investigated by using final concentrations of 5mM, 1mM, 0.1mM and 0mM.

8.4.2 Bacterial supernatants screened for lignin degrading ability

Liquid cultures of *S. viridosporus, B. subtilis, P. Putida, Rhodococcus RHA 1, Rhodococcus sp., N. autotrophic* and, *L. mesenteroides,* were grown for 16 hr LB. 2ml of these solutions were then centrifuged for four minutes at 10000 rpm, and the supernatant decanted. 30µl of the culture supernatant was

used for each well of the subsequent assay.

Assays had a total volume 200 µl and were carried out in 96 well plates, using a TECAN GENios plate reader. A stock solution of lignin-FITC solution (1 mg) was prepared in 750 mM Tris buffer pH 7.4 containing 50 mM NaCl, and then diluted into 4.5ml of the same Tris buffer. 160µl of this solution was then added to each well, followed by 30µl culture supernatant and then 10µl of 40mM H_2O_2 solution (2mM final concentration). Measurements (λ_{ex} 490 nm, λ_{em} 520 nm) were taken every minute for the first ten minutes and after this every ten minutes for two hours. Duplicates of each assay were carried out, and controls were included where the lignin and/or bacteria solutions were both replaced with buffer. The entire assay was repeated as above but with the H_2O_2 being replaced by buffer. The control without bacteria was subtracted from each data point. Concentration dependence was investigated using 10, 30 and 50 µl of culture supernatant.

8. 5 UV-visible screening assays

8.5.1 UV-visible screening assay general method

A stock solution of nitrated MWL from pine, wheat straw and miscanthus was prepared (1mg/100ml) in 750 mM Tris buffer pH 7.4 containing 50mM NaCl.

Assays (200 µl total volume) were carried out in 96 well plates, using a TECAN GENios plate reader. To each well was added 30µl of microorganism supernatant, 160µl nitrated lignin, 10 µl of 2 mM H_2O_2.

Absorbance at 430 nm was measured at one min intervals for 20 min. Each assay was carried out in duplicate, with controls in which nitrated lignin or bacterial culture supernatant was replaced with 750 mM Tris pH 7.4 containing 50mM NaCl. The whole plate was repeated without addition of H_2O_2. All readings where taken in duplicate. Concentration dependence was investigated using 10, 20, and 30 µl culture supernatant.

Control experiments were carried out where the nitrated lignin was replaced with glucose and cellulose that had previously been treated with tetranitromethane as detailed in 8.3.2. These experiments used the supernatant from *P. putida* and *R. jostii* RHA1.

8.5.2 Micro-organism growth for UV-visible screening assay

Liquid cultures of *S. viridosporus*, *B. subtilis*, *P. putida* 33015, *Rhodococcus sp. RHA* 1, *Rhodococcus sp.* DSM43230, *N. autotrophica*, *L. mesenteroides*, *P. putida* 4539, *R. erythropolis*, *Acetobacter* PC/4, *Arthrobacter globiformis* D45 and *B. licheniformis* were grown for 16 hours in LB. 2ml of these solutions were then centrifuged for 4 minutes at 10000 rpm, and the supernatant decanted. 30µl of the culture supernatant was used for each well of the subsequent assay.

Liquid cultures of *S. coelicoler* M110, *S. coelicoler JCM* 3279, *S. coelicoler* M145, *S. coelicoler* ISP 5233, *S. coelicoler* M1190, *S. coelicoler* 1010 and *S. avermittilis* 41443 DSM were grown for 24 hours in 25ml of LB in 250ml conical flasks with baffles, each flask also contained 1.25g of polyethylene glycol 8000 as a dispersant. After 24 hours growth was assessed by absorbance

at 600nm. If the growth was between 0.1 and 1.0 the solution was spun down and used as above.

Solid fungal cultures of *Agaricus bisporus, Lentinula edodes, Lepista nuda, Phanerochaete chrysosporium, Pleurotus ostreatus, Schizophyllum commune, Serpula lacrymans* and *Trametes versicolor* were grown on straw by Dr K. Burton and D. Eastwood at Warwick HRI. These cultures were then treated with 5ml of water and then shaken by hand and 2ml of this solution was then centrifuged for 4 minutes at 10000 rpm, and the supernatant decanted. 30μl of the culture supernatant was used for each well of the subsequent assay.

Liquid fungal cultures of *Suillus luteus, Paxillus involutus, Suillus bovinus, laccaria bicolour, Cenococcum geophilum, lactarius rufus* and *Lactarius controversus* were grown as liquid cultures on MMN media (For 1 L, KH_2PO_4 10ml of 5% stock, $(NH_4)H_2PO_4$ 10ml of 2.5% stock, $CaCl_2.2H_2O$ 10ml of 5% stock, NaCl 10ml of 0.25% stock, 10ml of 1.5% stock, Thiamine 1ml of 0.01% stock, Fe(EDTA) 1.2ml of 2% stock and make up to 1L adjust pH to 4.7 with HCl) were provided by Dr G. Bending from Warwick HRI. 1ml of this solution was then taken and filtered through a 0.2μm whatman filter with a 12mm diameter and 30μl of the culture supernatant was then used for each well of the subsequent assay.

8.5.3 Plate assay

Two plates of *B. subtilis, L. mesenteroides, P. putida* and *R. jostii RHA*1 were grown on LB agar plates. One of these plates for each bacteria was then sprayed

with nitrated miscanthus lignin (1mg/100ml). All the plates were then incubated for two days. After this time the plates were photographed.

8.6 Lignin degradation studies

8.6.1 Small-scale degradation trials with nitrated lignin

200 μl of nitrated lignin solution (1mg/ml) was added to 5 ml of LB or ISP media 1. The three LB solutions were then inoculated with either *P. putida*, *B. subtilis* or *R. jostii* RHA1. The ISP media 1 was inoculated with *S. viridosporus*. These solutions were then incubated overnight and then 1 ml samples were taken and spun at 10000 rpm for 4 minutes. After this the supernatant was cooled on ice, then treated with 50μl of cooled CCl_3COOH (1mg/ml) and left on ice for 3 minutes. The precipitate was removed by centrifugation, and the supernatant was then taken and analysed by reverse phase HPLC, using a Phenomenex Luna 5μ C18 100Å 50x4.6 mm on a Hewlett Packard Series 1100 analyser, at a flow rate of 0.5 ml/min. The HPLC gradient was 20-30% MeOH/H_2O over five min, then 30-50% MeOH/H_2O over 5-12 min, then 50-80% MeOH/H_2O over 12-25 min. Controls were done with each media where they were not inoculated with any bacteria.

8.6.2 Small scale degradation trials with *P. putida* and *R. jostii* RHA1 and miscanthus lignocellulose

A 20 ml culture of Luria Broth containing 0.5g of lignocellulose from miscanthus was inoculated with a 2 ml culture of log phase *P. putida* or *Rhodococcus* RHA1. The solutions were shaken (180 rpm) at 30^{o}C for one week. Samples (1ml) were removed after 2, 4, and 6 hr, and after 1, 2, 3, and

seven days.

Each sample was centrifuged (5 min, 10000 rpm) and the supernatant was cooled on ice, then treated with 50µl of cooled CCl_3COOH (1mg/ml) and left on ice for 3 minutes. The precipitate was removed by centrifugation and the supernatant was then taken and analysed by reverse phase HPLC, using a Phenomenex Luna 5µ C18 100Å 50x4.6 mm on a Hewlett Packard Series 1100 analyser, at a flow rate of 0.5 ml/min. The HPLC gradient was 20-30% MeOH/H_2O over five minutes, then 30-50% MeOH/H_2O over 5-12 min, then 50-80% MeOH/H_2O over 12-25 min. LC/MS was carried out using a reverse phase C-8 column, 250 x 4.6mm provided by Thermo Scientific, on a Finnigan LTQ machine, at a flow rate of 1.0 ml/min. Buffer A, H_2O with 0.1 % v/v formic acid; buffer B, 20% MeOH:MeCN 50:50 with 0.1% formic acid. Gradient 20-30% buffer B over five min, then 30-50% buffer B over 5-12 min, then 50-80% buffer B over 12-25 min.

Samples for GC-MS were extracted into dichlormethane (1ml) derivatised via silylation by treatment with N, O-bis(trimethylsilyl)acetamide (200µl) and chloro-trimethylsilane (10µl). The samples were left overnight and then further diluted by a factor of 100. GC-MS was carried out on a Varian 3800 machine, using a Varian Factor Four column, 30m x 0.25mm x 0.25µm, with electron impact ionisation at 750eV. Temperature gradient 75 ^oC 0-1 min, then raised by 25^oC/min for nine minutes to 300^oC, then held for nine minutes.

200µl of sample from each time point was taken and diluted into 500ml of H_2O. After this 100µl of 2,4-dinitrophenyl hydrazine (1mg/ml) was added in addition to 1 drop of concentrated HCl. This solution was left for an hour and then studied by HPLC and LC/MS.

Data for compound **59** LC-MS, RT = 4.29 min, *m/z* 235 MK^+; GC-MS (monosilylated), RT = 7.021 min, *m/z* 268 $(M)^+$, 253 $(M\text{-}CH_3)^+$, 180 $(M\text{-}CH_3\text{-}COCH_2CH_2OH)^+$, 122 $(M\text{-}SiMe_3\text{-}COCH_2CH_2OH)^+$.

Data for ferulic acid **22** LC-MS, RT = 5.25 min, 195 m/z MH^+; GC-MS (monosilylated), RT = 5.27 min, 251 $(M\text{-}CH_3)^+$, 193 $(M\text{-}SiMe_3)^+$, 149 $(M\text{-}SiMe_3\text{-}CO_2)^+$.

Data for compound **60** LC-MS, RT= 5.76 min, *m/z* 251 MK^+; GC-MS (disilylated) RT= 6.028 min, *m/z* 341$(M\text{-}CH_3)^+$, 283 $(M\text{-}SiMe_3)^+$, 268 $(M\text{-}SiMe_3\text{-}CH_3)^+$, 239 $(M\text{-}SiMe_3\text{-}CO_2)^+$.

Data for oxalic acid **61** GC-MS (disilylated) RT= 4.4 min, 189, $(M^+\text{-}3Me)$ 147 $(M^+\text{-}SiMe_3\text{-}Me)$, 132 $(M^+\text{-}SiMe_3\text{-}2Me)$, 116 $(M^+\text{-}SiMe_3\text{-}2Me\text{-}O)$, (monosilylated) RT= 5.3 147 $(M^+\text{-}Me)$, 132 $(M^+\text{-}2Me)$, 117 $(M^+\text{-}2Me)$.

Standards of oxalic acid, ferulic acid and compound **60** were run using the above method of derivatisation and analysis. When derivatising the chemical standards for GC/MS, DCM was used as the solvent with the exception of compound **60** where 1,4-dioxane was used. In all cases HPLC quality solvent was used.

8.7 Spectrophotometric assays of DypB

8.7.1 Nitrated lignin assay of DypB knockout mutants

A stock solution of nitrated wheat lignin was prepared (0.015mM) in 750 mM Tris buffer pH 7.4 containing 50mM NaCl. Liquid cultures of *R. jostii RHA* 1, *R. jostii* RHA1Δro577 (Δ*dypA*), *R. jostii* RHA1Δro2407 (Δ*dypB*) and *R. jostii* RHA1Δro2377 (Δ*mco*) were grown for 16 hrs in LB. 2ml of these solutions were then centrifuged for four minutes at 10000 rpm, and the supernatant decanted. 30μl of the culture supernatant was used for each well of the subsequent assay. These samples were assayed using the method given in 8.5.1.

8.7.2 Nitrated lignin assay of recombinant DypA and DypB

A stock solution of nitrate wheat lignin was prepared (0.015mM) in 750 mM Tris buffer pH 7.4 containing 50mM NaCl.

The total assay volume was 200μl. To each well was added 30 μl of protein solution (0.1mg/ml), 130μl nitrated lignin, 10 μl of 40 mM H_2O_2. Absorbance at 430 nm was measured at one minute intervals for 20 minutes. Each assay was carried out in triplicate, with controls in which nitrated lignin and protein solution was replaced with 750 mM Tris pH 7.4 containing 50mM NaCl. The whole plate was repeated without addition of H_2O_2.

8.7.3 Mn^{2+} and syringaldehyde dependency experiment

A stock solution of nitrated wheat lignin was prepared (0.015mM) in 750 mM Tris buffer pH 7.4 containing 50mM NaCl.

The total assay volume was 200μl. To each well was added 30 μl of protein solution (0.1mg/ml), 130μl nitrated lignin, 30ul of $MnCl_2$ (50 mM) or 30μl of syringaldehyde (50mM), 10 μl of 40 mM H_2O_2. Absorbance at 430 nm was measured at 1 min intervals for 20 min. Each assay was carried out in duplicate, with controls in which nitrated lignin, protein solution and $MnCl_2$ was replaced with 750 mM Tris pH 7.4 containing 50mM NaCl. The whole plate was repeated without addition of H_2O_2. All readings where taken in duplicate.

8.7.4 DypB with lignin and lignocellulose

Lignocellulose/ lignin (5mg) was added to succinate buffer (3ml, 50mM, pH 5.5) then Dyp B (100μl, 0.1mg/ml) was added, followed by H_2O_2 (100 μl, 40mM). The resulting solution was incubated at 30^oC for 48 hours. Aliquots (1ml) were taken at 1, 3, 5, 24 and 48 hours. These fractions were analysed by HPLC. Aliquots for HPLC (400μl) were mixed with CCl_3COOH (1 g/ml w/v, 40 μl), the solution was then spun for four minutes at 10 000 rpm. The experiment was also repeated with the hydrogen peroxide replaced by glucose (final concentration 0.3 mM) and glucose oxidase (final concentration 0.5 μg/ml). Both experiments were carried out with and without $MnCl_2$ (1 mM). HPLC analysis was carried out using the method given in 8.6.2.

8.7.5 Kraft lignin kinetic assay[85]

In a 1ml cuvette kraft lignin (500 μl, 0.5mg/ml), DypB (25 μl of 0.1mg/ml), H_2O_2 peroxide (100μl, 40mM), Mn^{2+} (200 μl, 50mM) and succinate buffer (175μl, pH5.5, 50mM) are mixed in the order stated. The absorbance was observed at 465 nm. Substrate concentrations were then varied for $MnCl_2$ (1.25-

10 mM final concentration) and Kraft lignin (0.05-0.25 mg/ml final concentration), with the total volume kept at 1.0 ml. Measurements were taken in duplicate. The molar concentration of Kraft lignin was calculated using an average molecular mass of 10,000.

8.7.6 Lignin dimer kinetics by HPLC

β-aryl ether **27**, (2ml, 5mM) dissolved in 9:1 water: acetone was diluted into succinate buffer (3ml, 50mM, pH 5.5) then Dyp B (100μl, 0.1mg/ml), $MnCl_2$ (100 μl, 50 mM) was added, followed by H_2O_2 (100 μl, 40mM). The resulting solution was incubated at 30^oC for two days. Two samples (1ml) where taken at 1, 3, 5, 24 and 48 hours. To stop the reaction each aliquot was placed in a 90^oC water bath for ten minutes immediately after being collected. These fractions were analysed by HPLC. Aliquotes for HPLC (400μl) were mixed with CCl_3COOH 1:1 w:v (40 μl). A control was run where no DypB was added. The reaction was repeated without $MnCl_2$.

8.7.7 Lignin Dimer Degradation experiment

Dimer (β-aryl ether, **27**-**29** pinresinol **31** and biphenyl dimer **64**) (2ml, 5mM stock solution) dissolved in 9:1 acetone water was diluted into succinate buffer (3ml, 50mM, pH 5.5) then Dyp B (25μl, 0.1mg/ml) was added, followed by H_2O_2 (100 μl, 40mM). The resulting solution was incubated at 30^oC for two days. Aliquotes (1ml) where taken at 1, 3, 5, 24 and 48 hours. These fractions were analysed by HPLC and LC/MS. Aliquotes for HPLC (400μl) were mixed with CCl_3COOH 1:1 w:v (40 μl). The HPLC method was the same as those used in 8.6.2. The LC/MS method was LC/MS analysis was carried out using a

Phenomenex Luna 5μ C_{18} reverse phase column (100Å, 50x4.6 mm) on a Agilent 1200, at a flow rate of 0.5 ml/min, with a Bruker HCT Ultra massspectrometer. The LC gradient was 20-30% MeOH/H_2O over five minutes; 30-50% MeOH/H_2O over 5-12 min; 50-80% MeOH/H_2O over 12-25 min. The solution is left for one hour and then diluted by a factor of 100, after which it is applied.

For each dimer a control was run where no DypB was added. The experiment was repeated with β-aryl ether **27** with the H_2O_2 peroxide solution replaced with glucose oxidase (0.5μg/ml) and glucose (0.3mM).The experiments with the three β-aryl ether lignin dimers were repeated with $MnCl_2$ (100 μl, 50 mM). The above experiment was also run with guaiacol as the substrate (2ml, 5mM).

8.7.8 Lignin Dimer Degradation experiment with diaphorase

β-aryl ether **27** (2ml, 5mM), dissolved in 9:1 acetone water, was diluted into succinate buffer (3ml, 50mM, pH 5.5) then Dyp B (25μl, 0.1mg/ml), diaphorase from *Clostridium kluyveri* (500 μl of 2mg/ml). NADH (2 ml, 5mM) was added, followed by H_2O_2 (100 μl, 40mM). The resulting solution was incubated at 30^{o}C for two days. Aliquotes (1ml) were taken at 1, 3, 5, 24 and 48 hours. These fractions were analysed by HPLC and LC/MS. Aliquotes for HPLC (400μl) were mixed with CCl_3COOH 1:1 w:v (40 μl). The HPLC method was the same as those used in 8.6.2. The LC/MS method was the same as 8.7.7.

A control was run where no DypB was added. The experiment was repeated with no NADH and with no NADH and no DypB.

8.7.9 pH rate profile of DypB

DypB (0.5mg/ ml), ABTS (10 mM), $MnCl_2$ (10mM) and H_2O_2 (10mM) were reacted together in citric acid 0.1M and phosphate 0.2M buffers of pH 2.8, 3.2, 3.6, 3.7, 4.1, 4.3, 4.6, 4.8, 5.7, 6.3 and 6.6. The increase in absorbance at 430 nm over five minutes was observed and an extinction coefficient of 36.8 mM^{-1} cm^{-1} [199] was used to calculate the activity. Each measurement was made in triplicate.

8.7.10 Stopped Flow kinetics analysis of DypB

Recombinant DypB (8 μM final concentration) in 30mM citrate- 60mM phosphate buffer, pH6.0, and was mixed with freshly prepared solutions of hydrogen peroxide, $MnCl_2$, and β-aryl ether **27** at 8 or 80 μM concentration final concentrations. All measurements were carried out in triplicate. The decay of DypB compound I was observed at 397 nm.[182] Compound II decay was observed at 417 nm, which is the isosbestic point between compound II and resting enzyme.[183] Kinetic transients were fitted to single and double exponential kinetic models, and in all cases, good fits were observed to single exponential functions. In the reactions of β-aryl ether **27**, more complex behaviour was observed at >1 s, in which case the data at 15-1000 ms was used to derive k_{obs}.

APPENDIX 1 LC-MS

Retention Time (Min)	m/z	Sample	Method	Possible Assignment
3.36	227	P. putida 6hrs; P. putida 1 day; P. putida 3 day; RHA1 5 days	LC/MS	aromatic triacid, **1**
3.39	227	R. RHA1 4hrs; R. RHA1 1 day; R. RHA1 1 week;	LC/MS	aromatic triacid, **1**
	249	R. RHA1 4hrs; R. RHA1 1 day; R. RHA1 1 week;	LC/MS	aromatic triacid, **9**
	317	R. RHA1 4hrs;	LC/MS	dimer, **40**
3.41	181	R. RHA1 2hrs;	LC/MS	?
	227	R. RHA1 2hrs;	LC/MS	aromatic triacid, **1**
	249	R. RHA1 2hrs;	LC/MS	aromatic triacid, **9**
	317	R. RHA1 2hrs;	LC/MS	dimer, **40**
3.43	227	P. putida 2 days;	LC/MS	aromatic triacid, **1**
3.52	155	R. RHA1 6 hrs	LC/MS	catechol, **12**
3.81	225	P. putida 2 days;	LC/MS	pyran, **16**
	252	P. putida 2 days;	LC/MS	?
	346	P. putida 2 days;	LC/MS	?
3.94	225	R. RHA1 2 day	LC/MS	pyran, **16**
4.22	245	P. putida 6hrs	LC/MS	?
4.29	235	R. RHA1 1 day; R. RHA1 5days; R. RHA1 5days	LC/MS	aromatic ketone, **2**; or diacid, **7**
4.46	209	R. RHA1 2 day	LC/MS	pyran, **15**
4.53	235	P. putida 6hrs; P. putida 1 day; P. putida 3 day; R. RHA1 2hrs; R. RHA1 4hrs	LC/MS	aromatic ketone, **2**; or diacid, **7**
4.56	209	R. RHA1 1 day	LC/MS	pyran, **15**
	225	R. RHA1 1 day	LC/MS	pyran, **16**
4.69	195	R.RHA1 5 days;	LC/MS	fereulic acid, **3**
4.81	258	P. putida 2 days;	LC/MS	aromatic ketone, **2**; or diacid, **7**
	259	P. putida 2 days;	LC/MS	?
	267	P. putida 2 days;	LC/MS	?
	346	P. putida 2 days;	LC/MS	dimer?
	348	P. putida 2 days;	LC/MS	dimer?
4.87	323	P. putida 2 days;	LC/MS	?
5.25	195	P. putida 6hrs; R. RHA 1 2hrs; R. RHA1 6hrs	LC/MS	fereulic acid, **3**
	254	P. putida 6hrs; RHA1 2hrs	LC/MS	?
5.33	362	P. putida 2 days;	LC/MS	dimer
	219	P. putida 2 days;	LC/MS	?
	199	P. putida 2 days;	LC/MS	syringic acid, **41**
5.45	155	R. RHA1 6hrs	LC/MS	catechol, **12**
	169	R. RHA1 6hrs	LC/MS	vannillic acid, **13**
5.58	251	R. RHA1 6hrs	LC/MS	aromatic diacid, **4**
5.76	251	P. putida 6hrs; R. RHA1 4hrs	LC/MS	aromatic diacid, **4**
6.10	227	RHA1 5 days	LC/MS	aromatic triacid, **1**

	249	RHA1 5 days	LC/MS	aromatic triacid, **9**
6.15	582	R. RHA1 6hrs	LC/MS	trimer?
	583	R. RHA1 6hrs	LC/MS	trimer, **17**
6.16	155	R. RHA1 6hrs	LC/MS	catechol, **12**
	169	R. RHA1 6hrs	LC/MS	vannillic acid, **13**
6.17	501	P. putida 6hrs	LC/MS	?
6.24	221	P. putida 2 days;	LC/MS	monomer, **21**
	235	P. putida 2 days;	LC/MS	diacid, **9**
	251	P. putida 2 days;	LC/MS	diacid, **4**
	254	P. putida 2 days;	LC/MS	?
6.26	560	R. RHA1 1 day	LC/MS	trimer?
6.31	344	R. RHA1 4hrs;	LC/MS	?
	366	R. RHA1 4hrs;	LC/MS	?
6.37	357	P. putida 1 day	LC/MS	diacid, **5**
	408	P. putida 1 day	LC/MS	?
6.48	675	R. RHA1 1 week	LC/MS	trimer?
6.54	675	P. putida 3 day	LC/MS	?
6.55	378	R. RHA1 5 days	LC/MS	?
6.65	166	P. putida 6hrs	LC/MS	?
6.68	675	P. putida 1 day	LC/MS	?
6.69	166	R. RHA1 4hrs;	LC/MS	?
	464	R. RHA1 4hrs;	LC/MS	?
	205	P. putida 2 days;	LC/MS	?
	229	P. putida 2 days;	LC/MS	?
6.93	473	R. RHA1 1 week	LC/MS	trimer?
6.97	746	P. putida 2 days;	LC/MS	tetramer?
	747	P. putida 2 days;	LC/MS	tetramer?
7.25	229	R. RHA1 4hrs;	LC/MS	?
8.05	188	P. putida 6hrs; P. putida 1 day, P. putida 3 day	LC/MS	?
8.09	188	R. RHA1 4hrs;	LC/MS	?
	697	R. RHA1 4hrs;	LC/MS	?
8.34	383	R. RHA1 1 week;	LC/MS	coumaryl dimer, **29**
	243	P. putida 2 days;	LC/MS	?
8.35	198	R. RHA1 5 days	LC/MS	?
8.65	604	P. putida 1 day	LC/MS	trimer?
	553	P. putida 1 day	LC/MS	?
	197	P. putida 1 day	LC/MS	aromatic ketone, **6**
8.95	245	P. putida 2 days;	LC/MS	?
	277	P. putida 2 days;	LC/MS	?
9.09	155	R. RHA1 6hrs	LC/MS	catechol, **12**
	169	R. RHA1 6hrs	LC/MS	vannillic acid, **13**
9.69	455	P. putida 3 day	LC/MS	?
	477	P. putida 3 day	LC/MS	?
	813	P. putida 3 day	LC/MS	tetramer, **37**
9.75	652	P. putida 6hrs; P. putida 1 day	LC/MS	?
9.75	652	R. RHA1 4hrs;	LC/MS	?
	813	R. RHA1 4hrs;	LC/MS	tetramer, **37**
	856	R. RHA1 4hrs;	LC/MS	?
9.99	514	R. RHA1 1 week	LC/MS	trimer?
10.05	380	P. putida 3 day	LC/MS	dimer?
	358	P. putida 3 day	LC/MS	?

	548	P. putida 3 day	LC/MS	?
10.21	241	R. RHA1 2 day;	LC/MS	triacid, **18**
10.24	397	RHA1 1 week;	LC/MS	dimer **30** or dimer **31**
10.27	397	P. putida 3 day	LC/MS	dimer **30** or dimer **31**
	419	P. putida 3 day	LC/MS	?
	657	P. putida 3 day	LC/MS	?
10.36	577	P. putida 1 day	LC/MS	trimer, **39**
	653	P. putida 1 day; RHA1 2hrs	LC/MS	trimer, **10**
10.41	155	R. RHA1 6hrs	LC/MS	catechol, **12**
	169	R. RHA1 6hrs	LC/MS	vannillic acid, **13**
10.72	684	P. putida 6hrs; P. putida 1 day	LC/MS	?
10.77	659	R. RHA1 2hrs;	LC/MS	trimer, **11**
	684	R. RHA1 2hrs;	LC/MS	?
10.84	243	P. putida 3 day	LC/MS	?
11.04	588	R. RHA1 1 day	LC/MS	trimer?
	589	R. RHA1 1 day	LC/MS	trimer, **38**
	753	R. RHA1 1 day	LC/MS	tetramer, **28**
	755	R. RHA1 1 day	LC/MS	tetramer, **27**
	756	R. RHA1 1 day	LC/MS	tetramer?
	778	R. RHA1 1 day	LC/MS	tetramer?
11.23	770	R. RHA1 2 day	LC/MS	tetramer?
	794	R. RHA1 2 day	LC/MS	tetramer, **26**
	991	R. RHA1 2 day	LC/MS	pentamer?
	1013	R. RHA1 2 day	LC/MS	pentamer, **22**
	1014	R. RHA1 2 day	LC/MS	pentamer?
11.82	588	R. RHA1 1 day	LC/MS	trimer?
	659	R. RHA1 1 week	LC/MS	trimer, **11**
	1009	R. RHA1 1 day	LC/MS	pentamer, **21**
11.89	751	R. RHA1 2hrs; R. RHA1 4hrs	LC/MS	tetramer, **36**
	1009	R. RHA1 2hrs; R. RHA1 4hrs	LC/MS	pentamer, **21**
	1010	R. RHA1 2hrs;	LC/MS	pentamer?
	1081	R. RHA1 2hrs; R. RHA1 4hrs	LC/MS	pentamer?
11.91	751	P. putida 6hrs; P. putida 1 day	LC/MS	tetramer, **36**
	1009	P. putida 6hrs; P. putida 1 day	LC/MS	pentamer, **21**
	1081	P. putida 6hrs	LC/MS	hexamer, **25**
12.42	572	P. putida 1 day	LC/MS	?
	1057	P. putida 1 day	LC/MS	pentamer, **20**
	1374	P. putida 1 day	LC/MS	heptamer, **24**
12.54	530	P. putida 6hrs; P. putida 1 day; R. RHA1 1 week;	LC/MS	trimer?
12.59	530	R. RHA1 2hrs; R. RHA1 4hrs	LC/MS	trimer?
	1026	R. RHA1 2hrs; R. RHA1 4hrs	LC/MS	?
	1101	R. RHA1 4hrs;	LC/MS	hexamer, **23**
	1102	R. RHA1 2hrs;	LC/MS	?
13.90	208	RHA1 5 days	LC/MS	?

14.04	348	P. putida 2 days;	LC/MS	?
16.87	343	R. RHA1 6hrs	LC/MS	diacid, 5 or dimer, **14**
27.16	469	P. putida 2 days;	LC/MS	?
27.95	470	R. RHA1 5 days	LC/MS	tetramer?
27.97	469	P. putida 3 day	LC/MS	tetramer?
43.89	417	P. putida 3 day	LC/MS	?
	591	P. putida 3 day	LC/MS	?
43.90	417	RHA1 5 days	LC/MS	?
	418	RHA1 5 days	LC/MS	?
	575	RHA1 5 days	LC/MS	trimer, **34**
	591	RHA1 5 days	LC/MS	?
	619	RHA1 5 days	LC/MS	trimer, **35**

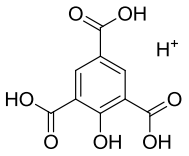

1

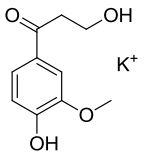

2

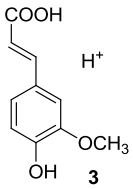

3

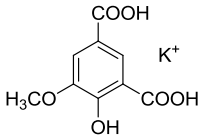

4

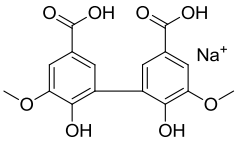

5

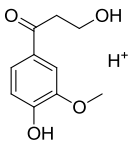

6

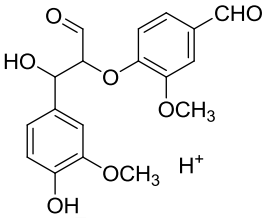

7

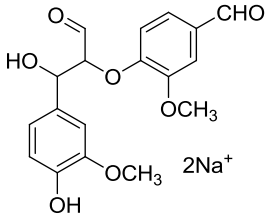

8

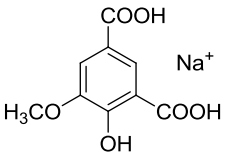

9

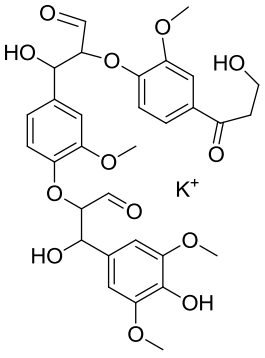

10

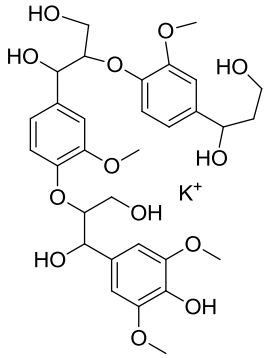

11

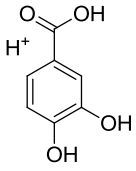

12

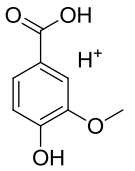

13

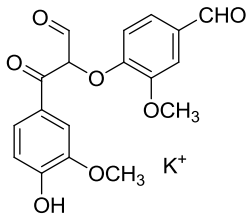

14

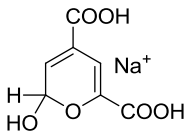

15

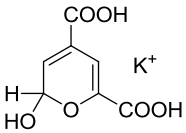

16

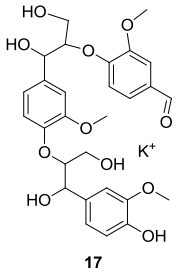

17

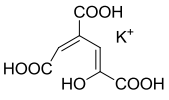

18

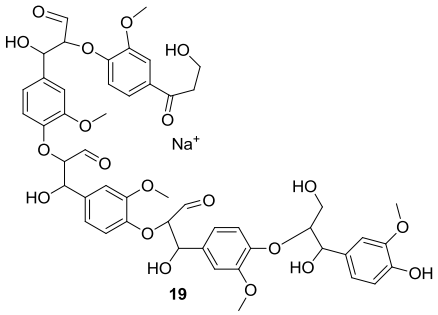

19

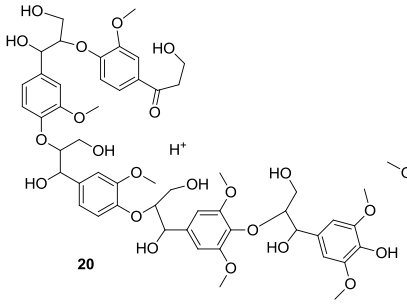

20

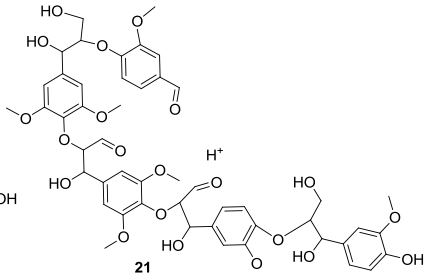

21

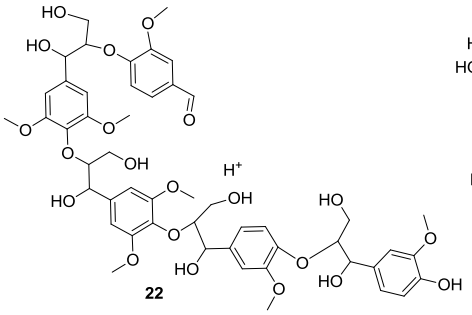

22

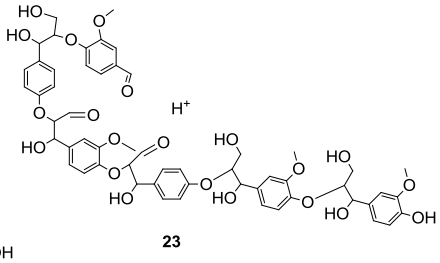

23

References

[1] "Sustainable biofuels: prospects and challenges", policy document, RSC, 2008, Londin.

[2] F. Cherubini, *Energy Convers. Manage.*, 2010, **51** 1412–1421.

[3] A. Ragauskas, C. Williams, B. Davison, G. Britovsek, J. Cairney, C. Eckert, W. Frederick Jr., J. Hallett, D. Leak, C. Liotta, J. Mielenz, R. Murphy, R. Templer and T. Tschaplinski, *Science*, 2006, **311**, 484-489.

[4] L. O. Wackett, *Curr. Opin. Chem. Biol.*, 2008**, 12**, 187-193.

[5] J. Gressel, *Plant Sci*, 2008, **174**, 246-264.

[6] S. M. Brumbley, M. P. Purnell, L. A. Petrasovitis, L. K. Nielsen and P. H. Twine, *Inter. Sugar J.*, 2007**, 109**, 5.

[7] F. Festel, *Chem. Eng. Technol.*, 2008, **31**, 715-720.

[8] Department for Environment Food and Rural Affairs, Survey of Agriculture and Horticulture: 1 June 2007 England – Final results, http://statistics.defra.gov.uk/esg/statnot/june_eng.pdf

[9] Department for Environment Food and Rural Affairs, CEREALS USAGE BY MILLERS, BREWERS AND MALTSTERS UK - JULY 2010, http://www.defra.gov.uk/evidence/statistics/foodfarm/food/cereals/cerealsusage.htm

[10] H. Das and S. K. Singh, *Crit. Rev. in Food Sci. Nutr.*, 2004, **44**, 77-89.

[11] A. Demirbas, *Energy Convers. Manage.*, 2009, **50**, 2782–2801.

[12] T. Werpy and G. Pedersen, in *Top value added chemicals from biomass*, vol. 1. US Department of Energy; 2005.

[13] J. Hayes, S. Fitzpatrick, M. Hayes and J. Ross, in Biorefienries – industrial processes and products (status quo and future directions), ed. B Kamm, P Gruber and M Kamm, editors., Wiley-VCH , 2006, vol.1.

[14] E. Sjöström, in Wood Chemistry Fundamentals and Applications, Academic Press, London, 2nd Ed., 1993, pp. 118.

[15] E. Sjöström, in Wood Chemistry Fundamentals and Applications, Academic Press, London, 2nd Ed., 1993, pp54-89

[16] http://www.life.ku.dk/forskning/online_artikler/artikler/marken_en_stor_solfanger.aspx?lg=print

[17] B. Davis and A. Fairbanks, in Carbohdrate Chemistry, Oxford University Press, Oxford, 1st Ed., 2002, pp80-81.

[18] J. Ralph, R. Helm and S. Quideau, *J. chem. Soc. Perkin Trans.*, 1992, **1**, 2971-2980.

[19] J. Mao, K. Holtman, J. Scott, J. Kadla, and K. Shcmidt Rohr, *J. Agric. Food Chem.*, 2006, **54**, 9677-9686.

[20] M. C. Carpinella, C. G. Ferrayoli and S. M. Palacios, *J. Agric. Food Chem.*, 2005, **53**, 2922-2927.

[21] Ángel T Martínez, F. Ruiz-Dueñas, M. Jesús Martínez, J. Río and A. Gutiérrez, *Curr. Opin. Biotechnol.*, 2009, **20**, 348–357.

[22] J. Ralph, K. Lundquist, G. Brunow, F. Lu, H. Kim, P. F. Schatz, J. Marita, R. D. Hatfield, S. A. Ralph, J. H. Christensen and W. Boerjan, *Phytochem. Rev.*, 2004, **3**, 29-60.

[23] J. Zakzeski, P. Bruijnincx, A. Jongerius, and B. Weckhuysen, *Chem. Rev.*, 2010**, 110**, 3552–3599.

[24] E. Adler, *Wood Sci. Technol.*, 1977, **11**, 169.

[25] A. Sakakibara, in Wood and Cellulose Chemistry, ed. N. Shiraishi, Marcel Dekker Inc., New York, 1991.

[26] K**.** Koda, A. Gaspar, L. Yu and D. Argyropoulos, *Holzforschung* ,2005, **59**, 612.

[27] J. Ralph, J. Marita, A. Ralph, R. Hatfield, F. Lu, R. Ede, J. Peng, S. Quideau, R. Helm, J. Grabber, H. Kim, G. Jimenez-Monteon, Y. Zhang, H. Jung, L. Landucci, J. MacKay, R. Sederoff, C. Chapple and A. Boudet, In *Advances in Lignocellulosics Characterization*, ed. D. Argyropoulos, Tappi Press, Atlanta, 1999.

[28] E. Capanema, M. Balakshin and J. Kadla, *Agric. Food. Chem.*, 2004, ***52***, 1850**.**

[29] Z. Lee, G. Meshitsuka, N. Cho and J. Nakano, *Mokuzai Gakkaishi*, 1981, **27**, 671.

[30] E. Capanema, M. Balakshin and J. Kadla, *J. Agric. Food. Chem.*, 2005, **53**, 9639.

[31] J. Rencoret, M. Gisela, A. Gutiérrez, L. Nieto, J. Jiménez-Barbero, A. Martínez and J. del Río, *Ind. Crops Prod.*, 2009, **30**, 137.

[32] L. B. Davin and N. G. Lewis, *Curr. Opio. Biotechnol.*, 2005, **16**, 407-415.

[33] D. Evtuguin and F. Amado, *Macromol. Biosci.*, 2003, **3**, 339-343.

[34] O. Faix, *Holtzforschung*, 1991, **45**, 21-27.

[35] E. Harris, J. D'Ianni and H. Adkins, *J. Am. Chem. Soc.* 1938, **60**, 1467.

[36] R. Thring and J. Breau, *Fuel*, 1996, **75**, 795.

[37] M. Nag, K. David, G. Britovsek and A. Ragauskas, *Holzforschung*, 2009, **63**, 513.

[38] E. Portjanskaja, K. Stepanova, D. Klauson and S. Preis, *Catal. Today*, 2009, **144**, 26.

[39] F. Chakar and A. Ragauskas, *Ind. Crops Prod.*, 2004, **20**, 131-141.

[40] North American Pulp and Paper Fact Book, 1997, p. 332

[41] W. Glassser and S. Kelley, in Encyclopedia of Polymer Science and Engineering, ed. H. Mark, N. Bikales, C. Overberger, G. Menges and J. Kroschwitz, 2nd edn., 1987, vol. 8, p795-848.

[42] R. Vicuña, *Enzyme Microbiol., Technol.*, 1988, **10**, 646-655

[43] M. H. Gold, M. Alic, *Microbiol. Rev.*, 1993, **57**, 605-622.

[44] T. Higuchi, *Proc. Jpn. Acad., Ser. B*, 2004, **80**, 204-214.

[45] http://botit.botany.wisc.edu/toms_fungi/may97.html

[46] B. Finzelt, T**.** Poulos, and J. Kraut, *J. Biol. Chem*., 1984, **259,** 13027-13036.

[47] T. Poulos, *Arch.Biochem. Biophys.* 2010, doi: 10.1016/j.abb.2010.02.008

[48] T. Poulos and J. Kraut, *J. Biol. Chem.*, 1980, **255** 8199–8205.

[49] T. Iizuka, M. Kotani and T. Yonetani, *J. Biol. Chem.*, 1971, **246**, 4731–4736.

[50] G. Lang, K. Spartalian and T. Yonetani, *Biochim. Biophys. Acta* , 1976, **451**, 250–258.

[51] J. Fajer, D.C. Borg, A. Forman, D. Dolphin and R.H. Felton, *J. Am. Chem. Soc.*, 1970, **92**, 3451–3459.

[52] T. Yonetani, H. Schleyer, A. Eherenberg, *J. Biol. Chem.*, 1966, **241**, 3240–3243.

[53] J.M. Mauro, L.A. Fishel, J.T. Hazzard, T.E. Meyer, Kraut, *Biochemistry*, 1988, **27**, 6243–6256.

[54] T. Choinowski, W. Blodig, K. Winterhalter and K. Piontek, *J. Mol. Biol.* 1999, **286**, 809-827.

[55] W .Blodig, A Smith, W Doyle, K Piontek, *J.Mol.Biol.*, 2001, **305**, 851-861.

[56] S. Jovanovic, S. Steenken and M. Simic, *J. Phys. Chem.*, 1991, **95**, 684-687.

[57] A. Khindaria, I. Yamazaki and S. Aust, *Biochemistry*, 1996, **35**, 6418-6424.

[58] T. Johjima, N. Itoh, M. Kabuto. F. Tokimura, Nakagawa, H. Wariishi and H. Tanaka, *Proc. Natl. Acad. Sci. USA*, 1999, **96**, 1989-1994.

[59] T. Umazawa, F. Nakatsubo and T. Higuchi, *Agric. Biol. Chem.*, 1983, **47**, 2677-2681; T. Umezawa and T. Higuchi, *Agric. Biol Chem.* 1987, **51**, 2282-2284.

[60] T. K. Jirk and C. Chang, *Holzfoschung*, 1975, **29**, 56-64.

[61] L. Marquez and H. Wariishi, H. Dunford, and M. Gold, *J. Biol. Chem.*, 1988, **263**, 10549-10552.

[62] J. Ruiz-Dueñas, M. Morales, M. Mate, A. Romero, M. Martínez, A. Smith and A. Martínez, *Biochemistry*, 2008, **47**,1685-1695.

[63] M. Hofrichter, *Enzyme Microb. Technol.*, 2002, **30**, 454-466.

[64] M. Sundaramoorthy., K. Kishi, M. Gold, T. Poulos, *J.Mol.Biol.*, 1994, **238,** 845-848.

[65] U. Tuor, H. Wariishi, H. E. Shoemaker and M. Gold, *Biochemistry*, 1992, **31**, 4986-4995; H. Wariishi, K. Valli and M. Gold, *Biochemistry,* 1989, **28**, 6017-6023.

[66] L. Banci, S. Ciofi-Baffoni and M. Tien, *Biochemistry*, 1999, **38**, 3205-3210.

[67] A. Heinfling, F. J. Ruitz-Dueñas, M. J. Martinez, M. Bergbauer, U. Szewzyk and A. T. Martinez, *FEBS Lett.*, 1998, **428**, 141-146.

[68] D. Wong, *Appl Biochem. Biotechnol.* 2009, **157**, 174-209

[69] R. Pongi, M. Camilla Barrato, C. Teutloff, S. Giansanti, F. Ruiz-Dueñas and T. Choinowski, *J. Biol. Chem.*, 2006, **281**, 9517-9526.

[70] M. Perez-Boada, J. Ruiz-Dueñas, F.J., R. Pogni, R. Basosi, T. Choinowski, M. Martinez, M.J., K. Piontek and A. Martinez, *J. Mol. Biol*., 2005, **354,** 385.

[71] W. Bavendamm, *Zeitschr. Pflanzenkrankh. Planzenschtz*, 1928, **38**, 257-276; T. Higuchi, in Formation and biological degradationof lignins, in Adv. Enzymology, ed. F. F. Nordm, **34**, Interscience Publisher, New York, pp207-283.

[72] M. Lahtinen, K. Kruus, P. Heinonen and J. Spilä, *J. Agric. Food Chem.*, 2009, **57**, 8357-8365.

[73] A. Potthast, T. Roxenau, H. Koch and K. Fischer, *Holzforschung*, 1999, **53**, 175-180.

[74] F. Ruiz-Dueñas and Á. Martínez, Microb. Biotechnol., 2009, **2**, 164–177.

[75] C. Eggert, U. Temp, and K. Eriksson, *FEBS Lett.*, 1997, **407**, 89-92.

[76] A. Gutierrez, J. Rencoret, D. Ibarra, S. Molina, S. Camareo, J. Romerro, J. Del Río,[†] and Á. Martínez, *Environ. Sci. Technol.*, 2007, **41**, 4124-4129.

[77] M. Lahtinen, K. Kruus, H. Boer, M. Kemell, M. Andberg, L. Viikari and J. Sipilä, *J. Mol. Catal. B: Enzym.*, 2009, **57**, 204-210.

[78] A. Leonowicz, N. Cho, J. Luterek, A. Wilokolazka, M. Wojtas-Wasilewska, A. Matuszewska, M. Hofrichter, D. Wesenberg and J. Rogalski, *J. Basic Microbiol.*, **41**, 2001, 185-227.

[79] J. Shi, R. Sharma-Shivappa, M. Chinn and N. Howell, *Biomass bioenergy*, 2009, **33**, 88-96.

[80] W. Zimmermann, *J. Biotechnol*., 1988, **10**, 646-655.

[81] M. Ramachandra, D. L. Crawford and G. Hertel, *Appl. Environ. Microbiol.*, 1988, **54**, 3057-3063.

[82] K. Haider, J. Trojanowski and V. Sundman, *Arch. Microbiol.*, 1978, **119**, 103-106.

[83] C. Trigo and A. S. Ball, *Appl. Microbial. Biotechnol.*, 1994, **41**, 366-372.

[84] F. Perestelo, A. Rodrigues, R. Pérez, A. Carnicero, G. De la Fuente and M. Falcón, *World J Microbiol. Biotechnol.*, 1996, **12**, 111-112.

[85] A. Raj, R. Chandra, M. K. Reddy, H. J. Purohit and A. Kapley, *World J. Microbiol. Biotechnol.*, 2007, **23**, 793-799.

[86] G. Singh, N. Capalash, R. Goel and P. Sharma, *Enzyme Microb. Technol.*, 2007, **41**, 794-799.

[87] V. Antonopoulos, M. Hernandez, M. Arias, E. Mavrakos and A. Ball, *Appl. Microbiol. Biotechnol.*, 2001, **57**, 92-97.

[88] T. Bugg, M. Ahmad, E. Hardiman and R. Singh**,** *Curr. Opin. Biotechnol.*, In Press.

[89] H. Kawakami, in *Lignin Biodegradation: Microbiology, Chemistry and Potential Applications Volume II*, ed. T. K. Kirk, T. Higuchi and H. Chang, CRC Press, Florida, 1980, pp 103-125.

[90] E. Masai, Y. Katayama and M. Fukuda, *Biosci. Biotechnol. Biochem.*,2007, **71,** 1-15.

[91] D. L. Crawford, A. L. Pometto III and R. Crawford, *Appl. Environ. Microbiol.*, 1983, **45**, 898-904.

[92] S. Anatai and A. Iyo, *J. Basic Microbiol*., 1990, **30**, 643-647.

[93] D. Crawfor, M. Barder, A. Pometto III and R. Crawford, *Arch. Microbiol.*, **131**, 140-145.

[94] S. Adav, C. Ng, M. Arulmani amd S. Sze, *J Proteome Res*. 2010, **9**, 3016-3024.

[95] H. Kern and T. Kirk, *Appl. Environ. Microbiol.*, 1987, 2242-2246.

[96] S. Haemmerli, M. Leisola and A. Fietchter, *Appl. Environ. Microbiol.*, 1986, **35**, 33-36.

[97] E. Masai, Y. Yamamoto, T. Inoue, K. Takamura, H. Hara, D. Kasai, Y. Katayama and M. Fukuda, *Biosci. Biotechnol. Biochem.*, 2007, ***71***, 2487-2492.

[98] Y. Otsuka, M. Nakamura, K. Shighara, K. Sugimura, E. Masai, S. Ohara and Y. Katayama, *Appl. Microbiol. Biotechnol.*, 2006, **71**, 608-614.

[99] T. Michinobu, M. Hishida, M. Sato, Y. Katayama, E. Masai, M. Nakamura, Y. Otsuka, S. Ohara and K. Shigehara, *Polym. J. (Tokyo, Jpn.)*, 2008, **40**, 68-75.

[100] T. Michinobu, Y. Inazawa, K. Hiraki, Y. Katayama, E. Masai, M. Nakamura, S. Ohara and K. Shigehara, *Chem. Lett.*, 2008, **37**, 154-155.

[101] T. Michinobu, M. Bito, M. Tanimura, Y. Katayama, E. Masai, M. Nakamura, Y. Otsuka, S. Ohara and K. Shigehara, *J. Macromol. Sci., Part A: Pure Appl.Chem.*, 2010 **47**, 564-570.

[102] T. Michinobu, K. Hiraki, N. Fujii, K. Shikinaka, Y. Katayama, E. Masai, M. Nakamura, Y. Otsuka, S. Ohara and K. Shigehara, *Chem. Lett.*, 2010, **39**, 400-401.

[103] Michinobu T, Bito M, Yamada Y, M. Tanimura, Y. Katayama, E. Masai, M. Nakamura, Y. Otsuka, S. Ohara and K. Shigehara, *Polym. J. (Tokyo, Jpn.)*, 2009, **41**, 1111-1116.

[104] J. Davis and J. Sello, *Appl. Microbiol. Biotechnol.*, 2010, **86**, 921-929.

[105] G. Singh, N. Ahuja, M. Batish, N. capalash and P. Sharma, *Bioresour. Technol.*, 2008, **99**, 7472-7479.

[106] A. Unall and N. Kolankaya, *Turk.j. Biol.*, 2001, **41**, 67-72.

[107] H. Kellner, P. Luis, B. Zimdars, B. Kiesel and F. Buscot, *Soil Biol. Biochem.*, 2008, **40**, 638-648.

[108] T. Kirk, *Annu. Rev. Phytopathol.*, 1971, **9**, 185-210.

[109] J. Rajan and V. Srinivasan, *Biotechnol. Tech.*, 1992, **6**, 219-222.

[110] J. B. Van Beilen and Y. Poirier, *Plant J.*, **2008**, 54, 684 -701.

[111] S. Hagedorn and B. Kaphammer, *Annu. Rev. Microbiol.*, 1994, **48**, 773-800.

[112] G. Clark, *Perfumer and Flavorist*, 1990, **15**, 45-54.

[113] H. Priefert, J. Rabenhorst and A. Steinbüchel, *Appl. Microbiol. Biotechnol.*, **56**, 2001, 296-314.

[114] A. Raj, M. Reddy and R. Chandra, *Int. Biodeter. Biodeg*. 2007, **59**: 292-296.

[115] V. Gupta, A. Minocha and N. Jain, *J. Chem. Tech. Biotech*. 2001, **76**: 547-552.

[116] S. Mathew and T. Abraham, *Crit Rev Biotechnol.*, 2004, **24**, 59-83.

[117] M Kampa, V. Alexaki, G. Notas, A. Nifli, A. Nistikaki, A. Hatzoglou, E. Bakogeorgou, E. Kouimtzglou, G. Blekas, D. Boskou, A. Gravanis and E. Castanas, *Breast Cancer Res.*, 2004,

6,63-74; H. Mori, K. Kawabata, N. Yoshimi, T. Takaka, T. Murakami, T. Okada and H. Murai, *Anticancer Res.*, 1999, **19**, 3775-3778*;* P. Lesca, *Carcinogenesis*, 1983, **4**, 1651-1653.

[118] B. Wang and J. Ou-Yang, *Cardiovasc. Drug Rev.*, 2005, **23**, 161–172.

[119] F. Lin, J. Lin, R. Gupta, J. Tournas, J. Burch, M. Selim, N. Monteiro-Riviere, J. Grichnik, J. Zielinski and S. Pinnell, *J. Invest. Dermatol.*, 2005, **125**, 826-832.

[120] *US Pat*., 5,336,513

[121] R Stabile and A. Dicks**,** *J. Chem. Edu.*, 2003, **80,** 313-315.

[122] T. Li and J. Rosazza, *Appl. Environ. Microbiol*, 2000, **66**, 684-687.

[123] Chemistry and Industry, 2008, **24,** 7

[124] E. Adler and E. Eriksoo, *Acta Chem. Scand.*, 1955, **9**, 341-342.

[125] F. Nakatsubo, K. Sato and T. Higuchi, 1975, **29**, 165-168.

[126] J. Sipillä and K. Syrjänen, *Holzforschung*, 1995, **49**, 325-331.

[127] B. G. Davis and A. J. Fairbanks, in Carbohydrate Chemistry, Oxford university press, New York, 2002, pp 4-5.

[128] C. Crestini and M. D' Auria, *Tetrahedron*, 1997, **53**, 7877-7888.

[129] H. Erdtman and L. Bengt, *Acta Chem. Scand.,* 1949, **3,** 1358-1371.

[130] T. Mukaiyama, *Pure & Appl. Chem.,* **55**, 1983, 1749-1758.

[131] D. Williams and I. Fleming, in Spectroscopic Methods in Orgainc Chemistry, 5th edn., 1995, McGraw Hill, London, p 93.

[132] B. Ruffin, S. Grelier, A. Nourmamode and A. Castellan, *Can. J. Chem.*, **80**, 2002, 1223-1231.

[133] A. Vogel, A. Tatchell, B. Furnis, A. Hannaford and P. Smith, in *Vogel's Textbook of Practical Organic Chemistry*, Prentice Hall, Harlow, England, 5th edn., 1989, pp524.

[134] M. Gold, J. Glenn and M. Alric, *Methods Enzymol.*, 1988, **161,** 74.

[135] M. Tekere, A. Mswaka, R. Zvauya and J. Read, *Enzyme Microb. Technol.,* 2001, **28**, 420-426.

[136] V. Sundman and L. Nase, *Paper and Timber*, 1971, **2**, 67-71

[137] D. Crawford and R. Crawfod, *Enztme Microb. Technol.*, 1980, **2**, 11-22.

[138] B. Chance and A. Maehly, *Methods Enzymol.*, 1955, **2**, 764-775.

[139] D. Mercer, M. Iqbal, P. Miller and A. McCarthy, *Appl. Environ. Microbiol*., 1996, **62**, 2186-2190.

[140] T. Sonoki, Y. Iimura E, E. Masai, S. Kajita and Y. Katayama, *J. Wood Sci.*, 2002, **48**, 429-433.

[141] A. Holmgren, G. Henriksson and L. Zhang, *Biomacromoleculs*, 2008, **9**, 3378-3382

[142] W. Zimmerman, A. Paterson and P. Broda, *Methods Enzymol.*, 1988, **161,** 191-199.

[143] J. Obst and T. Kirk, *Methods Enzymol.*, 1988, **161**, 3-12.

[144] O. Faix, *Holtzforschung*, 1991, **45**, 21-27.

[145] M. McLeod, R. Warren, , W. Hsiao, N. Araki, M. Myhre, C. Femandes, D. Miyazawa, W. Wong, A. Lillquist, D. Wang, M. Dosanjh, H. Hara, A. Petrescu, R. Morin, G. Yang, J. Stott, J. Schein, H.Shin, D. Smailus, A. Siddiqui, M. Marra, S. Jones, R. Holt, F. Brinkman, K. Miyauchi, M.Fukuda , J. Davies, W. Mohn and L. Eltis, *Proc. Natl. Acad. Sci. U. S. A*, 2006, **103**, 15582-15587.

[146] J. Riordan, M. Sokolovsky and B. Valee, *J. Am. Chem. Soc.*, 1966, **88**, 4104-4105.

[147] J. Colpaert and K. van Tichelen, *New Phytol.*, 1996, **134**, 123-132.

[148] C. Mai, U. Kues and H. Militz, *Appl. Environ. Microbiol.*, 2004, **63**, 477-494.

[149] C. Boyle, B. Kropp and I. Reid, *Appl. Environ. Microbiol.*, 1992, **58**, 3217-3224.

[150] A. Dahlberg and R. Finlay, in *Ectomycorrhizal Fungi*, eds. J.Ciarney and S. Chambers, Springer, New York, 1999, pp47-48.

[151] G. Bending and D. Read, *Mycol. Res.*, 1997, **101**, 1348-1354.

[152] K. Furukawa, F. Matsumura and K. Tonomura, Agric. Biol. Chem., 1978, **42**, 543-548.

[153] A. Pometto III and D. Crawford, *Methods Enzymol.*, 1988, **161,** 183-190.

[154] I. Chronakis, *J. Mater. Process. Technol.***,** 2005, **167**, 283.

[155] P. Keresten and K. Kirk, *J. Bacteriol.*, 1987, **169**, 2195-2201.

[156] P. Keresten, S. Stephens and K. Kirk, in *Biotechnology in the Pulp and Paper Manufacture*, eds. T. Kirk and C. Chang, Butterworth-Heinemannn, Stoneham, pp457-463.

[157] K. Hammel, K. Jensen Jr, M. Mozuch, L. Landucci, M. Tien and E. Pease, *J. Biol Chem*, 1993, **268**, 12274-12281.

[158] W. Riemenschneider and M. Tanifuji, in "Oxalic Acid" in Ullmann's Encyclopedia of Industrial Chemistry, eds Barbara Elvers, Heike Noethe, 2002, Wiley-VCH, Weinheim. doi: 10.1002/14356007.a18_247

[159]J. Ishikawa, A. Yamashita, Y. Mikami, Y. Hoshino, H. Kurita, K. Hotta and T. Shiba, M. Hattori, *Proc. Natl. Acad. Sci. U. S. A.*, 2004, **41**, 14925-14930.

[160] C. Zubieta, R. Joseph, S. Krishna, D. McMullan, M. Kapoor, H. Axerod, M. Miller, P. Abdubeck, C. Acosta, T. Astakhova, D. Carlton, H. Chiu, T. Clayton, M. Deller, L. Duan, Y. Elias, M. Elsligier, J. Feuerhelm, S. Gzechnik, J. Hale, G. Han, L. Jaroszewski, K. Jin, H. Klock, M. Knuth, P. Kozbial, A. Kumar, D. Marciano, A. Morse, K. Murphy, E. nigoghossian, L. Okach, S. Oommachen, R. Reyes, C. Rife, P. Schimmel, C. Trout, H. Bedem, D. Weekes, A. White, Q. Xu, K. hodgson, J. Wooley, A. Deacon, A. Godzik, S. Lesley and I. Wilson, *Proteins*, 2007, **69**, 234-243.

[161] D. Goodin and D. McRee, *Biochemistry*, 1993, **32**, 3313-3324.

[162] M. Sutter, D. Boehringer, S. Gutmann, S. Gunther, D. Prangishvili, M. Loessner, K. Stetter, E. Weber-Ban and N. Ban, *Nat. Struct. Mol. Biol.*, 2008, **15**, 939-946.

[163] T. Khimerik, and Mikrobiol. Zh., 1977 **39**, 355-356; K. Kadam, S. Drew, *Biotechnol. Bioeng.*, **28**, 394-404.

[164] J. Coleman, S. Rounsley, M. Rodriguez-Carres, A. Kuo, C. Wasmann, J. Grimwood, J. Schmutz, M. Taga, G. White, S. Zhou, D. Schwartz, M. Freitag, L. Ma, E. Danchin, B. Henrissat, P. Coutinho, D. Nelson, D. Straney, C. Napoli, B. Barker, M. Gribskov, M. Rep, S. Kroken, I. Molnár, C. Rensing, J. Kennell, J. Zamora, M. Farman, E. Selker, A. Salamov, H. Shapiro, J. Pangilinan, E. Lindquist, C. Lamers, I. Grigoriev, D. Geiser, S. Covert, E. Temporini, and H. VanEtte, *PLoS Genet*., 2009, **5**, e1000618, doi: 10.1371/journal.pgen.1000618.

[165] A. Rodríguez, A. Carnicero, F. Perestelo, G. DE LA Fuente, O. Milstein and M. A. Falcón, *Appl Environ Microbiol*., 1994, **60,** 2971-2976.

[166] Valerie F. Crepin, Craig B. Faulds and Ian F. Connerton, *Protein Expression Purif*., 2003, **29**, 176-184.

[167] K. Piontek, M. Antorini, and T. Choinowski**,** *J. Biol. Chem.*, 2002, **277**, 37663–37669.

[168] L. Munoz and M. Riley, *Biotechnol. Bioeng.*, 2008, **100**, 882-888.

[169] S. Kunkeaw, S. Tan and G. Coaker, *Mol. Plant-Microbe Interact*., 2010, **23**, 415-424.

[170] J. Gogarten, W. Doolittle and J. Lawrence, *Mol. Biol. Evol.*, 2002, **19**, 2226-2238.

[171] S. Létoffé, G. Heuck, P. Delepelaire, N. Lange and C. Wandersman, *Proc. Natl. Acad. Sci. U. S. A*, 2009, **106**, 11719-11724.

[172] Y. Sugano, R. Muamatsu, A. Ichiyangi, T. Sayo and M. Shoda, *J. Biol. Chem.*, 2007, **282**, 36652-36658

[173] A. Hiner, E. Raven, R. Thorneley, F. García-Cánovas and J. Rodriguez-López, *J. Inorg. Biochem.*, 2002, **91**, 27-34.

[174] S. Kim and M. Shoda, *Appl. Environ. Microbiol.*, 1999, **65**, 1029-1035; Y. Sugano, K. Sasaki and M. Shoda, *Appl. Environ. Microbiol.*, 2000, **66**, 1754-1758.

[175] V. Renganathan, K. Miki and M. Gold, *Arch. Biochem. Biophys.*, 1985, **241**, 304-414; M. Tien, T. Kirk, C. Bull and J. Fee, *J. Biol. Chem.*, 1986, **261**, 1687-1693; V. Renganathan, K. Miki and M. Gold, *Biochemistry*, 1987, **26**, 5127-5132.

[176] Y. Sugano, *Cell. Mol. Life Sci.*, 2009, **66**, 1387-1403.

[177] N.Shintani, Y. Sugano and M. Shoda, *J. Wood Sci.*, 2002, **48**, 402-408.

[178] Prof. L. Eltis, personal communication.

[179] S. Camarero, D. Ibarra, M. Martinez and A. Martinez, *Appl. Environ. Microbiol*., 2005, **71**, 1775-1784.

[180] R. Koduri and M. Tien, *J. Biol. Chem.*, 1995, **270**, 22254-22258.

[181] K. Schmalzl, C. Forsyth and P. Evans, *Wood Sci. Technol.*, 1995, **29**, 307-319.

[182] J. Roberts, R. Singh, T. Bugg and L. Eltis, 2010, in preparation.

[183] H. Wariishi, H. Dunford, I. MacDonald, and M. Gold, *J. Biol. Chem*., 1989, **264**, 3335-3340.

[184] H. Erdtman and L. Bengt, *Acta Chem. Scand.,* 1948, **2,** 535-537.

[185] D. Learmonth, M. Vieira-Coelho, J. Benes, P. Alves, N. Borges. A. Freitas and P. Soares-da-Silva, *J. Med. Chem.*, 2002, **45**, 685-694

[186] T. Althuis and H. Hess, *J. Med. Chem.*, 1977, **20**¸ 146-149.

[187] C. J. Bennett, S. I. Caldwell, D. B. McPhail, P.C. Morrice, G. G. Duthie and R. C. Hartley, *Bioorg. Med. Chem.*, **12**, 2004, 2079-2098.

[188] R. Borchardt and D. Thakker, *J. Med. Chem.*, 1975¸ **18**, 152-158.

[189] M. Zwakysta, H. Timerman, M. Tamura, T. Tohmia, Y. Wada and K. Onogi, Zhang, *J. Med. Chem.*, **40**, 1997, 1075-1089.

[190] A. Fauq, C. Ziani-Cherif and E. Richelson, *Tetrahedron: Asymmetry*, 1998, **9**, 2333-2338.

[191] I. Berndtsson and K. Lundquist, *Acta Chem. Scand. Ser. B*, **31**, 1996, 725-726.

[192] K. Lundquist, R Stomberg and S.Venunge, *Acta Chem. Scand. Ser. B*, 41, 1987, 499-510.

[193] T. L Jacobs, *J. Am. Chem. Soc.*, **58**, 1936, 2272.

[194] F. Nakatsubo, *Meth. Enz.*, 1988, **161**, 3-11.

[195] F. Nakatsubo, K. Sato and T. Higuchi; *Holzforschung*,1975, **5**, 165-168; F. Nakatsubo, *Meth. Enz.*, 1988, **161**, 3-11.

[196] R. Chapman and G. Swan, *J. Chem. Soc. C*, 1970,865-872.

[197] P. Claus, P. Schilling, J. Gratzl and K. Kratzl, Monatshefte Für Chemie, **103**, 1178-1193.

[198] W. Hareland, R. Crawford, P. Chapman and S. Dagley, *J. Bact.*, 1975, **121**, 272-285.

[199] J. Keesey, in *Biochemica Information*, Boehringer Mannheim Biochemicals, Indianapolis, 1st Edition, 1987, pp. 49.